Intramolecular Electron Transfer in an Iridium d^8-d^8 Donor-Acceptor System

Thesis by

Lucius Seiberling Fox

In Partial Fulfillment of the Requirements

for the Degree of

Doctor of Philosophy

California Institute of Technology

Pasadena, California

1989

(Submitted January 31, 1989)

Acknowledgment

Well, at this point with all of the experiments done and the body of my thesis written, it is time to reflect on my tenure at Caltech and try to thank many of the people who have enriched my graduate career. I owe a special debt of thanks to my research advisor and friend Harry Gray. Apart from being an outstanding scientist, Harry is probably the most generous and supportive person I have ever had the opportunity to work for. I can not count the number of meals at the Acapulco Lounge that I have enjoyed at Harry's expense; each accompanied by numerous rounds of Margaritas! He has cheered me on in lab, thumbs always pointing toward the ceiling, and cheered me up when things weren't going so well. Most importantly, he has provided me with the opportunity to independently seek out my own graduate education. When I joined his group in 1983, I found this "hands off approach" somewhat frustrating. Over the years I believe that the "Gray Way" of graduate education has developed my ability to identify and pursue interesting chemical problems. I value this single skill more than any other and know that I will continue to appreciate it as my career unfolds.

One of the exciting aspects of my graduate research was that it involved collaborating with several outstanding scientists at Caltech, SERI, and Brookhaven National Laboratory. Dan DuBois at SERI was responsible for initiating research surrounding the preparation of the redox phosphine ligands and was a valuable source of information during the synthesis phase of this project. Janet Marshall coached me in preparing the iridium dimer complexes and was involved in their inital characterization. Professor Dick Marsh at Caltech solved the crystal structure of $[Ir_2(Pz^*)_2(CO)_2(Ph_2POCH_2CH_2\text{-}Py^+)_2](Ph_4B)_2$ and my interactions with him enhance my appreciation for the science of crystallography and proper data analysis. I thank him for the time he took to make sure that our data were sound, our interpretations were correct and to answer all of my questions. During the winter

quarter of 1987 I had the unique opportunity to travel to Brookhaven National Laboratory to conduct picosecond laser experiments on my compounds with Jay Winkler. Needless to say without these data my thesis would not be complete. I thank Jay and his wife Melissa for their hospitality during my visit. It was certainly nice to spend Sunday afternoons having dinner with the Winklers rather than having the "entree du jour" at the Brookhaven caferteria. Through my interactions with Jay I learned what I know about reaction kinetics and picosecond laser spectroscopy and I am grateful to him for his advice and insights.

As I read about the many theories of electron transfer, I found that they are based on readily understandable concepts which are often enshrouded in technical jargon and complicated mathematical formalisms. Luckly for me John Hopfield employed two of electron-transfer's up and coming theoreticians who were willing to answer many of my questions. Jose and Dave, I think I understand your latest papers but I'll give you a call just to be sure.

When I arrived at Caltech in 1983, the photogroup was inhabited by three seasoned group members. Mike Hopkins, Tom Zeitlow, and Janet Marshall made key contributions to my education by showing me the ropes in lab, talking to me about potential projects, and teaching me the ins and outs of inorganic photochemistry. Mike and I became good friends and I thank him for the many hours we spent talking about research ideas and graduate school survival techniques. "Jedi Master" Walther Ellis provided me with seemingly endless torture at the hands of his Ligand Field Theory course. Walther is a man who continues to amaze me; master scientist, master drinker, and photocopy machine expert! I certainly wish him and the Xerox machine at Utah all the best. Special thanks go to David Smith, Miriam Zeitlow, and Steve Mayo as my comrades at arms during graduate school and for their friendship. It has been a lot of fun being in the Gray Group thanks to the great people that I have had the oppportunity to

work with and count among my friends. John Brewer and Mike Therien proofread and critiqued my thesis and I thank them for their insights.

Outside of the Gray Group there are several people who have had an influence on my development both prior to and during my graduate career. Gary Christoph and Bruce Bursten gave me my first opportunity to conduct research in inorganic chemistry. Both men have helped me realize many of my goals and I thank them for their friendship and support. Sunney Chan has been a valuable friend and sounding board during graduate school and I truly appreciate his kindness. He introduced me to real chinese food and I will miss our regular trips to "Sun Tung Loc" for dim sum.

Most Importantly, I want to thank my mother, father, and my lovely wife Jayne for all the love and support they have given me during my education. My parents have stood behind me through out college and graduate school and Jayne has made these last two years at Caltech my happiest. Mom, Dad, I think I am finished with school now. Jayne, I promise that we'll never live near an earthquake fault again! I also want to thank my good friend Chris Thompson for helping me keep things in perspective.

Finally, I thank the British Petroleum America Corporation for a fellowship during the spring quarter of 1988.

To Mom, Dad, and Jayne

Abstract: A series of donor-acceptor complexes, $[Ir_2(\mu\text{-}Pz^*)_2(CO)_2(Ph_2POCH_2CH_2\text{-}Py^+\text{-}R)_2](Ph_4B)_2$ (Py^+-R= 2,4,6-trimethylpyridinium, 4-methylpyridinium, pyridinium, and 4-phenylpyridinium; Pz*=3,5-dimethylpyrazole), have been synthesized for studying the rate of photoinduced electron transfer from the metal localized ($d\sigma^*p\sigma$) excited states of d^8-d^8 chromophores. The pyridinium electron acceptors are covalently attached to the iridium metal centers (donor) via a three atom hydrocarbon linker bound to the terminal phosphine ligands. The x-ray crystallographic structure of $[Ir_2(\mu\text{-}Pz^*)_2(CO)_2(Ph_2POCH_2CH_2\text{-}Py^+)_2](Ph_4B)_2$ reveals a metal-metal distance of 3.219(1) Å and a solid state donor-acceptor separation of 5.84(1) Å. Additional donor-acceptor separations and orientations are available to the compounds in fluid solution through rotations about the Ir-P and linker group C-O, C-N, and C-C bonds. Steady state emission spectra show that the fluoresence and phosphoresence quantum yields in these compounds are substantially reduced relative to a appropriate model complex. To date the excited state reactivity of d^8-d^8 metal dimers has been exclusively attributed to their $^3(d\sigma^*p\sigma)$ states. These findings represent the first evidence for reactivity from a shorter lived $^1(d\sigma^*p\sigma)$ state.

Picosecond and nanosecond laser flash-photolysis techniques were employed to measure the rates of photoinduced electron transfer and charge recombination in these systems. Values of k_{ET}, obtained from these studies, vary between 10^6 sec^{-1} and 10^{12} sec^{-1} as a function of reaction exoergicity ($\Delta G^{o\prime}$= -0.8 eV to 1.92 eV). Clear evidence for the inverted behavior predicted by classical and semiclassical electron transfer models is seen at high driving force. Rate constants for reactions involving the $^1(d\sigma^*p\sigma)$ and $^3(d\sigma^*p\sigma)$ excited states, as well as the rates of charge recombination are characterized by very similar values of λ and H_{ab} . Our data are adequately modeled by the classical theory of electron transfer proposed by Marcus (λ=1.0 eV, H_{ab}=35 cm^{-1}) or by a semiclassical model for k_{ET} where nuclear tunneling involves a low frequency metal-ligand mode (λ=1.0 eV, H_{ab}=35 cm^{-1}, ω=400 cm^{-1}). These findings are

explored with regard to utilizing the donor-acceptor complexes as molecular photochemical energy storage systems.

Contents

List of Figures

Chapter 1

Chapter 2

Chapter 3

Chapter 4

List of Tables

Chapter 2

Chapter 3

Chapter 4

Chapter 1

Introduction

Electron transfer (ET) is one of Nature's most fundamental chemical reactions. Charge transfer processes are of central importance in.a wide number of complex biological and chemical systems that are currently being explored in the scientific community. For example, photosynthesis continues to be an area of interest in chemistry and chemical biology,[1] especially due to the recent crystallographic characterization of the photosynthetic reaction center of *Rhodopseudamonas viridis* by Deisenhofer and coworkers.[1c] Electron-transfer studies concerning model systems[1a] and the reaction center itself[1a,3] have greatly enhanced our understanding of this remarkable photoredox system. Efficient long distance electron-transfer events are also important in the energy storage reactions that take place via the membrane-bound proteins in the mitochondria of cells.[2] Here, electron-transfer reactions, which are coupled to a proton pumping process, produce a membrane potential that is used to synthesize ATP from ADP and inorganic phosphate. Electron transfer is also a fundamental solid state process and an area of significant interest with regard to the renaissance taking place in solid state chemistry.[4] Many of the same fundamental principles that govern electron transfer between molecules must also play a role in the transport of charges through a semiconducting solid. In fact, some of the theories for molecular electron-transfer reactions have been developed by analogy to the theories of small polarons in solid state systems. One area where a fundamental understanding of electron-transfer processes will certainly have an impact in coming years is Scanning Tunneling Microscopy (STM).[5] STM is of intense interest to the physics and chemistry communities, because this technique offers the unique capability of being able to record real time images of surfaces and surface adsorbates with molecular and, in some instances, atomic resolution. Because the STM technique is based on electron tunneling between the tunneling-tip and surface, an understanding of the molecular properties that govern charge-transfer processes will be important for interpreting images of surface-bound molecular species. In addition to being of academic interest, electron-

transfer processes are also important to a number of current and developing commercial technologies. Electron-transfer reactions form the basis of the photographic and xerographic processes.[6] From exposure to development, the transformations required to capture an image on photographic film involve both solid state and molecular redox reactions. Finally, photoinduced and thermal electron-transfer reactions are intimately linked to developing solar energy storage technologies. Recent reports have indicated that solar energy conversion efficiencies as high as 28% can be attained using solid state photoelectrochemical devices.[7] These considerations indicate that detailed studies, concerning the fundamental parameters which control the rates of electron transfer, are certainly warranted.

This thesis deals with the mechanistic aspects of excited state intramolecular electron transfer in an iridium d^8-d^8 A-frame metal complex. A long range goal of our electron-transfer research is to couple photoinduced charge separation to bond forming chemical reactions. Our studies have focused on d^8-d^8 complexes, because they are powerful excited state reductants[21d,22i] and their d^8-d^7 counterparts are reactive toward C-X and C-H bond activation.[24] The following chapter introduces the concepts and terminology surrounding electron transfer and d^8-d^8 compounds that are called upon in later discussions. We first review some of the theoretical models associated with electron-transfer reactions followed by some background information on d^8-d^8 metal dimers and an outline of the objectives of this research program.

Electron-Transfer Theory: Over the past two decades the theoretical models for electron-transfer reactions have played a central role in developing an understanding of these fascinating chemical processes.[8] These models have provided a central framework for designing and interpreting experiments that explore the roles played by various molecular parameters in determining k_{et}. Because many of the concepts expressed in these theories will be important in later discussions, we will give a brief overview of these concepts and introduce some of the terminology associated with electron-transfer

models. A detailed treatment of these models can be obtained by referring to the review articles and original papers cited at the end of this chapter.

In principle, a redox system must overcome two types of barriers to electron transfer in going from reactants to products. The first of these is related to the energy required to reorganize the reactant bond distances, angles, and solvation environments to a configuration indicative of the transition state. While bonds are neither formed nor broken in an outer-sphere electron-transfer reaction, the bond distances, angles, and solvation environments in the reactants and products are different. Thus, to form the transition state, these degrees of freedom in the donor and acceptor must rearrange to some configuration intermediate between the reactants and the products. This reorganization process assures that energy is conserved in the transition state by equalizing the energy levels of the transferring electron on the donor and acceptor. Once a transition state configuration has been achieved, the system must overcome an electronic barrier to electron transfer imposed by the intervening medium between the donor and acceptor. If the medium between the redox partners is a good electron-transfer mediator, then the electronic barrier is small and electron transfer occurs with near unit efficiency. Conversely, if the intervening medium is an insulator, then electron transfer will be a less probable event. According to the classical, semiclassical, and quantum mechanical theories of electron transfer, k_{et} for a given reaction can be described by the three kinetic quantities seen in equation 1.1.

$$k_{et} = \nu\kappa(FC) \qquad \text{eq. 1.1}$$

Here, ν is the frequency of the vibrations that destroy the transition state, κ is an electronic transmission factor that expresses the probability of charge transfer in the transition state region, and FC is the Frank-Condon factor for electron transfer. These quantities represent the different barriers to electron transfer encountered by a

reactive redox system along its reaction coordinate. They have been treated using several different theoretical approaches.

The thermal barriers to electron transfer or Frank-Condon factors have been described using both classical and quantum mechanical models. Most notable amongst the classical models is the theory proposed by Marcus for the rate of outer-sphere electron-transfer reactions (equations 1.2 to 1.4).[8f,g,h]

$$k_{et} = \kappa A \sigma^2 \exp\left[-\frac{\Delta G^*}{RT}\right] \quad \text{eq. 1.2}$$

$$\Delta G^* = \frac{(\lambda + \Delta G^{o'})^2}{4\lambda} \quad \text{eq. 1.3}$$

$$\lambda = \lambda_i + \lambda_o \quad \text{eq. 1.4}$$

The total activation free energy in the Marcus model is a function of the reaction free energy ($\Delta G^{o'}$) and the intrinsic thermal barrier λ, which is the sum of a molecular (λ_i) and solvent related component (λ_o). λ_i is referred to as the *inner-sphere* reorganization energy and represents the energy required to rearrange the bond distances and angles of the reactants to their transition state configurations. The later quantity, λ_o, represents the energy required to reorganize the solvation environment of the reactants. Marcus derived specific expressions for these parameters by assuming that the molecular degrees of freedom could be modeled by classical harmonic oscillators and that the surrounding solvent was a dielectric continuum. One feature of the Marcus model that has stimulated considerable experimental interest concerns its predictions regarding the variation of k_{et} as a function of reaction exoergicity. Taking the natural log of equation 1.2 and plotting $RT\ln(k_{et})$ versus $\Delta G^{o'}$ reveals that the rate of electron transfer should increase as a function of driving force in what has been termed the *normal region* until $\Delta G^{o'}=\lambda$ and then decrease as a function of driving force into what

Marcus labeled the *inverted region* . In addition to the Marcus model, several quantum mechanical and semiclassical models for electron-transfer reactions have also been proposed. One of the more popular semiclassical relationships for k_{et} is has been developed by Jortner and Bixon (equations 1.5 and 1.6).[8i,j,k,l]

$$k_{et} = \left(\frac{\pi}{\hbar^2 \lambda_s k_b T}\right)^{1/2} |V|^2 \sum_{w=0}^{\infty} \left(e^{-S} S^w / w!\right) \exp\left\{\frac{(\lambda_s + \Delta G + w h\nu)^2}{4 \lambda_s k_b T}\right\} \quad \text{eq. 1.5}$$

$$S = \frac{\lambda_v}{h\nu} \quad \text{eq. 1.6}$$

In equations 1.5 and 1.6 the outer-sphere reorganization energy (λ_s) is treated classically using a dielectric continuum model. However, the higher frequency molecular vibrations of the donor and acceptor are treated quantum mechanically to allow for nuclear tunneling. This equation reduces to the Marcus relationships at high temperature and has been useful in describing electron-transfer reactions at low temperature and at high driving force where nuclear tunneling effects are most important. While electron transfer in the normal region is for the most part understood, reactions in the inverted region have remained largely unexplored. A lack of information regarding the mechanism of electron transfer at large reaction exoergicities is directly related to the fact that prior to 1984 little experimental evidence for inverted behavior had been observed.[9] Thus, high driving force reactions are of continued interest in electron-transfer research.[10]

The electronic transmission coefficient (κ) controls the rate of electron transfer in the transition state region. When multiplied by the nuclear frequency, ν, it represents the activationless reaction rate constant. This factor is determined by the electronic coupling between the two redox partners, the velocity of the reaction

coordinate through the transition state region, and the time scale for energy exchange between the reaction coordinate and other degrees of freedom.[11] As stated earlier, κ represents the probability that charge transfer will take place once the system has reached the transition state. When $\kappa=1$ charge transfer takes place with unit efficiency and the reaction is termed *adiabatic*. A $\kappa<1$ is associated with a less efficient *nonadiabatic* electron-transfer process. The reaction adiabaticity is directly related to the relative magnitudes of the electronic coupling between the redox partners and the kinetic energy of their nuclei near the top of the col (figure 1.1). If the kinetic energy of the reaction coordinate (k_BT) is less than the electronic interaction (Δ), then the system is confined to the lower energy surface and passes ballistically from reactants to products. In contrast, if $\Delta<k_BT$, then the system can make transitions to an excited state surface (i.e. follow the dashed line figure 1.1) and remain in an electronic state corresponding to the reactants. This makes electron transfer a less probable event and requires that the system make multiple crossings through the transition state region before forming products. Recent theories have indicated that the electronic coupling between two redox partners is an exponential function of their through space separation and is related to the structural and electronic properties of the intervening medium.[12] Understanding the molecular factors that govern the electronic interactions between donor and acceptor is an area of significant interest in experimental electron-transfer research and is currently being investigated in a number of synthetic[10a,g,13e-h] and biological redox systems.[10b, 13a-d,24d]

In addition to being sensitive to electronic coupling effects, κ is also a function of the rate of energy exchange between the reaction coordinate and *bath modes*.[14] Bath modes correspond to degrees of freedom that are not included in the reaction coordinate but are coupled to it. They essentially accept excess energy associated with the transition state and allow the products to relax to an equilibrium configuration. Energy exchange between the RC and bath has been explored in theoretical studies by associating

Figure 1.1: A schematic representation of an electron-transfer hypersurface near the transition state region. If electron transfer is adiabatic, the reactants are confined to the lower surface and pass ballistically through the transition state region. If the reaction is nonadiabatic, the system can be excited to higher energy surface in the transtion state region and retain an electronic configuration indicative of the reactants. * marks the position of the transiton state along the reaction coordinate. TS labels the transition state region, which is defined as that portion of phase space within k_BT of the transition state. LZ (Landau-Zener region) is that portion of phase space where the electronic coupling between the redox partners is strong. It includes an area within Δ of the transition state.

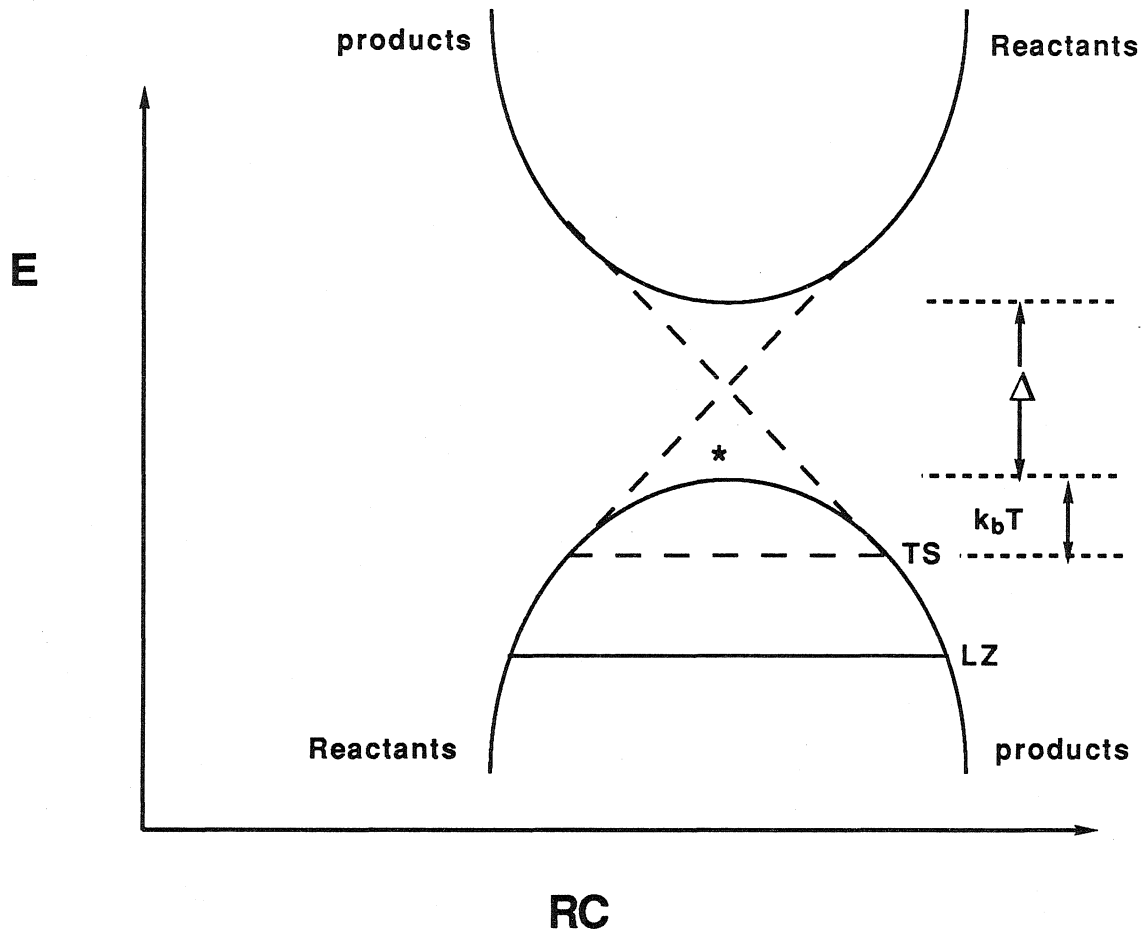
products
Reactants
E
*
k_bT
TS
LZ
Reactants
products
RC

a classical friction with motion of the system through the transition state region. Under conditions of low friction (i.e. slow energy exchange between the RC and bath modes) the system can not relax rapidly enough to an equilibrium "products configuration" and must make multiple crossings before being trapped in the products well. Such a situation is referred to as *underdamped*. Under conditions of high friction (i.e. rapid energy exchange between the RC and bath modes), the system moves through the transition state region by Brownian diffusion. In this *overdamped* situation the system also makes multiple crossings through the transition state region before forming products. Finally, when the reaction friction is optimal (i.e. *critically damped*) energy exchanges between the RC and bath on a time scale commensurate with the formation of products. Under these conditions, the reaction adiabaticity is controlled predominantly by electronic coupling. Behavior characteristic of an overdamped ET system has recently been observed by Kosower,[15] Simon,[16] and Eisenthal[17] in organic charge transfer systems dissolved in alcoholic solutions. In these studies the rate of electron transfer was shown to directly correlate with the longitudinal relaxation time of the solvent medium. A greater understanding of the role played by solvent dynamics in electron-transfer reactions will unfold as additional systems with ET rates greater than or equal to 10^{13} sec^{-1}become available.

d^8-d^8 Metal Dimers:The electronic structure and excited properties of d^8-d^8 transition metal complexes are areas of current interest in inorganic photochemistry.[18] Recent research has indicated that their low lying excited states display a variety of different chemical reactivities including the excited state oxidative addition of halocarbons,[19] carbon-hydrogen bond activation,[20] and outer-sphere electron transfer.[21] These diverse photochemical and photophysical properties can be traced to their ($d\sigma^*p\sigma$) excited states, which result from the axial metal-metal interactions inherent in these compounds. According to Gray and coworkers,[22] the electronic structure of these intriguing chromophores can be schematically represented by the

Figure 1.2: A simplified MO diagram for a d^8-d^8 metal dimer showing the ground state electronic configuration. The ($d\sigma^* \rightarrow p\sigma$) excited states can be accessed by exciting the complex with visible light as indicated by the white arrow.

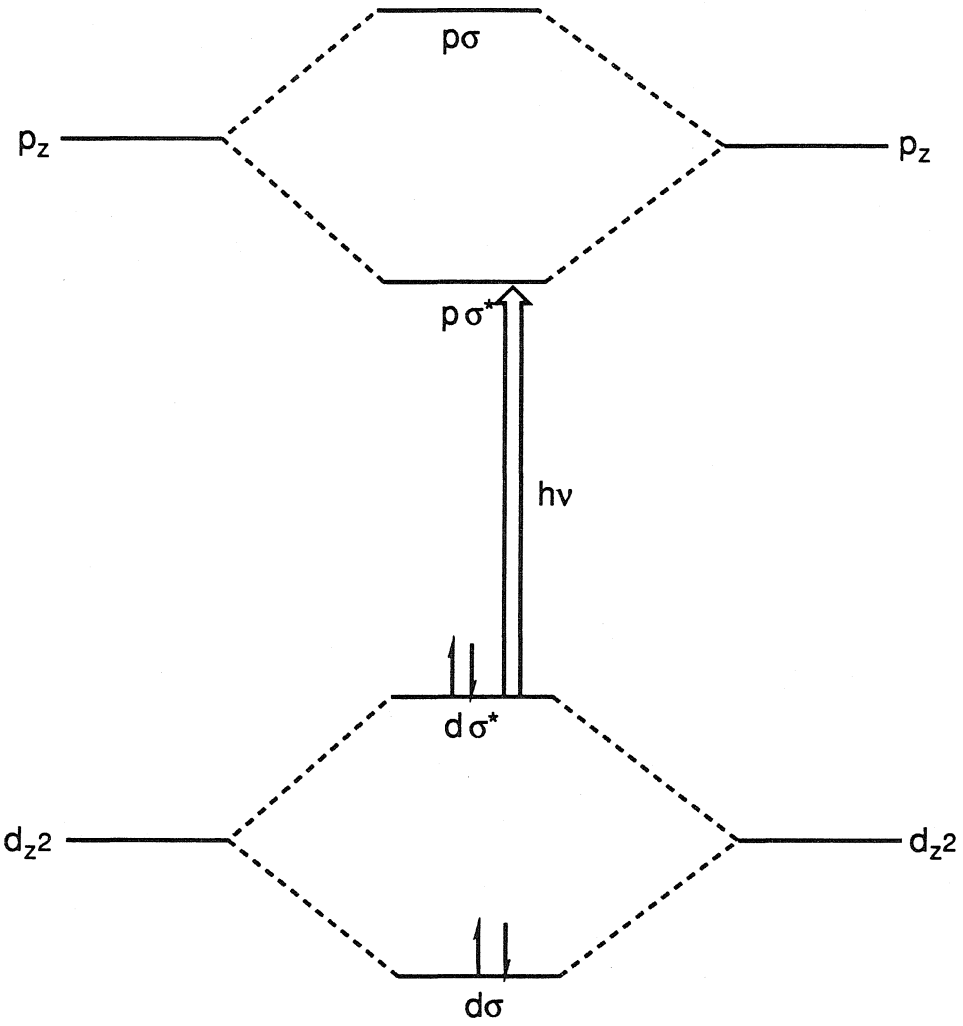
pσ
p_z
p_z
pσ*
hν
dσ*
d_{z2}
d_{z2}
dσ

molecular orbital diagram in figure 1.2. Covalently linking two square planar d^8 complexes into a dimer molecule forces an axial interaction between the d_z2 and p_z orbitals of the monomer fragments, which leads to the formation of $d\sigma$ and $p\sigma$ bonding and antibonding dimer MOs. Filling this MO scheme with the 16 metal electrons from the two monomer fragments leaves the $d\sigma^*$ level as the compound's highest occupied molecular orbital. The long lived excited states in these complexes are generated by exciting one $d\sigma^*$ electron into a vacant $p\sigma$ orbital. This electronic configuration yields a singlet and corresponding triplet state as the reactive excited states in these systems.

At the inception of this research, our studies regarding excited state electron transfer in d^8-d^8 compounds had centered around a series of iridium pyrazolate bridged COD complexes first prepared by Stobart and coworkers (figure 1.3).[23] Marshall *et al.* conducted a thorough examination of the driving force dependence of the bimolecular triplet electron-transfer quenching reactions in $[Ir_2(Pz)_2(COD)_2]$ using a homologous series of pyridinium electron acceptors.[21d,22i] Results from this study are summarized in figure 1.4. Several important conclusions were drawn from these findings: 1) In contrast to the predictions made by the Marcus model, the rate of triplet electron transfer in this photoredox system tends to a diffusion limit at high driving force. We, like others, speculated that our failure to observe inverted behavior in this study was tied to the limitations placed on rapid electron transfer reactions by diffusion. 2) Steady-state quenching experiments showed that the excited state electron-transfer reactivity in this complex was restricted to its triplet state. Because, the singlet state in this compound lies approximately 4000 cm^{-1} above its triplet state, in it principle should be a powerful reductant. This lack of reactivity was presumed to be due to the subnanosecond fluorescence lifetime in $[Ir_2(Pz)_2(COD)_2]$. These key observations suggested that our understanding of electron-transfer reactions involving d^8-d^8 A-frame compounds could potentially be extended by designing a redox system which eliminated bimolecular diffusion as a rate limiting kinetic process.

Figure 1.3: The iridium dimer complex used by Marshall *et al.* in their bimolecular quenching studies. This complex possesses terminal chelating COD ligands.

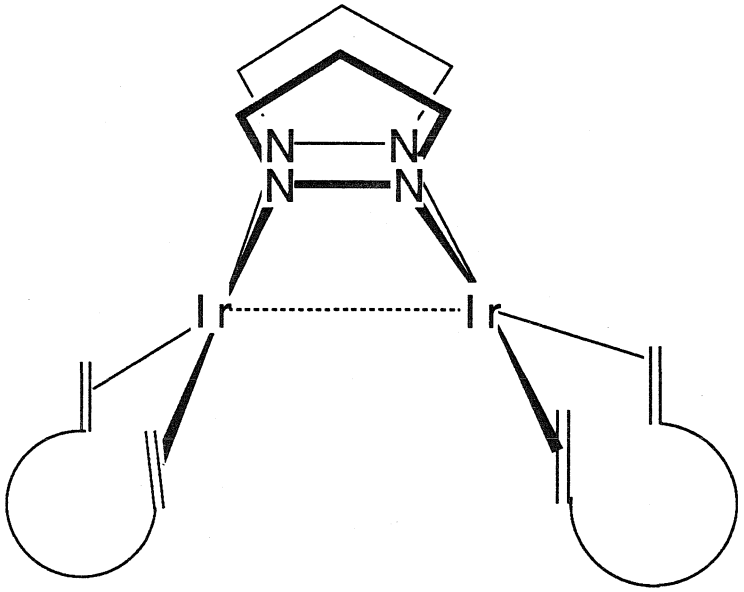
N
N
N
N
Ir
Ir

Figure 1.4: The driving force dependence data of Marshall et al. adapted from reference 22i.

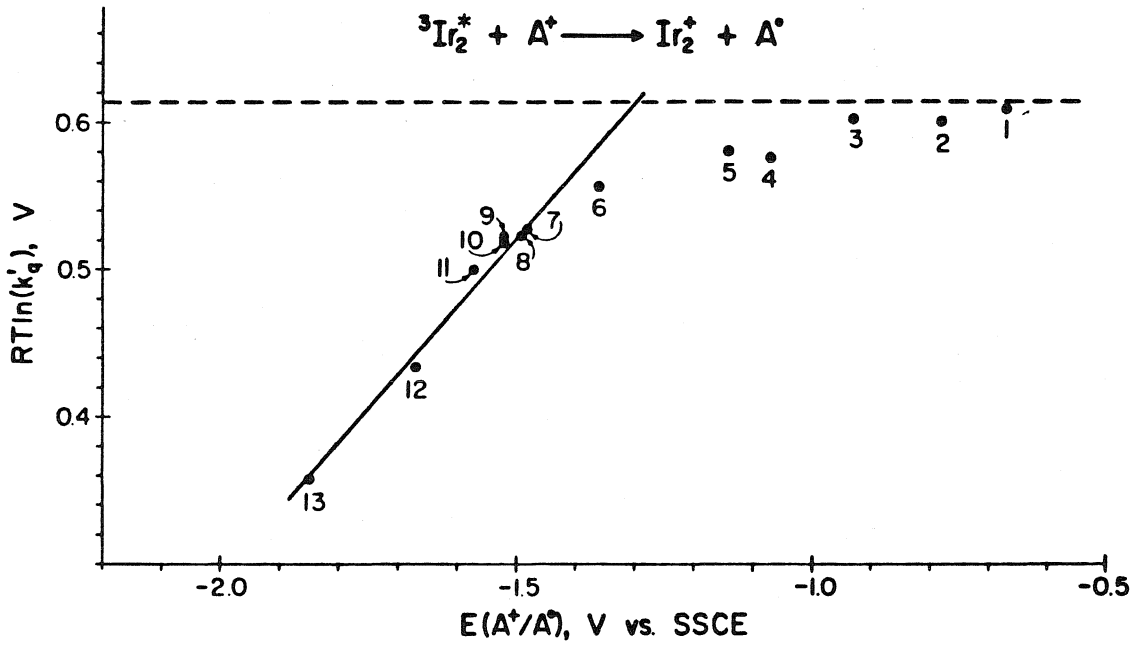
$^3Ir_2^* + A^+ \longrightarrow Ir_2^+ + A^\circ$
0.6
0.5
0.4
RTln(k_q'), V
1
2
3
4
5
6
7
8
9
10
11
12
13
-2.0
-1.5
-1.0
-0.5
E(A^+/A°), V vs. SSCE

In this study we remove the constraints place on excited state electron-transfer reactions due to diffusion, by covalently linking an iridium dimer chromophore (donor) and a pyridinium cation (acceptor) into a single molecular unit. An analogous approach has been recently demonstrated in a number of synthetic[10a,c,13e-h,24a-c] and biological redox systems.[10b,13a-d,24d] Our particular strategy employs a series of redox-active phosphinite ligands. We feel this approach has potential generality, because phosphine ligands are found in a wide variety of inorganic and organometallic compounds. In principle our ligands could be used to prepare and study a number of different inorganic photoredox compounds. Our objectives in this study are; 1) to further characterize the driving force dependence of electron transfer reactions in d^8-d^8 A-frame complexes and look for evidence of inverted behavior, 2) to explore the possibility of observing singlet quenching reactions that might readily occur in an intramolecular electron-transfer complex, and 3) to determine what differences, if any, exist between the factors that govern the triplet, singlet and charge recombination ET processes in these compounds. Evidence for singlet electron-transfer quenching would be of significant interest, because at present the excited state reactivity of d^8-d^8 metal dimers has been exclusively attributed to their long lived triplet states. Our research regarding these issues is organized as follows. Chapter 2 outlines the preparation and characterization of our d^8-d^8 donor-acceptor complexes. Careful consideration is given to their structural properties determined by NMR spectroscopy and from a crystal structure of $[Ir_2(Pz^*)_2(CO)_2(Ph_2POCH_2CH_2\text{-}Py^+)_2](Ph_4B)_2$. Chapter 3 summarizes our results concerning the spectroscopic and electrochemical properties of the complexes. These data are used to construct an approximate state diagram for their metal localized and charge-transfer excited states. Finally, in chapter 4, rate constants for their photoinduced electron-transfer and charge recombination reactions are measured using nanosecond and picosecond laser spectroscopy.

These data are analyzed with regard to the photophysical properties of the compounds and the driving force dependence of k_{et}.

References

1a. Budil, D. E.; Gast, P.; Chang, C.-H.; Schriffer, M.; Norris, J. R., *Ann. Rev. Phys. Chem.*, **1987**, *38*, 561-583.

b. Boxer, S. G., *Biochim. Biophys. Acta*, **1983**, *726*, 265-292.

c. Deisenhofer, J.; Epp, O.; Miki, K.; Huber, M. R., *Mol. Biol.*, **1984**, *180*, 385-398.

2. Hatefi, Y., *Ann. Rev. Phys. Chem.*, **1985**, *54*, 1015-1069.

3a. Gunner, M. R.; Robertson, D. E.; Dutton, P. L., *J. Phys. Chem.*, **1986**, *90*, 3783-3795.

b. Ogrodnik, A.; Remy-Richter, N.; Michel-Beyerele, M. E.; Feick, R., *Chem. Phys. Lett.*, **1987**, *135*, 576-581.

4. Mikkelsen, K. V.; Ratner, M. A., *Chem. Rev.*, **1987**, *87*, 113-153.

5a. Hansma, P. K.; Tersof, J., *J. Appl. Phys.*, **1987**, *61*, R1-R23.

b. Hansma, P. K.; Elings, V. B.; Marti, C. E.; Bracker, C. E., *Science*, **1988**, *242*, 209-216.

6. James, T. H., *"Theory of the Photographic Process"*, **1977**, Macmillan Publishing Co., New York.

7a. *C&E News*, **1988**,*66*, 30.

b. *C&E News*, **1988**,*66*, 15.

8a. Marcus, R. A.; Sutin, N., *Biochim. Biophys. Acta*, **1985**, *811*, 265-322.

b. Newton, M. D.; Sutin, N., *Ann. Rev. Phys. Chem.*, **1984**, *35*, 437-480.

c. Sutin, N., *Prog. Inorg. Chem.*, **1984**, *30*, 441-498.

d. Jortner, J., *Biochim. Biophys. Acta*, **1980**, *594*, 193-230.

e. Sutin, N., *Acc. Chem. Res.*, **1982**, *15*, 275-282.

f. Marcus, R. A., *J. Chem. Phys.*, **1956**, *24*, 966-978.

g. Marcus, R. A., *J. Chem. Phys.*, **1957**, *26*, 867-871.

h. Marcus, R. A., *J. Chem. Phys.*, **1957**, *26*, 872-877.

i. Kestner, N. R.; Logan, J.; Jortner, J., *J. Phys. Chem.*, **1984**, *78*, 2148-2166.

j. Jortner, J., *J. Chem. Phys.*, **1976**, *64*, 4860-4867.

k. Efrima, S.; Bixon, M., *Chem. Phys.*, **1976**, *13*, 447-460.

l. Van Duyne, R. P.; Fischer, S. F. M., *Chem. Phys.*, **1974**, *5*, 183-197.

m. Jotrner, J., *J. Amer. Chem. Soc.*, **1980**, *102*, 6676-6686.

n. Siders, P.; Marcus, R. A., *J. Amer. Chem. Soc.*, **1981**, *103*, 748-752.

9. Miller, J. R.; Beitz, J. V.; Huddleston, R. K., *J. Amer. Chem. Soc.*, **1984**, *106*, 5057-5068.

10a. Closs, G. L.; Miller, J. R., *Science*, **1988**, *240*, 440-447.

b. McLendon, G., *Acc. Chem. Res.*, **1988**, *21*, 160-167.

c. Wasieleski, M. R.; Niemczyk, M. R.; Svec, W. A.; Pewitt, E. B., *J. Amer. Chem. Soc.*, **1985**, *107*, 1080-1082.

d. Ohno, T.; Yoshimura, A.; Shioyama, H.; Mataga, N., *J. Phys. Chem.*, **1987**, *91*, 4365-4370.

e. Ohno, T.; Yoshimura, A.; Mataga, N., *J. Phys. Chem.*, **1986**, *90*, 3295-3297.

f. Gould, I. R.; Ege, D.; Mattes, S. L; Farid, S., *J. Amer. Chem. Soc.*, **1987**, *89*, 3675-3679.

g. Meade, T. J.; Gray, H. B.; Winkler, J. R., *manuscript in preparation.*

h. Elias, H.; Chou, M. H.; Winkler, J. R., *J. Amer. Chem. Soc.*, **1988**, *110*, P.

11. Frauenfelder, H.; Wolynes, P. G., *Science*, **1985**, *229*, 337-345.

12a. Beratan, D. N.; Onuchic, J. N.; Hopfield, J. J., *J. Chem. Phys.*, **1987**, *86*, 4488-4498.

b. Onuchic, J. N.; Beratan, D. N., *J. Amer. Chem. Soc.*, **1987**, *109*, 6771-6778.

c. Beratan, D. N.; Hopfield, J. J., *J. Amer. Chem. Soc.*, **1984**, *106*, 1584-1594.

13a. Lieber, C. M.; Karas, J. L.; Mayo, S. L.; Axup, A. W.; Albin, M.; Crutchley, R. J.; Ellis, W. R.; Gray, H. B., *"Trace Elements in Man and Animals"* , Plenum, New York, **1987.**

b. Crutchley, R. J.; Ellis, W. R.; Gray, H. B., *"Frontiers in Bioinorganic Chemistry"* ; VCH Verlagsgesellschaft: Weinheim, FRG, **1986,** 679-693.

c. Gray, H. B., *Chem. Soc. Rev.*, **1986**, *15*, 17-30.

d. Mayo, S. L.; Ellis, W. R.; Crutchley, R. J.; Gray, H. B., *Science*, **1986**, *233*, 948-952.

e. Verhoven. J. W., *Pure & Appl. Chem.*, **1986**, *58*, 1285-1290.

f. Oevering, H.; Paddon-Row, M. N.; Heppener, M.; Oliver, A. M.; Cotsaris, E.; Verhoven, J. W.; Hush, N. S., *J. Amer. Chem. Soc.*, **1987**, *109*, 3258-3269.

g. Oliver, A. M.; Craig, D. C.; Paddon-Row, M. N.; Kroon, J.; Verhoven, J. W., *Chem. Phys. Lett.*, **1988**, *150*, 366-373.

h. Leland, B. A.; Joran, A. D.; Felker, P. M.; Hofield, J. J.; Zewail, A. H.; Dervan, P. B., *J. Phys. Chem.*, **1985**, *89*, 5571-5573.

14a. Garg, A.; Onuchic, J. N.; Ambegaokar, V., *J. Chem. Phys.*, **1985**, *83*, 4491-4503.

b. Onuchic, J. N., *J. Chem. Phys.*, **1987**, *86*, 3925-3943.

15a. Kosower, E. M., *Acc. Chem. Res.*, **1982**, *15*, 259-266.

b. Kosower, E. M.; Huppert, D., *Chem. Phys. Lett.*, **1983**, *96*, 433-435.

16a. Su, S.-G.; Simon, J. D., *J. Phys. Chem.*, **1987**, *91*, 2693-2696.

b. Su, S.-G.; Simon, J. D., *J. Phys. Chem.*, **1986**, *90*, 6475-6479.

c. Su, S.-G.; Simon, J. D., *Chem. Phys. Lett.*, **1986**, *132*, 345-350.

17a. Crawford, M. K.; Wang, Y.; Eisenthal, K. B., *Chem. Phys. Lett.*, **1981**, *79*, 529-533.

b. Wang, Y.; Eisenthal, K. B., *J. Chem. Phys.* , **1982**, *77*, 6076-6082.

18a. Zipp, A. P., *Coord. Chem. Rev.*, **1988**, *84*, 47-83.

b. Marshall, J, L.; Stiegman, A. E.; Gray, H. B., *ACS Symp. Ser.*, **1986**, *307*, 166-176.

c. Roundhill, D. M., *J. Amer. Chem. Soc.*, **1985**, *107*, 4354-4356.

d. Che, C.-M.; Lee, W.-M., *J. Chem. Soc. Chem. Comm.*, **1986**, 512-513.

e. Alexander, K. A.; Stein, P.; Hedden, D. B.; Roundhill, D. M., *Polyhedron*, **1983**, 1389-1392.

f. Roundhill, D. M.; Atherton, S. F., *submitted for publication.*

g. Roundhill, D. M.; Atherton, S. J.; Shen, Z.-P, *J. Amer. Chem. Soc.*, **1987**, *109*, 6076-6079.

19. Caspar, J. V.; Gray, H. B., *J. Amer. Chem. Soc.*, **1984**, *106*, 3029-3030.

20a. Vlcek, A.; Gray, H. B, *Inorg. Chem..*, **1987**, *26*, 1997-2001.

b. Harvey. E. L.; Stiegman, A. E.; Vlcek, A.; Gray, H. B., *J. Amer. Chem. Soc.*, **1987**, *109*, 5233-5235.

c. Vlcek, A.; Gray, H. B., *J. Amer. Chem. Soc.*, **1987**, *109*, 286-287.

d. Harvey, P. D.; Gray, H. B, *Nouv. J. Chem.*, **1987**, *11*, 595-596.

21a. Che, C.-M.; Butler, L. G.; Gray, H. B., *J. Amer. Chem. Soc.*, **1981**, *103*, 7796-7797.

b. Che, C.-M., Cho, K.-C.; Chan, W.-S.; Gray, H. B., *Inorg. Chem..*, **1986**, *25*, 4906-4909.

c. Milder, S. J.; Goldbeck, R. A.; Kliger, D. S.; Gray. H. B., *J. Amer. Chem. Soc.*, **1980**, *102*, 6761-6764.

d. Marshall, J, L.; Stobart, S. R.; Gray, H. B., *J. Amer. Chem. Soc.*, **1984**, *106*, 3027-3029.

22a. Rice, S. F., Ph.D. Dissertation, California Institute of Technology, Pasadena, CA, 1982.

b. Rice, S. F.; Miskowski, V. M.; Gray, H. B., *Inorg. Chem..*, **1988**, *manuscript in press.*

c. Rice, S. F.; Gray, H. B., *J. Amer. Chem. Soc.*, **1981**, *103*, 1593-1595.

d. Rice, S. F.; Gray, H. B., *J. Amer. Chem. Soc.*, **1983**, *105*, 4571-4575.

e. Mann, K. R.; Thich, J. A.; Bell, R. A.; Coyle, C. A.; Gray, H. B., *Inorg. Chem..*, **1980**, *19*, 2462-2468.

f. Stiegman, A. E.; Rice, S. F.; Gray, H,. B.; Miskowski, V. M., *Inorg. Chem.*, **1987**, *109*, 1112-1116.

g. Mann, K. R.; Gordon, J. G.; Gray, H. B., *J. Amer. Chem. Soc.*, **97**, *1975*, 3553-3555.

h. Smith, T. P., Ph.D. Dissertation, California Institute of Technology, Pasadena, CA, 1982.

i. Marshall, J. L., Ph.D. Dissertation, California Institute of Technology, Pasadena, CA, 1987.

23. Beveridge, K. A.; Bushnell, G. W.; Dixon, K, R.; Eadie, D. T.; Stobart, S. R., *J. Amer. Chem. Soc.*, **1982**, *104*, 920-922.

24a. Westmoreland, T. D.; Le Bozec, H.; Murray, R. W.; Meyer, T. J., *J. Amer. Chem. Soc.*, **1983**, *105*, 5952-5954.

b. Chen, P.; Westmoreland, T. D.; Danielson, E.; Schanze, K. S.; Anthon, D.; Neveux. P. E.; Meyer, T. J., *Inorg. Chem.*, **1987**, *26*, 1116-1126.

c. Danielson, E.; Elliot, C. M.; Merkert, J. E.; Meyer, T. J., *J. Amer. Chem. Soc.*, **1987**, *109*, 2519-2520.

d. Heitele, H.; Michek-Beyerle, M. E.; Finckh, P., *Chem. Phys. Lett.*, **1987**, *134*, 273-278.

e. Peterson-Kennedy, S. E.; McGourty, J. L.; Ho, P. S.; Sutaris, C. J.; Learig, N.; Zernel, H.; Blough, N. V.; Margoliash, E.; Hoffman, B. M., *Coord. Chem. Rev.*, **1985**, *64*, 125-133.

25a. Boyd, D. C.; Rodman, G. S.; Mann, K. R., *J. Amer. Chem. Soc.*, **1986**, *108*, 1779-1784.

b. Smith, D. C.; Gray, H. B., *manuscript in preparation.*

Chapter 2

Synthesis and Structure

Introduction

The basic components of an intramolecular electron-transfer system are an electron donor, an electron acceptor, and a bridging group, which covalently links the two redox partners into a single molecular unit. Each component plays a crucial role in determining the rate of photoinduced and thermal electron transfer in such a system by controlling fundamental electron-transfer parameters such as reaction free energy; donor-acceptor separation, orientation, and electronic coupling; and inner-sphere reorganization energies.[1] By varying the chemical and physical properties of these three elements, information concerning the factors that control electron-transfer reactions can be obtained. For example, the driving force dependence of k_{ET} has been traditionally investigated by systematically varying the redox energy of a structurally homologous series of electron acceptors.[2] This type of study provides valuable information concerning the reorganization energy controlling the charge-transfer process and probes the system for the inverted behavior predicted by current theoretical models.[1a] Bridging groups can play a number of roles in intramolecular ET systems. In addition to holding the two redox partners at a well-defined separation and orientation, they can also act as a "conducting medium" for transmitting an electron between the donor and acceptor.[3] This type of through-bond mechanism may be important in the long range electron-transfer reactions seen in metalloproteins[4] and is an area of intense interest. These considerations suggest that a successful donor-acceptor system is one that can be systematically modified so that k_{ET} can be studied as a function of different donor, acceptor, and bridging group properites. Thus, our goal has been to develop synthetic routes that are flexible enough to allow for these types of

Figure 2.1: Structure of the iridium d^8-d^8 donor-acceptor complexes.

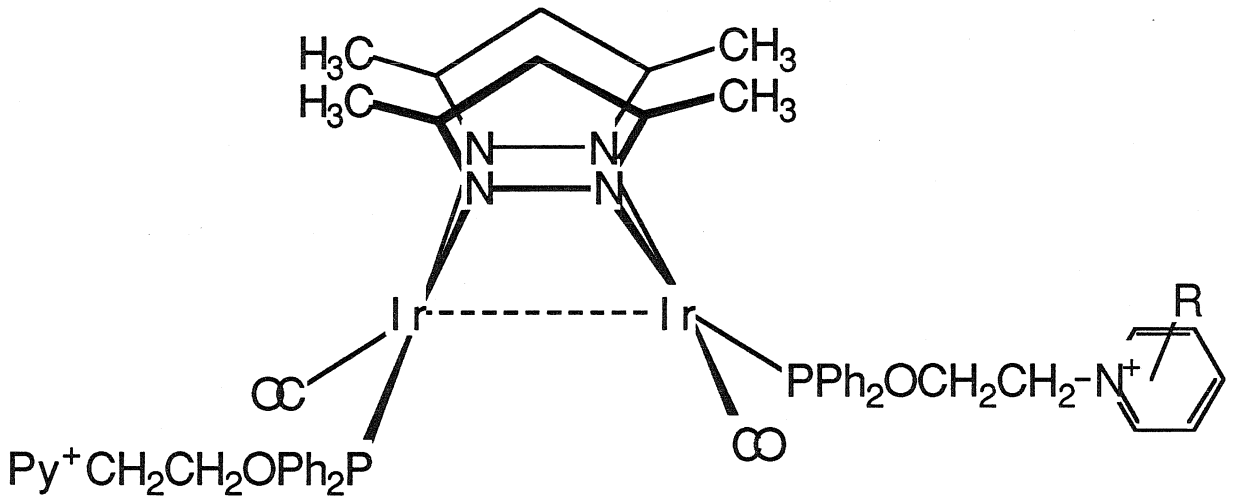
H3C
CH3
H3C
CH3
N
N
N
N
Ir
Ir
CO
CO
PPh2OCH2CH2-N+
R
Py+CH2CH2OPh2P

systematic modifications.

This chapter details the preparation and characterization of the series of donor-acceptor molecules schematically represented in figure 2.1. These compounds are similar to the d^8-d^8 compounds used in a previous bimolecular electron-transfer study in that they are based on an Ir(I) A-frame metal dimer chromophore.[5] The reaction driving force for excited state electron transfer in these systems can be controlled by varying the aromatic substituents on their pyridinium electron acceptors. These acceptors are covalently attached to the terminal phosphinite ligands in the complexes via a three atom hydrocarbon spacer. Because the distance dependence of an electron-transfer reaction is difficult to predict *apriori* , compounds with short simplistic spacers represent the best starting point for initiating studies surrounding a new intramolecular redox system. The short donor-acceptor separations imposed by this bridging group should insure that electron transfer will occur during the lifetime of the iridium dimer's electronic excited states.[6]

In the results section of this chapter a detailed account of the preparation of these compounds is given. The complexes have been characterized by high field proton and phosphorous NMR spectroscopy, IR spectroscopy, and x-ray diffraction crystallography. Results from these studies are subsequently discussed in terms of the synthetic routes reported here, the structural properties of the molecules, and the possible solution dynamics of the bridging group.

Experimental

Materials

Solvents

All solvents used in the preparation of the phosphinite redox ligands and iridium dimer complexes were of reagent grade quality or better. Acetonitrile was dried over Linde 4Å sieves, vacuum transferred to a Schlenk storage flask, and blanketed with dry nitrogen. Tetrahydrofuran and diethyl ether were distilled from sodium/benzophenone. Methylene chloride was distilled from CaH_2 and acetone was distilled from activated alumina. Toluene and ethanol were spectral grade in quality and used as received. THF, ethanol, diethyl ether, methylene chloride, and acetone were degassed by evacuation at 80° C for one hour and then stored under a nitrogen atmosphere. Benzene-d6, acetone-d6, DMSO-d6 and acetonitrile-d3 were purchased from MSD Isotopes and used without further purification.

Ligands

Chlorodiphenylphosphine, diphenylethoxyphosphine, diphenylmethoxyphosphine, and butoxydiphenylphosphine were purchased from Strem Chemical Company and used as received. Pyridine, 4-methylpyridine, 4-phenylpyridine, and triethylamine were purchased from Aldrich Chemical Company and were used without further purification. 2-Bromoethanol, also purchased from Aldrich, was vacuum distilled prior to use to remove polymeric impurities. Dimethylamine was purchased in 2 lb lecture bottles from Matheson Company and used as received. 3-isobutyl acetylacetone was obtained from Pfaltz and Bauer Chemical Company and used without further purification.

3,5-dimethyl-4-isobutylpyrazole was prepared using a published procedure for the preparation of 3,5-dimethylpyrazole.[7]

Metal Complexes

Iridium trichloride trihydrate was purchased from Johnson Matthey (AESAR). 3,5-Dimethylpyrazole and 1,5-cyclooctadiene were purchased from Aldrich Chemical Company. Carbon monoxide was obtained from Matheson Company. Each was used as received.

Synthetic Procedures

General Procedures

All manipulations involving both the phosphinite ligands and iridium dimer complexes were conducted under a nitrogen atmosphere using standard Schlenk techniques or in a Vacuum Atmospheres Co. dry box. ^{1}H and ^{31}P NMR spectra were recorded on either a Jeol FX-90-Q or a Jeol GX-400 fourier transform spectrometer. IR spectra were recorded as fluorolube mulls on a Beckman Instruments IR-4240 Spectrometer.

Phosphinite Redox Ligands

Preparation of $(C_6H_6)_2P\text{-}N(CH_3)_2$: N,N-dimethyl-P,P-diphenylphosphine was synthesized using a procedure similar to that reported for related compounds.[8] 300 mls of dry deoxygenated diethyl ether was placed in a 1000 ml round bottom Schlenk flask and charged with 10g (45 mmoles) of chlorodiphenylphosphine. The reaction mixture was cooled to 0° C and dimethylamine was slowly bubbled through cold ethereal solution. Almost immediately, dimethylamine hydrochloride began to form as a flocculent white

precipitate. The reaction mixture was stirred and dimethylamine was added until hydrochloride salt formation ceased. The resulting suspension was stirred for an additional hour to ensure that all of the starting materials had been consumed. Dimethylamine hydrochloride was separated by cannula filtration and washed with two 100 ml portions of ether. The washings and filtrate were transferred to a second 1000 ml Schlenk flask and rinsed with three 50 ml portions of deoxygenated distilled water to remove any residual hydrochloride salt, which was complexed to the phosphine product. The ether solution was dried first over anhydrous Li_2CO_3 for 15 minutes and subsequently stirred over CaH_2 for 24 hours. CaH_2 was separated by filtration through a fine porosity glass frit. The filtrate was concentrated to one-tenth of its original volume and transferred to a 100 ml round bottom flask fitted with a short path distillation head[9]. The residual ether was removed in vacuo leaving a white waxy residue. This crude product was purified by vacuum distillation producing a clear viscous liquid which solidified upon cooling (b.p. 76-85 °C/0.04 mm Hg). The product was characterized by ^{31}P and ^{1}H NMR spectroscopy. ^{1}H: 2.5(d; NCH_3) and 7.3(m; $(C_6H_6)_2P$); ^{31}P: 64.0 ppm (versus ext. H_3PO_4).

Preparation of 1-(2-hydroxyethyl)pyridinium and (2-hydroxyethyl)triethylammonium Salts: With the exception of 1-(2-hydroxyethyl)-2,4,6-trimethylpyridinium tetraphenylborate, all other pyridinium salts were synthesized using a procedure analogous to that reported earlier for preparing 1-alkylpyridinium compounds[6]. 1-(2-hydroxyethyl)-2,4,6-trimethylpyridinium tetraphenylborate was prepared from 2-aminoethanol and 2,4,6-trimethylpyrylium tosylate by the method of Balaban *et al.*[10] Each compound was characterized by ^{1}H NMR spectroscopy and their spectra were compared to those reported in the literature.[11]

Preparation of [$Ph_2POCH_2CH_2$-R](Ph_4B): The general methodology outlined below was used in the preparation of all the phosphinite redox ligands, except where noted. In all cases a slight excess of N,N-dimethyl-P,P-diphenylphosphine was used to ensure complete consumption of the hydroxyethylpyridinium starting material. 2.0g (9.0 mmoles) of N,N-dimethyl-P,P-diphenylphosphine and 8.0 mmoles of a 1-(2-hydroxyethyl)pyridinium salt were dissolved in approximately 150 mls of oxygen free acetonitrile. 0.1g of benzoic acid was added and the reaction mixture was stirred for four hours at room temperature under an inert atmosphere. The solvent was removed in vacuo leaving an oily residue, which was rinsed with three 20 ml portions of either diethyl ether or toluene until it began to solidify into a crude powder. With the exception of ($Ph_2POCH_2CH_2$-4Ph-Py)(Ph_4B), the product was purified by recrystallization from acetonitrile/toluene solutions. All of phosphinite ligands were characterized by elemental analysis, and ^1H NMR and ^{31}P spectroscopy. The NMR spectra are summarized in table 2.3a.

($Ph_2POCH_2CH_2$-NEt_3)(Ph_4B): Anal. Calcd. for $C_{44}H_{49}NOBP$: C,81.4; H,7.6; N,2.2. Found: C,80.8; H,7.7; N,2.5.

($Ph_2POCH_2CH_2$-Py)(Ph_4B): Anal. Calcd. for $C_{43}H_{39}NOBP$: C,82.3; H,6.3;N,2.2. Found: C,82.7; H,6.5; N,2.4.

($Ph_2POCH_2CH_2$-4Me-Py)(Ph_4B): Anal. Calcd. for $C_{44}H_{41}NOBP$: C,82.4; H,6.3;N,2.2. Found: C,82.2; H,6.4; N,2.4.

($Ph_2POCH_2CH_2$-2,4,6Me_3-Py)(Ph_4B): Anal. Calcd. for $C_{46}H_{45}NOBP$: C,82.6; H,6.7;N,2.1. Found: C,82.3; H,6.7; N,2.1.

($Ph_2POCH_2CH_2$-NEt_3)(PF_6): Anal. Calcd. for $C_{20}H_{29}NOF_6P$: C,49.5; H,5.97; N,2.88. Found: C,50.1; H,6.2; N,3.1.

Preparation of ($Ph_2POCH_2CH_2$-4Ph-Py)(Ph_4B): Because this compound had greater propensity to form oils in acetonitrile/toluene solutions, the crude product was

rinsed with three 50 ml portions of ethanol containing 0.5 mls of dichloromethane. This procedure yielded a crude powder, which was purified by recrystallization from acetone/diethyl ether solutions.

($Ph_2POCH_2CH_2$-4Ph-Py)(Ph_4B): Anal. Calcd. for $C_{49}H_{33}BNOP$: C,83.8; H,6.1;N,2.0. Found: C, 83.8; H, 6.1; N, 1.9.

Inorganic Complexes

Starting Materials: Di-μ-chloro-bis(1,5-cyclooctadiene)diiridium(I), bis(1,5-cyclooctadiene)bis(μ-3,5–dimethylpyrazole)diiridium(I), tetracarbonylbis(μ-3,5-dimethylpyrazole)diiridium(I), bis(1,5-cyclooctadiene)bis(μ-3,5-dimethyl-4-isobutylpyrazole)diiridium(I), and tetracarbonylbis(μ-3,5-dimethyl-4-isobutylpyrazole)diiridium(I) were prepared according to previously established procedures.[12,6] The bis μ-3,5-dimethyl-4-isobutyl pyrazolate bridge complexes had not been previously reported and were characterized by elemental analysis and ^1H NMR spectroscopy.

Bis(1,5-cyclooctadiene)bis(μ-3,5-dimethyl-4-isobutylpyrazole)diiridium(I): Anal. Calcd. for $C_{26}H_{38}N_4Ir_2$: C,44.93; H,6.60; N,6.16. Found: C,44.97; H,5.98; N,6.15. ^1H NMR (d6-Benzene): δ = 2.6 (m; COD), δ = 4.0 (m; COD), δ = 4.4 (m, COD), δ =1.85 (m; COD), δ = 0.8 (d; isobutyl CH_3), δ =1.5 (septet; isobutyl -CH), δ = 2.4 (s; pyrazole CH_3), δ =1.9 (d; isobutyl CH_2).

Tetracarbonylbis(μ-3,5-dimethyl-4-isobutylpyrazole)diiridium(I): Anal. Calcd. for $C_9H_{14}N_4O_4Ir_2$: C,33.07; H,3.78; N,7.01. Found: C,33.09; H,3.79; N,7.01. ^1H NMR (d6-Benzene): δ = 2.2 (s; pyrazole CH_3), δ =1.9 (d; isobutyl CH_2), δ =1.45 (septet; isobutyl -CH), δ = 0.7 (d; isobutyl CH_3).

Preparation of the $[Ir_2(Pz^*)_2(CO)_2(Ph_2POCH_2CH_2R)_2](Ph_4B)_2$ and $[Ir_2(Pz^{**})_2(CO)_2(Ph_2POCH_2CH_2R)_2](Ph_4B)_2$ Complexes: The same

general procedure outlined for preparing $[Ir_2(Pz^*)_2(CO)_2(Ph_2POCH_2CH_2\text{-}Py)_2](Ph_4B)_2$ was used in the synthesis of all the iridium dimer complexes, except where noted. Each of the compounds was characterized by elemental analysis, ^1H NMR and ^{31}P NMR spectroscopy. Their proton and ^{31}P NMR spectra are summarized in table 2.3b.

$[Ir_2(Pz^*)_2(CO)_2(Ph_2POCH_2CH_2\text{-}Py)_2](Ph_4B)_2$(1): 0.1g (0.14mmoles) of $Ir_2(Pz^*)_2(CO)_4$ was placed in a 250 round bottom Schlenk flask and dissolved in 150 mls of dry THF. A THF (ca. 50 mls) solution containing 0.30 mmoles of $(Ph_2POCH_2CH_2\text{-}Py)(Ph_4B)$ was added to the reaction mixture dropwise over the course of approximately 2 to 3 minutes. With each addition of phosphinite ligand, carbon monoxide gas was liberated from the solution. The reaction mixture was stirred for four hours under a nitrogen atmosphere to ensure that all of the reactants had been consumed. During this time period the solution changed color from orange to red/orange. THF was removed in vacuo leaving an orange/red residue, which was taken up in 10 mls of acetonitrile. The solution was chilled to 0° C and toluene was slowly added until the product began to crystallize. $[Ir_2(Pz^*)_2(CO)_2(Ph_2POCH_2CH_2\text{-}Py)_2](Ph_4B)_2$ was isolated by cannula filtration as a bright red solid. Anal. Calcd. for $C_{98}H_{92}B_2N_6O_4P_2Ir_2$: C,62.41; H,4.91; N,4.45. Found: C,62.26; H,5.05; N,4.53.

[Ir2(Pz*)2(CO)2(Ph2POCH2CH2-4Me-Py)2](Ph4B)2(2):
0.1g (0.14mmoles) of $Ir_2(Pz^*)_2(CO)_4$ was placed in a 250 ml round bottom Schlenk flask and dissolved in 150 mls of THF. 50 mls of THF containing 0.3 mmoles of $(Ph_2POCH_2CH_2\text{-}4Me\text{-}Py)(Ph_4B)$ was added over a period of 2 to 3 minutes. The reaction mixture was sealed under a nitrogen atmosphere and allowed to stand undisturbed for 48 hours during which time the product formed as bright red crystals. The product was separated by cannula filtration and washed with three 20 ml portions of

THF. Anal. Calcd. for $C_{100}H_{96}B_2N_6O_4P_2Ir_2$: C,63.40; H,5.32; N,4.26. Found: C,63.63; H,5.37; N,4.30.

$Ir_2(Pz^*)_2(CO)_2(Ph_2POCH_2CH_3)_2$(3): 0.1g(0.14mmoles) of $Ir_2(Pz^*)_2(CO)_4$ was placed in a 250 round bottom Schlenk flask and dissolved in 150 mls of THF. 0.1 ml (0.7 mmoles) of $Ph_2POCH_2CH_3$ was added via a gas tight syringe. An immediate liberation of carbon monoxide gas was observed followed by a change in solution color from orange to orange/red. The reaction mixture was stirred for four hours to ensure complete consumption of the starting materials. THF was removed in vacuo leaving an orange/red residue, which was taken up in 20 mls of 2:1 ethanol/dichloromethane. Slow evaporation of this solution under a steady stream of nitrogen afforded the product as bright orange crystals. Anal. Calcd. for $C_{40}H_{44}N_4O_2P_2Ir_2$: C,44.04; H,4.03; N,5.13. Found: C,43.74; H,4.08; N,5.06.

$[Ir_2(Pz^*)_2(CO)_2(Ph_2POCH_2CH_2\text{-}NEt_3)_2](PF_6)_2$(4): This complex was prepared using the same procedure as that outlined for complex 1 except that a slightly different isolation procedure was employed. After the solvent was removed from the reaction mixture, the orange/red residue was rinsed with three 20 ml portions of ethanol containing 0.1 ml of dichloromethane. This produced a crude solid, which was purified by soxholet extraction into dichloromethane. Anal. Calcd. for $C_{52}H_{72}F_{12}N_6O_4P_4Ir_2$: C,39.5; H,5.46; N,5.323. Found: C,39.32; H,5.16; N,4.58.

The following complexes were prepared using the procedure outlined for complex 1.

$[Ir_2(Pz^*)_2(CO)_2(Ph_2POCH_2CH_2\text{-}2,4,6Me_3\text{-}Py)_2](Ph_4B)_2$(5): Anal. Calcd. for $C_{104}H_{104}B_2N_6O_4P_2Ir_2$: C,63.40; H,5.32; N,4.26. Found: C,63.63; H,5.37; N,4.30.

$[Ir_2(Pz^*)_2(CO)_2(Ph_2POCH_2CH_2\text{-}4Ph\text{-}Py)_2](Ph_4B)_2$(6): Anal. Calcd. for $C_{110}H_{100}B_2N_6O_4P_2Ir_2$: C,64.62; H,4.95; N,4.10. Found: C,63.52; H,4.96; N,3.94.

$[Ir_2(Pz^*)_2(CO)_2(Ph_2POCH_2CH_2\text{-}NEt_3)_2](Ph_4B)_2$(7): Anal. Calcd. for $C_{100}H_{112}B_2N_6O_4P_2Ir_2$: C,62.23; H,5.85; N,4.35. Found: C,62.3; H,5.70; N,4.37.

The following complexes were prepared using the procedure outline for complex 3.

$Ir_2(Pz^*)_2(CO)_2(Ph_2POCH_2CH_2CH_2CH_3)_2$(8): Anal. Calcd. for $C_{44}H_{50}N_4O_4P_2Ir_2$: C,46.15; H,4.40; N,4.88. Found: C,46.06; H,4.53; N,4.87.

$Ir_2(Pz^*)_2(CO)_2(Ph_2POCH_3)_2$(9): Anal. Calcd. for $C_{38}H_{40}N_4O_4P_2Ir_2$: C,42.94; H,3.76; N,5.27. Found: C,43.10; H,3.83; N,5.22.

$Ir_2(Pz^*)_2(CO)_2(Ph_3P)_3{\cdot}CH_2Cl_2$(10): Anal. Calcd. for $C_{49}H_{46}Cl_2N_4O_4P_2Ir_2$: C,46.27; H,3.62; N,4.41. Found: C,47.50; H,3.95; N,5.38.

[Ir2(Pz)2(CO)2(Ph2POCH2CH2-Py)2](Ph4B)2**(11): Anal. Calcd. for $C_{106}H_{108}B_2N_6O_4P_2Ir_2$: C,63.60; H,5.69; N,4.20. Found: C,63.58; H,5.36; N,4.23.

[Ir2(Pz)2(CO)2(Ph2POCH2CH2-4Me-Py)2](Ph4B)2**(12): Anal. Calcd. for $C_{108}H_{112}B_2N_6O_4P_2Ir_2$: C,64.02; H,5.57; N,4.14. Found: C,63.52; H,5.60; N,4.13.

[Ir2(Pz)2(CO)2(Ph2POCH2CH2-4Ph-Py)2](Ph4B)2**(13): Anal. Calcd. for $C_{118}H_{116}B_2N_6O_4P_2Ir_2$: C,65.94; H,5.40; N,3.91. Found: C,65.80; H,5.59; N,3.55.

X-Ray Crystallography

Crystals of $[Ir_2(Pz^*)_2(CO)_2(Ph_2POCH_2CH_2\text{-}Py)_2](Ph_4B)_2$ suitable for x-ray diffraction studies were grown from DMF solutions layered with dry diethyl ether. An irregularly shaped crystal with approximate dimensions 0.10x0.40x0.70 mm was sealed inside a glass capillary tube under an inert atmosphere and centered on a CAD4 diffractometer equipped with graphite-monochromated MoKα radiation for intensity data collection. Unit cell dimensions were obtained from the angle settings of 25 reflections

with $25° < 2\theta < 31°$. The space group $P2_{1/c}$ was chosen based on the systematic absences h0l (l=2n+1) and 0k0 (k=2n+1). Three data sets were collected in the quadrants h,k,l; -h,-k,-l; h,-k,l; and -h,k,-l with a total of 18453 reflections and were successfully merged into a final data set having 8019 independent reflections. Check reflections were monitored every 10000 seconds to record crystal decay; only minor variations were observed and the data were corrected accordingly.

The data were corrected for absorption, Lorentz, and polarization effects. An absorption coefficient of 26 cm^{-1} was found to yield the best correction of both the high and low intensity reflections. Special considerations were given to correcting individual reflections for background x-ray scatter. The unusually long c axis of this particular monoclinic lattice lead to partial overlap between adjacent reflections in approximately 1/3 of the data and precluded the use of standard correction procedures. To circumvent this problem an "average" background correction factor was calculated from the remaining well resolved reflections and was applied to the entire data set. Because systematic errors arising from this procedure should affect the low intensity data to the greatest extent, least squares refinements were carried out, which included and excluded the low intensity reflections. The minor differences observed between values of R, the GOF, and the atomic coordinates for each of these different refinements were taken to indicate that this background correction procedure was valid.

Initial coordinates for the four iridium atoms were determined by interpreting Patterson maps. The remaining non-hydrogen atoms were located from structure-factor Fourier calculations. The iridium atoms were given anisotropic thermal factors, while the remaining atoms were treated isotropically. Several cycles of least squares refinement lead to convergence with R of 0.0697 for 7212 reflections. For the strong

Table 2.1a Coordinates ($\times 10^4$)

x, y, z and $U_{eq}{}^a \times 10^4$

Atom	x	y	z	U_{eq} or B
IR1	3025(.4)	394(.3)	7838(.1)	317(1)
IR2	2296(.4)	580(.3)	7152(.1)	311(1)
P1	1995(2)	−267(2)	8137(1)	355(9)
P2	3001(2)	−269(2)	6832(1)	327(8)
C1	4015(10)	−443(9)	7894(3)	4.2(3)*
O1	4683(7)	−1023(6)	7906(2)	5.9(2)*
C2	1031(11)	193(9)	7085(3)	4.7(3)*
O2	66(8)	−102(7)	7030(2)	6.7(3)*
ND1A	1937(7)	1382(6)	7719(2)	3.1(2)*
ND1B	1694(7)	1476(6)	7427(2)	2.7(2)*
CD1A	1443(9)	2069(8)	7840(3)	3.6(3)*
CD1B	1078(10)	2192(9)	7370(3)	4.1(3)*
CD1C	918(10)	2592(9)	7631(3)	4.8(3)*
CD1D	1578(11)	2165(10)	8163(3)	6.0(4)*
CD1E	745(12)	2480(10)	7068(4)	6.4(4)*
ND2A	4052(7)	1102(6)	7587(2)	2.8(2)*
ND2B	3791(7)	1144(6)	7298(2)	2.8(2)*
CD2A	4977(10)	1553(9)	7669(3)	4.3(3)*
CD2B	4556(10)	1669(8)	7200(3)	3.9(3)*
CD2C	5311(11)	1918(9)	7417(3)	4.8(3)*
CD2D	5457(12)	1665(10)	7976(4)	6.8(4)*
CD2E	4469(11)	1872(9)	6878(3)	5.3(3)*
OA1	2182(6)	49(5)	8476(2)	3.8(2)*
CA1	3234(11)	477(9)	8585(3)	5.5(3)*
CB1	3153(11)	697(10)	8896(3)	5.8(4)*
NP1	3277(8)	−68(7)	9093(2)	4.2(2)*
CP1A	2385(10)	−458(9)	9179(3)	4.8(3)*
CP1B	2481(12)	−1195(10)	9344(3)	5.9(4)*
CP1C	3516(14)	−1545(11)	9414(4)	7.4(4)*
CP1D	4397(13)	−1133(11)	9328(4)	7.2(4)*
CP1E	4283(12)	−410(10)	9170(4)	6.2(4)*
OA2	2921(6)	123(5)	6501(2)	3.1(2)*
CA2	1929(9)	618(8)	6405(3)	3.4(3)*
CB2	2015(10)	824(8)	6079(3)	4.3(3)*
NP2	1829(8)	37(7)	5897(2)	3.7(2)*
CP2A	786(11)	−251(9)	5826(3)	5.2(3)*
CP2B	617(13)	−1032(11)	5675(4)	6.7(4)*
CP2C	1479(13)	−1465(11)	5596(4)	6.9(4)*
CP2D	2517(12)	−1159(10)	5657(3)	6.0(4)*
CP2E	2689(10)	−414(9)	5813(3)	4.8(3)*
CB1A	2208(10)	−1433(8)	8182(3)	3.9(3)*
CB1B	2420(12)	−1836(10)	8451(4)	6.2(4)*
CB1C	2593(14)	−2756(13)	8475(4)	8.5(5)*
CB1D	2484(14)	−3199(12)	8228(5)	8.1(5)*
CB1E	2243(14)	−2893(13)	7949(5)	8.8(5)*

Table 2.1a (Cont.)

Atom	x	y	z	U_{eq} or B
CB1F	2148(12)	−1969(11)	7940(4)	6.8(4)*
CB2A	506(8)	−204(7)	8078(3)	2.7(3)*
CB2B	−137(9)	−369(8)	8299(3)	3.8(3)*
CB2C	−1280(10)	−392(9)	8239(3)	4.6(3)*
CB2D	−1779(11)	−213(9)	7974(3)	5.4(3)*
CB2E	−1155(12)	−27(10)	7757(3)	5.8(4)*
CB2F	15(10)	−4(8)	7805(3)	4.2(3)*
CB3A	2407(9)	−1340(8)	6765(3)	3.0(3)*
CB3B	2446(10)	−1759(8)	6500(3)	4.1(3)*
CB3C	1961(11)	−2580(10)	6439(3)	5.6(4)*
CB3D	1502(12)	−2976(10)	6658(4)	5.9(4)*
CB3E	1481(11)	−2629(10)	6923(3)	5.6(4)*
CB3F	1921(10)	−1773(8)	6975(3)	4.2(3)*
CB4A	4449(9)	−517(8)	6883(3)	3.1(3)*
CB4B	5150(10)	−460(8)	6669(3)	4.2(3)*
CB4C	6248(11)	−682(9)	6731(3)	5.2(3)*
CB4D	6670(12)	−916(10)	7004(4)	5.7(4)*
CB4E	6020(13)	−987(10)	7221(4)	6.8(4)*
CB4F	4889(11)	−770(9)	7155(3)	5.0(3)*
B1	1474(10)	741(9)	694(3)	2.6(3)*
C11A	2199(9)	734(8)	416(3)	3.0(3)*
C11B	2666(9)	1493(8)	311(3)	3.2(3)*
C11C	3360(10)	1468(9)	91(3)	4.4(3)*
C11D	3656(10)	692(9)	−16(3)	4.5(3)*
C11E	3243(10)	−73(9)	78(3)	4.8(3)*
C11F	2519(10)	−54(8)	296(3)	4.0(3)*
C12A	2420(9)	678(8)	972(3)	3.4(3)*
C12B	2854(10)	−113(9)	1081(3)	4.3(3)*
C12C	3651(12)	−204(10)	1316(4)	6.1(4)*
C12D	4058(12)	562(12)	1434(4)	7.2(4)*
C12E	3748(13)	1339(11)	1344(4)	7.1(4)*
C12F	2911(11)	1421(10)	1107(3)	5.5(4)*
C13A	620(9)	−79(7)	680(3)	3.0(3)*
C13B	−19(10)	−285(9)	421(3)	4.7(3)*
C13C	−771(12)	−985(10)	400(4)	6.2(4)*
C13D	−914(11)	−1470(10)	631(4)	5.8(4)*
C13E	−352(11)	−1275(9)	900(3)	5.2(3)*
C13F	395(10)	−569(8)	917(3)	4.1(3)*
C14A	707(9)	1623(8)	708(3)	3.2(3)*
C14B	379(11)	1903(9)	971(3)	4.8(3)*
C14C	−355(12)	2618(11)	981(4)	6.7(4)*
C14D	−707(12)	3036(11)	737(4)	6.7(4)*
C14E	−465(12)	2790(10)	469(4)	6.2(4)*
C14F	265(11)	2054(9)	462(3)	4.9(3)*
B2	3507(11)	671(9)	4313(3)	3.3(3)*

Table 2.1a (Cont.)

Atom	x	y	z	U_{eq} or B
C21A	4306(9)	1550(8)	4312(3)	3.4(3)*
C21B	4633(10)	1879(9)	4047(3)	4.7(3)*
C21C	5348(12)	2614(10)	4052(4)	5.9(4)*
C21D	5715(12)	2993(10)	4302(4)	6.0(4)*
C21E	5460(12)	2690(10)	4560(4)	6.2(4)*
C21F	4764(10)	1948(9)	4561(3)	4.4(3)*
C22A	2814(9)	645(8)	4596(3)	3.2(3)*
C22B	2354(10)	1401(8)	4704(3)	3.7(3)*
C22C	1648(10)	1387(9)	4920(3)	4.5(3)*
C22D	1375(10)	611(9)	5032(3)	5.0(3)*
C22E	1796(11)	−149(9)	4937(3)	5.4(4)*
C22F	2509(10)	−148(9)	4718(3)	4.5(3)*
C23A	2546(9)	731(8)	4044(3)	3.1(3)*
C23B	2020(9)	1(8)	3901(3)	3.1(3)*
C23C	1131(9)	46(8)	3684(3)	3.4(3)*
C23D	689(10)	864(8)	3605(3)	4.1(3)*
C23E	1137(10)	1599(8)	3750(3)	4.1(3)*
C23F	2033(10)	1514(8)	3955(3)	3.7(3)*
C24A	4320(9)	−178(7)	4302(3)	2.9(3)*
C24B	4978(10)	−436(9)	4553(3)	4.7(3)*
C24C	5701(11)	−1160(10)	4552(3)	5.5(4)*
C24D	5763(12)	−1614(10)	4308(4)	6.1(4)*
C24E	5155(11)	−1389(9)	4053(3)	5.0(3)*
C24F	4448(9)	−640(8)	4053(3)	3.3(3)*

[a] $U_{eq} = \frac{1}{3}\sum_i \sum_j [U_{ij}(a_i^* a_j^*)(\vec{a}_i \cdot \vec{a}_j)]$
*Isotropic displacement parameter, B

Table 2.1b Anistropic Temperature Factors

Atom	U_{11}	U_{22}	U_{33}	U_{12}	U_{13}	U_{23}
IR1	346(3)	336(3)	281(4)	−42(3)	82(2)	31(3)
IR2	345(3)	310(3)	284(4)	31(3)	62(2)	−17(3)
P1	401(20)	350(21)	322(23)	−64(17)	77(16)	74(18)
P2	353(19)	322(20)	311(22)	17(16)	61(16)	−11(18)

The form of the displacement factor is:

$$\exp -2\pi^2(U_{11}h^2a^{*2} + U_{22}k^2b^{*2} + U_{33}\ell^2c^{*2} + 2U_{12}hka^*b^* + 2U_{13}h\ell a^*c^* + 2U_{23}k\ell b^*c^*)$$

Table 2.2: Final Crystallographic Parameters

Mol. Wt. 1828.98

Cell Dimensions

a, Å 12.189(1)

b, Å 15.298(2)

c, Å 46.372(6)

α, deg. 90

β, deg. 90.406(10)

γ, deg. 90

V, $Å^3$ 8646(7)

Z 4

ρ, g/cm^3 1.41

μ, cm^{-1} 26.0

Crystal Dimensions 0.1 x 0.4 x 0.7 mm

Scan Width ω scans (1°)

No. of Observed Reflections

Total 8019

> 0 7212

$>3\sigma$ 6131

No. of Parameters Varied 477

R 0.0697

$R_{3\sigma}$ 0.055

GOF 2.32

Space Group $P2_{1/c}$

data with $F_o^2 > 3\sigma F_o^2$, R = 0.055 for 6131 reflections. The goodness of fit was 2.32 for n = 8019 data and p= 477 parameters. Atomic coordinates and final unit cell parameters are found in tables 2.1 and 2.2.

Calculational Details

Molecular mechanics calculations were carried out on $[Ir_2(Pz^*)_2(CO)_2(Ph_2POCH_2CH_2\text{-}Py)_2](Ph_4B)_2$ using Biograf III version 1.40.[13] Initial atom positions were taken from its crystallographic coordinates. Energy minimizations for the three ligand rotational conformations seen in figure 2.16 were carried out using a Dreiding force field, which had been modified to reproduce the experimentally observed bond distances and angles. In each case the coordinates of the Ir, P, CO, and pyrazolate nitrogen atoms were held fixed to preserve their coordination geometries. All calculations were carried out in the absence of atom charges, counter-ions, and solvent molecules in an extended atom approximation.

Rigid geometry conformational mapping involving the four torsional angles seen in figure 2.15 was carried out using procedures described previously by Karplus *et al.*[14]. It was found that conformations in which ϕ_{B1} and ϕ_{B2} are both acute were physically impossible. Thus, calculations were carried out in which $\phi_{B1}(\phi_{B2})$ was held at 180° and $\phi_{B2}(\phi_{B1})$ was varied between 60° and 300° in 120° increments. For pairs of values in ϕ_{B1} and ϕ_{B2}, ϕ_{B3} varied between 60° and 300° in 120° increments and ϕ_{B4} varied between 90° and 270° in 30° increments. The van der Waals energy of each conformation was determined using a Lennard-Jones 6-12 potential function of the form

$$E_{vdW} = \sum_{R_{ij} \leq R_{cut}} \left\{ \left[\frac{(R_o)_{ij}}{R_{ij}} \right]^{12} - 2 \left[\frac{(R^*_o)_{ij}}{R_{ij}} \right]^{6} \right\} (D_o)_{ij}$$

where D_0 is the van der Waals bond energy in Kcal/mole, R_0 is the van der Waals bond length in Å and R is the interatomic distance in Å. Only those interactions within an interval less that a cutoff distance (R_{cut}) of 9.0 Å were included in this sum. This procedure was repeated for each of the three different Ir-P conformations.

Results

Phosphinite Redox Ligands

The two step reaction sequence outlined in figure 2.3 was used to synthesize a series of redox phosphinite ligands with different electrochemical reduction potentials (figure 2.2). A number of 1-(2-hydroxyethyl)pyridinium salts were prepared in good yield by reacting pyridine or a para-substituted pyridine with 2-bromoethanol using a previously established procedure (reaction 1a.).[6] 1-(2-hydroxyethyl)-2,4,6-trimethylpyridinium tosylate was synthesized using a ring open reaction between a corresponding pyrylium cation and (2-hydroxyethyl)amine, due to the poor nucleophilicity of ortho disubstituted pyridines (reaction 1b.).[10a,b] Each of the pyridinium salts was metathesized to its corresponding tetraphenylborate salt to enhance the solubility of the phosphinite ligands and iridium dimer complexes in organic solvents. ^{1}H NMR spectra of these compounds compared favorably with spectra found in the literature.[11]

Step two involved the alcoholysis of N,N-dimethyl-P,P-diphenylphosphine by a 1-(hydroxyethyl)pyridinium compound to produce its corresponding phosphinite ligand (reaction 2.).[15] This transformation was carried out at room temperature in approximately 90% isolated yield by catalyzing the reaction with a small amount of benzoic acid. This approach avoided the higher reaction temperatures and forcing conditions associated with more traditional methods of preparing alkoxy diphenylphosphines and minimized the possibility of Arbuzov rearrangements[15] and side reactions involving the pyridinium cations.[16] Each of the redox ligands prepared in this manner was characterized by ^{1}H and ^{31}P NMR spectroscopy. These data are summarized in table 2.3a.

Figure 2.2: Structures of the phosphinite redox ligands and their abbreviations.

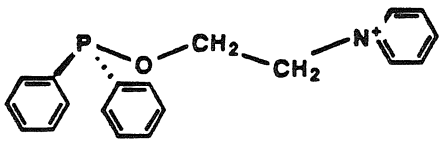

$Ph_2POCH_2CH_2$-Py

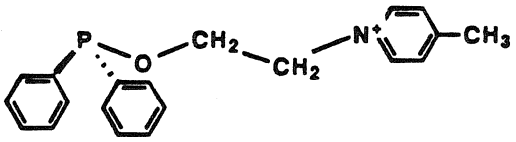

$Ph_2POCH_2CH_2$-4Me-Py

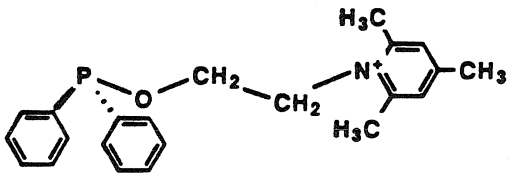

$Ph_2POCH_2CH_2$-2,4,6Me_3-Py

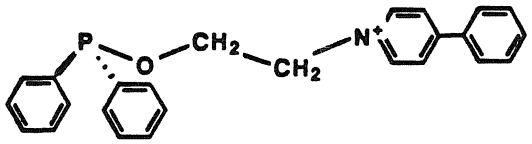

$Ph_2POCH_2CH_2$-4Ph-Py

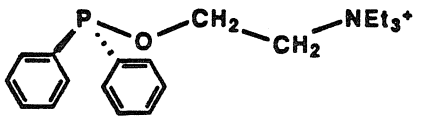

$Ph_2POCH_2CH_2$-NEt_3

Figure 2.3: Synthetic scheme for preparing the phosphinite redox ligands.

(Reaction 1a.)

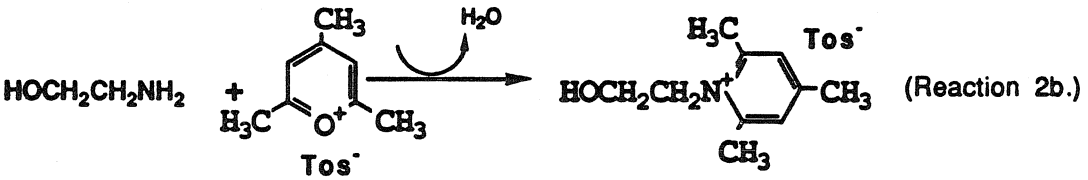

(Reaction 2b.)

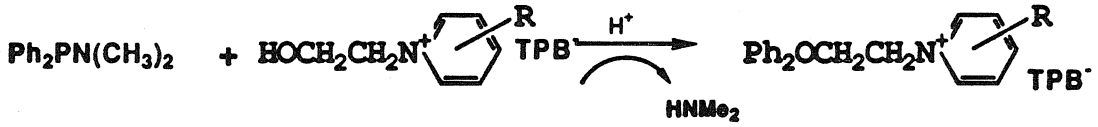

(Reaction 2)

Table 2.3a: ^{1}H and ^{31}P NMR Data for Phosphinite Redox Ligands

Compound	Assignment	δ/ppm[a]	
		^{1}H	^{31}P[b]
$(Ph_2POCH_2CH_2\text{-}Py)(Ph_4B)$	Ph_2P-	----	116.1
	-Py (ortho H)	9.00(d)	
	-Py (para H)	8.50(t)	
	-Py (meta H)	8.00(t)	
	-O***CH₂***CH_2-	4.28(dt)	
	-OCH_2***CH₂*** -	4.84(t)	
$(Ph_2POCH_2CH_2\text{-}4\text{-}MePy)(Ph_4B)$	Ph_2P-	----	115.6
	-Py-***CH₃***	2.50(s)	
	-Py (ortho H)	8.70(d)	
	-Py (meta H)	7.75(d)	
	-O***CH₂***CH_2-	4.25(dt)	
	-OCH_2***CH₂*** -	4.69(t)	
$(Ph_2POCH_2CH_2\text{-}4\text{-}PhPy)(Ph_4B)$	Ph_2P-	----	115.1
	-Py (ortho H)	8.10(d)	
	-Py (meta H)	7.75(d)	
	-Ph (ortho H)	7.80(d)	
	-Ph (meta H)	7.55(m)	
	-Ph (para H)	7.55(m)	
	-O***CH₂***CH_2-	4.20(dt)	
	-OCH_2***CH₂*** -	4.50(t)	
$(Ph_2POCH_2CH_2\text{-}246Me_3\text{-}Py)(Ph_4B)$	Ph_2P-	----	117.8
	-Py (meta H)	7.50(s)	
	-Py (ortho CH_3)	2.65(s)	
	-Py (para CH_3)	2.40(s)	
	-O***CH₂***CH_2-	4.25(dt)	
	-OCH_2***CH₂*** -	4.69(t)	
$(Ph_2POCH_2CH_2\text{-}NEt_3)(Ph_4B)$	Ph_2P-	----	116.1
	-O***CH₂***CH_2-	3.52(dt)	
	-OCH_2***CH₂*** -	4.12(t)	
	(***CH₃***CH_2)-	1.20(t)	
	(CH_3***CH₂***)-	3.30(q)	
$(Ph_2POCH_2CH_2\text{-}NEt_3)(PF_6)$	Ph_2P-	----	118.5
	PF_6	----	-143.5
	-O*CH₂*CH_2-	3.77(dt)	
	-OCH_2*CH₂* -	4.27(t)	
	(***CH₃***CH_2)-	1.29(t)	
	(CH_3***CH₂***)-	3.53(q)	

a. Spectra were measured in d^6-DMSO. b. Chemical shifts are versus ext.H_3PO_4.

NMR spectra of the ligands show proton chemical shifts and multiplicities for the pyridinium aromatic protons and ring substituents, which are similar to those seen in spectra of their 1-(2-hydroxyethyl)pyridinium precursors. The phosphine phenyl groups show up as a pair of complex multiplets at $\delta = 7.6$ and $\delta = 7.3$ ppm. Notably, the β-methylene protons appear as a doublet of triplets at 4.2 ppm due to proton-phosphorous coupling ($J_{PH} = 6.50$ Hz). In addition, ^{31}P NMR spectra show ligand phosphorous chemical shifts ranging from $\delta = 115.1$ to $\delta = 118.5$ ppm. These spectroscopic data identify the ligands as esters of diphenylphosphinous acid.[17]

Iridium Dimer Preparation

Synthetic Methodology: The series of iridium(I) donor-acceptor complexes and corresponding model compounds reported in this study were prepared using procedures similar to those described previously for a number of analogous rhodium[18] and iridium[19] pyrazolate bridge compounds. Initial attempts at preparing redox phosphinite complexes of diiridium bis(μ-pyrazolate) using the two step method of Stobart and coworkers (figure 2.4) were complicated by the propensity of the products to form as intractable oils. This oil formation was attributed to small amounts of cyclooctadiene released during the preparation of the tetracarbonyl intermediate, $Ir_2(Pz)_2(CO)_4$ (reaction 3a.). $Ir_2(Pz)_2(CO)_4$ could not be isolated and purified for use as a primary starting material because it percipitates from concentrated solutions as a black intractable polymer. However, Nussbaum *et al.*[20] had reported a procedure for preparing its bis μ-3,5-dimethylpyrazolate bridge analog in good overall yield. By reacting pure $Ir_2(Pz^*)_2(CO)_4$ with two equivalents of a phosphinite ligand of choice, its corresponding bis carbonyl, bis phosphinite iridium dimer was isolated as an orange/red crystalline solid in approximately 90% overall yield (reaction 4.). This

Figure 2.4: Synthetic scheme for preparing $Ir_2(Pz^*)_2(CO)_2(Ph_2POCH_2CH_2R)_2$ complexes.

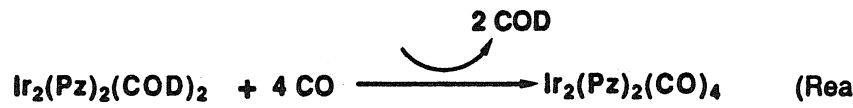

(Reaction 3a.)

(Reaction 3b.)

(Reaction 4.)

approach proved to be general for a variety of phosphine ligands and permitted the preparation of a complete series of donor-acceptor molecules and their corresponding model complexes.[21]

The donor-acceptor complexes based on the 3,5-dimethylpyrazole bridge framework proved to be soluble in most polar organic solvents, but were fairly insoluble in lower polarity solvents such as dichloromethane. Because some of the electrochemical and spectroscopic studies discussed in later chapters had to be carried out in less polar organic solvents, a second series of compounds was prepared containing 3,5-dimethyl-4-isobutylpyrazole ligands. Each of the complexes was characterized by ^{1}H and ^{31}P NMR spectroscopy. These data are summarized in table 2.3b.

^{1}H NMR: Unlike d^8-d^8 A-frame compounds containing identical terminal ligands, the carbon monoxide phosphine complexes can exist as cis and trans structural isomers as seen in figure 2.5. Based on x-ray crystallographic data available for a number of rhodium and iridium pyrazolate bridge systems,[22] the trans substitutional isomer is favored in the solid state. In solution, however, these two entities could exist in dynamic equilibrium. While Stobart and coworkers have reported that $Ir_2(Pz)_2(CO)_2(Ph_3P)_2$ exists as its trans isomer in solution and in the solid state,[19] evidence for the presence of both the cis and trans isomers of $Rh_2(Pz^*)_2(CO)_2(Ph_3P)_2$ has been observed in its proton NMR spectra.[23] The structural and electronic similarities between these two complexes and the donor-acceptor compounds prepared in this study suggest that structural isomerism should be considered in assigning their NMR spectra. Previous studies have indicated that the bridge substituent magnetic environments in d^8-d^8 A-frame complexes are perturbed by the nature and disposition of the dimer's terminal ligands.[23,12,19] Thus, a careful analysis of the signals due to the pyrazole methyl

Table 2.3b: ^{1}H and ^{31}P NMR Data for Iridium Dimer Complexes

Compound	Assignment	δ(ppm)
$[Ir_2(Pz^*)_2(CO)_2(Ph_2POCH_2CH_2\text{-}Py)_2$[b]	Pz*-***CH_{3A}***	1.4(s)
$(Ph_4B)_2$[d]	Pz*-***CH_{3B}***	2.2(s)
δ_P = 97.79[e]	Pz*-***H***	5.35(s)
	-OCH_2***CH_2***-	5.1(m)
	-O***CH_2***CH_2-	4.9(m)
		4.3(m)
	Py ortho	9.3(d)
	Py para	9.6(t)
	Py meta	9.2(t)
	Ph_2P- ortho	7.85(d,d)
		7.6(d,d)
	Ph_2P- para	7.45(t)
		7.15(m)
	Ph_2P- meta	7.35(t)
		7.15(m)
$Ir_2(Pz^*)_2(CO)_2(Ph_2POCH_2CH_2\text{-}4CH_3\text{-}Py)_2$[b]	Pz*-***CH_{3A}***	1.42(s)
$(Ph_4B)_2$	Pz*-***CH_{3B}***	2.2(s)
δ_P = 100.8	Pz*-***H***	5.4(s)
	-OCH_2***CH_2***-	5.0(m)
	-O***CH_2***CH_2-	4.9(m)
		4.25(m)
	Py ortho	9.1(d)
	Py meta	8.0(d)
	Py-***CH_3***	2.6(s)
	Ph_2P- ortho	7.6(d,d)
		7.85(d,d)
	Ph_2P- meta	7.35(t)
		7.15(t)
	Ph_2P- para	7.45(t)
		7.22(t)
$Ir_2(Pz^*)_2(CO)_2(Ph_2POCH_2CH_2\text{-}4Ph\text{-}Py)_2$[b]	Pz*-***CH_{3A}***	2.2(s)
$(Ph_4B)_2$	Pz*-***CH_{3B}***	1.4(s)
δ_P = 99.04	Pz*-***H***	5.35(s)
	-OCH_2***CH_2***-	5.2(m)
	-O***CH_2***CH_2-	4.4(m)
		5.0(m)
	Py-Ph ortho	9.4(d)
	Py-Ph meta	8.65(d)
	Py-***Ph*** ortho	8.1(d)
	Py-***Ph*** para+meta	7.65(m)
	Ph_2P- ortho	7.9(d,d)
		7.65(d,d)

Table 2.3b: (cont.)

Compound	Assignment	δ(ppm)
	Ph_2P- meta	7.55(d,d)
		7.1(d,d)
	Ph_2P- para	7.4(d,d)
		7.2(d,d)
$Ir_2(Pz^*)_2(CO)_2(Ph_2POCH_2CH_2\text{-}2,4,6Me_3\text{-}Py)_2$[a]	Pz*-CH_{3A}	1.6(s)
$(Ph_4B)_2$	Pz*-CH_{3B}	2.25(s)
δ_P = 95.20	Pz*-H	5.5(s)
	Py-CH_3 ortho	2.67(s)
	Py-CH_3 para	2.45(s)
	Py-H	7.62(s)
	Ph_2P- ortho	7.8(d,d)
		7.6(d,d)
	Ph_2P- para	7.48(t)
		7.30(t)
	Ph_2P- meta	7.4(t)
		7.22(t)
$Ir_2(Pz^*)_2(CO)_2(Ph_2POCH_2CH_2\text{-}NEt_3)_2$[b]	Pz*-CH_{3A}	1.85(s)
$(Ph_4B)_2$	Pz*-CH_{3B}	2.3(s)
δ_P = 104.29	Pz*-H	5.65(s)
	-OCH_2CH_2-	3.55(m)
		3.65(m)
	-OCH_2CH_2-	4.35(m)
		4.45(m)
	-$N(CH_2CH_3)_3$	1.2(t)
	-$N(CH_2CH_3)_3$	3.3(q)
	Ph_2P- ortho	8.1(d,d)
		7.8(d,d)
	Ph_2P- para	7.4(t)
		7.2(m)
	Ph_2P- meta	7.3(t)
		7.2(m)
$Ir_2(Pz^*)_2(CO)_2(Ph_2POCH_3)_2$[c]	Pz*-CH_{3A}	2.45(s)
$(Ph_4B)_2$	Pz*-CH_{3B}	2.10(s)
δ_P = 100.82	Pz*-H	5.6(s)
	P-O-CH_3	3.8(d)
	Ph_2P- ortho	8.2(m)
	Ph_2P- para	7.0(t)
		6.95(t)
	Ph_2P- meta	7.1(m)
$Ir_2(Pz^*)_2(CO)_2(Ph_2POCH_2CH_3)_2$[c]	Pz*-CH_{3A}	2.05(s)
$(Ph_4B)_2$	Pz*-CH_{3B}	2.55(s)
δ_P = 96.15	Pz*-H	5.60(t)

Table 2.3b: (cont.)

Compound	Assignment	δ(ppm)
	-$OCH_2\boldsymbol{CH_3}$	1.3(t)
	-$O\boldsymbol{CH_2}CH_3$	4.31(m)
		4.55(m)
	$\boldsymbol{Ph_2}$P- ortho	8.23(d,d)
		8.30(d,d)
	$\boldsymbol{Ph_2}$P- para	6.95(t)
		7.04(t)
	$\boldsymbol{Ph_2}$P- meta	7.2(m)
$Ir_2(Pz^*)_2(CO)_2(Ph_2POCH_2CH_2CH_2CH_3)_2$[c] $(Ph_4B)_2$ δ_P = 96.11	Pz*-$\boldsymbol{CH_{3A}}$	2.2(s)
	Pz*-$\boldsymbol{CH_{3B}}$	2.5(s)
	Pz*-$\boldsymbol{H}$	5.6(s)
	$OCH_2CH_2CH_2\boldsymbol{CH_3}$	0.87(t)
	$OCH_2CH_2\boldsymbol{CH_2}CH_3$	1.44(sextet)
	$OCH_2\boldsymbol{CH_2}CH_2CH_3$	1.68(d,quintet)
	$O\boldsymbol{CH_2}CH_2CH_2CH_3$	4.16(m)
		4.56(m)
	$\boldsymbol{Ph_2}$P- ortho	8.37(d,d)
		8.23(d,d)
	$\boldsymbol{Ph_2}$P- para	6.95(t)
		7.05(t)
	$\boldsymbol{Ph_2}$P- meta	7.15(m)
$Ir_2(Pz^*)_2(CO)_2(Ph_2POCH_2CH_2$-$NEt_3)_2$[a] $(PF_6)_2$ δ_P = 100.5	Pz*-$\boldsymbol{CH_{3A}}$	2.0(s)
	Pz*-$\boldsymbol{CH_{3B}}$	2.4(s)
	Pz*-$\boldsymbol{H}$	5.55(s)
	-$OCH_2\boldsymbol{CH_2}$-	3.45(m)
		3.49(m)
	-$O\boldsymbol{CH_2}CH_2$-	4.6(m)
		4.45(m)
	-$N(CH_2\boldsymbol{CH_3})_3$	1.3(t)
	-$N(\boldsymbol{CH_2}CH_3)_3$	3.3(q)
	$\boldsymbol{Ph_2}$P- ortho	8.16(d,d)
		7.95(d,d)
	$\boldsymbol{Ph_2}$P- para	7.53(t)
		7.65(m)
	$\boldsymbol{Ph_2}$P- meta	7.47(t)
		7.65(m)
$Ir_2(Pz^{**})_2(CO)_2(Ph_2POCH_2CH_2$-$Py)_2$[a] $(Ph_4B)_2$ δ_P = 99.17	Pz**-$CH_2CH(\boldsymbol{CH_3})_2$	0.54(d)
		0.39(d)
	Pz**-$CH_2\boldsymbol{CH}(CH_3)_2$	1.05(septet)
	Pz**-$\boldsymbol{CH_2}CH(CH_3)_2$	1.72(d)
	Pz*-$\boldsymbol{CH_{3A}}$	1.5(s)

Table 2.3b: (cont.)

Compound	Assignment	δ(ppm)
	Pz*-CH_{3B}	2.2(s)
	-OCH_2CH_2-	4.9(m)
	-OCH_2CH_2-	4.41(m)
		5.02(m)
	Ph_2P- ortho	7.77(d,d)
		7.61(d,d)
	Ph_2P- para	7.34(t)
		7.14(t)
	Ph_2P- meta	7.08(t)
		7.25(t)
	Py- ortho	8.68(d)
	Py- para	8.45(t)
	Py- meta	8.20(t)
$Ir_2(Pz^{**})_2(CO)_2(Ph_2POCH_2CH_2$-4Me-Py$)_2$[a] $(Ph_4B)_2$	Pz**-$CH_2CH(CH_3)_2$	0.63(d,d)
δ_P = 99.54	Pz**-$CH_2CH(CH_3)_2$	1.2(octet)
	Pz**-$CH_2CH(CH_3)_2$	1.87(d)
	-OCH_2CH_2-	4.6(m)
	-OCH_2CH_2-	5.0(m)
		4.4(m)
	Ph_2P- ortho	7.89(d,d)
		7.77(d,d)
	Ph_2P- para	7.47(t)
		7.26(m)
	Ph_2P- meta	7.42(m)
	Py-*H* ortho	8.23(d)
	Py-*H* meta	7.63(d)
$Ir_2(Pz^{**})_2(CO)_2(Ph_2POCH_2CH_2$-4Ph-Py$)_2$[a] $(Ph_4B)_2$	Pz**-$CH_2CH(CH_3)_2$	0.6(d)
		0.65(d)
δ_P = 99.34	Pz**-$CH_2CH(CH_3)_2$	1.2(m)
	Pz**-$CH_2CH(CH_3)_2$	1.9(t)
	Pz*-CH_{3A}	1.6(s)
	Pz*-CH_{3B}	2.2(s)
	-OCH_2CH_2-	4.9(m)
	-OCH_2CH_2-	4.6(m)
		5.2(m)
	Ph_2P- ortho	8.0(d,d)
		7.8(d,d)
	Ph_2P- para	7.45(d,d)
		7.40(d,d)
	Ph_2P- meta	7.2(m)
	Py-Ph ortho	8.55(d)
	Py-Ph meta	8.15(d)
	Py-*Ph* ortho	7.9(d)
	Py-*Ph* para+meta	7.7(m)

Table 2.3b: (cont.)

Compound	Assignment	δ(ppm)
$Ir_2(Pz^*)_2(CO)_2(Ph_3)_2$[c]	Pz*-CH_{3A}	1.8(s)
δ_P = 17.56	Pz*-CH_{3B}	2.6(s)
	Pz*-H	5.6(s)
	Ph_3P ortho	7.8(m)
	Ph_3P meta+para	7.0(s)

a. d3-Acetonitrile. b. d6-DMSO c. d6-Benzene. d. Signals for the tetraphenylborate counterions appeared at 6.9(t), 7.0(t), and 7.2(m). e. Chemical shifts are referenced to external H_3PO_4.

Figure 2.5: Molecular structures for the *cis* and *trans* isomers of $Ir_2(Pz^*)_2(CO)_2(Ph_2POCH_2CH_3)_2$. The bridging pyrazole substituents are labeled according to their magnetic environments.

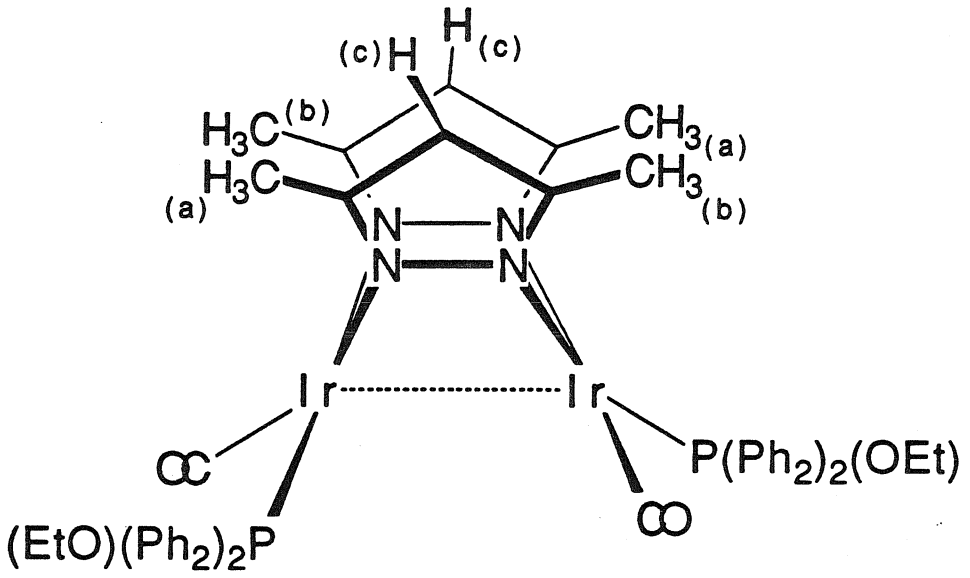
(c)H
H(c)
H3C(b)
CH3(a)
H3C(a)
CH3(b)
N
N
N
N
Ir
Ir
CO
P(Ph2)2(OEt)
CO
(EtO)(Ph2)2P

Trans

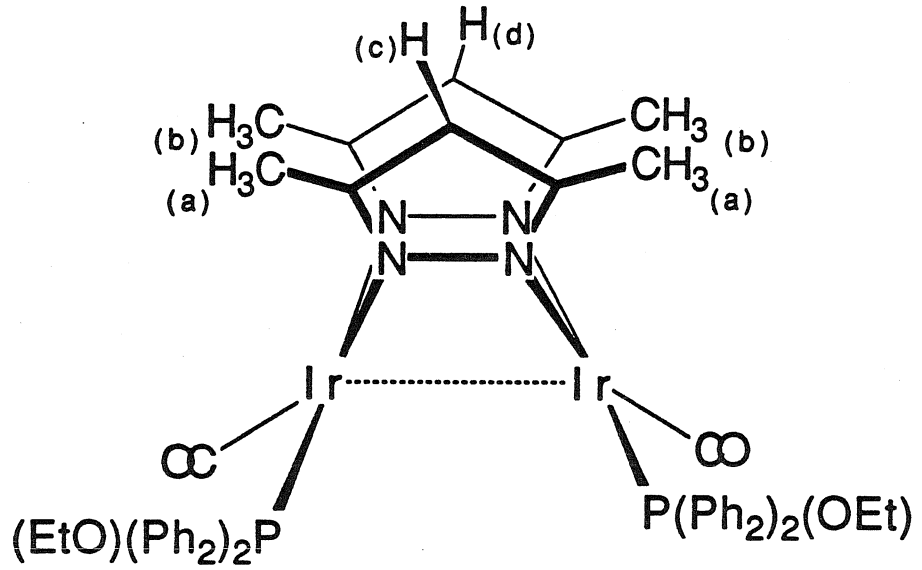
(c)H
H(d)
(b)H3C
CH3(b)
H3C(a)
CH3(a)
N
N
N
N
Ir
Ir
CO
CO
(EtO)(Ph2)2P
P(Ph2)2(OEt)

Cis

Figure 2.6: a) ^{1}H NMR spectrum of $Ir_2(Pz^*)_2(CO)_4$ in d6-benzene; δ = 2.13 ppm (s; pyrazole CH_3), δ = 5.60 ppm (s; pyrazole C-4 H). b) ^{1}H NMR spectrum of $Ir_2(Pz^*)_2(CO)_2(Ph_2POCH_2CH_3)_2$ in d6-benzene.

a

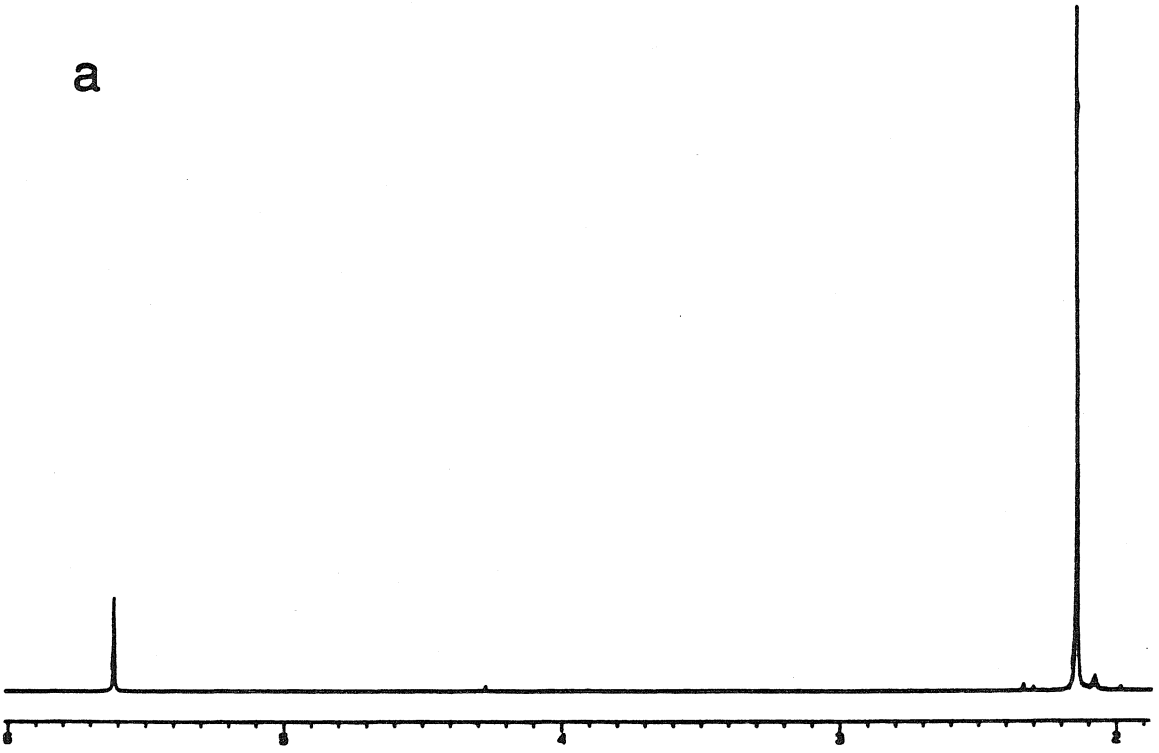

b

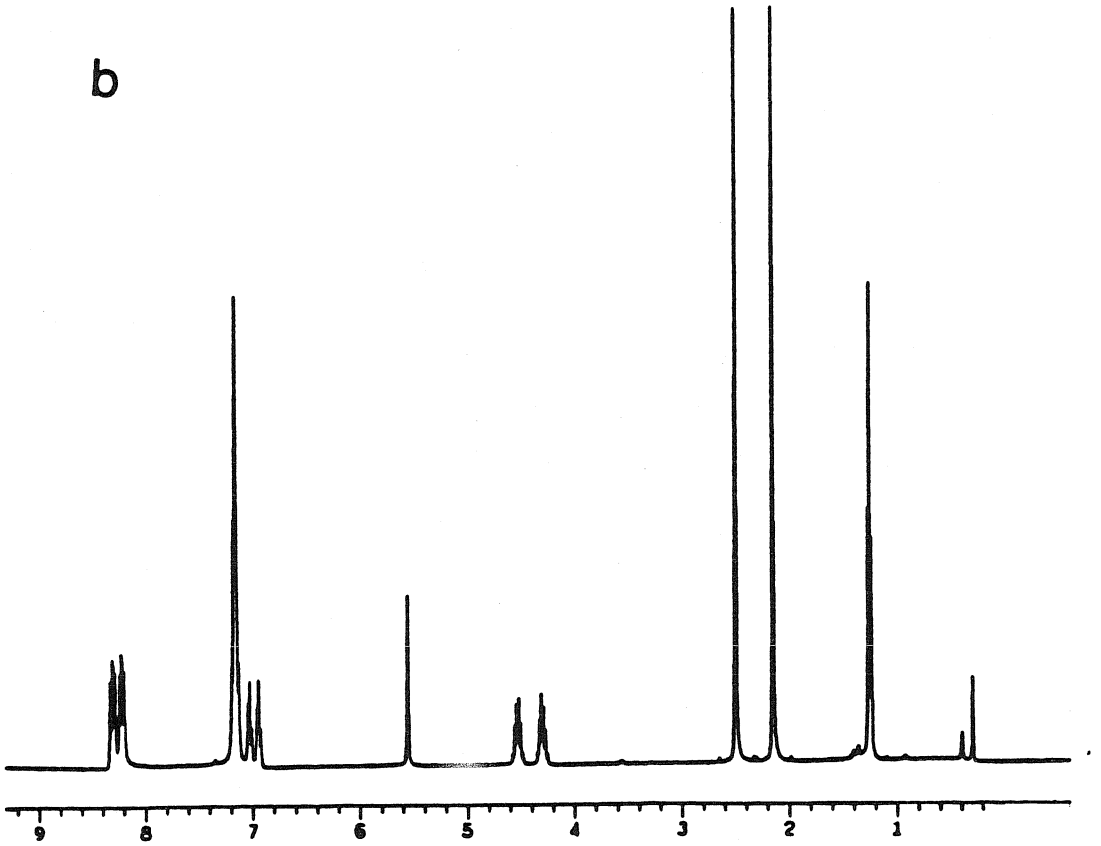

groups and C-4 protons in our complexes should disclose their solution coordination geometry.

In addition to containing a number of multiplets for the phenyl and ethoxy substituents on the phosphinite ligands, the ^1H NMR spectrum of $Ir_2(Pz^*)_2(CO)_2(Ph_2POCH_2CH_3)_2$ (figure 2.6b) shows three signals at $\delta = 5.60$, $\delta = 2.50$, and $\delta = 2.05$ ppm (integration 1:3:3), which are assigned to the pyrazole C-4 proton and the two pair of inequivalent bridge methyl groups respectively. These spectral data indicate that a solitary isomer of $Ir_2(Pz^*)_2(CO)_2(Ph_2POCH_2CH_3)_2$ is present in solution. This conclusion is substantiated by the presence of a single pair of singlet bands for the pyrazole methyl groups. Spectra of a mixture would show at least four bands for the magnetically inequivalent methyl groups in the cis and trans isomers. The unique singlet band assigned to pyrazole C-4 protons suggests that this complex exists as its trans isomer. In the corresponding cis isomer these protons occupy magnetically inequivalent C-4 sites (figure 2.5). In addition, based on the assignments made for the pyrazolate substituents in $Ir_2(Pz^*)_2(CO)_4$ (figure 2.5a), the chemical shifts of the pyrazole methyl groups in $Ir_2(Pz^*)_2(CO)_2(Ph_2POCH_2CH_3)_2$ can be assigned according to the labeling scheme seen in figure 2.7.

Due to the trans configuration of its terminal ligands, $Ir_2(Pz^*)_2(CO)_2(Ph_2POCH_2CH_3)_2$ lacks internal mirror symmetry. As prepared, this compound is, presumably, a racemic mixture of its two enantiomers. The chiral nature of the complex is manifested in its NMR spectra through the diastereotopic chemical shifts observed for magnetically inequivalent protons bound to the phosphinite ligand alkoxy and phenyl substituents. Figure 2.8a shows the aromatic region of a 400 MHz ^1H spectrum of $Ir_2(Pz^*)_2(CO)_2(Ph_2POCH_2CH_3)_2$ taken in d6-benzene. The

Figure 2.7: Chemical shift assignments for the bridging pyrazole substituents in $Ir_2(Pz^*)_2(CO)_2(Ph_2POCH_2CH_3)_2$.

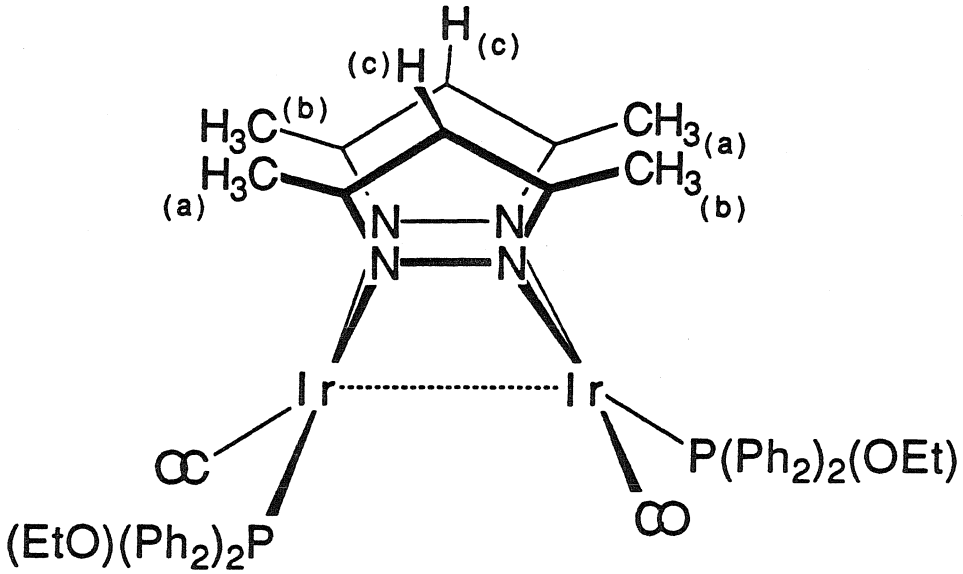

$\delta_{(a)}$= 2.05 ppm

$\delta_{(b)}$= 2.50 ppm

$\delta_{(c)}$= 5.60 ppm

Figure 2.8: a) ^{1}H NMR spectrum of $Ir_2(Pz^*)_2(CO)_2(Ph_2POCH_2CH_3)_2$ showing diasteriotopic chemical shifts for the phosphinite phenyl substituents. b) Diasteriotopic chemical shifts for the ethoxy group methylene protons.

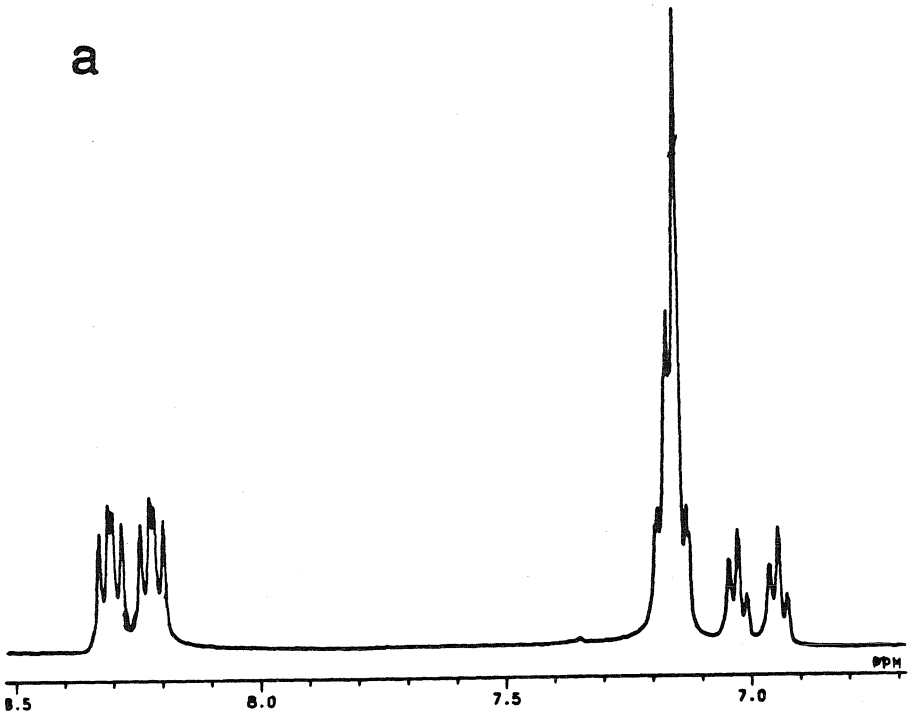
a
PPM
8.5
8.0
7.5
7.0

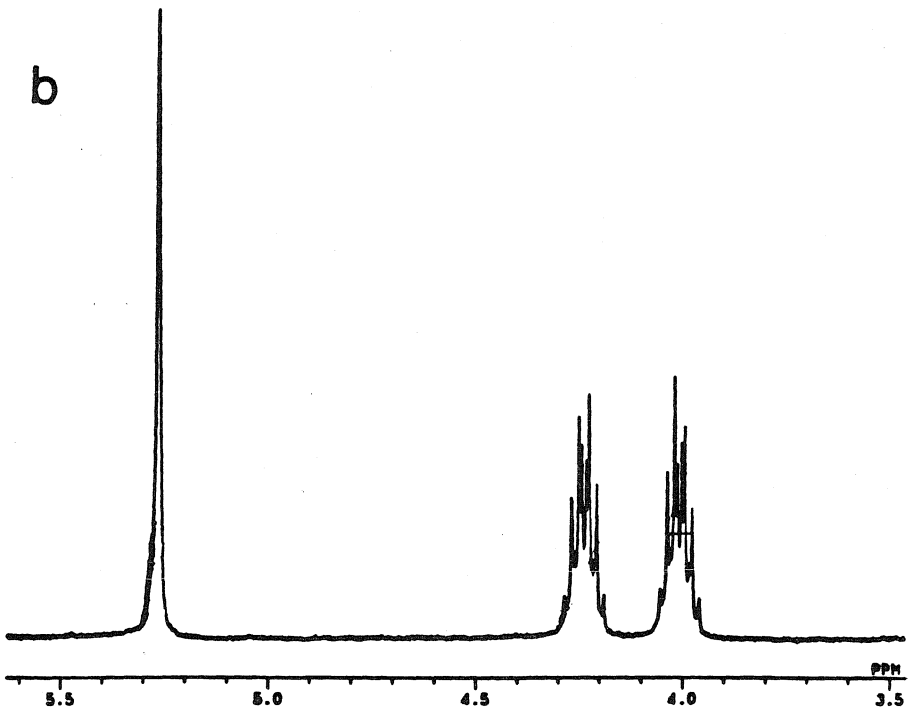
b
PPM
5.5
5.0
4.5
4.0
3.5

phenyl group ortho protons appear as a pair of closely spaced doublets at δ = 8.23 and δ = 8.30 ppm (J_{PH} = 6.25 Hz) along with a pair of slightly second order triplets at δ = 6.95 and δ = 7.04 ppm assigned to pairs of magnetically distinct para protons. The meta proton chemical shifts are not affected as much by the magnetic inequivalence of the ligand phenyl groups and are observed as a complex multiplet at δ = 7.2 ppm. A similar effect is seen in the phosphine ethoxy group β–methylene protons (figure 2.8b.), which appear as a pair of complex multiplets at δ_1 = 4.30 and δ_2 = 4.55 ppm.

The spectroscopic properties of all of the donor-acceptor complexes reported here are similar to those seen in the $Ir_2(Pz^*)_2(CO)_2(Ph_2POCH_2CH_3)_2$ (table 2.3b). The proton NMR spectra of $[Ir_2(Pz^*)_2(CO)_2(Ph_2POCH_2CH_2\text{-}2,4,6\ Me_3\text{-}Py)_2](Ph_4B)_2$ in d3-acetonitrile, seen in figures 2.9-2.10, exemplify those spectral features common to this series of compounds. The singlet bands at δ = 1.6, δ = 2.25, and δ = 5.5 ppm, which are assigned to the pyrazole bridge methyl groups and C-4 proton, establish that this complex exists in solution as its trans isomer. This conclusion is further substantiated by the diastereotopic doubling of bands due to protons on the phosphinite ligand phenyl and alkoxy substituents. Figure 2.10a shows the aromatic region of this compound's 400 MHz NMR spectrum. The pair of overlapping doublets at δ = 7.8 and δ = 7.6 ppm are assigned to phosphinite ligand ortho protons. Signals for the corresponding meta and para protons appear as pairs of second order tiplets at δ= 7.4 , δ = 7.22 ppm and at δ = 7.48, δ = 7.30 ppm respectively. Figure 2.10b shows signals for the β and γ -methylene protons on the ligand alkoxy group. The β-methylene protons occupy significantly different magnetic environments in the metal complex and are split into a pair of complex mutiplets at δ = 4.8 and δ = 4.25 ppm. In contrast, the γ–methylene protons are not resolved into their individual diastereotopic bands at 400

Figure 2.9: ^{1}H NMR spectrum of $[Ir_2(Pz^*)_2(CO)_2(Ph_2POCH_2CH_2\text{-}2,4,6Me_3\text{-}Py)_2](Ph_4B)_2$ in d3-acetonitrile.

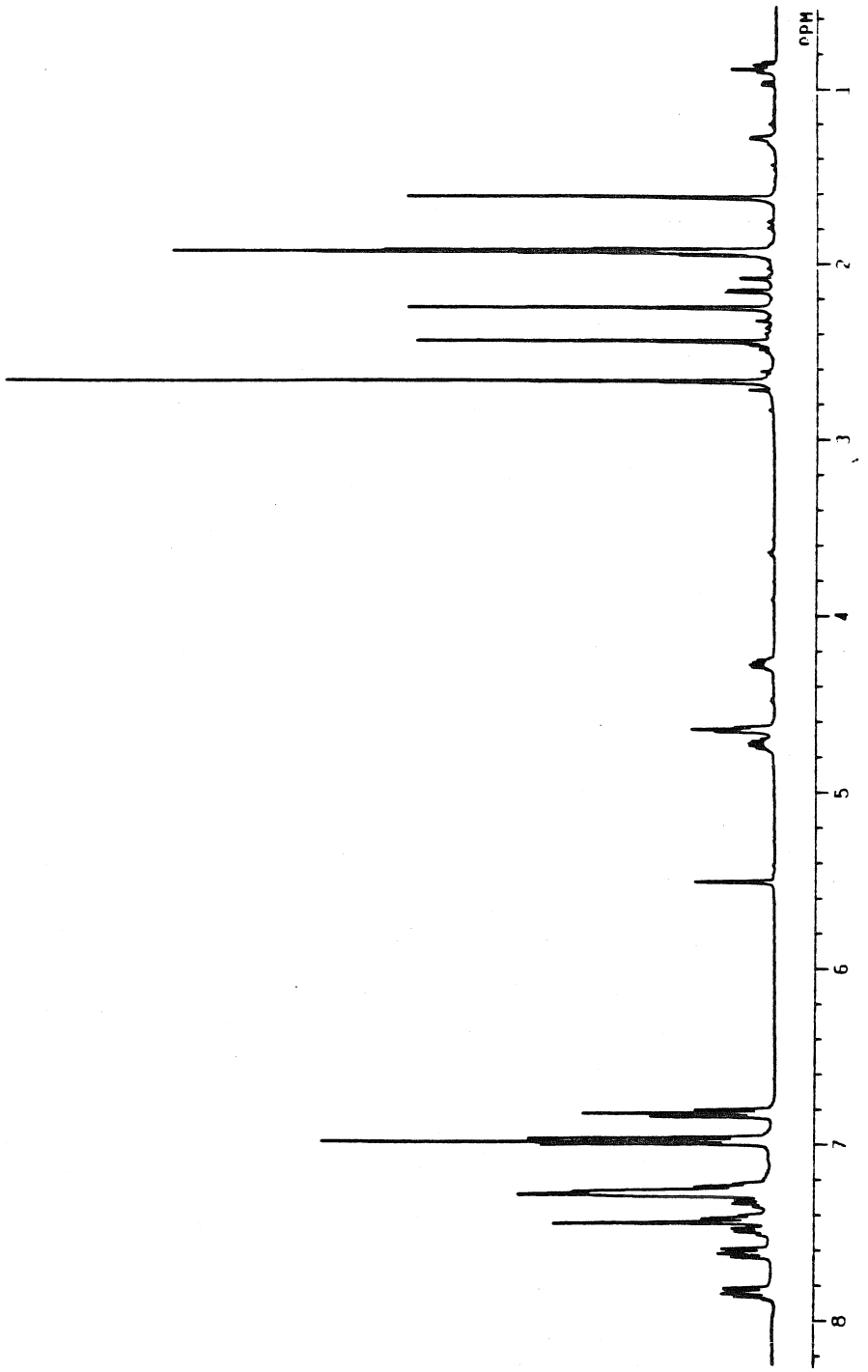
PPM
1
2
3
4
5
6
7
8

Figure 2.10: a) ^{1}H NMR spectrum of $[Ir_2(Pz^*)_2(CO)_2(Ph_2POCH_2CH_2\text{-}2,4,6Me_3\text{-}Py)_2](Ph_4B)_2$ showing the diasteriotopic chemical shifts for the phosphinite phenyl substituents. The pair of triplets (δ = 7.0 and δ = 7.15 ppm) and the complex multiplet (δ = 7.45 ppm) are due to the tetraphenylborate counterions. b) Diasteriotopic chemical shifts for the alkoxy group methylene protons.

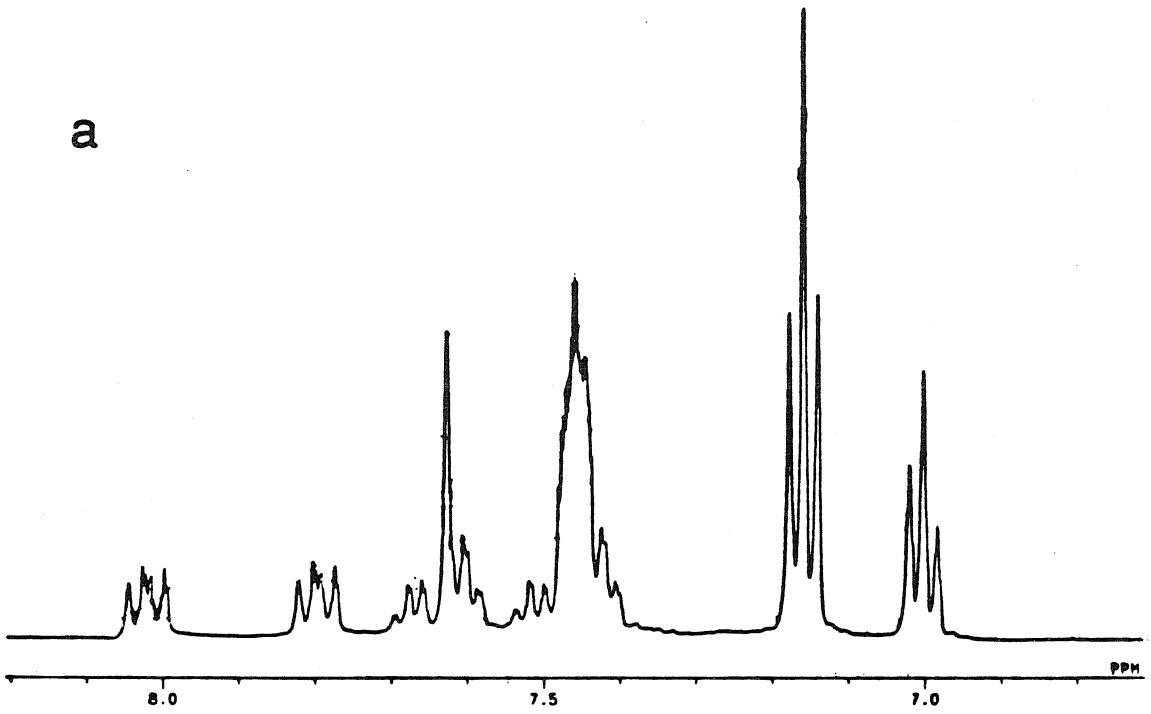
a
PPM
8.0
7.5
7.0

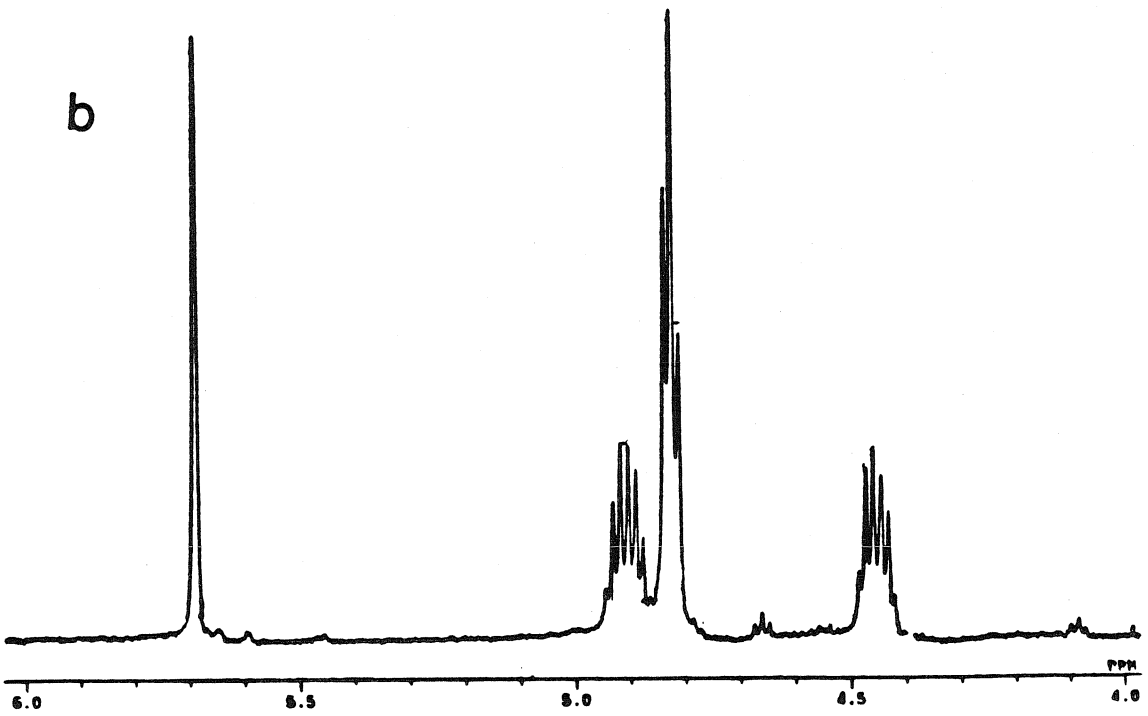
b
PPM
6.0
5.5
5.0
4.5
4.0

Figure 2.11 a and b: ^{1}H NMR spectra of $Ir_2(Pz^*)_2(CO)_2(Ph_2POCH_2CH_2CH_2CH_3)_2$ showing the change in the magnetic emvironments of the alkoxy group methylene protons as a function of distance from the compound's chiral center.

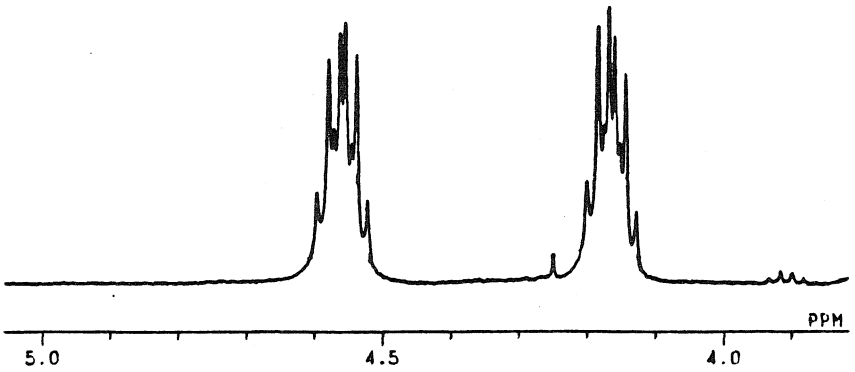

a

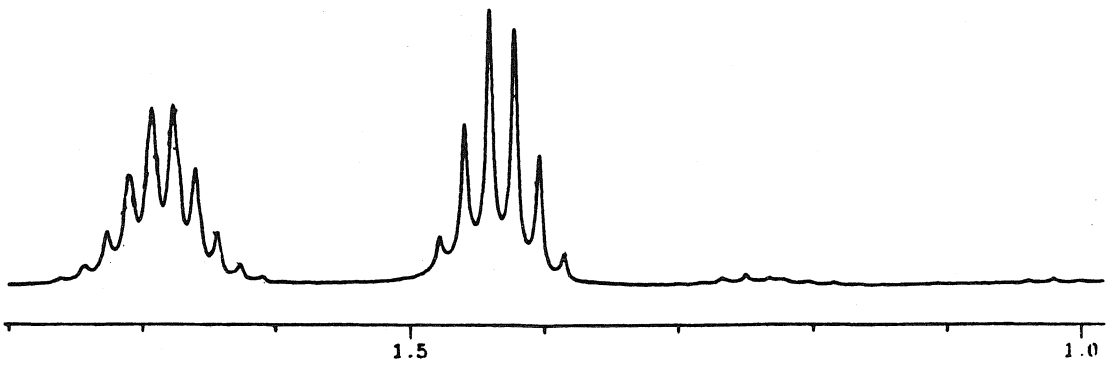

b

Figure 2.12: a) ^{1}H NMR spectrum of $Ir_2(Pz^{**})_2(CO)_4$ in d6-benzene. δ = 2.20 ppm (s; pyrazole CH_3), δ = 1.90 ppm (d; -CH_2 $CH(CH_3)_2$), δ = 1.45 (septet; -CH_2CH $(CH_3)_2$), δ = 0.7 ppm (d; -$CH_2CH(CH_3)_2$). b) ^{1}H NMR spectrum of $[Ir_2(Pz^{*})_2(CO)_2(Ph_2POCH_2CH_2$-4Ph-$Py)_2](Ph_4B)_2$ in d6-DMSO showing diasteriotopic chemical shifts for the pyrazole isobutyl substituents.

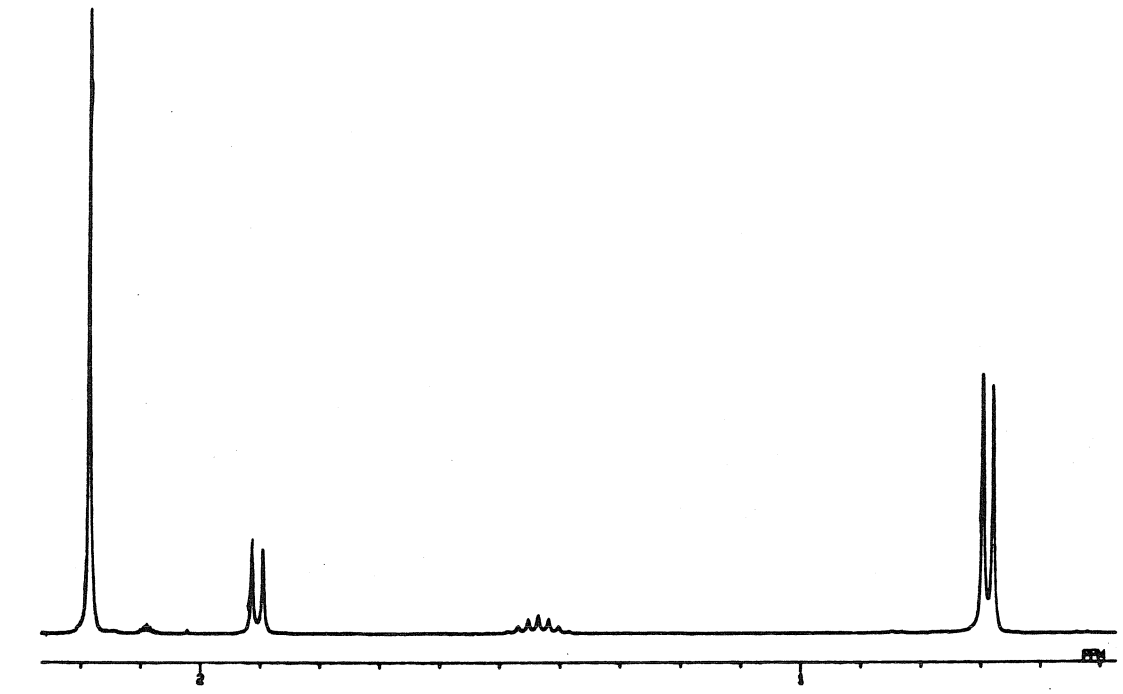

a

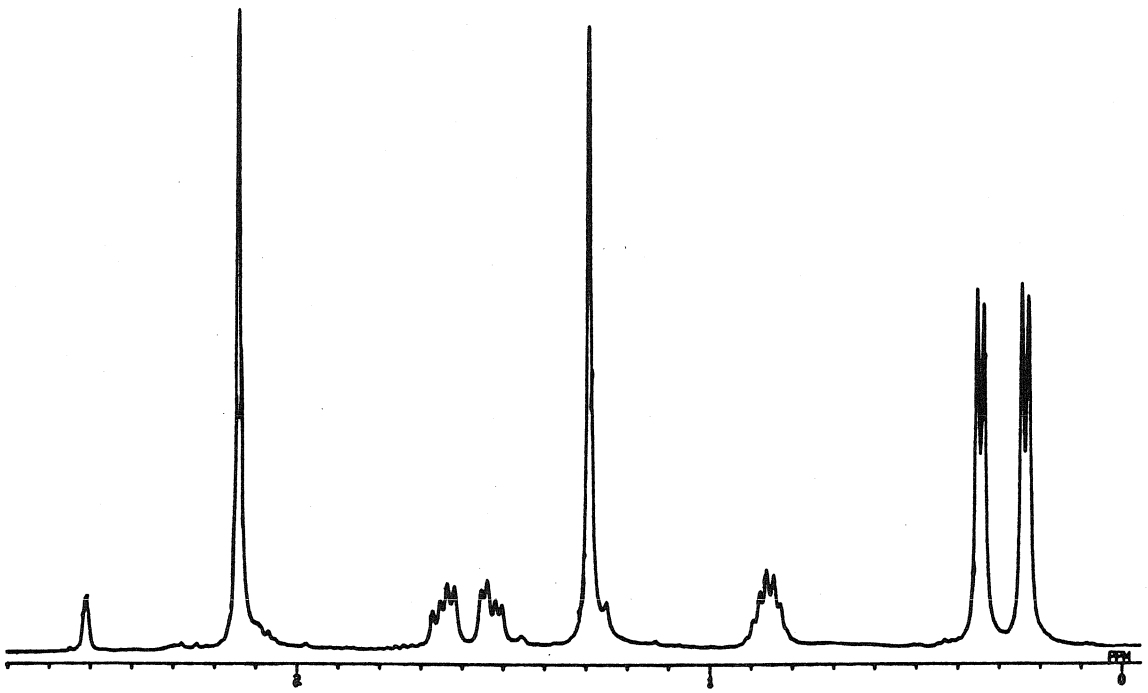

b

MHz and appear as a slightly second order triplet at δ = 4.74 ppm. A similar trend is observed for the β, γ, and δ-methylene bands in spectra of $Ir_2(Pz^*)_2(CO)_2(Ph_2POCH_2CH_2CH_2CH_3)_2$ (figure 2.11).

The diastereotopic chemical shifts seen in spectra of the bis (μ-3,5-dimethyl-4-isobutylpyrazole) complexes indicate that these compounds also possess a trans configuration of their terminal ligands. Figure 2.12a shows a 400 MHz proton spectrum of $[Ir_2(Pz^{**})_2(CO)_4]$(d6-benzene) and figure 2.12b the same spectral region for $[Ir_2(Pz^{**})_2(CO)_2(Ph_2POCH_2CH_2\text{-}4\text{-}Ph\text{-}Py)_2(Ph_4B)_2]$ (d6-DMSO) . The familiar doubling of signals for asymmetric ligand substituents seen earlier, is observed for the methyl and α-methylene protons of the pyrazole bridge isobutyl groups (δ = 0.35 and δ = 0.23; δ =1.63 and δ =1.55 ppm respectively). In addition to the diastereotopic doubling, the methylene protons are split into pairs of doublets most likely indicative of slowly introconverting rotational isomers along the isobutyl chain.

IR and ^{31}P NMR Spectra: Infrared spectra of $Ir_2(Pz^*)_2(CO)_2(Ph_2POCH_2CH_3)_2$ as fluorolube mulls show two strong bands attributable to CO stretches at ν_{CO} = 1955 cm^{-1} and 2010 cm^{-1}. The lower energy band is analogous to the CO bands seen in the redox active complexes and previously reported phosphine CO dimer compounds.[19,18,22] The higher energy band has not been reported previously and is most likely due to a solid state effect as it is not seen in solution spectra of this complex. Spectra of the remaining complexes all show a single broad CO stretch at 1955 cm^{-1}. ^{31}P NMR spectra showed a solitary singlet with chemical shifts between 95.02 and 104.29 ppm consistent with coordination of the phosphinite ligands to an Ir(I) metal center.[24]

Crystallographic Structure

To probe the structural properties of the iridium donor-acceptor complexes, the structure of $[Ir_2(Pz^*)_2(CO)_2(Ph_2POCH_2CH_2\text{-}Py)_2](Ph_4B)_2$ was determined using x-ray crystallographic structure techniques. Results from this study indicate that this complex possesses structural properties similar to those seen in a number of related iridium and rhodium pyrazolate bridge dimers.[19,18,22,25] An ORTEP drawing of this compound with atomic numbering is shown in figure 2.13; selected bond distances and angles are summarized in table 2.4.

The complex consists of two d^8 monomer fragments held in a face-to-face, A-frame configuration by a pair of 3,5-dimethylpyrazole bridging ligands. These ligands are nearly perpendicular to each other in the complex ($\theta = 94.2°$) and deviate only slightly from a planar geometry. The ND1A, ND1B, CD1A, CD1B, CD1C, CD1D, and CD1E atoms of the first pyrazole ring are displaced from the mean plane passing through them by 0.0, 0.0, 0.01, 0.03, 0.02, -0.02, and -0.03 Å; the ND2A, ND2B, CD2A, CD2B, CD2C, CD2D, CD2E atoms deviate from the plane passing through their pyrazolate ring by 0.0, -0.1, -0.02, 0.0, -0.04, -0.04, and -0.03 Å. The torsional angles summarized in table 2.5 indicate that the two iridium atoms and four pyrazole nitrogen atoms define a nearly perfect boat comformation. Interestingly, the two pairs of Ir-N-N angles in the boat differ by approximately 5° and are related by the molecule's C_2 axis. These minor deviations may reflect the different steric requirements of the complex's terminal CO and phosphine ligands. The metal-metal separation of 3.219(1) Å found in this complex is intermediate between those seen in the structures of $Ir_2(Pz)_2(CO)_2(Ph_3)_2$ and $Ir_2(Pz)_2(CO)_2(Ph_3)_2(C_6H_6)$ and is indicative of a

Figure 2.13: ORTEP drawing of $[Ir_2(Pz^*)_2(CO)_2(Ph_2POCH_2CH_2\text{-}Py)_2](Ph_4B)_2$.

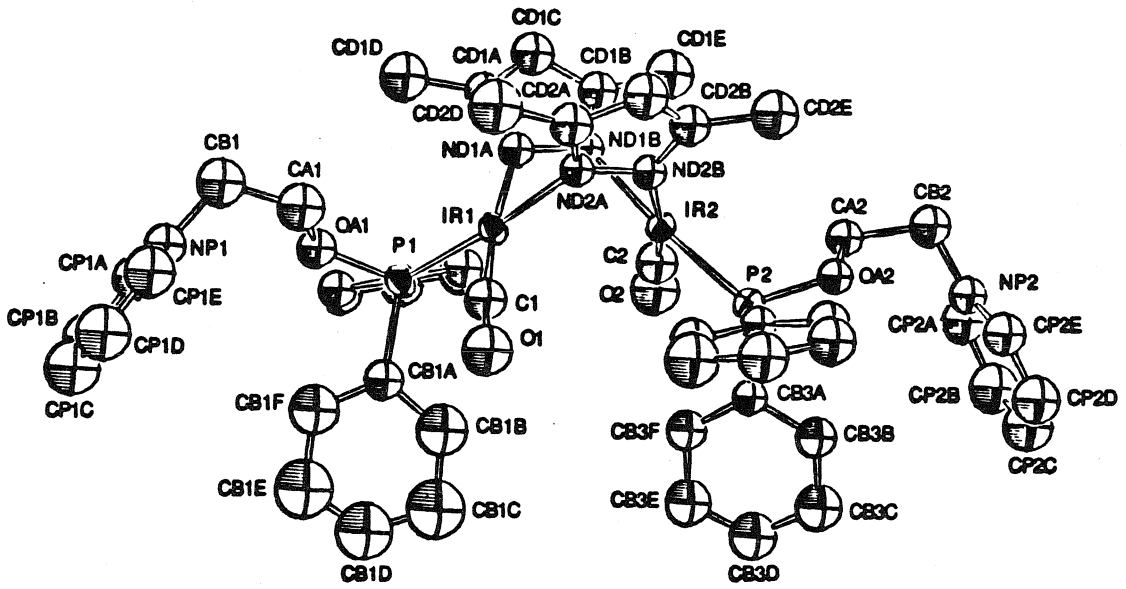
CD1C
CD1D
CD1A
CD1B
CD1E
CD2A
CD2D
CD2B
CD2E
ND1A
ND1B
ND2B
ND2A
IR1
IR2
CB1
CA1
OA1
NP1
P1
CP1A
CP1E
CP1B
CP1D
CP1C
C1
O1
C2
O2
P2
CA2
CB2
OA2
NP2
CP2A
CP2E
CP2B
CP2D
CP2C
CB1A
CB1F
CB1B
CB1E
CB1C
CB1D
CB3A
CB3F
CB3B
CB3E
CB3C
CB3D

Table 2.4 Selected Distances and Angles

Iridium Coordination Sphere

Distance(Å)		Angle(°)	
IR1 –IR2	3.219(1)	ND1A–IR1 –ND2A	83.0(4)
IR1 –C1	1.759(13)	C1 –IR1 –P1	90.1(4)
IR2 –C2	1.648(13)	ND2A–IR1 –C1	91.0(5)
IR1 –P1	2.217(3)	P1 –IR1 –ND1A	96.3(3)
IR2 –P2	2.216(3)	C1 –IR1 –ND1A	172.6(5)
IR2 –ND1B	2.066(9)	P1 –IR1 –ND2A	174.4(3)
IR1 –ND1A	2.045(9)	ND1B–IR2 –ND2B	83.2(3)
IR2 –ND2B	2.061(9)	C2 –IR2 –P2	95.1(5)
IR1 –ND2A	2.101(9)	ND1B–IR2 –C2	87.9(5)
		P2 –IR2 –ND2B	94.1(3)
		C2 –IR2 –ND2B	170.4(5)
		P2 –IR2 –ND1B	174.3(3)
		IR1 –ND2A–ND2B	119.2(7)
		IR1 –ND1A–ND1B	114.2(7)
		IR2 –ND1B–ND1A	119.5(7)
		ND2A–ND2B–IR2	114.2(7)

CO Ligands

Distance(Å)		Angle(°)	
C1 –O1	1.201(16)	O2 –C2 –IR2	179.1(12)
C2 –O2	1.260(17)	O1 –C1 –IR1	174.0(11)

Iridium to Pyridinium Distances

Distance(Å)	
IR1 –NP1	5.838(10)
IR2 –NP1	9.003(10)
IR2 –NP2	5.841(10)
IR1 –NP2	8.971(10)

Phosphine Ligands

Distance(Å)		Angle(°)	
P1 -OA1	1.635(8)	IR1 -P1 -OA1	116.1(3)
P1 -CB1A	1.812(13)	IR1 -P1 -CB1A	115.9(4)
P1 -CB2A	1.809(11)	IR1 -P1 -CB2A	120.6(4)
OA1 -CA1	1.478(16)	CB1A-P1 -CB2A	101.4(6)
CA1 -CB1	1.49(2)	CB1A-P1 -OA1	100.3(5)
CB1 -NP1	1.482(18)	CB2A-P1 -OA1	99.2(5)
P2 -OA2	1.639(8)	CB2A-P1 -CB1A	101.4(6)
P2 -CB3A	1.803(12)	P1 -OA1 -CA1	118.8(7)
P2 -CB4A	1.795(12)	OA1 -CA1 -CB1	106.3(11)
OA2 -CA2	1.454(14)	CA1 -CB1 -NP1	113.8(12)
CA2 -CB2	1.557(17)	IR2 -P2 -OA2	115.1(3)
CB2 -NP2	1.474(16)	IR2 -P2 -CB3A	117.9(4)
		IR2 -P2 -CB4A	118.9(4)
		CB3A-P2 -CB4A	101.6(5)
		CB3A-P2 -OA2	101.0(5)
		CB4A-P2 -OA2	99.1(5)
		CB4A-P2 -CB3A	101.6(5)
		P2 -OA2 -CA2	116.1(7)
		OA2 -CA2 -CB2	105.1(9)
		CA2 -CB2 -NP2	111.5(10)

Pyrazole Bridging Ligands

Distance(Å)		Angle(°)	
ND1A-ND1B	1.359(13)	CD1A-ND1A-IR1	139.6(8)
ND1A-CD1A	1.365(15)	CD1A-ND1A-ND1B	105.7(9)
ND1B-CD1B	1.337(16)	CD1B-ND1B-ND1A	109.8(9)
CD1A-CD1C	1.360(18)	CD1B-ND1B-IR2	130.7(8)
CD1A-CD1D	1.49(2)	CD1C-CD1A-ND1A	110.7(11)
CD1B-CD1C	1.39(2)	CD1D-CD1A-ND1A	118.9(11)
CD1B-CD1E	1.48(2)	CD1D-CD1A-CD1C	130.3(12)
ND2A-ND2B	1.345(13)	CD1C-CD1B-ND1B	108.6(11)
ND2A-CD2A	1.340(16)	CD1E-CD1B-ND1B	121.2(12)
ND2B-CD2B	1.347(15)	CD1E-CD1B-CD1C	130.0(12)
CD2A-CD2C	1.39(2)	CD1B-CD1C-CD1A	105.1(12)
CD2A-CD2D	1.49(2)	CD2A-ND2A-ND2B	110.8(9)
CD2B-CD2C	1.34(2)	CD2B-ND2B-IR2	139.3(8)
CD2B-CD2E	1.52(2)	CD2B-ND2B-ND2A	105.6(9)
		CD2C-CD2A-ND2A	106.6(11)
		CD2D-CD2A-ND2A	123.9(12)
		CD2D-CD2A-CD2C	129.4(13)
		CD2C-CD2B-ND2B	111.1(11)
		CD2E-CD2B-ND2B	118.6(11)
		CD2E-CD2B-CD2C	130.4(12)
		CD2B-CD2C-CD2A	105.9(12)

Table 2.5 Selected Torsional Angles

Atoms	Angle (°)
Ir1-P1-OA1-CA1	-22.03
P1-OA1-CA1-CB1	-180.74
OA1-CA1-CB1-NP1	-285.02
Ir2-P2-OA2-CA2	-36.19
P2-OA2-CA2-CB2	185.65
OA2-CA2-CB2-NP	272.19
Ir1-ND1A-ND1B-Ir	25.76
Ir1-ND2A-ND2B-Ir	25.61
ND1A-ND1B-Ir2-ND2B	-68.88
ND2B-ND2A-Ir1-ND1A	-68.45
ND2A-ND2B-Ir2-ND1B	58.25
ND1B-ND1A-Ir1-ND2A	58.18

ground state metal-metal interaction similar to that described earlier for a number of d^8-d^8 metal dimers.[26,19,6] Notably, the terminal phosphinite and carbon monoxide ligands adopt a trans configuration with respect to the compound's metal-metal axis, which is consistent with the NMR spectroscopic data discussed in the previous section.

The coordination environment around each of the two iridium atoms in $[Ir_2(Pz^*)_2(CO)_2(Ph_2POCH_2CH_2\text{-}Py)_2](Ph_4B)_2$ is approximately square planar. The bond angles between adjacent ligands in each of the square planes are close to 90° with the N-Ir-N angles consistently smaller than the other L-P-L angles. Both of the d^8 monomer fragments deviate from a rigorous planar geometry. The displacements of the Ir1, ND1A, ND2A, C1, P1 and Ir2, ND1B, ND2B, C2, P2 atoms from the mean planes passing through them are -0.015, -0.076, 0.095, -0.087, 0.083 and 0.017, -0.082, 0.061, 0.072, -0.068 Å, respectively. The Ir1-C1 and Ir2-C2 bond lengths differ by approximately 0.1 Å. This difference can be attributed to systematic errors in correcting the diffraction intensities for iridium absorption effects based on two observations made during the structure refinement process. Least squares refinements were carried out on two different data sets. One was corrected for heavy atom absorption, while a second data set was left in its uncorrected form. With the exception of the Ir1-C1 and Ir2-C2 bonds, structures refined from both data sets were nearly identical. It was found that the disparity in the Ir-CO bond lengths was larger in structures refined from uncorrected diffraction data. Secondly, structures refined using only high angle reflections had Ir-CO bond lengths that were the same within their estimated standard deviations. Because low angle reflections are more sensitive to errors incurred from heavy atom absorption, this result further substantiates that the 0.1Å difference in the Ir-CO bond lengths is due to Ir x-ray absorption effects.

The bond lengths and angles for comparable substituents on each of the phosphinite ligands in this complex are the same within their estimated standard

deviations. In additon, the torsional angles along the ligands' alkoxy subtituents are similar indicating that the molecules possess implicit C_2 symmetry in the solid state. Both ligands adopt a rotational conformation about the Ir-P bond which avoids less favorable steric interactions between the phosphine phenyl groups and the bridging pyrazole ligands. While this solid state conformation represents a lower energy configuration of the Ir-P rotational coordinate, other conformations are most likely accessible in fluid solution (vida infra). The Ir-P-O-C and P-O-C-C torsional angles in the ligand alkoxy groups are substantially less than 180° and leave the three atom bridging group linking the pyridinium cation to the metal complex partially extended. This particular solid state conformation occurs, most likely, as a results of crystal packing forces. The 5.9 Å through space distance between the two redox partners is intermediate in value between that for a fully extended chain (6.9 Å) and for their Van der Waals contact distance.

Discussion

In the previous sections a detailed description was given of the preparation and characterization of the d^8-d^8 intramolecular redox molecules, which will form the focus of the subsequent chapters of this thesis. These results will now be examined with regards to: 1) the scope of the synthetic methodologies developed toward preparing a wide variety of donor-acceptor molecules. 2) Structural relationships amongst these complexes and related d^8-d^8 A-frame complexes. 3) The conformational properties of the redox ligands and the range of intramolecular electron-transfer distances available in these complexes.

Synthetic Methodology: A long term goal of this research program is to design, synthesize, and study intramolecular electron-transfer systems to understand kinetic

factors such as reaction exoergicity, donor-acceptor separation and orientation, and solvent dynamical effects in electron-transfer reactions. Central to the pursuance of this goal is the development of synthetic methodologies that are flexible enough to allow the redox potentials of the donor and acceptor, the electronic properties of the bridging group, and the donor-acceptor separation to be readily varied within a series of redox complexes. The approach to forming a covalent linkage between an electron donor and acceptor presented in this study posseses two important features for developing a range of different donor-acceptor systems. In contrast to some recently reported excited state donor-acceptor systems based on porphyrins[27,2b] and bipyridyl transition metal complexes,[28] the redox active phosphine approach outlined in this study is not restricted to a particular inorganic complex. In principle, redox phosphinite ligands could be used to probe excited state ET reactions in any chromophore containing phosphine ligands. Studies spanning a range of different inorganic chromophores will be important in understanding variations in electron transfer rates as a function of the nature of the excited donor. In addition, the synthetic methodology developed here may prove to be general enough to allow for detailed studies of the medium effects that control excited state ET processes. The range of electronically different bridging groups, which could be incorporated into a series of redox active ligands, should be limited only by the availability of a corresponding haloalcohol. Research involving the preparation and study of new ligands and complexes is currently being pursued in our laboratories.

Future studies designed to explore the driving force dependence of electron transfer in the $[Ir_2(Pz^*)_2(CO)_2(Ph_2POCH_2CH_2\text{-}Py\text{-}R)_2]$ systems will require a series of complexes spanning a range of reaction driving forces. The reaction exoergicity in these complexes can, in principle, be controlled by varying substituents on the pyridinium aromatic ring. The viability of this approach has been demonstrated in bimolecular driving force studies.[5,6] While the synthetic methodologies developed in

this chapter can be used to prepare ligands containing several different pyridinium cations, there were some notable exceptions, which warrant further discussion. The alcoholysis reaction of N,N-dimethyl-P,P-diphenylphosphine proved useful in synthesizing a number of redox ligands with higher electrochemical reduction potentials, but it could not be extended to the preparation of ligands containing more activated pyridinium cations. Based on the current literature, the difficulties surrounding these reactions were attributed to irreversible ring opening reactions between dimethylamine and the more reactive cyano and carbomethoxy pyridinium cations.[16] Several different R_2NH leaving groups were assayed with regard to their reactivity toward 4-cyano-1-methylpyridinium, but none were found to be inert enough to avoid pyridinium ring opening as a rapid side reaction. Thus, reactions that avoid secondary amines as a reaction side product must be developed to prepare ligands with lower electrochemical reduction potentials.

Two alternative approaches to preparing diphenylphosphine esters, which would circumvent this problem, are shown in figure 2.14. Reaction 5 is based on the facile alcoholysis reactions of phosphinous acid chlorides.[15] In this particular case, polyvinylpyridine (PVP) acts as a proton sponge for scavanging HCl liberated during the reaction. Features of this approach, which make it attractive, are its mild reaction conditions and the ease with which the products can be isolated from PVP-HCl. Preliminary results along these lines have shown promise.[29] Reaction 6 is based on some recent work published by Batyeva[30] and coworkers and represents an extension of Nifant'ev's research on acid catalyzed reactions of phosphrous III amides.[31] Attractive features of this approach are that it could be carried out under mild reaction conditions and that the dimethylamine liberated during the reaction is sequestered as its corresponding acetamide. Either of these approaches could serve as viable routes to

Figure 2.14: Alternative reactions for preparing high driving force redox ligands.

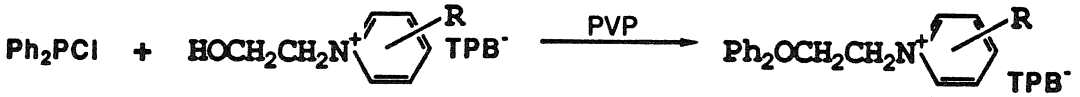

(Reaction 5.)

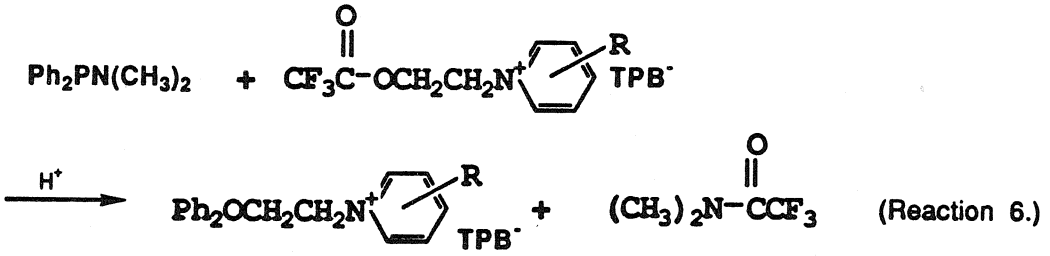

(Reaction 6.)

ligands with redox potentials outside the range available with the current compounds.

Structural Properties: An understanding of intramolecular electron transfer in the donor-acceptor systems prepared here will be developed by making comparisons between the photophysical properties of the redox active complexes and their corresponding "model compounds." An underlying assumption of this approach is that the complexes represent a structurally and electronically homologous series of compounds. The electronic properties of the redox complexes and model compounds are investigated in detail in chapter three. The structural similarity between these molecules follows from the NMR and IR spectroscopic results presented in this chapter. These data clearly establish that all of the d^8-d^8 complexes contain two terminal carbon monoxide and phosphinite ligands arranged in a trans configuration with respect to the metal-metal axis.

The crystal structure of $[Ir_2(Pz^*)_2(CO)_2(Ph_2POCH_2CH_2\text{-}Py)_2](Ph_4B)_2$ shows that the complexes are structurally related to perviously reported d^8-d^8 A-frame complexes.[38] As seen in table 2.16 the metal-metal separation in this complex is similar to those reported earlier for a number of analogous metal dimers. Previous studies have shown that the unique electronic and photophysical properties of d^8-d^8 A-frame metal dimers arise from the pseudoaxial interactions between their Ir(I) metal centers.[39] These data (table 2.16) suggest that the photophysical models developed for $[Ir_2(Pz\text{-}R)_2(COD)_2]$[6] and $Ir_2(Pz^*)_2(CO)_2(Ph_3P)_2$[32] may serve as reference points for understanding the photophysics of the donor-acceptor complexes. This concept will be explored to a greater extent in chapter 3.

ET Distance: During the past decade detailed theoretical and experimental studies concerning the electronic factors that control electron-transfer reactions have

Table 2.6: Metal-Metal Bond Distances for Selected A-Frame Complexes

Compound	d(Å)
$[Ir_2(Pz^*)_2(CO)_2(Ph_2POCH_2CH_2\text{-}Py)_2](Ph_4B)_2$	3.219(1)
[a] $Ir_2(Pz)_2(CO)_2(Ph_3P)_2$	3.163(2)
[b] $Ir_2(Pz)_2(COD)_2$	3.216(1)
[b] $Ir_2(3,4,5\ Me_3)_2(COD)_2$	3.096(1)

a. See reference 19.
b. See reference 6 and references cited there.

indentified donor-acceptor separation and orientation as two primary ET variables. Hopfield has proposed an approximately exponential distance dependence for ET reactions as a consequence of long range overlap between the "wavefunction tails" for the transfering electron.[33] Explicit models directed toward understanding the roles played by bridging groups in donor-acceptor systems have more recently been developed by Beratan and Onuchic within this general framework.[34] Concurrent with developing theories, a number of fixed distance, fixed orientation donor-acceptor systems have appeared in the literature for studying medium effects in electron-transfer reactions. Such systems have employed a variety of bridging groups, ranging from synthetically prepared organic spacers to genetically engineered metalloproteins.[4a] Central to this area of electron-transfer research is understanding what constitutes the "electron-transfer medium" and how this medium facilitates the ET process. A detailed understanding of these effects will develop from the design and study of systems that carefully vary molecular ET parameters in a systematic fashion.

While the donor-acceptor systems reported in this chapter lack the structural rigidity necessary for studying distance and orientation effects in electron transfer, the three atom linker in these d^8-d^8 complexes should restrict the distances and orientations for ET to a more limited range of values than those available in bimolecular reactions. A qualitative understanding of this range of values can be developed by using NMR spectra of $[Ir_2(Pz^*)_2(CO)_2(Ph_3P)_2]$ in conjunction with results from a molecular graphics and mechanics analysis of $[Ir_2(Pz^*)_2(CO)_2(Ph_2POCH_2CH_2\text{-}Py)_2](Ph_4B)_2$.

A consideration of CPK models of $[Ir_2(Pz^*)_2(CO)_2(Ph_2POCH_2CH_2\text{-}Py)_2](Ph_4B)_2$ shows that there are essentially two types of internal rotations that alter the distance and orientation between the iridium atoms and pyridinium aromatic

Figure 2.15: Structure showing the torsional angles pertinent to variations in the electron-transfer distance in $[Ir_2(Pz^*)_2(CO)_2(Ph_2POCH_2CH_2\text{-}Py)_2](Ph_4B)_2$.

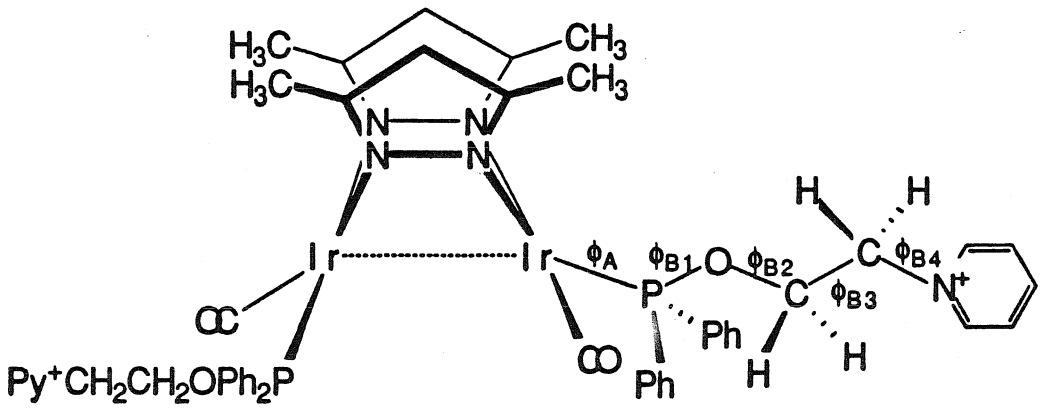
H3C
CH3
H3C
CH3
N
N
N
N
Ir
Ir
CC
CO
Py+CH2CH2OPh2P
ϕA
ϕB1
O
ϕB2
ϕB3
P
Ph
Ph
C
H
H
H
H
C
ϕB4
N+

Figure 2.16 a, b, and c: Structures showing three different phosphinite ligand rotational conformations, which are related by a 120° rotation about the Ir-P bond (ϕ_A). R_1 and R_2 are the through space distances between the lefthand pyridinium nitrogen and its proximal and distal iridium atoms respectively. Cross hatched spheres represent the heteroatoms. Sphere sizes were chosen for the purpose of clarity and should not be interpreted as thermal ellipsoids. In each case $\phi_{B1} = \phi_{B2} = \phi_{B3} = 180°$; $\phi_{B4} = 90°$.

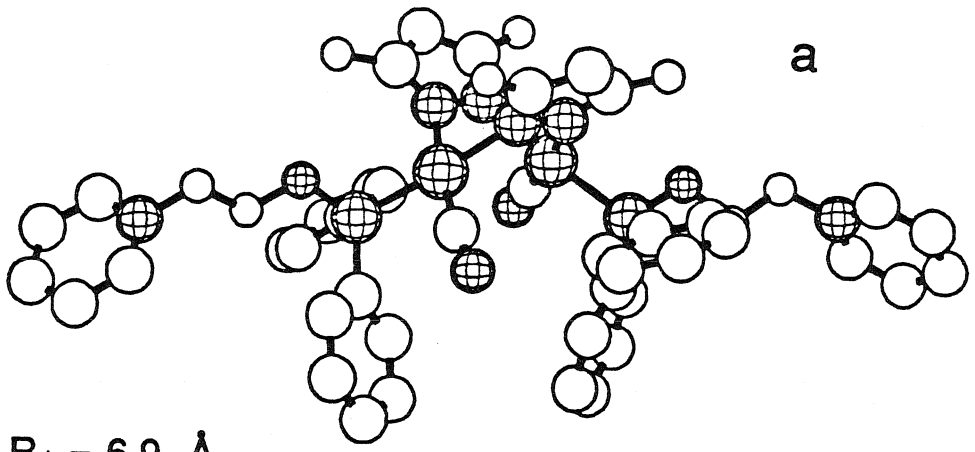

R_1 = 6.9 Å

R_2 = 9.8 Å

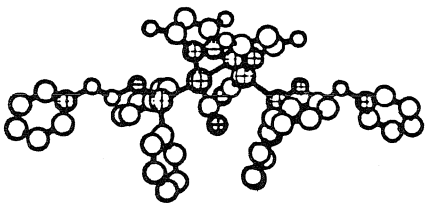

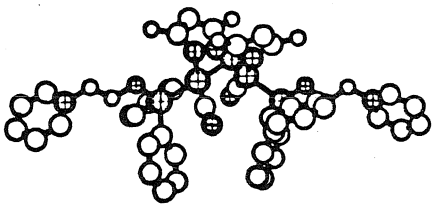

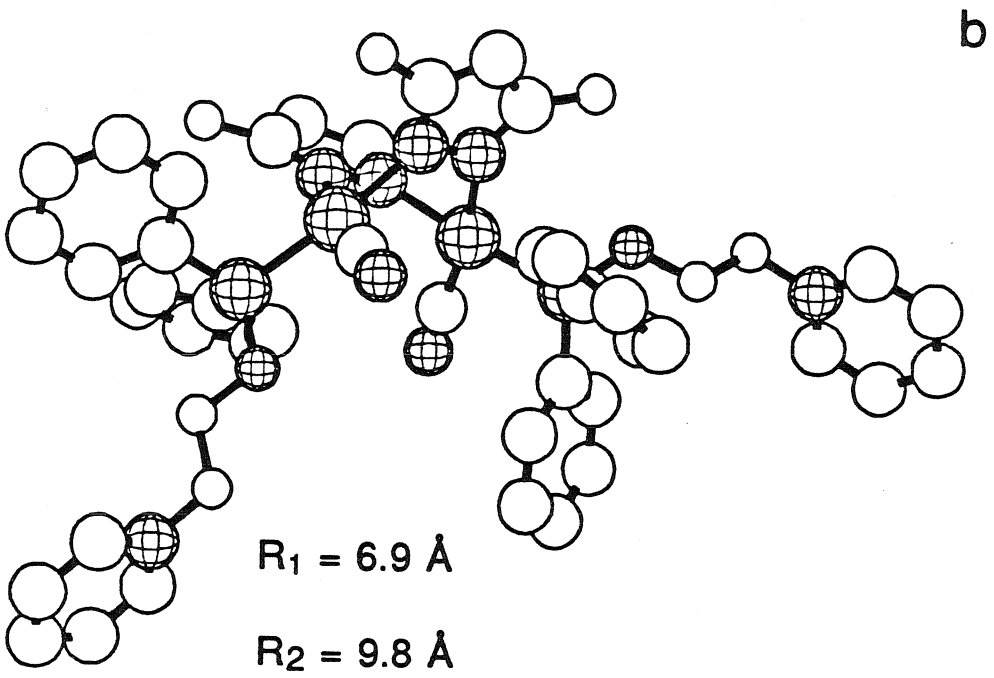
b
R_1 = 6.9 Å
R_2 = 9.8 Å

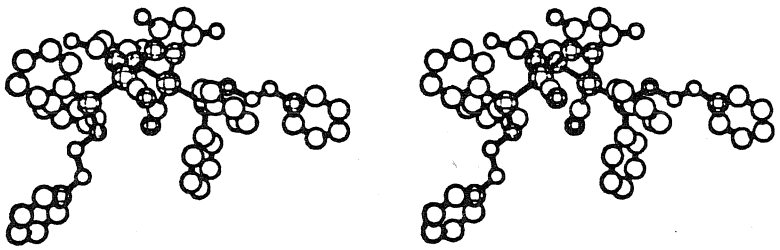

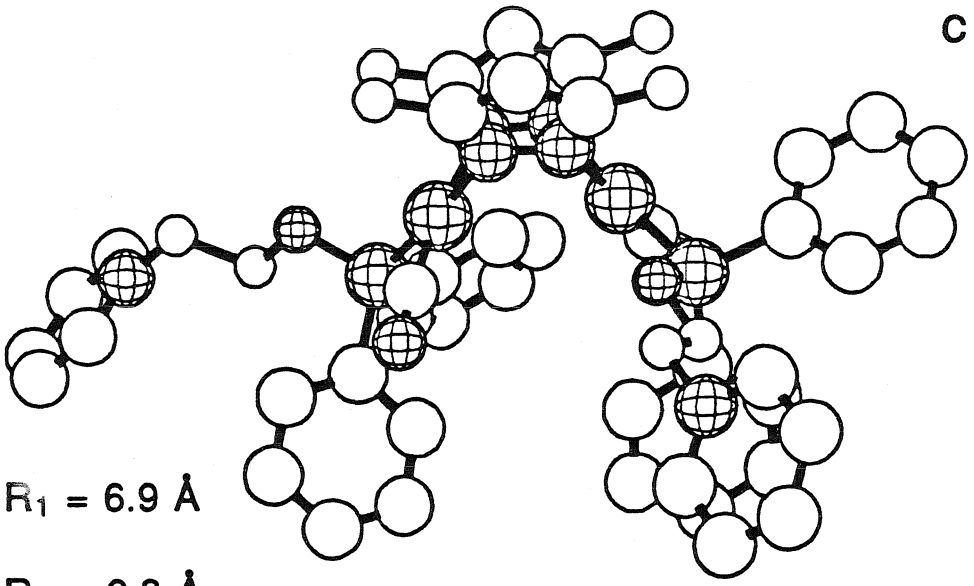
C
R_1 = 6.9 Å
R_2 = 9.8 Å

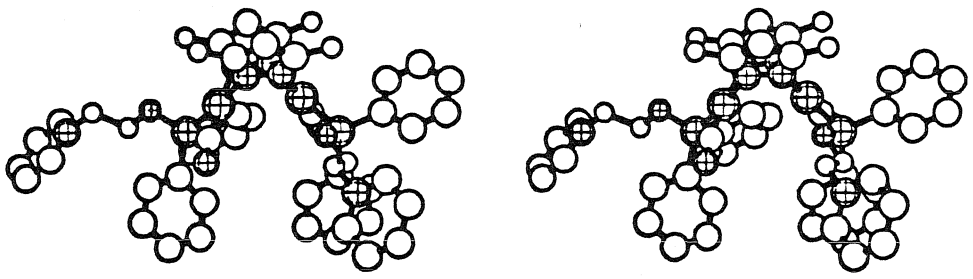

ring (figure 2.15). Rotations about either of its Ir-P bonds (ϕ_A) drastically affects the relative orientation of the two redox partners. As seen in figures 2.16 a,b,c this rotation essentially allows the pyridinium cation to access different regions of the iridium dimer chromophore. Conformation I (figure 2.16a) probes distances and orientations over one of the square planar ends of the molecule, while conformations II (figure 2.16b) and III (figure 2.16c) access regions below the terminal ligands and approximately perpendicular to the pyrazole ligands, respectively. Within each of these three Ir-P conformers, rotations about bonds along the linker backbone(ϕ_{B1}, ϕ_{B2}, ϕ_{B3},ϕ_{B4}) change the donor-acceptor distance over a region of the iridium dimer dictated by ϕ_A. Rigid geometry conformational mapping calculations indicate that the through space distance separating the two redox partners varies between limiting values of 6.9 to 5.0 Å as a function of ϕ_{B1}, ϕ_{B2}, ϕ_{B3}, and ϕ_{B4}. Examples of the different ligand geometries found from this analysis are shown in figures 2.17a-k. In some configurations, the through space separation[35] between each of the complex's iridium metal centers and pyridinium ring are almost identical, while in other conformations these distances are very different. Therefore, distances from a pyridinium nitrogen atom to both of the iridium metal centers are reported with each structure.

This analysis indicates that there are a considerable number of orientations and donor-acceptor separations available to the $[Ir_2(Pz^*)_2(CO)_2(Ph_2POCH_2CH_2\text{-}Py\text{-}R)_2]$ redox systems. The true range of conformers present in solutions of these complexes will depend on the activity of each of their internal rotational degrees of freedom. C^{13} NMR T_1 measurements have indicated that internal rotations in aliphatic hydrocarbons produce a distribution of solution conformers that exchange on a picosecond time scale. At the present time, the activity of the spacer group rotations can be inferred from these results. Further studies will be necessary to characterize these degrees of freedom and their effect on photoinduced electron transfer processes in our compounds. Careful

consideration of the proton NMR spectrum of $[Ir_2(Pz^*)_2(CO)_2(Ph_3P)_2]$ indicates that motion about the Ir-P bonds in the $[Ir_2(Pz^*)_2(CO)_2(Ph_2POCH_2CH_2\text{-}Py\text{-}R)_2]$ complexes must also be important in determining their range of solution conformations. If the triphenylphosphine phenyl groups in $[Ir_2(Pz^*)_2(CO)_2(Ph_3P)_2]$ interconvert via intramolecular rotations, NMR spectra of this complex should show at most three groups of multiplets for its ligand aromatic protons. As seen in figure 2.18 the ortho, meta and para protons in this complex appear a complex mutiplet at δ = 7.8 ppm (ortho) and a singlet at δ = 7.0 ppm (meta+para), indicating that the ligand phenyl groups exchange magnetic environments on an NMR timescale. Based on Tolman cone angle arguments,[36] rotations about ϕ_A in $[Ir_2(Pz^*)_2(CO)_2(Ph_2POCH_2CH_2\text{-}Py])_2]$ should be hindered mainly by its phosphinite phenyl substituents. Because this rotational degree of freedom is active in $[Ir_2(Pz^*)_2(CO)_2(Ph_3P)_2]$, it should be active in the donor-acceptor complexes as well.

In a bimolecular electron-transfer reaction the value of k_{obs} is controlled by the relative rates of electron transfer and molecular diffusion. Under steady-state conditions, "reactive pairs" of redox partners are formed via diffusional processes and are subsequently transformed into products[37]. If $k_{ET} >> k_{diff}$, as is the case in many excited state ET reactions, then the observed reaction rate becomes diffusion limited. In a "fixed site" donor-acceptor system the redox partners are held at a constant distance and orientation by a rigid covalent linkage. Here, k_{obs} is determined solely by factors that govern k_{et}, because the reactants have been synthetically preassembled into reactant pairs. The structural analysis presented above suggests that electron transfer in these $[Ir_2(Pz^*)_2(CO)_2(Ph_2POCH_2CH_2\text{-}Py\text{-}R])_2]$ complexes may occur under the influence of a pairwise diffusional process not found in either bimolecular reactions or in fixed site ET systems. The redox partners in these complexes are assembled into

Figure 2.17 a-d: Structures showing variations in the orientation and distance between the pyridinium cation and iridium dimer as a function of $\phi B1$, $\phi B2$, $\phi B3$, and $\phi B4$ for ligand conformation I (figure 2.15a). R_1 and R_2 are the through space distance between the lefthand pyridinium nitrogen and its proximal and distal iridium atoms respectively.

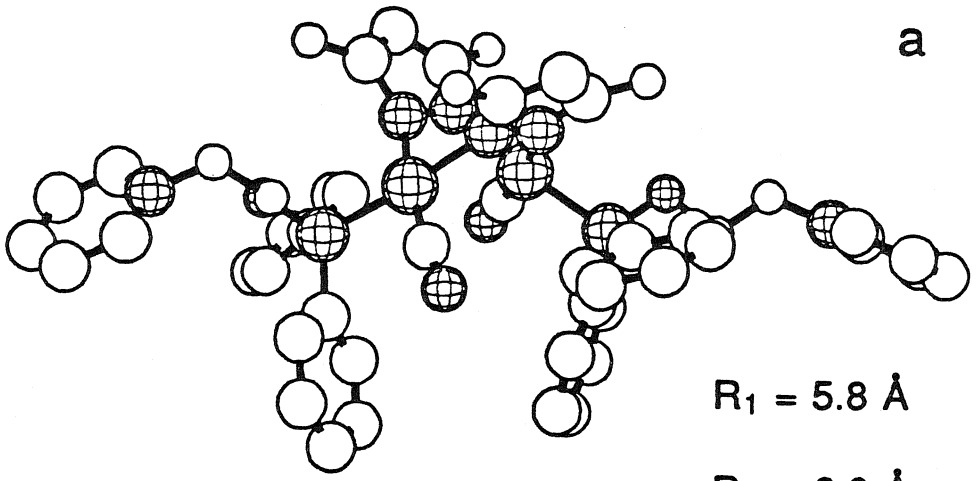
a
R_1 = 5.8 Å
R_2 = 8.9 Å

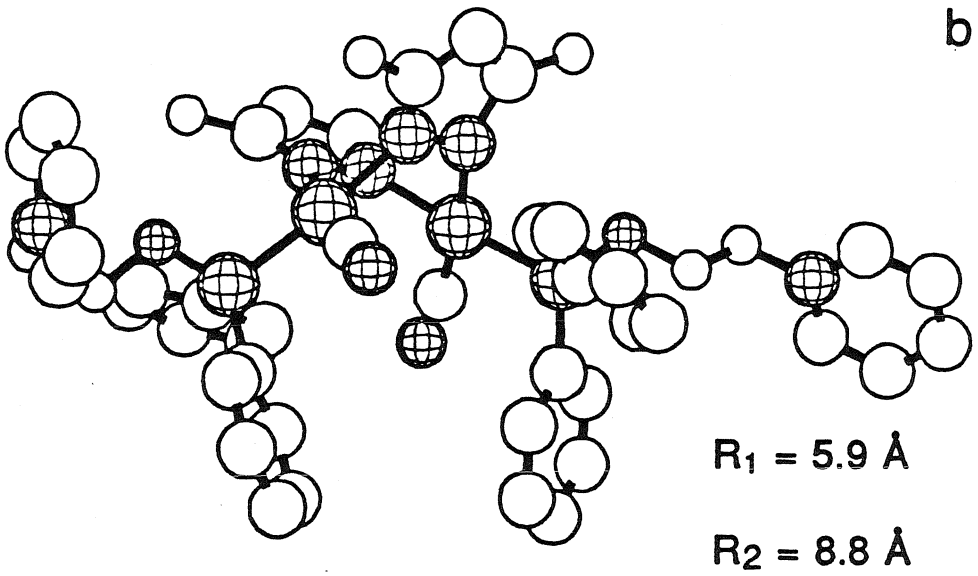
b
R_1 = 5.9 Å
R_2 = 8.8 Å

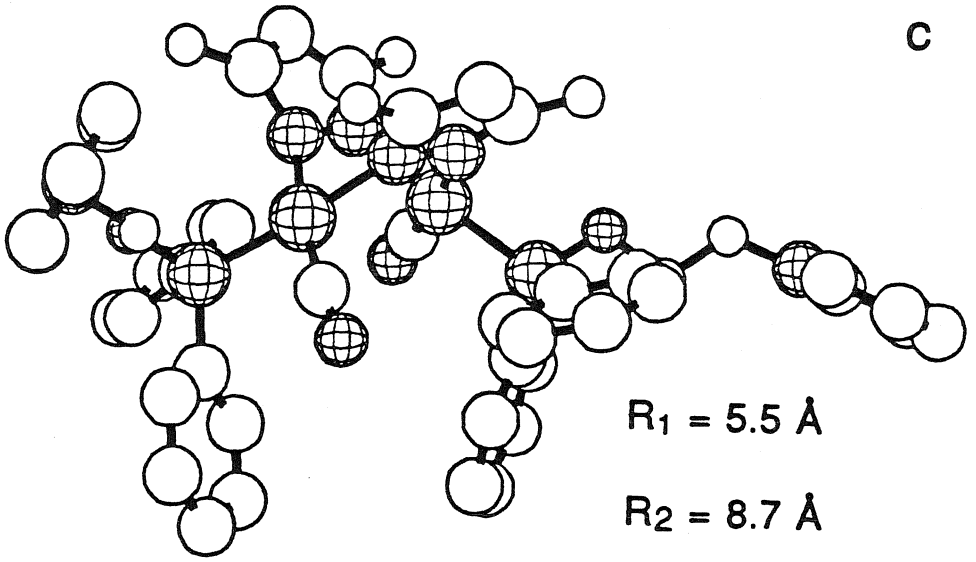
c
R_1 = 5.5 Å
R_2 = 8.7 Å

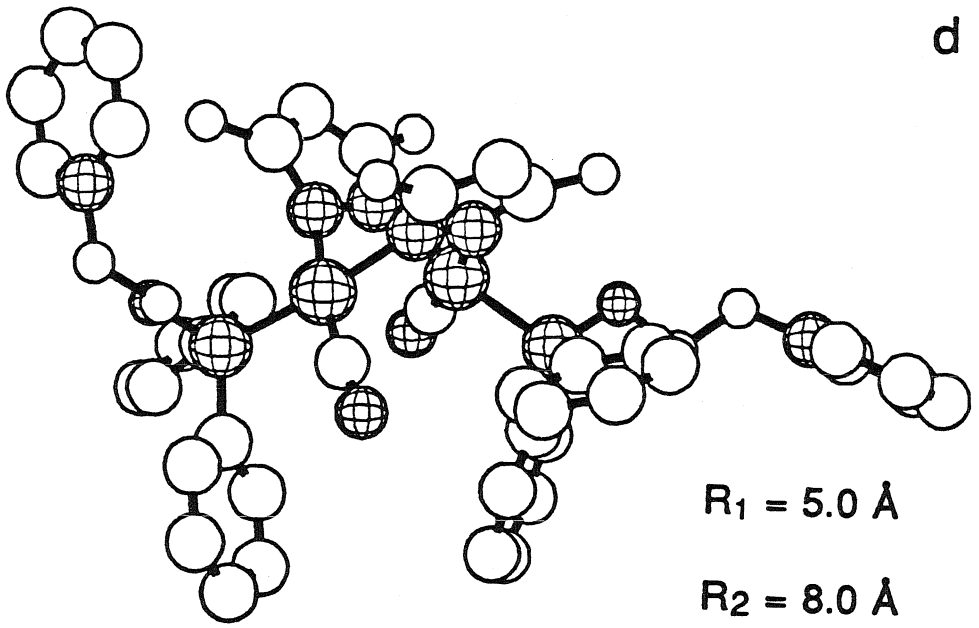
d
R_1 = 5.0 Å
R_2 = 8.0 Å

Figure 2.17 e-h: Structures showing variations in the orientation and distance between the pyridinium cation and iridium dimer as a function of $\phi B1$, $\phi B2$, $\phi B3$, and $\phi B4$ for ligand conformation II (figure 2.15b). R_1 and R_2 are the through space distance between the lefthand pyridinium nitrogen and its proximal and distal iridium atoms respectively.

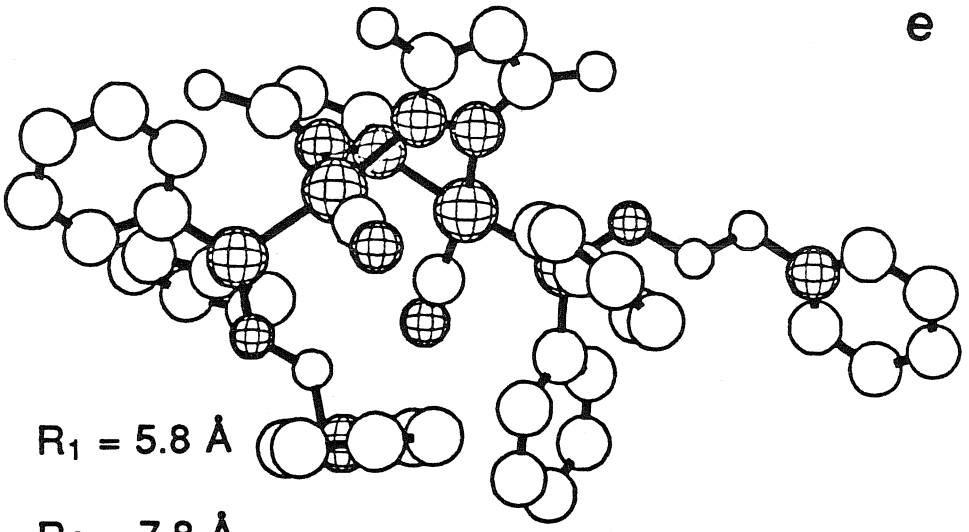
e
R_1 = 5.8 Å
R_2 = 7.8 Å

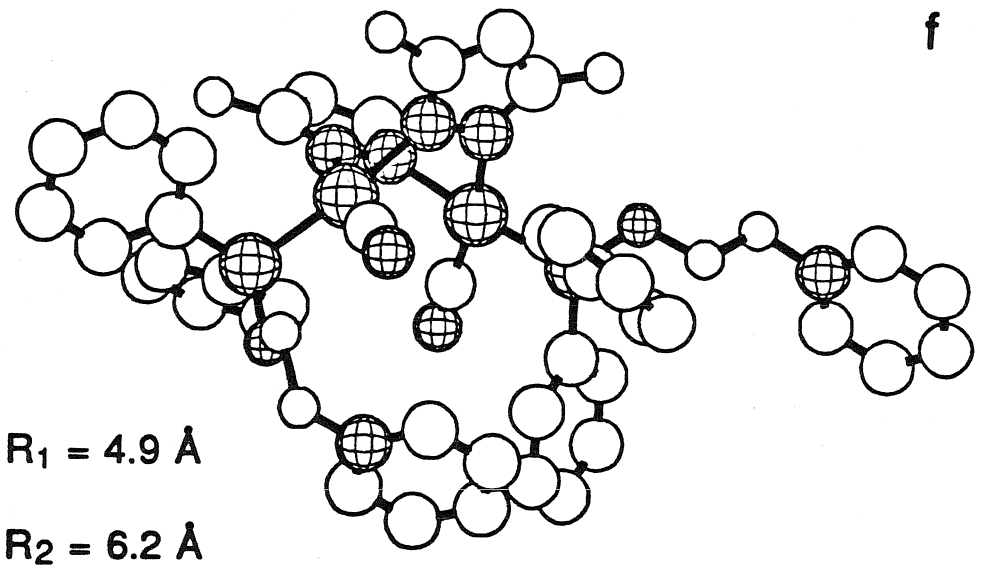
f
R_1 = 4.9 Å
R_2 = 6.2 Å

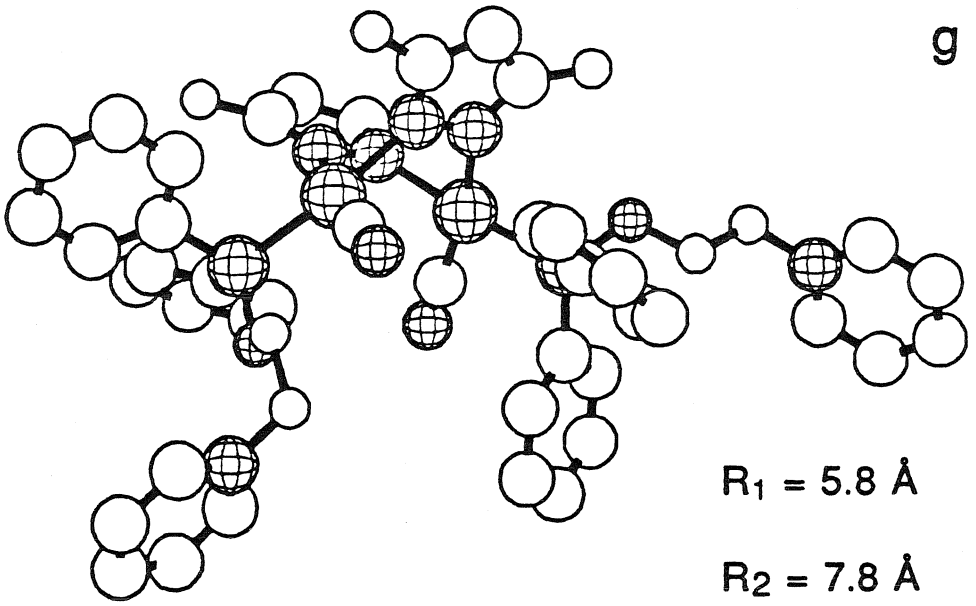
g
R_1 = 5.8 Å
R_2 = 7.8 Å

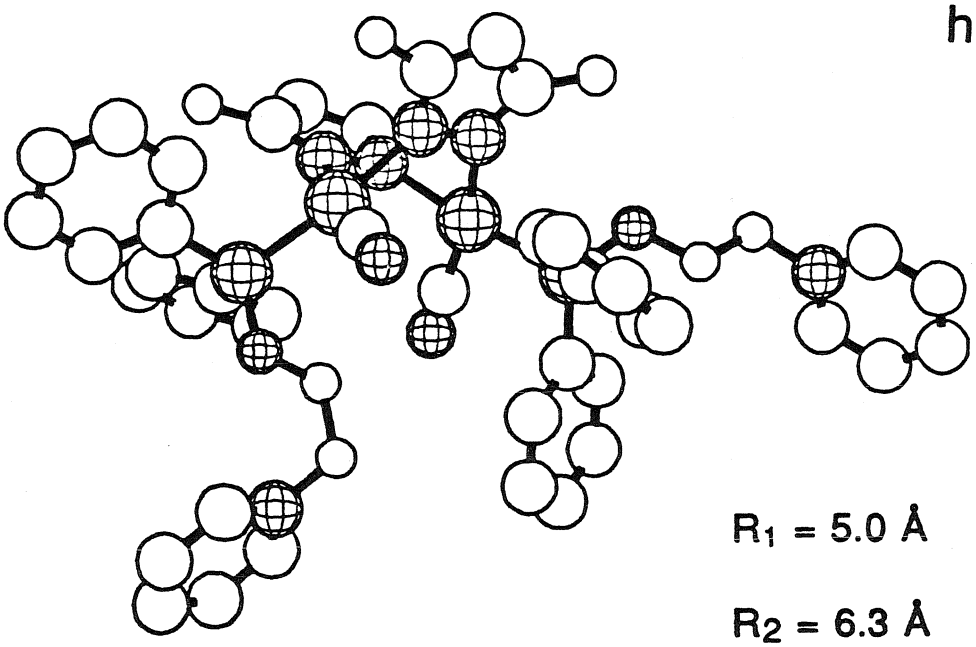
h
R_1 = 5.0 Å
R_2 = 6.3 Å

Figure 2.17 i-k: Structures showing variations in the orientation and distance between the pyridinium cation and iridium dimer as a function of $\phi B1$, $\phi B2$, $\phi B3$, and $\phi B4$ for ligand conformation III (figure 2.15c). R_1 and R_2 are the through space distance between the righthand pyridinium nitrogen and its proximal and distal iridium atoms respectively.

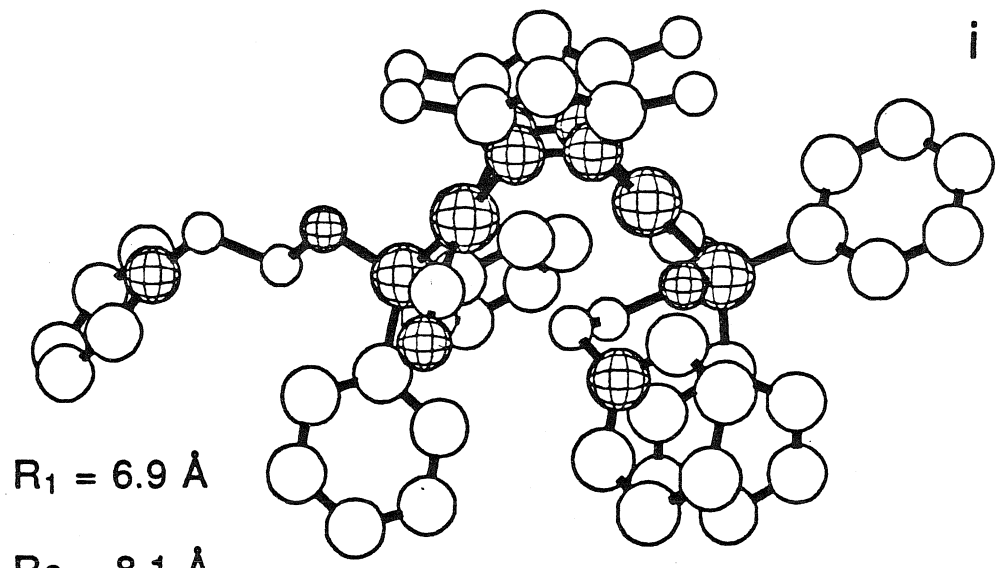

i

R_1 = 6.9 Å

R_2 = 8.1 Å

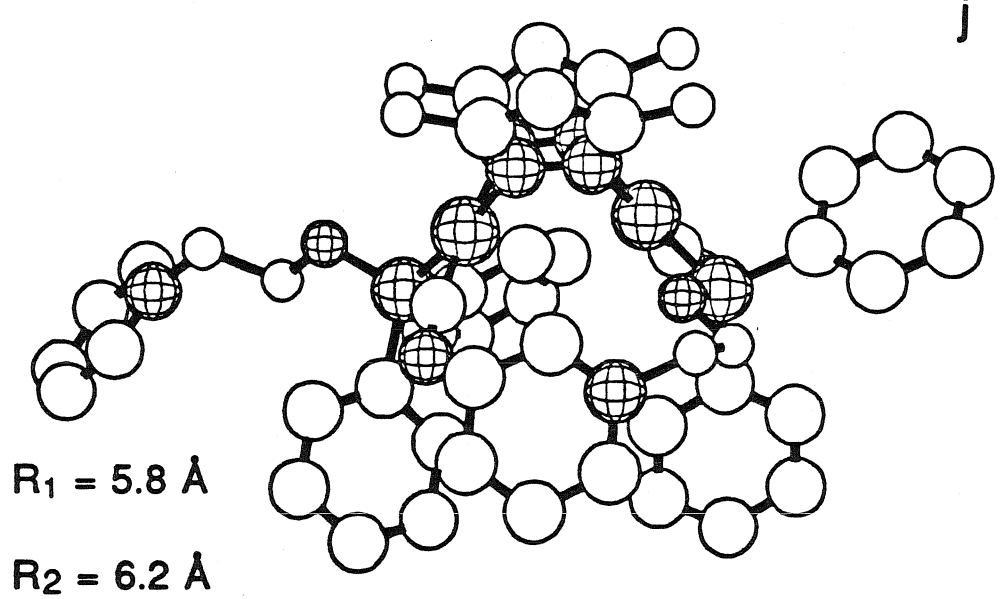

j

R_1 = 5.8 Å

R_2 = 6.2 Å

k

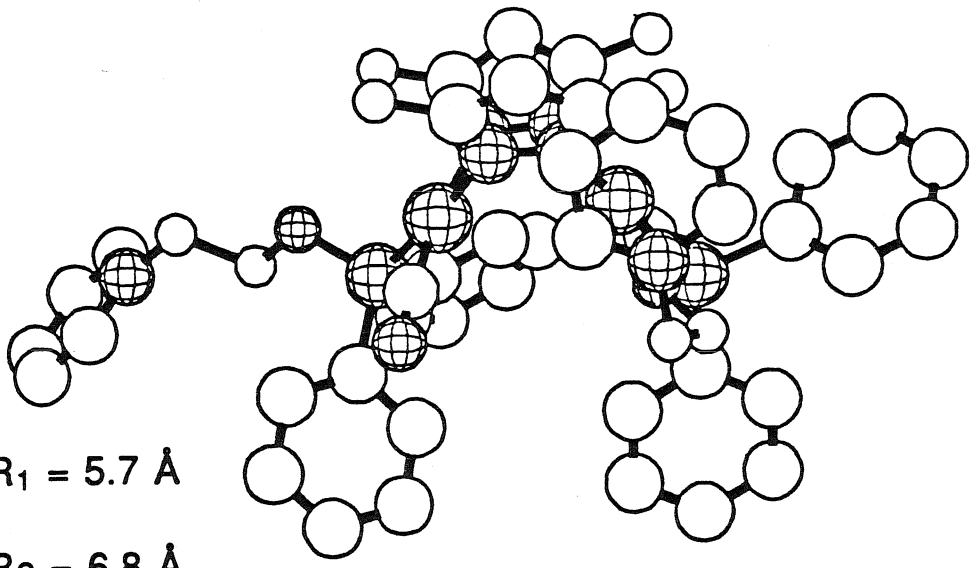

R_1 = 5.7 Å

R_2 = 6.8 Å

Figure 2.18: ^{1}H NMR spectrum of $[Ir_2(Pz^*)_2(CO)_2(Ph_3P)_2]$ in d6-benzene.

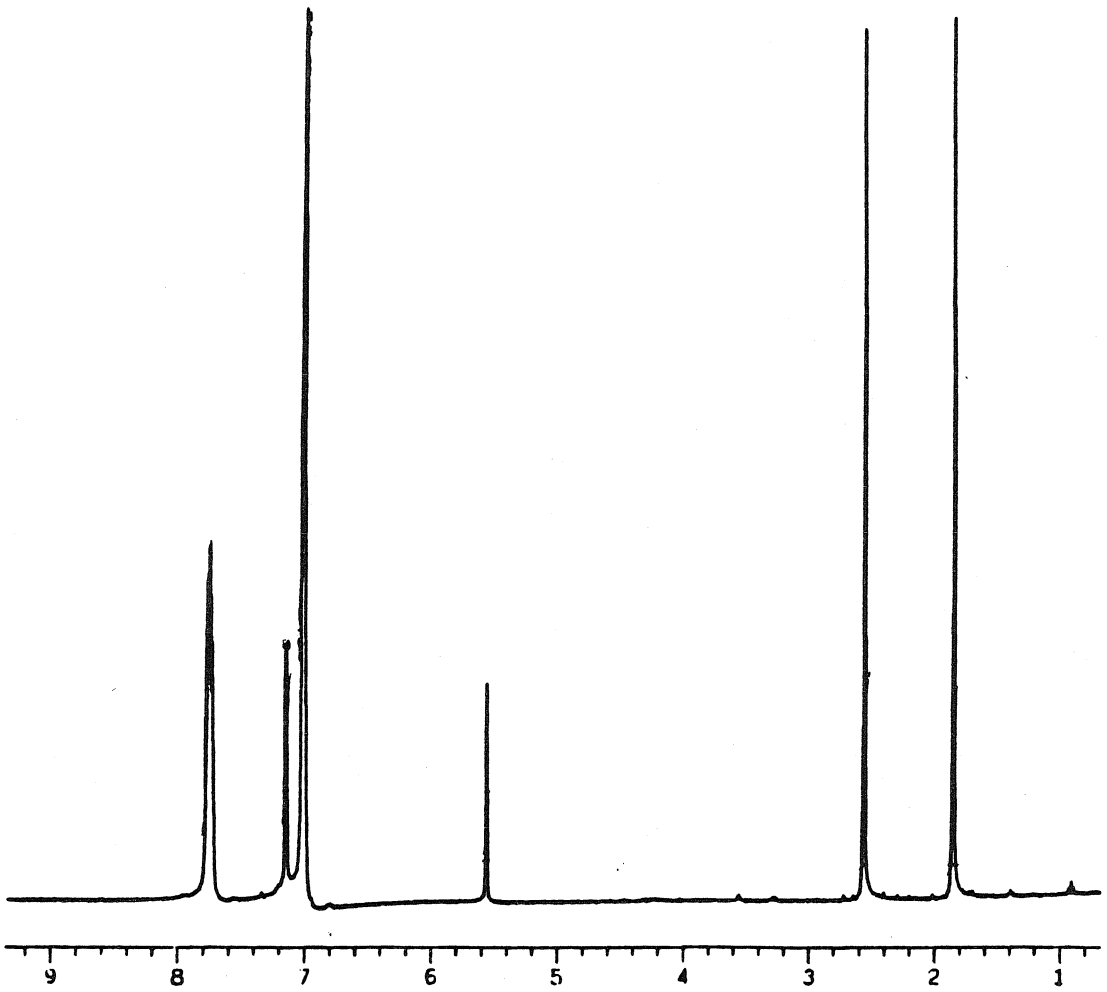
9
8
7
6
5
4
3
2
1

reactant pairs as in a fixed site compound, but are free to diffuse within a restricted region of solution defined by the conformational properties of the phosphinite ligands. The effect that intramolecular motion has on the observed rate of electron transfer in these complexes is at present poorly understood and represents an important area for future research. However, as we will see in chapters 3 and 4 the restrictions placed on bimolecular diffusion in these systems will be sufficient for studying excited state ET reactions with rate constants well above k_{diff}.

References

1a. Marcus, R. A.; Sutin, N., *Biochim. Biophys. Acta*, **1985**, *811*, 265-322.

b. Guarr. T.; McLendon, G., *Coord. Chem. Rev.*, **1985**, *68*, 1-52.

c. Sutin, N., *Prog. Inorg. Chem.*, **1983**, *30*, 441-498.

d. Newton, M. D.; Sutin, N., *Ann. Rev. Phys. Chem.*, **1984**, *35*, 437-480.

e. Meyer, T. J., *Prog. Inorg. Chem.*, **1983**, *30*, 389-440.

f. Sutin, N., *Acc. Chem. Res.*, **1982**, *15*, 275-282.

2a. Gould, I. R.; Ege, D.; Mattes, S. L.; Farid, S., *J. Amer. Chem. Soc.*, **1987**, *109*, 3794-3796.

b. Wasielewski, M. R.; Niemczyk, M. P.; Svec, W. A.; Pewitt, E. B., *J. Amer. Chem. Soc.*, **1985**, *107*, 1080-1082.

c. Closs, G. L.; Miller, J. R., *Science*, **1988**, *240*, 440-447.

d. Bock, C. R.; Connor, J. A.; Gertierrez, A. R.; Meyer, T. J.; Whitten, D. G.; Sullivan,B. P.; Nagel, J. K., *J. Amer. Chem. Soc.*, **1979**, *101*, 4815-?.

3a. Closs, G. L.; Calcaterra, L. T.; Green, N. J.; Penfield, K. W.; Miller, J. R., *J. Phys. Chem.*, **1986**, *90*, 3673-3683.

b. Oevering, H.; Paddon-Row, M. N.; Heppener, M.; Oliver, A. M.; Cotsaris, E.; Verhoven, J. W.; Hush, N. S., *J. Amer. Chem. Soc.*, **1987**, *109*, 3258-3269.

4a. Mayo, S. L.; Ellis, W. R.; Crutchley, R. J.; Gray, H. B., *Science*, **1986**, *233*, 948-952.

b. Isied, S. S., *Prog. Inorg. Chem.*, **1984**, *32*, 443-?.

5. Marshall, J. L.; Stobart, S. R.; Gray, H. B., *J. Amer. Chem. Soc.*, **1984**, *106*, 3027-3029.

6. Marshall, J. L., Ph.D. Dissertation, California Institute of Technology, 1986.

7. Wiley, R. H.; Hexner, P. E., *Org. Synth.*, **1951**, *31*, 43-44.

8a. Ewart, G.; Payne, D. S.; Porte, A. L.; Lane, A. P., *J. Chem. Soc.*, **1962**, 3984-3990.

b. Noth, H.; Vetter, H. J., *Chem. Ber.*, **1963**, *96*, 1109-1118.

c. Maier, L., *Helv. Chim. Acta*, **1964**, *47*, 2129-2137.

9. The distillate has a tendency to solidify upon cooling and clog condensers. To avoid this problem, the distillation head and condenser should be wrapped with heating tape and kept warm.

10a. Balaban, A. T.; Boulton, A. J., *Org. Synth.*,*3*, 1112-1117.

b. Balaban, A. T.; Toma, C., *Tetrahedron*, Supplement No. 7, 9-25.

11. Katritzky, A. R.; Bopart, J. B.; Clarament-Elguero, R. M.; Yates, F. S.; Dinculescu, A.; Balaban, A. T.; Chiraleu, F., *J. Chem. Res. (M)*, **1978**, 4783-4797.

12. Bushnell, G. W.; Fjeldsted, D. O.K.; Stobart, S. R.; Zaworotko, M. J.; Knox, S. A. R.; MacPherson, K. A., *Organomet.*, **1985**, *4*, 1107-1114.

13. Biograf III was licensed from Bio-Design Inc., Pasadena, CA.

14a. Gelin, B. R.; Karplus, M., *Biochem..*, **1979**, *18*, 1256-1268.

b. Gelin, B. R.; Karplus, M., *Proc. Nat. Acad. Sci.*, **1975**, *72*, 2002-2006.

c. Brooks, B.R.; Bruccoleri, R. B.; Olafson, B. P.; States, D. J.; Swaminathan, S.; Karplus, M., *J. Comp. Chem.*, **1983**, 187-217.

15. Maier, L.; Karsolapoff, G. M., *" Organic Phosphorous Compounds"*, **1972**, Wiley-Interscience, New York.

16a. Moracci, F. M.; Di Rienzo, B.; Tortorella, S.; Liberatore, F., *Tetrahedron*, **1980**, *36*, 785-787.

b. Landquist, *J. Chem. Soc. Perkin I*, **1976**, 454-456.

c. Moracci, F. M.; Liberatore, F.; Tortorella, S.; Di Rienzo, B., *Tetrahedron*, **1979**, *35*, 809-812.

17. Mavel, G., *Ann. Rev. NMR Spectr*, **1973**, *58*, 1-89.

18. Powell, J.; Kuksis, A.; Nyberg., S. C.; Ng, W. W., *Inorg. Chim. Acta*, **1982**, *64*, L211-L212.

19. Atwood, J. L.; Beveridge, K. A.; Bushnell, G. W.; Dixon, K. R.; Eadie, D. T.; Stobart, S. R.; Zaworotko, M. J., *Inorg. Chem.*, **1984**, *23*, 4050-4057.

20. Nussbaum, S.; Rettig, S. J.; Storr, A.; Trotter, J., *Can. J. Chem.*, **1985**, *63*, 692-702.

21. Model compounds have ligands, which are similar to those found in the donor-acceptor complexes, but lack pyridinium electron acceptors.

22a. Uson, R.; Oro, L. A.; Ciriano, M. A.; Carmona, D.; Tiripicchio, A.; Camellini, M. T., *J. Organomet. Chem.*, **1982**, *224*, 69-80.

b. Uson, R.; Oro, L. A.; Ciriano, M. A.; Pinillos, M. T.; Tiripicchio, A.; Camellini, M. T., *J. Organomet. Chem.*, **1981**, *205*, 247-257.

23. Banditelli, G.; Bandini, A. L.; Bonati, F.; Mingghetti, G., *J. Organomet. Chem.*, **1981**, *218*, 229-239.

24. Nixon, J. F.; Pidcock, A., *Ann. Rev. NMR Spec.*, **1969**, *2*, 346-422.

25a. Coleman, A. W.; Eadie, D. T.; Stobart, S. R., *J. Amer. Chem. Soc.*, **1982**, *104*, 922-923.

b. Beveridge, K. A.; Bushnell, G. W.; Stobart, S. R.; Atwood, J. L.; Zaworotko, M. J., *Organomet.*, **1983**, *2*, 1447-1451.

26a. Rice, S. F.; Gray, H. B., *J. Amer. Chem. Soc.*, **1981**, *103*, 1593-1596.

b. Dallinger, R. F.; Miskowski, V. M.; Gray, H. B.; Woodruff, W. H.., *J. Amer. Chem. Soc.*, **1981**, *103*, 1595-1596.

27a. McMahon, R. J..; Force, R. K.; Patterson, H. H.; Wrighton, M. S., *J. Amer. Chem. Soc.*, **1988**, *110*, 2670-2672.

b. Gust, D.; Moore, T. A.; Liddell, P. A.; Nemeth, G. A.; Makings, L. R. ; Moore, A. L.; Barrett, D.; Pessiki, P. J.; Bensasson, R. V.; Ronger, M.; Chachaty, C; De Schyver, F. C.; Van der Anwerau, M.; Holzwarth, A. R.; Connolly, J. S., *J. Amer. Chem. Soc.*, **1987**, *109*, 846-856.

28. Chen, P.; Westmoreland, T. D.; Danielson, E.; Schanze, K, S.; Anthon, D.; Neveux, P. E.; Meyer, T. J., *Inorg. Chem.*, **1987**, *26*, 1116-1126.

29. Fox, L. S.; Farid, R. S.; Gray, H, B.; *unpublished results.*

30a. Batyeva, E. S.; Ofitserov, E. N.; Ivanyuk, N,. V.; Pydovik, A. N., *Zh. Obsh. Khim.*, **1976**, *46*, 2282.

b. Papers from Zhurnal Obshchei Khimi are cited with pages numbers from their english translations.

31a. Nifant'ev, E. E.; Borisov, E. V., *Zh. Obsh. Khim.*, **1985**, *55*, 1478-1480.

b. Petrov, K. A.; Nifant'ev, E. E.; Lysenko, T. N.; Evdokov, V. P., *Zh. Obsh. Khim.*, **1961**, *31*, 2214-2217.

c. Nifant'ev, E. E.; Ivanova, N. L.; Fursenko, I. V., *Zh. Obsh. Khim.*, **1969**, *46*, 2282.

d. Evdakov, V. P.; Beketov, V. P.; Svergun, V. I., *Zh. Obsh. Khim.*, **1973**, *43*, 51-55.

e. Evdakov, V. P.; Beketov, V. P.; Bryantsev, B. I., *Zh. Obsh. Khim.*, **1977**, *47*, 1579-1583.

f. Batyeva, E. S.; Al'fonsov, V. A.; Zamaletdinova, G. U.; Pudivik, A. N,, *Zh. Obsh. Khim.*, **1976**, *46*, 2120-2123.

32. Smith, T., *Ph. D. Dissertation, California Institute of Technology*, **1982**.

33a. Hopfield, J. J., *Biophys. Journ.*, **1977**, *18*, 311-321.

b. Redi, M.; Hopfield, J. J., *J. Chem. Phys.*, **1980**, *72*, 6651-6660.

c. Beratan, D. N.; Hopfield, J. J., *J. Amer. Chem. Soc.*, **1984**, *106*, 1584-1594.

34. Onuchic, J. N.; Beratan, D. N., *J. Amer. Chem. Soc.*, **1987**, *109*, 6771-6778.

35. The through space distance is arbitrarily defined using the iridium metal atoms and pyridinium nitrogen atom.

36. Tolman, C. A., *Chem. Rev.*, **1977**, *77*, 313-348.

37. Marcus, R. A.; Siders, P. J., *J. Phys. Chem.*, **1982**, *86*, 622-630.

Chapter 3

Electronic Spectra

and

Electrochemistry

Introduction

Having prepared and characterized a series of d^8-d^8 donor-acceptor complexes, our attention will now turn toward investigating their photophysical properties. As we saw in the previous chapter, one consequence of covalently binding electron acceptors to an iridium dimer chromophore was to restrict the range of available distances and orientations between the metal centers and acceptors. This binding together of redox partners also has some important photophysical implications. In principle the donor-acceptor complexes represent unique molecular electronic systems. They possess an additional charge-separated excited state that arises solely due to interactions between their redox partners. This state can potentially be accessed from the donor (acceptor) localized levels through radiative and nonradiative processes. Depending upon the nature of the interactions between these charge-transfer and donor (acceptor) localized states, certain photophysical properties of the donor-acceptor molecules will be perturbed. For example, if the charge-transfer state is populated via an electron transfer from a donor localized excited state, then the emission quantum yield and lifetime of the donor state should be diminished relative to an appropriate model compound. Previous studies have established that d^8-d^8 metal dimers possess low lying singlet and triplet excited states which arise from a ($d\sigma^*p\sigma$) electronic configuration. Thus, an important aspect of our studies was to determine how the photophysical properties of these d^8-d^8 excited states are perturbed by the presence of a covalently attached electron acceptor. $Ir_2(Pz^*)_2(CO)_2(Ph_2POCH_2CH_3)_2$ and $Ir_2(Pz^*)_2(CO)_2(Ph_2POCH_2CH_2\text{-}NEt_3^+)_2$ were employed as two model systems for these investigations. In terms of their composition, both compounds are similar to the donor-acceptor complexes. The later compound contains two non-reducible NEt_3^+ groups to model the effects that positive charges have on the quantum yields and lifetimes of the metal localized ($d\sigma^*p\sigma$) excited states.

In the following chapter the electronic and photophysical properties of the donor-acceptor complexes are examined using steady-state absorption and emission

spectroscopy, and electrochemical techniques. Important objectives of this aspect of our research were; 1) to determine, either spectroscopically or through some indirect means, the relative energies of the ($d\sigma^*p\sigma$) and charge-transfer states in these complexes, and 2) to obtain photophyscial evidence for excited state electron transfer. Objective number one is clearly important with regard to characterizing the electron transfer reactions in the donor-acceptor complexes as a function of reaction driving force. Cyclic voltammetry and constant potential bulk electrolysis experiments were conducted to determine potentials for the ground state redox processes available in these systems. In the discussion section of this chapter these electrochemical data are used in conjunction with our spectroscopic results to evaluate the energies of the ($d\sigma^*p\sigma$) and charge-transfer excited states in these redox systems. Objective number two was important with regard to some of the time-resolved spectroscopic experiments discussed in chapter 4. In interpreting spectra from these studies, it was essential to know which of the ($d\sigma^*p\sigma$) excited states was involved in electron-transfer reactions. In the past the reactivity of d^8-d^8 compounds has been exclusively associated with their long lived triplet states. The quantum yield data presented in this chapter represent the first evidence that their shorter lived singlet states are also highly reactive under the appropriate kinetic conditions. In addition, it was important to characterize the spectroscopic properties of the charge-transfer states in these systems. In principle these states should relax ground via both radiative and nonradiative processes. Absorption and emission spectra of the compounds were central to identifying the dominant deactivation pathways available to the charge-transfer states in the complexes.

Experimental

General Procedures: All manipulations involving the iridium dimer complexes were carried out using standard Schlenk and high vacuum techniques. Solvents used in

spectroscopic and electrochemical experiments were reagent grade or better in quality. They were purified as indicated, subjected to a minimum of five freeze/pump/thaw cycles, and stored in a round bottom storage flask fitted with a Kontes teflon stopcock. 2-Methyltetrahydrofuran was purified by distillation from a 0.5% (w/w) suspension of cuprous chloride, followed by distillation from CaH_2 and finally from sodium/benzophenone. It was stored under vacuum over sodium/benzophenone as an indicator. Acetonitrile and propionitrile were distilled from CaH_2 under nitrogen and stored in vacuo. Methylene chloride was distilled from CaH_2, subjected to five freeze/pump/thaw cycles and stored in a Schlenk storage flask under a nitrogen atmosphere.

Electronic Absorption Spectroscopy: Electronic Absorption spectra were recorded using a Cary 17 UV-Vis Spectrometer. Room temperature spectra were obtained from 2:1 2-methyltetrahydrofuran/propionitrile solutions that were prepared under vacuum in a 1 cm quartz cuvette attached to a Kontes Teflon stopcock. Low temperature spectra were measured using a quartz optical dewar of local design. Samples were chilled to 77° K in liquid nitrogen and maintained at that temperature via thermal contact with a copper block, which was immersed in a liquid nitrogen bath. Spectra were corrected for absorption due to the solvent, cuvette, and dewar. They were hand digitized using a Calcomp 2000 digitizing pad, an IBM-AT clone PC, and Pro-Design II version 2.5. Extinction coefficients and band widths (fwhm) were determined by fitting the observed band shapes to gaussian envelope functions using Peakfit version 1.2 (EMF Software). Oscillator strengths were calculated using equation 3.1.

$$f = 4.6 \times 10^{-9} \varepsilon_{max} \bar{\nu}_{1/2} \qquad \text{eq. 3.1}$$

Electronic Emission Spectroscopy: Electronic emission spectra were recorded on an in-house emission spectrometer whose construction and specifications have been previously described.[5a] Samples were excited with the 436 nm line of an oriel 200 watt Hg/Xe lamp. This line was selected with a Spex 1670 monochromator and filtered with an Oriel 436 nm (#5645) interference filter (fwhm = 80 cm^{-1}) to remove stray excitation frequencies. Sample emission was collimated, focused on the slit of a Spex 1870 monochromator, and detected with a Hamamatsu R955 PMT. Scattered excitation was removed using a Corning 3387 sharp-cut filter. The signal was amplified with an EG&G 182-A lock-in amplifier and transferred to a Horizon North Star computer where it was digitized and corrected for PMT response. The corrected intensity data were transformed to a linear energy scale and plotted as a function of emission frequency. Room temperature spectra were measured of solutions consisting of an iridium dimer complex in dry oxygen-free acetonitrile. Samples were handled in a 1 cm high precision quartz fluorimetery cell that was attached to a Kontes Teflon stopcock. Low temperature spectra were obtained from 2:1 2-methyltetrahydrofuran/propionitrile solutions that were prepared under vacuum in an NMR tube attached to a Kontes Teflon stopcock. The samples were cooled to 77° K by immersing them in a liquid nitrogen bath contained in a quartz finger dewar. Room temperature quantum yields were determined by the optically dilute solution method of Crosby and Demas.[37] Integrated emission intensities were determined by the cut and weigh method of integration and used to calculated quantum yields according to equation 3.2. $Ru(Bipy)_3^{2+}$ served as a reference.[38]

$$Q_s = Q_r\left[\frac{I_s}{I_r}\right]\left[\frac{n_s}{n_r}\right]^2 \qquad \text{eq. 3.2}$$

The ODs of the samples and reference at 436 nm were adjusted so that they were equivalent within experimental error and were less than or equal to 0.1.

Temperature dependent emission spectra of $Ir_2(Pz^*)_2(CO)_2(Ph_2POCH_2CH_3)_2$ were recorded using a CTI-Cryogenics model 70 Cryodyne Cryocooler. Samples were prepared under vacuum as 2-methyltetrahydrofuran solutions and flame sealed in 1 mm path length optical glass cuvettes. Cuvettes were mounted on a copper block, which was attached to the cold stage of the Cryocooler. Thermal contact between the sample and cold stage was achieved via copper grease. The sample temperature was measured using a copper/constantan thermocouple and was controlled with a CTI temperature controller. Samples were allowed to thermally equilibrate at each temperature for 1/2 hour.

Excitation Spectroscopy: Electronic excitation spectra of optically dilute solutions were recorded using a Perkin-Elmer model WPF-66 fluorimeter. Intensity data were corrected for variations in the lamp intensity profile using a Rhodamine B quantum counter and were plotted as a function of excitation frequency.

Electrochemistry: Cyclic voltammetry (CV) and constant potential bulk electrolysis experiments were performed using an EG&G 173 Potentiostat/Galvanostat, a 175 Universal Programmer, and a 179 Digital Coulometer. CVs were plotted on a Houston Instruments Omnigraphic 2000 XY-Recorder. Two different cell geometries were used to measure cyclic voltammograms and conduct constant potential coulometry experiments. CVs were measured at BAS platinum and glassy carbon electrodes using the electrochemical cell seen in figure 3.1. An SSCE, fitted with a vycor salt bridge, and a platinum basket electrode were employed as reference and counter electrodes respectively. Contact between the reference electrode and working electrode compartment was made through a luggin-capillary with a cracked glass tip. Positioning the luggin-capillary tip close to the surface of the working electrode reduced effects due to IR-drop inherent in electrochemical cells containing organic solvents. The properties of this cell were checked periodically using ferrocene as a test system. This cell

Figure 3.1. A schematic drawing of the electrochemical cell used in cyclic voltammetry experiments. The Luggin capillary arrangement used in this cell reduces effects due to IR drop, which are inherent in electrochemical experiments.

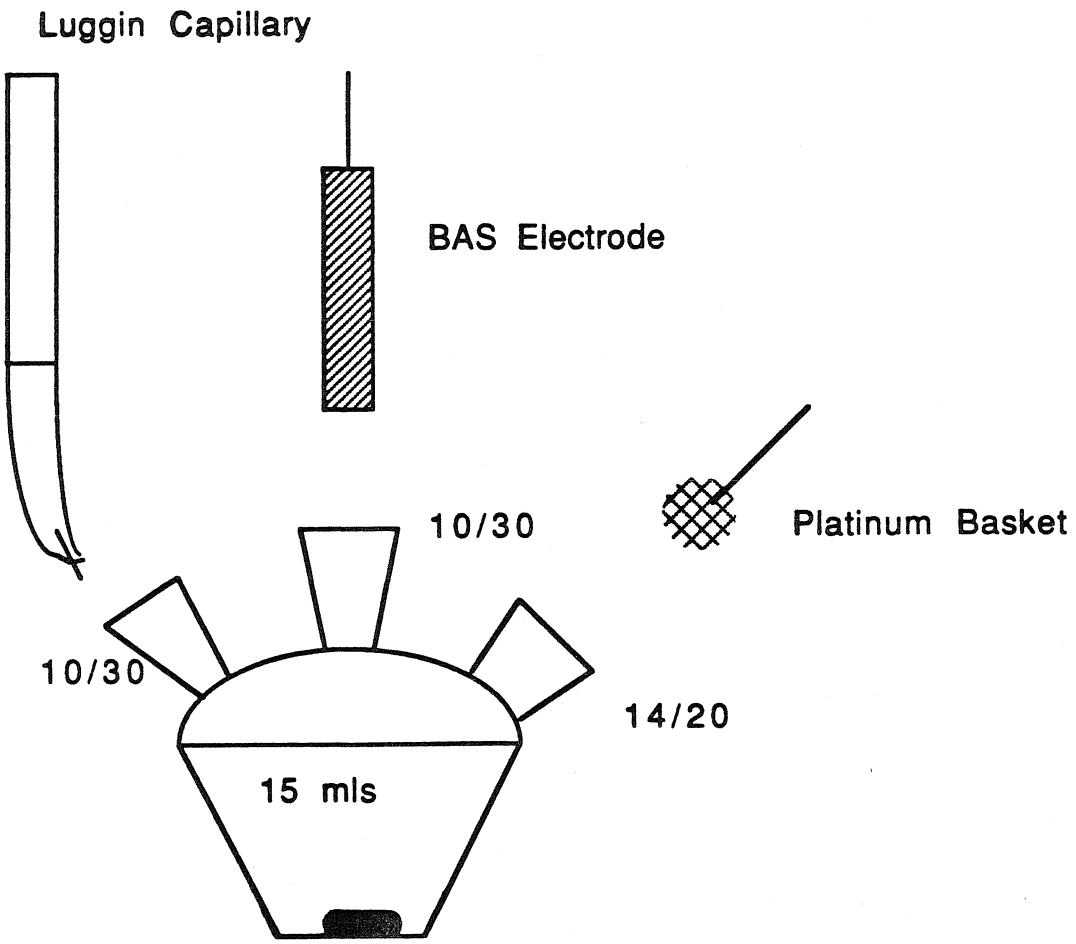
Luggin Capillary
BAS Electrode
10/30
Platinum Basket
10/30
14/20
15 mls

design and electrode geometry consistently reproduced literature $E_{1/2}$ values for ferrocene and showed minor IR drop effects.

Interfacial electron-transfer kinetics between platinum electrodes and the iridium dimers were sensitive to the electrode pretreatment procedure. The following pretreatment suggested by Anson and Long[42] was used to obtain active platinum electrode surfaces. 1) Polish to a metallic luster using 0.3 μm polishing alumina. 2) Sonicate in a 1:1 methanol/ water solution for 15 minutes. 3) Cycle the electrode in 0.5 M sulfuric acid between 1.0 V and -0.05 V versus SSCE until good H_2/O_2 characteristics are seen. 4) Sonicate in the solvent used in the experiment at hand for 15 minutes. 5) Cycle the electrode in the supporting electrolyte solution to be used in the experiments until a constant background is observed. Cyclic voltammograms were typically measured on 0.5×10^{-3} M solutions of an iridium dimer complex in 10 mls of 0.1 M $TBAPF_6/CH_2Cl_2$. Measurements were carried out under an argon atmosphere.

Constant potential coulometry experiments were conducted in an H-tube type electrolysis cell. Electrolysis experiments were carried out at either a platinum basket or pyrolytic graphite working electrode and a platinum basket counter electrode. The working and counter electrode compartments were separated by a medium porosity glass frit. Potentials were measured with respect to an SSCE, which made contact with the working electrode compartment via a cracked glass luggin-capillary. Measurements were made in 0.1 M $TBAPF_6/CH_2Cl_2$ solutions under an argon atmosphere.

Results

Electronic Spectroscopy

The electronic structure and excited state properties of d^8-d^8 transition metal complexes are areas of current interest in inorganic photochemistry.[1] Recent research in our laboratories has indicated that the low lying excited states in these compounds display a variety of different chemical reactivities including the excited state oxidative addition of halocarbons,[1b,2] carbon-hydrogen bond activation,[1b,3] and outer-sphere electron transfer.[1b,4] These diverse photochemical and photophysical properties can be traced to the electronic excited states, which result from the axial metal-metal interactions inherent in these compounds. In the past, electronic spectroscopy has played a central role in understanding the electronic structure and excited state reactivity of these unique inorganic chromophores.[5,6] Thus, a logical starting point for research directed toward investigating the photophysics and photochemistry of a new class of d^8-d^8 complexes is an examination of their electronic spectra.

The current body of spectroscopic data concerning face-to-face d^8-d^8 complexes, such as $[Pt_2(P_2O_5H_2)_4]^{2-}$ and $[Rh_2(Bridge)_4]^{2+}$, indicates that the electronic structure of these systems can be schematically represented by the molecular orbital diagram shown in figure 3.2. Covalently linking two square planar d^8 complexes into a dimeric molecule forces an axial interaction between the d_z2 and p_z orbitals of the monomeric fragments, which leads to the formation of $d\sigma$ and $p\sigma$ dimer MOs. Filling this MO scheme with the 16 metal electrons from the two monomer fragments leaves the $d\sigma^*$ level as the compound's highest occupied molecular orbital. The low-lying electronic excited states in these complexes are generated by exciting one $d\sigma^*$ electron into a vacant $p\sigma$ orbital. This model makes some important predictions concerning the electronic

Figure 3.2. Molecular orbital diagram showing the metal based orbitals important to the electronic structure of d^8-d^8 metal dimers adapted from reference 22.

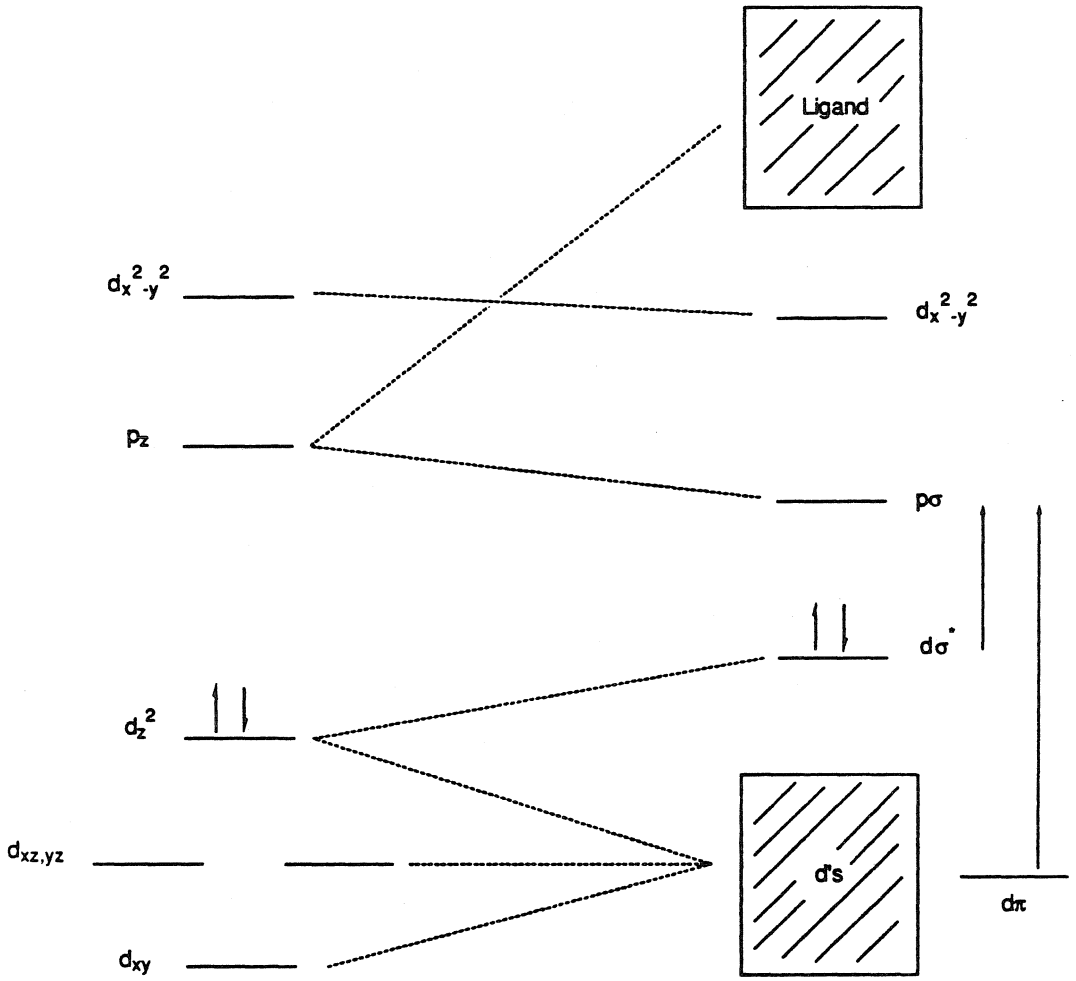
Ligand
$d_{x^2-y^2}$
$d_{x^2-y^2}$
p_z
$p\sigma$
$d\sigma^*$
d_{z^2}
$d_{xz,yz}$
d's
$d\pi$
d_{xy}

spectra and excited properties of d^8-d^8 metal complexes. First, the metal-metal interactions in these compounds should red shift their $d \rightarrow p$ charge-transfer transitions with respect to transitions localized on a single d^8 monomer. Thus, the electronic absorption spectra of d^8-d^8 metal dimers should show low energy $d \rightarrow p$ bands that are well removed from a manifold of higher energy monomer transitions. In addition, because their low energy excited states involve $d\sigma^* \rightarrow p\sigma$ electronic excitations, the strength of the metal-metal bond in these complexes should be greater in their $d\sigma^*p\sigma$ excited states. Both of these predictions have been verified by recent single crystal spectroscopic studies[5a,b,f,g] and excited state resonance raman experiments[7] involving $[Pt_2(P_2O_5H_2)_4]^{2-}$ and $[Rh_2(Bridge)_4]^{2+}$. While the MO model predicts that the energies of the $(d\sigma^* \rightarrow p\sigma)^1$ and $(d\sigma^* \rightarrow p\sigma)^3$ electronic transitions in d^8-d^8 complexes are a function of a compound's metal-metal separation, the current body of data concerning face-to-face and A-frame metal dimers indicates that these energies are more intimately related to the type of metal centers, the bridging and terminal ligands, and the metal-metal separations found in these complexes. In this respect some care must be exercised when using this approach to make comparisons between d^8-d^8 dimers with substantially different coordination environments. However, within a structurally homologous series of complexes with identical metal centers and similar ligands, an MO approach should be adequate for understanding the $(d\sigma^*p\sigma)$ excited states in these chromophores.

Recent spectroscopic studies, concerning a series of $Ir_2(\mu\text{-pyrazolate})_2(COD)_2$ complexes, have indicated that the molecular orbital model developed for face-to-face d^8-d^8 compounds can be extended to describe the spectroscopic properties of A-frame metal dimers.[8,3d] The low energy excited states in these chromophores have been identified as the $(d\sigma^*p\sigma)^1$ and $(d\sigma^*p\sigma)^3$ states by virtue of their visible absorption bands and fluid solution emission spectra. Because detailed experiments, regarding

Table 3.1: Spectral Parameters for the Iridium Donor-Acceptor Complexes.

Complex[a]	Room T			77° K		
$Ir_2(Pz^*)_2(CO)_2L_2$	ν_{max}[f] cm^{-1}	ε_{max}[g] $M^{-1}cm^{-1}$	$\nu_{1/2}$[f] cm^{-1}	ν_{max} cm^{-1}	ε_{max} $M^{-1}cm^{-1}$	$\nu_{1/2}$ cm^{-1}
Band I ($d\sigma^* \rightarrow p\sigma$)[1]						
$Ph_2OCH_2CH_3$	22,100	8900	2400	22,300	12,000	1600
$Ph_2OCH_2CH_2$-NEt_3	21,300	8500	24000	22,000	12,000	1600
$Ph_2OCH_2CH_2$-Me_3Py	21,600	8500	2300	22,000	13,000	1600
$Ph_2OCH_2CH_2$-4MePy[b]	21,500	7800	2400	21,500	11,000	1500
$Ph_2OCH_2CH_2$-Py	21,700	7700	2600	21,800	11,000	1500
$Ph_2OCH_2CH_2$-4PhPy[c]	21,900	6800	2500	--[d]	- -	- -
Band II ($d\sigma^* \rightarrow p\sigma$)[3]						
$Ph_2OCH_2CH_3$	19,200[h]	- -	- -	19,300	420	1400
$Ph_2OCH_2CH_2$-4MePy	--[e]	- -	- -	18,600	450	1800
$Ph_2OCH_2CH_2$-NEt_3	--[e]	- -	- -	19,600	410	1700
Band III						
$Ph_2OCH_2CH_3$	28,200	5000	3800	28,100	5700	3200
$Ph_2OCH_2CH_2$-NEt_3	27,700	5000	4600	28,200	6000	3000
$Ph_2OCH_2CH_2$-Me_3Py	28,300	5600	3700	28,700	8500	4200
$Ph_2OCH_2CH_2$-4MePy	27,300	5300	5300	27,000	5800	2900
$Ph_2OCH_2CH_2$-Py	27,600	4000	4500	27,600	--[d]	4500
$Ph_2OCH_2CH_2$-4PhPy[c]	28,400	4400	4400	--[d]	- -	- -

a. Spectra were measured in 2:1 2-methyltetrahydrofuran/propionitrile solutions unless otherwise indicated. b. A 3,5-dimethyl-4-isobutylpyrazole complex was used due to the poor solubility of the corresponding 3,5-dimethylpyrazole complex. c. Spectra measured in acetonitrile. d. Spectral parameters could not be determined due to the presence of intense $Ph_4B \rightarrow$ 4-PhPy charge-transfer bands. e. Not observed at room temperature. f. +,- 100 cm^{-1}.
g. +,- 10%. h. Determined from room temperature excitation spectra.

Table 3.2: Oscillator Strengths for the $(d\sigma^* \rightarrow p\sigma)^{1,3}$ and Band III Electronic Transitions.

Complex	Room T[a] f	77° K[a] f
$(d\sigma^* \rightarrow p\sigma)^1$		
$Ph_2OCH_2CH_3$	0.1	0.09
$Ph_2OCH_2CH_2$-NEt_3	0.09	0.09
$Ph_2OCH_2CH_2$-Me_3Py	0.09	0.10
$Ph_2OCH_2CH_2$-4MePy	0.09	0.08
$Ph_2OCH_2CH_2$-Py	0.09	0.08
$Ph_2OCH_2CH_2$-4PhPy	0.08	--[b]
Band III		
$Ph_2OCH_2CH_3$	0.09	0.08
$Ph_2OCH_2CH_2$-NEt_3	0.10	0.08
$Ph_2OCH_2CH_2$-Me_3Py	0.09	0.10
$Ph_2OCH_2CH_2$-4MePy	0.10	0.08
$Ph_2OCH_2CH_2$-Py	0.08	--[b]
$Ph_2OCH_2CH_2$-4PhPy	0.09	--[b]
$(d\sigma^* \rightarrow p\sigma)^3$		
$Ph_2OCH_2CH_3$	- -	0.03
$Ph_2OCH_2CH_2$-NEt_3	- -	0.03
$Ph_2OCH_2CH_2$-4MePy	- -	0.04

a. +,- 0.01

b. Not determined due to $Ph_4B \rightarrow$ Py charge-transfer bands which distorted the transition's band shape

complexes with terminal phosphine and carbon monoxide ligand have not been carried out , spectroscopic studies of the donor-acceptor and model complexes were undertaken to characterize their low lying excited states.[6]

Electronic absorption and emission spectra of the model compounds and donor-acceptor complexes were for the most part identical within their experimental uncertainties. Spectroscopic parameters for all of the d^8-d^8 dimers are summarized in tables 3.1 to 3.3. The spectroscopic properties common to this series of compounds are discussed below by referring to absorption, emission, and excitation spectra of $Ir_2(Pz^*)_2(CO)_2(Ph_2POCH_2CH_3)_2$ as illustrative examples.

Absorption Spectra: The room temperature absorption spectra of the donor-acceptor complexes and model compounds in 2:1 2-methylTHF/propionitrile solutions show two intense absorption features with maxima at approximately 21,000 cm^{-1} ($\varepsilon = 8500$) and 27,900 cm^{-1} ($\varepsilon = 5000$). These transitions are labeled Band I and Band II in figure 3.3a. As seen in figure 3.3b Bands I and II sharpen and blue shift slightly in 77° K glass spectra of the complexes, revealing three lower intensity transitions with maxima at approximately 19,000 cm^{-1} (Band III), 24,000 cm^{-1} (Band IV), and 26,000 cm^{-1} (Band V). Band III represents the lowest energy spectroscopic transition in these compounds and is well resolved from the low energy wing of Band I at low temperature. Bands IV and V appear as shoulders on the high energy side of Band I and the low energy side of Band II, respectively. In terms of the relative intensities and energies of Bands I, II, and III, the electronic absorption spectra of the carbon monoxide, phosphine metal dimers, are strikingly similar to spectra of a series of $[Ir_2(Pz)_2(COD)_2]$ complexes.[8] Thus, assignments for each of these transitions can be made by analogy to similar spectral features observed for the corresponding cyclooctadiene systems. Based on its intensity and temperature independent oscillator strength, Band I is assigned to a fully

Figure 3.3. Absorption spectrum of $Ir_2(Pz^*)_2(CO)_2(Ph_2POCH_2CH_3)_2$ in 2:1 2-methyltetrahydrofuran/propionitrile solutions. a) Room temperature. b) 77° K.

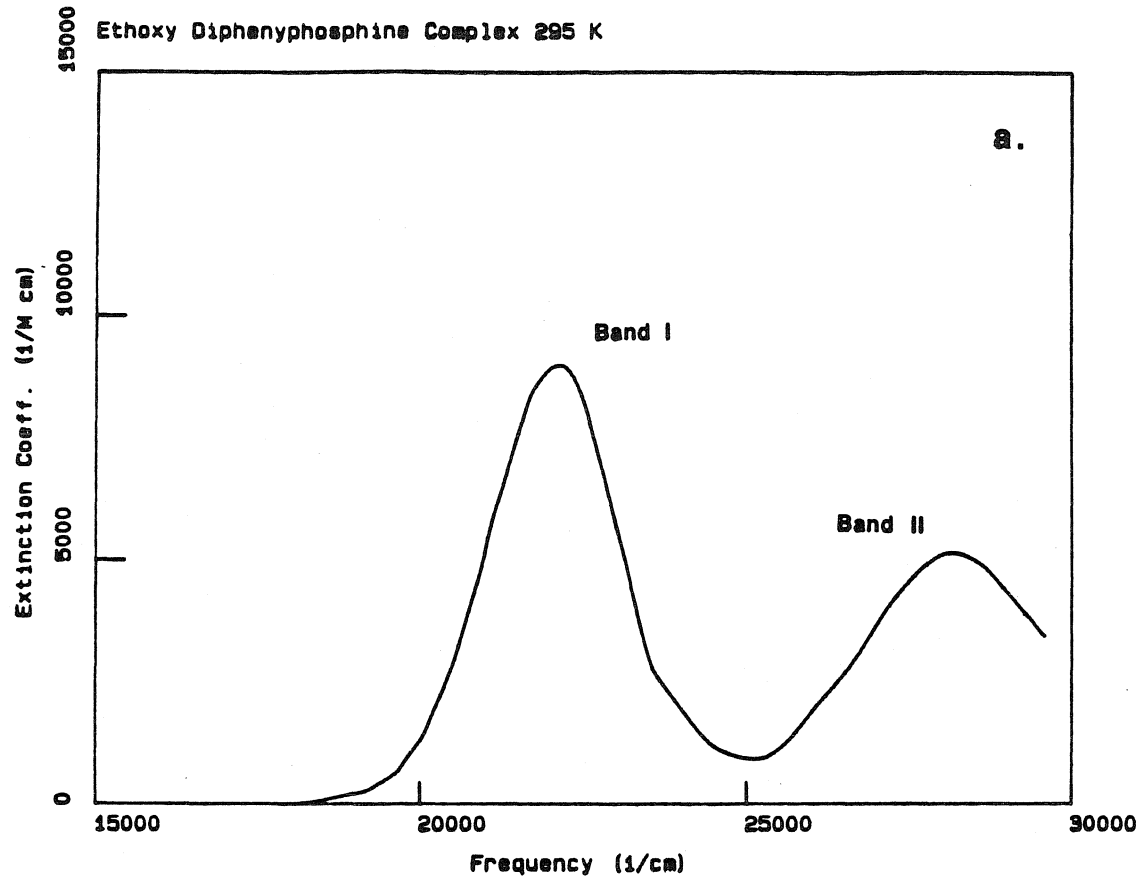
Ethoxy Diphenyphosphine Complex 295 K
a.
Band I
Band II
Extinction Coeff. (1/M cm)
15000
10000
5000
0
15000
20000
25000
30000
Frequency (1/cm)

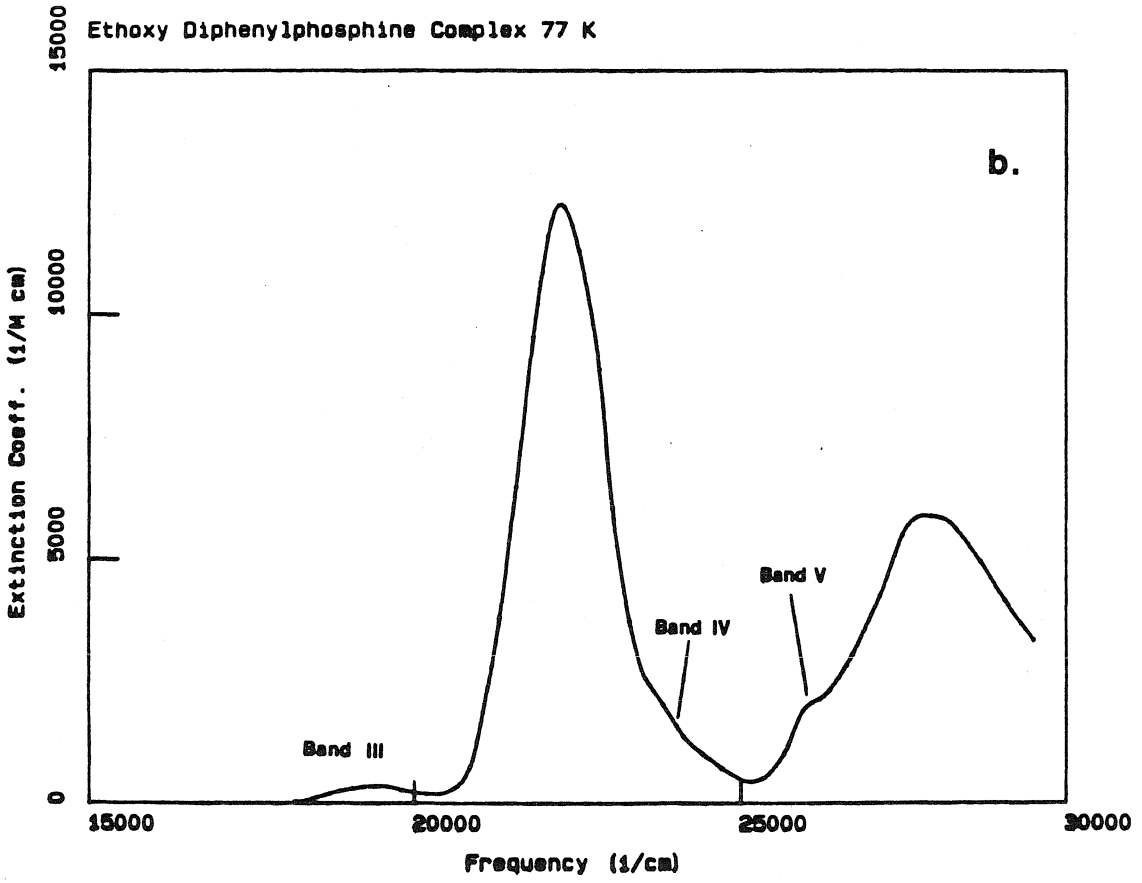
Ethoxy Diphenylphosphine Complex 77 K
b.
Band III
Band IV
Band V
Extinction Coeff. (1/M cm)
15000
10000
5000
0
15000
20000
25000
30000
Frequency (1/cm)

allowed $^1A \rightarrow {}^1B$ ($d\sigma^* \rightarrow p\sigma$) electronic transition. Band III is logically assigned to the corresponding triplet transition, $^1A \rightarrow {}^3B$ ($d\sigma^* \rightarrow p\sigma$), due to its substantially weaker intensity. These assignments are consistent with the MO diagram seen figure in 3.2 and are supported by previous arguments, regarding the spectra of several A-frame and face-to-face d^8-d^8 complexes.[3d,5,6,8,9]

The higher energy excited states of d^8-d^8 A-frame metal dimers are poorly understood. In contrast to the face-to-face complexes, definitive assignments for the higher lying electronic transitions in these complexes are precluded by their lower symmetry, their more complicated ligand systems, and a lack of information concerning spectra of their corresponding monomers.[10] In general, these states rapidly internally convert to the lower energy $(d\sigma^*p\sigma)^{1,3}$ states and are not responsible for the photochemical reactivity associated with d^8-d^8 systems.[5a,13] While a complete assignment of the higher energy absorption bands in spectra of the donor-acceptor molecules is outside the scope of this thesis, some parallels can be drawn between these bands and analogous features in spectra of related A-frame systems.

Absorption features similar to Band II have been observed in spectra of $[Ir_2(Pz)_2(COD)_2]$ (381 nm), $[Ir_2(Pz)_2(CO)_4]$ (325 nm), and their analogs. These bands have been attributed to ($d_{xz},d_{yz} \rightarrow p_z$) transitions in the $[Ir_2(Pz)_2(COD)_2]$ systems by analogy to assignments made for $Rh_2(Bridge)_4^{2+}$ and $Ir_2(TMB)_4^{2+}$.[5a,b] However, in comparison to the bandshapes observed for the $d_\pi \rightarrow p$ transitions in face-to-face d^8-d^8 systems, Band II has a much larger half-width at both room temperature and 77° K. This distinction in bandshapes indicates that Band II involves excited state distortions not found in the d_π excited states of face-to-face metal dimers. One possible explanation for the substantial half-widths associated with Band II is that this transition contains a considerable amount of metal-to-pyrazole charge transfer character. This interpretation is suggested by the low energy MLCT transitions seen in orthometallated Ir(III) monomers.[11] Careful inspection of Bands IV and V at 77° K shows that they are

Figure 3.4. 77° K absorption spectrum of $Ir_2(Pz^*)_2(CO)_2(Ph_2POCH_2CH_3)_2$ showing a 587 cm^{-1} progression in $\nu_{Ir\text{-}C}$ superimposed on Bands IV and V.

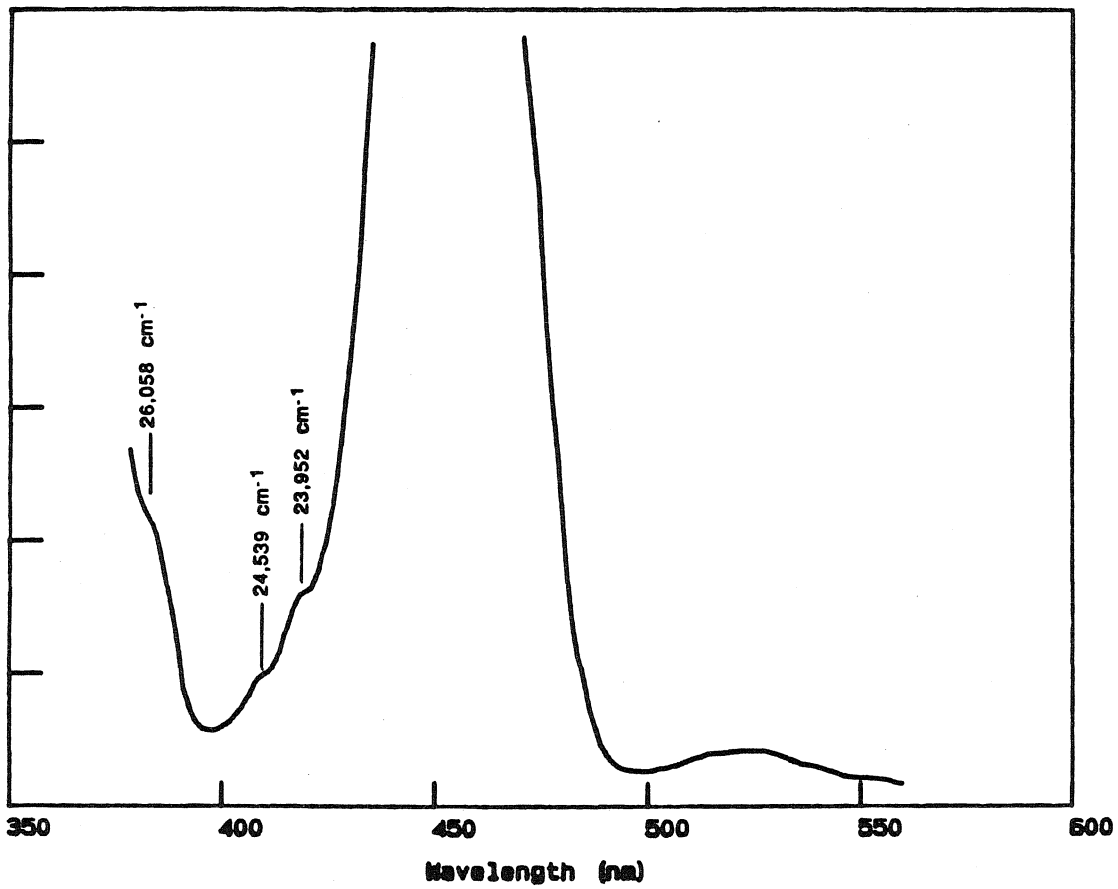
26,058 cm-1
24,539 cm-1
23,952 cm-1
350
400
450
500
550
600
Wavelength (nm)

weakly structured in a 587 cm^{-1} vibrational progression (figure 3.4). Similar bands appear in spectra of $[Ir_2(Pz)_2(CO)_4]$ and its analogs, but are absent in spectra of the corresponding pyrazolate bridged COD systems.[8] These bands have been tentatively assigned to ($d_\pi \rightarrow p,\pi^*CO$) transitions based on their 500 cm^{-1} vibrational progressions and their similarity to features observed in monomer spectra.[12] Their low intensity in spectra of the $Ir_2(Pz^*)_2(CO)_2(Ph_2POR)_2$ systems and absence in spectra of the COD dimers suggests that they are forbidden transitions, which gain substantial intensity via vibronic coupling to an Ir-C vibrational mode. Further detailed spectroscopic studies, involving both the pyrazolate bridged dimers and their corresponding monomers, will be necessary to definitively assign these higher energy bands.

Emission Spectra: Electronic emission spectra of the donor-acceptor complexes and model compounds at 77° K show two emission bands in the spectral region between 10,000 and 25,000 cm^{-1} with maxima at approximately 19,000 cm^{-1} and 15,000 cm^{-1} (figure 3.5). These bands are logically assigned to $^1B \rightarrow {}^1A(p\sigma \rightarrow d\sigma^*)$ and $^3B \rightarrow {}^1A(p\sigma \rightarrow d\sigma^*)$ electronic transitions, respectively, by analogy to emission features observed for a number of A-frame and face-to-face dimer compounds.[3d,5,6,8,9] At 77° K the singlet and triplet emission intensities of donor-acceptor compounds were similar to the intensities of the $Ir_2(Pz^*)_2(CO)_2(Ph_2POCH_2CH_3)_2$ and $Ir_2(Pz^*)_2(CO)_2(Ph_2POCH_2CH_2\text{-}NEt_3^+)_2$. Further, the 77° K phosphorescence lifetimes of the donor-acceptor and model compounds were the same within their experimental uncertainties. These indicate that rapid photoinduced electron transfer does not take place from either the ^1B or ^3B excited states in a rigid low temperature matrix. Spectral parameters for all the complexes are summarized in table 3.3.

The energies and intensities of the $^1B \rightarrow {}^1A$ and $^3B \rightarrow {}^1A$ emission bands in the model and donor-acceptor compounds change substantially as a function of temperature between 77° K and 295° K. As seen in figure 3.6, at room temperature both emission bands broaden and are red shifted with respect to their 77° K band maxima. Table 3.4

Figure 3.5. a) Electronic emission spectrum of $Ir_2(Pz^*)_2(CO)_2(Ph_2POCH_2CH_3)_2$ at 77° K. b) Higher sensitivity spectrum showing the singlet emission band at 77° K.

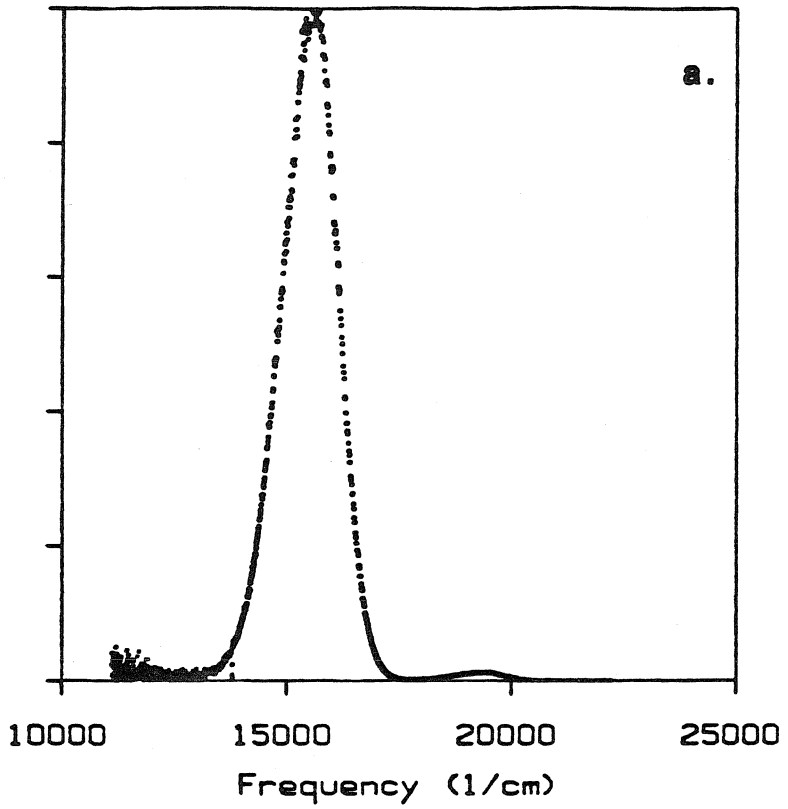
a.
10000
15000
20000
25000
Frequency (1/cm)

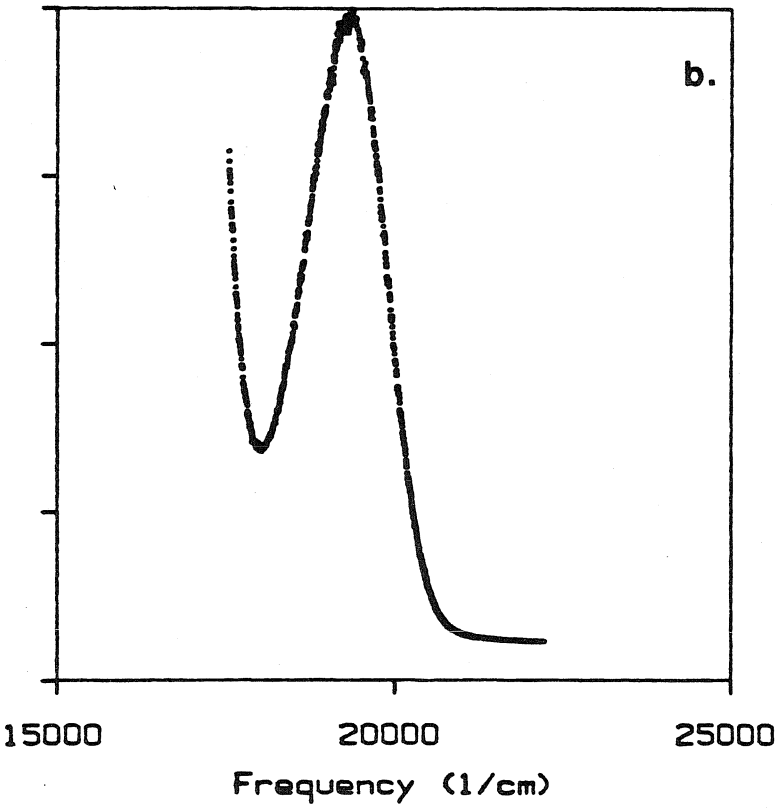
b.
15000
20000
25000
Frequency (1/cm)

Table 3.3: 77° K Emission Parameters for the Iridium Dimer Complexes.[a]

Complex	$(^1B \rightarrow {}^1A)$		$(^3B \rightarrow {}^1A)$	
$Ir_2(Pz^*)_2(CO)_2L_2$	ν_{max} cm^{-1}	$\nu_{1/2}$ cm^{-1}	ν_{max} cm^{-1}	$\nu_{1/2}$ cm^{-1}
$Ph_2OCH_2CH_3$	19,300	1500	15,500	1500
$Ph_2OCH_2CH_2$-NEt_3	19,200	1500	15,400	1600
$Ph_2OCH_2CH_2$-Me_3Py	19,200	1600	15,400	1600
$Ph_2OCH_2CH_2$-4MePy	19,300	1500	15,500	1500
$Ph_2OCH_2CH_2$-Py	19,300	1600	15,500	1500
$Ph_2OCH_2CH_2$-4PhPy	19,300	1800	15,500	1500

a. Spectra were measured of 2:1 2-methyltetrahydrofuran/propionitrile solutions.
b. A 4-isobutyl-3,5-dimethylpyrazole complex was used due to the poor solubility of the corresponding 3,5-dimethylpyrazole complex.

Table 3.4: Spectral Data for Selected A-Frame Complexes.

Complex	ν_{max} ($^1B \rightarrow {}^1A$) cm^{-1}	ν_{max} ($^3B \rightarrow {}^1A$) cm^{-1}	T °K
$Ir_2(Pz^*)_2(CO)_2(Ph_2POCH_2CH_3)_2$[a]	17,900	13,500	298
	19,400	15,500	77
$Ir_2(Pz^*)_2(CO)_2(Ph_2PO(CH_2)_2NEt_3)_2$[b]	18,200	13,300	298
	19,200	15,400	77
$Ir_2(Pz^*)_2(CO)_4$[c,d]	18,800	13,600	298
	20,000	14,900	77
$Ir_2(Pz)_2(CO)_4$[c,d]	18,800	13,300	298
	19,600	15,400	77
Ir_2(3-Methyl-Pz)$_2(CO)_4$[c,d]	18,800	13,300	298
	19,400	14,800	77
$Ir_2(Pz)_2(COD)_2$[a]	17,900	14,600	298
	18,000	14,700	77

a. 2-Methyltetrahydronfuran solutions.
b. 2:1 2-methylTHF/propionitrile solutions
c. 2-Methylpentane solutions
d. See reference 8.

Figure 3.6. a) Room temperature emission spectra of (1) $Ir_2(Pz^*)_2(CO)_2(Ph_2POCH_2CH_2NEt_3^+)_2$, (2) $Ir_2(Pz^*)_2(CO)_2(Ph_2POCH_2CH_2$-$246Me_3Py^+)_2$, (3) $Ir_2(Pz^*)_2(CO)_2(Ph_2POCH_2CH_2$-$4MePy^+)_2$, and (4) $Ir_2(Pz^*)_2(CO)_2(Ph_2POCH_2CH_2$-$Py^+)_2$ in acetonitrile comparing their relative intensities and band maxima. Note that the spectrum of $Ir_2(Pz^*)_2(CO)_2(Ph_2POCH_2CH_2NEt_3^+)_2$ has been reduced by a factor of five. b) Spectra 2,3, and 4 enlarged. The feature at 500 nm is a mercury line.

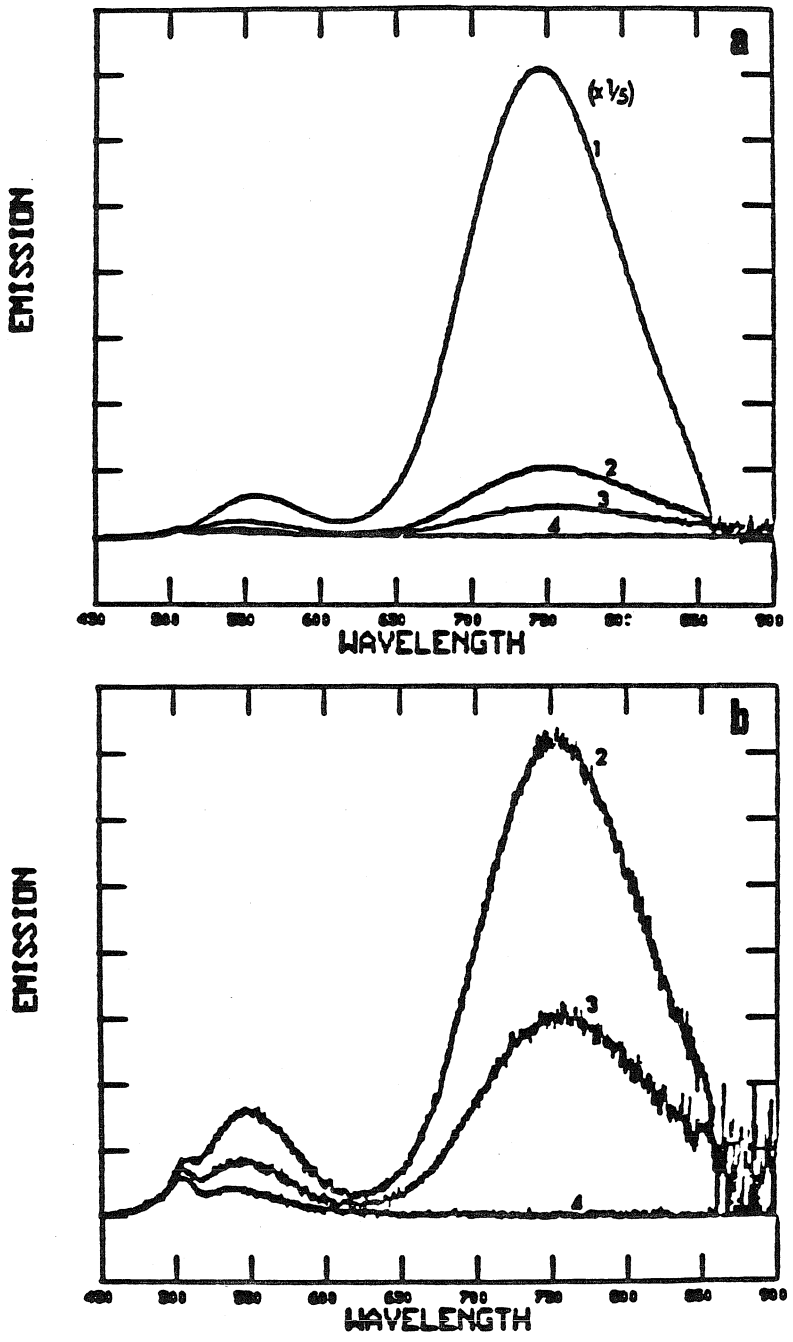
a
(x 1/5)
1
2
3
4
EMISSION
WAVELENGTH
b
2
3
4
EMISSION
WAVELENGTH

Figure 3.7. Electronic excitation spectra of $Ir_2(Pz^*)_2(CO)_2(Ph_2POCH_2CH_3)_2$ in 2-methyltetrahydrofuran. a) and b) Room temperature and 77° K singlet spectra. c) and d) Room temperature and 77° K triplet spectra.

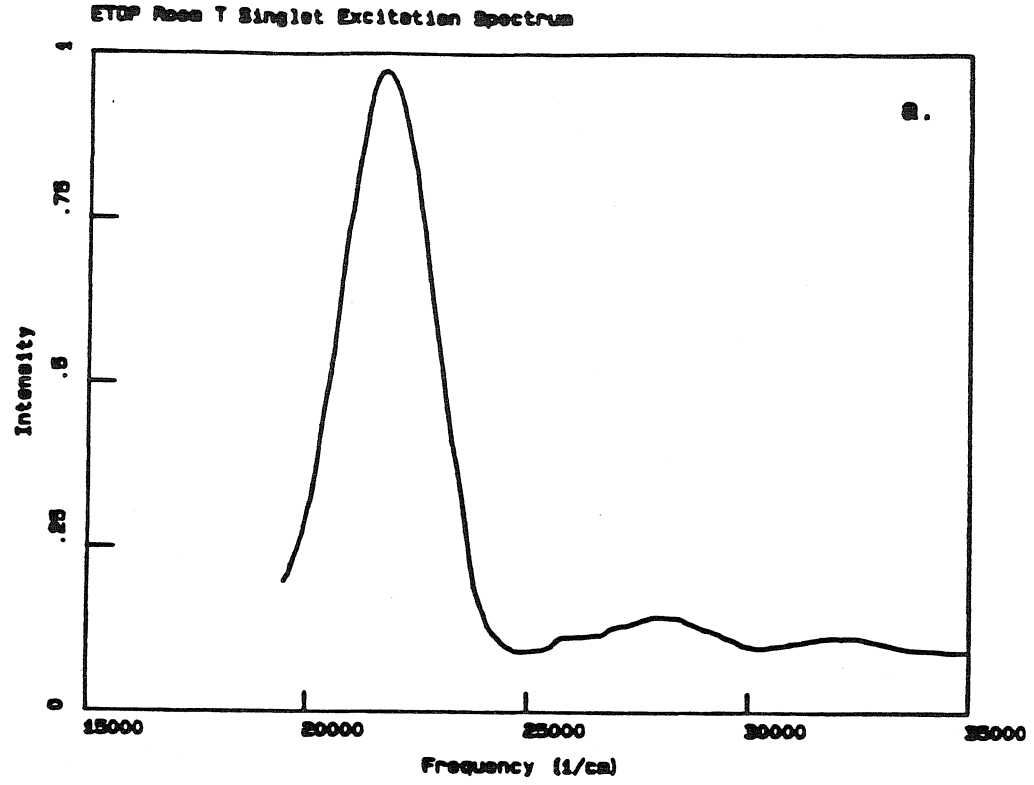
ETOP Room T Singlet Excitation Spectrum
a.
Intensity
0
.25
.5
.75
1
15000
20000
25000
30000
35000
Frequency (1/cm)

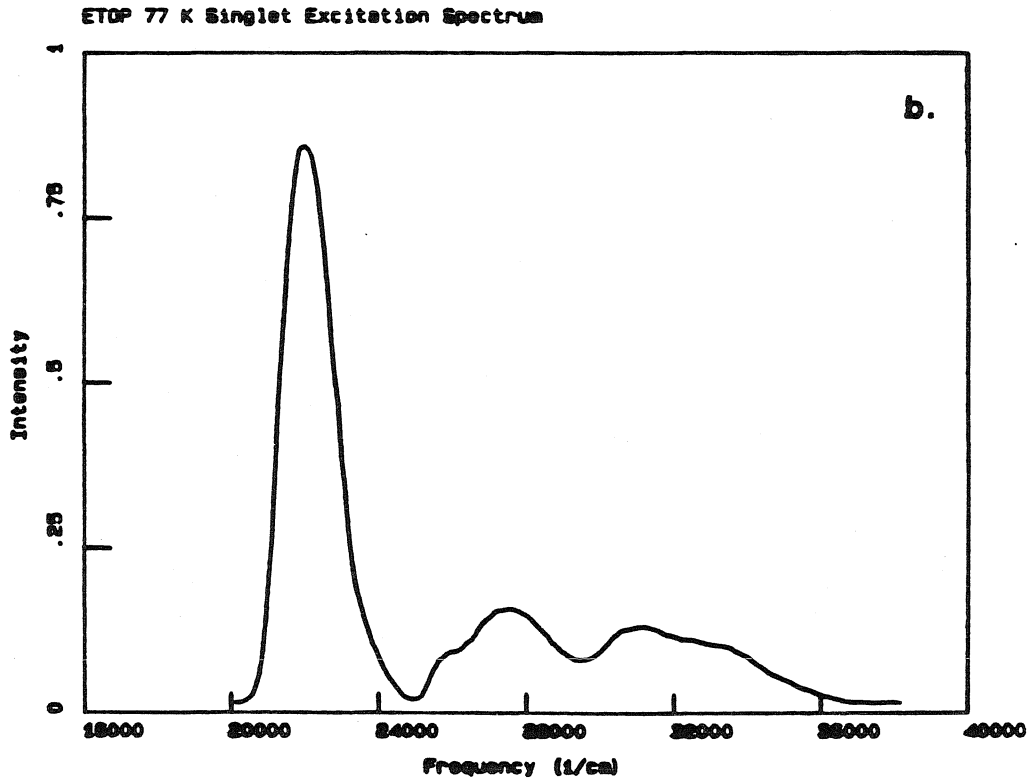
ETOP 77 K Singlet Excitation Spectrum
b.
Intensity
0
.25
.5
.75
1
16000
20000
24000
28000
32000
36000
40000
Frequency (1/cm)

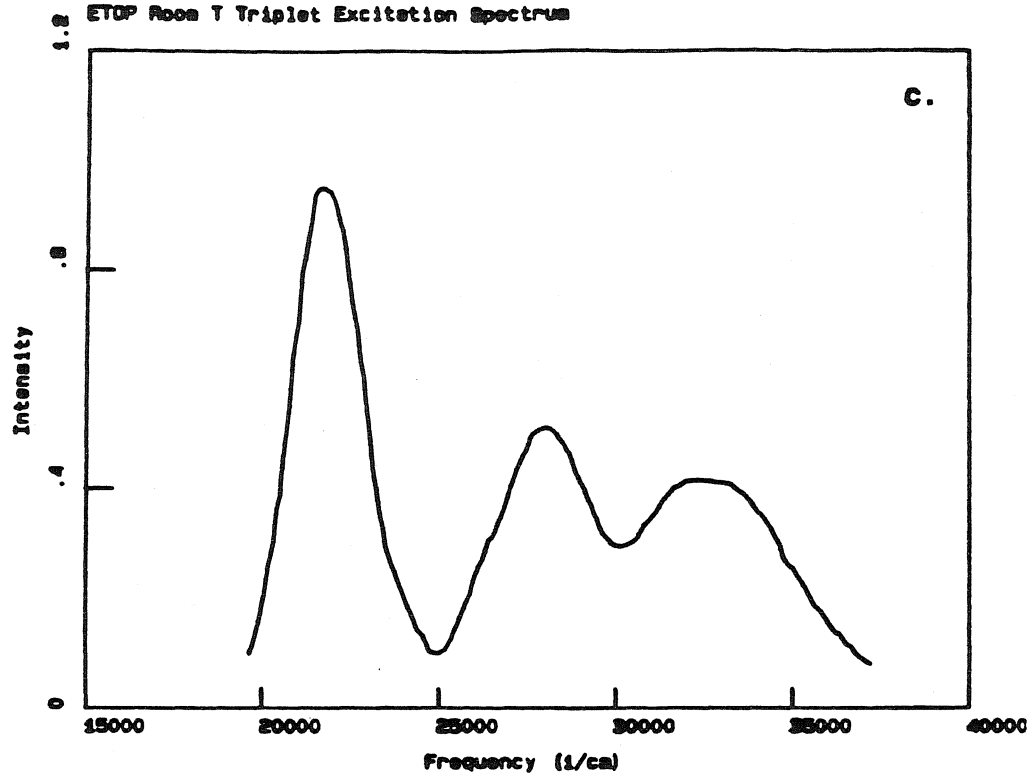
ETOP Room T Triplet Excitation Spectrum
c.
Intensity
1.2
.8
.4
0
15000
20000
25000
30000
35000
40000
Frequency (1/cm)

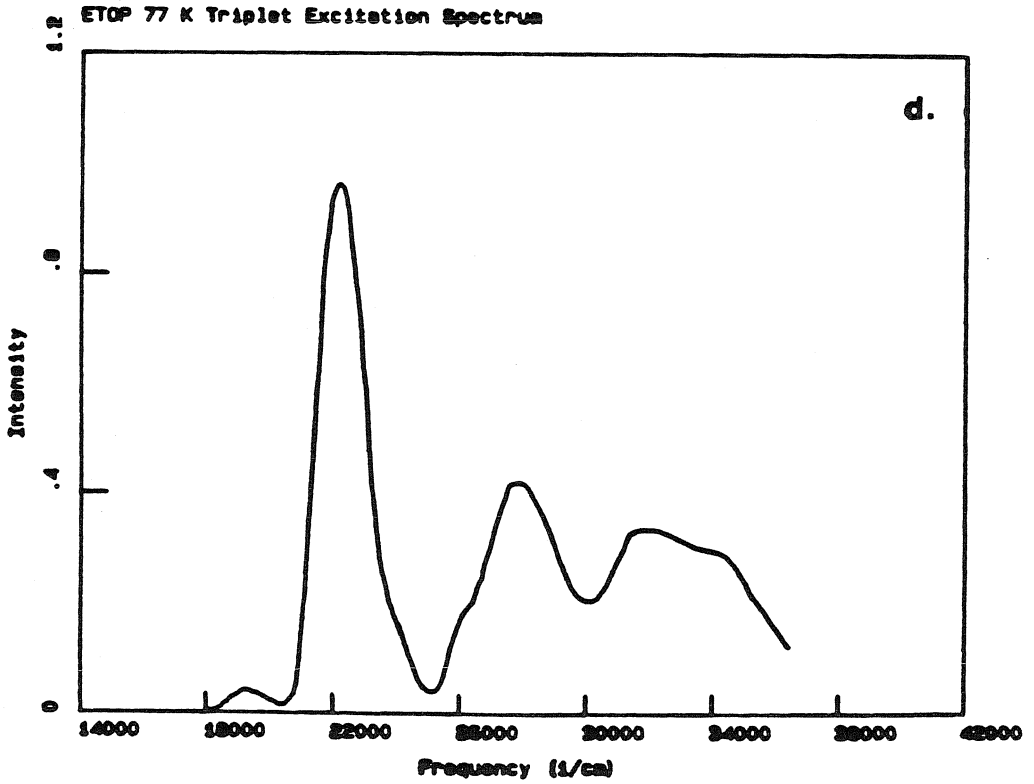
ETOP 77 K Triplet Excitation Spectrum
d.
Intensity
1.2
.8
.4
0
14000
18000
22000
26000
30000
34000
38000
42000
Frequency (1/cm)

shows that similar changes as a function of temperatures are observed in emission spectra of $[Ir_2(Pz)_2(CO)_4]$ and its analogs, but are curiously absent in spectra of the corresponding $[Ir_2(Pz)_2(COD)_2]$ systems.[8] One plausible explanation for this phenomenon is that photoemission in the tetra-CO and CO-phosphine systems occurs from different electronic excited states as a function of temperature. This possibility can be ruled out by examining the excitation spectra of $Ir_2(Pz^*)_2(CO)_2(Ph_2POCH_2CH_3)_2$ seen in figure 3.7. In terms of their band maxima and relative extinctions, the transitions observed in room temperature excitation spectra of this complex correlate well with those observed in its 77° K spectra. In addition, its triplet excitation spectrum is superimposable with its absorption spectrum. These findings indicate that the emission bands found in the high and low temperature spectra of $Ir_2(Pz^*)_2(CO)_2(Ph_2POCH_2CH_3)_2$ both correspond to its ($p\sigma \rightarrow d\sigma^*$) electronic transitions. The intense high energy bands ($\nu > 25{,}000\ cm^{-1}$) seen in triplet excitation spectra of $Ir_2(Pz^*)_2(CO)_2(Ph_2POCH_2CH_3)_2$ lose intensity in the correpsonding singlet spectrum, due to efficient intersystem crossing between its ($d\pi p\sigma$) and ^3B excited states. Enhancement in the intersystem crossing rates in this complex can be attributed to spin-orbit effects associated with the iridium metal centers.[13] Similar intensity differences have been observed in spectra of other d^8-d^8 systems.[5a,14,13b]

Further insight into the origin of this "blue shift" effect can be obtained by examining the spectral data for $Ir_2(Pz^*)_2(CO)_2(Ph_2POCH_2CH_3)_2$ summarized in tables 3.5 and 3.6. Room temperature and 77° K solid state emission spectra of this complex show phosphorescence band maxima that are isoenergetic with those found in its 77° K solution spectrum. In addition, the blue shift in both its singlet and triplet emission band maxima takes place via a completely reversible process over an approximately 10° temperature range between 90° and 100° K. (table 3.6). These data are consistent with a medium induced alteration of $Ir_2(Pz^*)_2(CO)_2(Ph_2POCH_2CH_3)_2$ that modifies its

Table 3.5: Emission Spectral Parameters for $Ir_2(Pz^*)_2(CO)_2(Ph_2POCH_2CH_3)_2$

Phase	ν_{max} ($^1B \rightarrow {}^1A$) cm^{-1}	ν_{max} ($^3B \rightarrow {}^1A$) cm^{-1}	T °K
Solid	--[b]	15,300	298
Solid	--[b]	15,400	77
Solution[a]	17,900	13,500	298
Solution	19,400	15,500	77

a. 2-Methyl THF solutions
b. Not observed

Table 3.6: Temperature Dependent Emission Data for $Ir_2(Pz^*)_2(CO)_2(Ph_2POCH_2CH_3)_2$

ν_{max} ($^3B \rightarrow {}^1A$)	$\nu_{1/2}$ cm^{-1}	T °K
13,600	1940	302
13,500	1800	270
13,400	1700	230
13,400	1700	200
13,400	1600	180
13,400	1600	160
13,400	1500	150
13,400	1500	140
13,400	1500	120
13,400	1500	100
15,000	1800	90
15,400	1600	80
15,500	1600	70

emission bandshapes. Analogous effects were first observed by Wrighton and coworkers in the emission spectra of $Re(Phen)(CO)_3Cl$ and were labeled "rigidochromic luminescence."[15]

The origin of luminescence rigidochromism has been discussed in detail by Dellinger and Kasha and can be understood in terms of the potential energy surfaces portrayed in figure 3.8.[16] The extent to which a molecular system can distort in response to any perturbation (i.e., electronic or vibrational) is determined not only by its normal modes and vibrational force constants but also by the ability of its surrounding medium to respond to changes in its overall shape. In a fluid solution the surrounding solvent molecules define a mutable cage, which can readily respond to changes in the shape of an enclosed solute. However, in a low temperature matrix or in a molecular crystal, the surrounding medium is more rigidly fixed and is less able to accommodate changes in a molecule's structure. These limitations alter the nature of the normal vibrational modes of a solute molecule by restricting certain low frequency molecular distortions. As seen in figure 3.8, these restrictions effectively change the shape of the molecule's potential surface along one or more of its normal coordinates. In terms of its electronic spectra, these changes effect the Frank-Condon factors for emission (absorption) which can drastically change its emission (absorption) band maximum and half width.

While our spectroscopic data do not point to a particular molecular distortion as being primarily responsible for the rigidochromic effects in spectra of d^8-d^8 A-frame metal dimers, it can be safely concluded that these distortions must be coupled to the metal-metal coordinate. It is well known from the low temperature single crystal spectra of $Rh_2(Bridge)_4^{2+}$ and $Pt_2(P_2O_5H_2)_4^{2-}$ that metal-metal vibrations are strongly coupled to their ($d\sigma^* \rightarrow p\sigma$) electronic transitions.[5a,f,g] The metal-metal bond distances in A-frame dimer complexes has both an angular as well as a distance

Figure 3.8. A schematic representation of a pair of potential energy surfaces illustrating the origin of rigidochromic spectroscopic effects according to the Dellinger-Kasha model. Medium rigidity effects spectroscopically relevant normal modes by restricting the low frequency torsional motions of the chromophore.

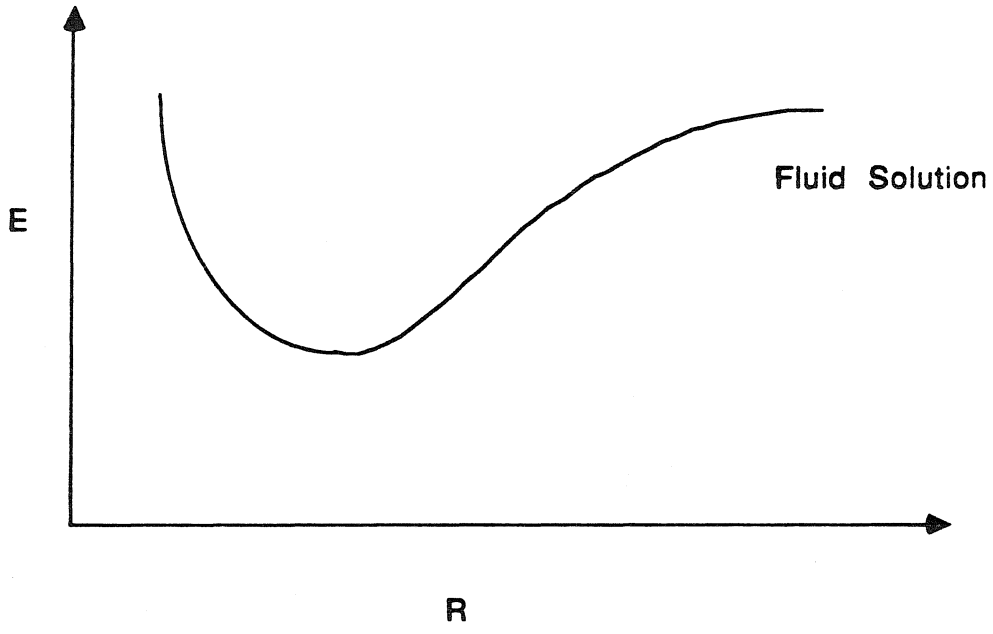
E
Fluid Solution
R

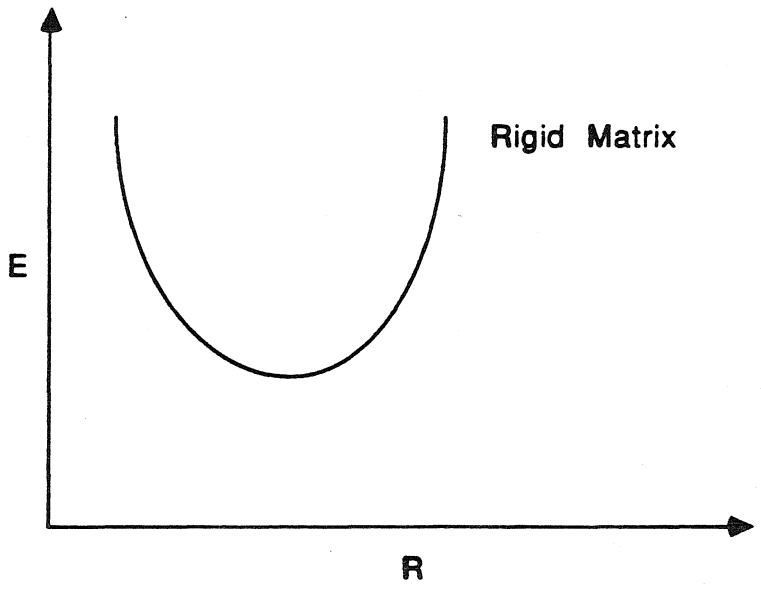
Rigid Matrix
E
R

dependence.[6] Thus, changes in the metal-metal separation in these systems may involve rearrangement of their bridging pyrazole ligands. This type of torsional motion would be susceptible to medium rigidity effects.[15c] Further conclusions, regarding rigidochromic effects in d^8-d^8 A-frame complexes, can be drawn by examining the spectroscopic data summarized in table 3.4. As mentioned earlier, rigidochromic emission appears only in spectra of the $[Ir_2(Pz)_2(CO)_4]$ and $[Ir_2(Pz)_2(CO)_2(Ph_2POR)_2]$ systems but is curiously absent in spectra of $[Ir_2(Pz)_2(COD)_2]$ and its analogs. These differences can be understood by considering the distinct steric environments provided by the various terminal ligands found in these complexes. Recent x-ray crystallographic results have indicated that the 0.375 Å difference in metal-metal distances found in oxidative addition adducts of $[Ir_2(Pz)_2(COD)_2]$ and $[Ir_2(Pz)_2(CO)_2(Ph_3P)_2]$ can be attributed in part to the larger steric repulsion between opposing COD ligands in the former compounds.[17] Similar types of steric interactions must also play a role in controlling the excited state metal-metal contractions in these A-frame metal dimers. This premise is supported by comparing the room temperature Stoke's shift seen in $[Ir_2(Pz^*)_2(CO)_4]$ (5000 cm^{-1}), $[Ir_2(Pz^*)_2(CO)_2(Ph_2POCH_2CH_3)_2]$ (5,800 cm^{-1}), and $[Ir_2(Pz)_2(COD)_2]$. The larger Stoke's shifts in the former two cases are consistent with a larger excited state metal-metal contraction made possible by their less sterically demanding terminal ligands. In contrast to these less sterically hindered systems, contractions along metal-metal coordinate in $[Ir_2(Pz^*)_2(COD)_2]$ are restricted by steric repulsion between its COD ligands; therefore, this compound does not exhibit rigidochromic effects.

In contrast to the low temperature emission data presented earlier, the room temperature emission intensities of both the singlet and triplet excited states in the donor-acceptor complexes are substantially quenched when compared to the corresponding model compounds (figure 3.6).[40] This pronounced emission intensity quenching can be attributed to an excited state intramolecular electron-transfer process

based on several lines of evidence. In some instances the excited state lifetimes and emission quantum yields of inorganic chromophores can be affected by simple nonchromophoric changes in the nature of their ligands. Nonchromophoric lifetime effects have been previously reported for a series of $Mo_2X_4(PR_3)_4$ complexes[18] and were interpreted within the frame work of Engleman and Jortner's model for nonradiative processes.[19] As seen in table 3.7, the quantum yields and triplet lifetimes of the four model complexes are essentially unperturbed by changes in the phosphinite ligand alkyl substituents. Thus, the intensity quenching seen in spectra of the donor-acceptor complexes can not be attributed to changes in k_{nr} brought on by the introduction of additional accepting or promoting vibrational modes. This emission quenching must be due to an additional nonradiative deactivation pathway involving intramolecular electron transfer. This conclusion is substantiated by the fact that the decrease in emission intensities across the series of donor-acceptor compounds, presented in figure 3.6, parallels changes in the redox potentials of their covalently attached pyridinium cations (vida infra).

Of significant interest is the intensity quenching observed in the singlet emission bands of the donor-acceptor compounds. These changes can be attributed to a *direct* singlet quenching process rather than a diminished back intersystem crossing yield due to a reactive triplet state. Control experiments show that the singlet emission intensity in $Ir_2(Pz^*)_2(CO)_2(Ph_2POCH_2CH_3)_2$ is not diminished when > 75% of its triplet emission is quenched via bimolecular energy transfer reactions. Thus, back intersystem crossing is not an active photophyscial process in the donor-acceptor and model complexes. This conclusion is in agreement with equilibrium constants (K_{eq}^{isc}) calculated from the 3700 cm^{-1} singlet-triplet energy gap in these complexes. In addition, triplet electron-transfer quenching in these systems can be inferred from the quantum yield data in table 3.7. Because $\phi_f^o/\phi_f < \phi_p^o/\phi_p$, some of the intensity quenching observed in the triplet

Table 3.7: Photophysical Parameters for the Donor-Acceptor Complexes.[a]

Complex $Ir_2(Pz^*)_2(CO)_2L_2$	Φ_f	Φ_p	τ_p μs
$Ph_2OCH_2CH_2$-NEt_3[b]	0.0015	0.032	1.2
$Ph_2OCH_2CH_3$	0.0023	0.025	1.1
Ph_2OCH_3	0.0027	0.040	1.2
$Ph_2O(CH_2)_3CH_3$	0.0025	0.030	1.1
$Ph_2OCH_2CH_2$-Me_3Py[c]	0.00017	0.0013	- -
$Ph_2OCH_2CH_2$-4MePy	0.00006	0.0004	- -
$Ph_2OCH_2CH_2$-Py	0.00003	--[d]	- -
$Ph_2OCH_2CH_2$-4PhPy	--[d]	- -	- -

a. Quantum yields taken from spectra measured in acetonitrile solutions at room temperature using $Ru(Bipy)_3^{2+}$ as a standard.
b. Singlet quantum yields for the model compounds are accurate to ±10%; triplet quantum yields are accurate to ±30%.
c. Quantum yields for the donor-acceptor compounds are accurate to ±80% .
d. Emission too weak to measure.

emission bands of the donor-acceptor complexes must be due to a direct triplet electron-transfer process.[20]

To date, the photochemical reactivity of d^8-d^8 complexes has been solely attributed to their long-lived triplet excited states. The spectra, reported here, represent the first evidence for reactivity from the shorter lived singlet states. Analyzing the quantum yield data in table 3.7 along with a singlet lifetime for $Ir_2(Pz^*)_2(CO)_2(Ph_2POCH_2CH_3)_2$ of 100 ps, places the singlet electron-transfer rates in these complexes between $5x10^{10}$ sec^{-1} and 10^{12} sec^{-1}. In comparison to the singlet reactivity reported here, the singlet state of $[Ir_2(Pz)_2(COD)_2]$ was found to be unreactive in an earlier bimolecular electron-transfer study.[3d,8] This lack of reactivity was attributed to its subnanosecond fluorescence lifetime. This shorter lived state can be intercepted by a rapid quenching process in the donor-acceptor complexes, presumably because the two redox partners are only several bond rotations away from being within the required distance for rapid electron transfer. Thus, covalently linking pyridinium cations to an iridium dimer chromophore appears to be essential for observing singlet excited state ET reactions. In addition, these reactions must have almost activationless thermal barriers, considering their substantial unimolecular rate constants. A more detailed account of the electron-transfer reactions seen in the donor-acceptor systems will be presented in chapter 4.

Electrochemistry

Previous studies regarding the electrochemical properties of d^8-d^8 metal dimers have played an important role in our understanding of the thermodynamic and kinetic factors that control their ground and excited state redox reactions. Electrochemical studies have lead to the generation and characterization of both d^8-d^7 and d^7-d^7 complexes. These species have been identified as key intermediates in photocatalytic cycles involving $Pt_2(P_2O_5H_2)_4^{2-}$ and $Ir_2(TMB)_4^{2+}$.[22,1,3] In some instances stable d^8-d^7 complexes have been generated and characterized by electronic spectroscopy and x-ray crystallography.[21e,f] In addition, recent electrochemical studies involving $Rh_2(TMB)_4^{2+}$ have indicated that its one electron oxidized state, $Rh_2(TMB)_4^{3+}$, is a reactive C-H bond activation catalyst.[22] These results have greatly enhanced our understanding of the excited state properties of d^8-d^8 complexes by uncovering a new type of ground state reactivity.

The electrochemical properties of the donor-acceptor and model compounds were of interest from several different standpoints. An understanding of the reaction exoergicities found in the donor-acceptor systems is important in characterizing their excited state electron-transfer reactions. Based on arguments presented below, a good estimate of the reaction driving force for photoinduced electron-transfer in our compounds can be obtained from the one electron redox potentials of their iridium metal centers and pyridinium cations and the spectroscopic energies of their ^1B, ^3B excited states. Thus, one goal of our electrochemical studies was to measure the one electron redox potentials for the iridium dimer chromophores and pyridinium cations. In chapter four, the photophysics of the donor-acceptor complexes is explored using picosecond time-resolved absorption spectroscopy. In principle an iridium dimer cation species, $[Ir_2(Pz^*)_2(CO)_2(Ph_2POR)_2]^+$, should be one of several transients produced in these experiments. Identifying this species in time-resolved absorption spectra of the donor-acceptor complexes would be greatly facilitated, if an

$[Ir_2^+(Pz^*)_2(CO)_2(Ph_2PR)_2]$ d^8-d^7 complex could be electrochemically generated and characterized. Finally, it was of interest to determine how covalently linking two pyridinium electron acceptors to an iridium dimer complex perturbs its one electron oxidation potentials. If sufficient ground state electronic coupling exists between the iridium metal centers and pyridinium cations in these systems, the electronic properties of both redox partners should be affected. While evidence for ground state donor-acceptor interactions was not observed in any of the electronic spectra presented earlier, electrochemical experiments offered an additional opportunity for investigating electron coupling effects.

Previous studies have indicated that the electrochemical behavior of d^8-d^8 dimers strongly depends on the nature of the solvent and supporting electrolyte.[21d,e,g] Much like d^8 monomers, these complexes have a propensity to acquire axial ligands upon oxidation. Thus, the presence of axial ligands as either a coordinating solvent or supporting electrolyte can drastically effect the shape of the waves in cyclic voltammograms of these compounds. Cyclic voltammograms (CV) of $Ir_2(Pz^*)_2(CO)_2(Ph_2POCH_2CH_3)_2$ in 0.1 M $TBAPF_6/CH_3CN$ showed a single irreversible oxidation wave with E_{pa}= 0.33 V and an irreversible electrode process at E_{pc}= -0.84 V corresponding to the reduction of an $[Ir_2(Pz^*)_2(CO)_2(Ph_2POCH_2CH_3)_2]^{n+}$ species.[43] While this behavior was not investigated in detail, it is presumed that the irreversible nature of both these couples is related to a complex process involving the coordination of one or more acetonitrile molecules to the oxidized iridium dimer. To avoid these complicating factors, CV experiments concerning the donor-acceptor complexes and model compounds were carried out in 0.1 M $TBAP_6/CH_2Cl_2$ solutions. In some instances complexes containing 3,5-dimethyl-4-isobutyl-pyrazole ligands were used due to the poor solubility of the corresponding 3,5-dimethylpyrazole complexes in methylene chloride. Differences between these compounds and those containing 3,5-dimethylpyrazole bridging ligands

will be discussed when necessary. The following section details our results concerning the electrochemistry of $Ir_2(Pz^*)_2(CO)_2(Ph_2POCH_2CH_3)_2$, $Ir_2(Pz^*)_2(CO)_2(Ph_3P)_3$, and the donor-acceptor complexes as seen in their cyclic voltammograms and bulk electrolysis data.

[$Ir_2(Pz^*)_2(CO)_2(Ph_2POCH_2CH_3)_2$]: Cyclic voltammograms of $Ir_2(Pz^*)_2(CO)_2(Ph_2POCH_2CH_3)_2$ in 0.1 M $TBAPF_6/CH_2Cl_2$ solutions, taken at a BAS platinum button working electrode, show two electrochemical couples within the potential window between -1.5 and 1.5 volts (figure 3.9). Values of E_{pc}, E_{pa}, ΔE, and $E_{1/2}$ for the first electrode process ($E_{p,a}$=0.34 volts) were constant as a function of scan rate(ν) for ν=20 to 500 mv/sec. Ratios of the anodic and cathodic peak currents for this couple varied between 1.3 and 1.1 and approached unity with increasing scan rate. Similar results were obtained at BAS glassy carbon electrodes. Constant potential bulk electrolysis experiments carried out at a pyrolytic graphite electrode (E_{app}=0.6 volts) yielded values of n=1 for this oxidation process. These data are consistent with a quasireversible one electron oxidation of $Ir_2(Pz^*)_2(CO)_2(Ph_2POCH_2CH_3)_2$ at $E_{1/2}$=0.30 volts which is followed by a slow chemical reaction. The second electrode process, seen in figure 3.9 at more positive potentials, was found to be irreversible for ν=20 to 500 mv/sec. This couple is logically assigned to a second one electron oxidation of $Ir_2(Pz^*)_2(CO)_2(Ph_2POCH_2CH_3)_2^+$ by analogy to results from a recent study concerning $[Ir_2(Pz)_2(COD)_2]$.[21g] Because our interest in this study was focused primarily on the one electron oxidation of the model compounds and donor-acceptor complexes, this couple and its analogs in other systems were not investigated in detail.

Additional information regarding the nature of the chemical reactions which follow the one electron oxidation of $Ir_2(Pz^*)_2(CO)_2(Ph_2POCH_2CH_3)_2$ was obtained by examining cyclic voltammograms and infrared spectra of methylene chloride solutions of

Figure 3.9. Cyclic voltammograms of $Ir_2(Pz^*)_2(CO)_2(Ph_2POCH_2CH_3)_2$ in 0.1 M $TBAPF_6/CH_2Cl_2$. This compound shows two single electron oxidations between 0.0 and 1.5 volts versus SSCE.

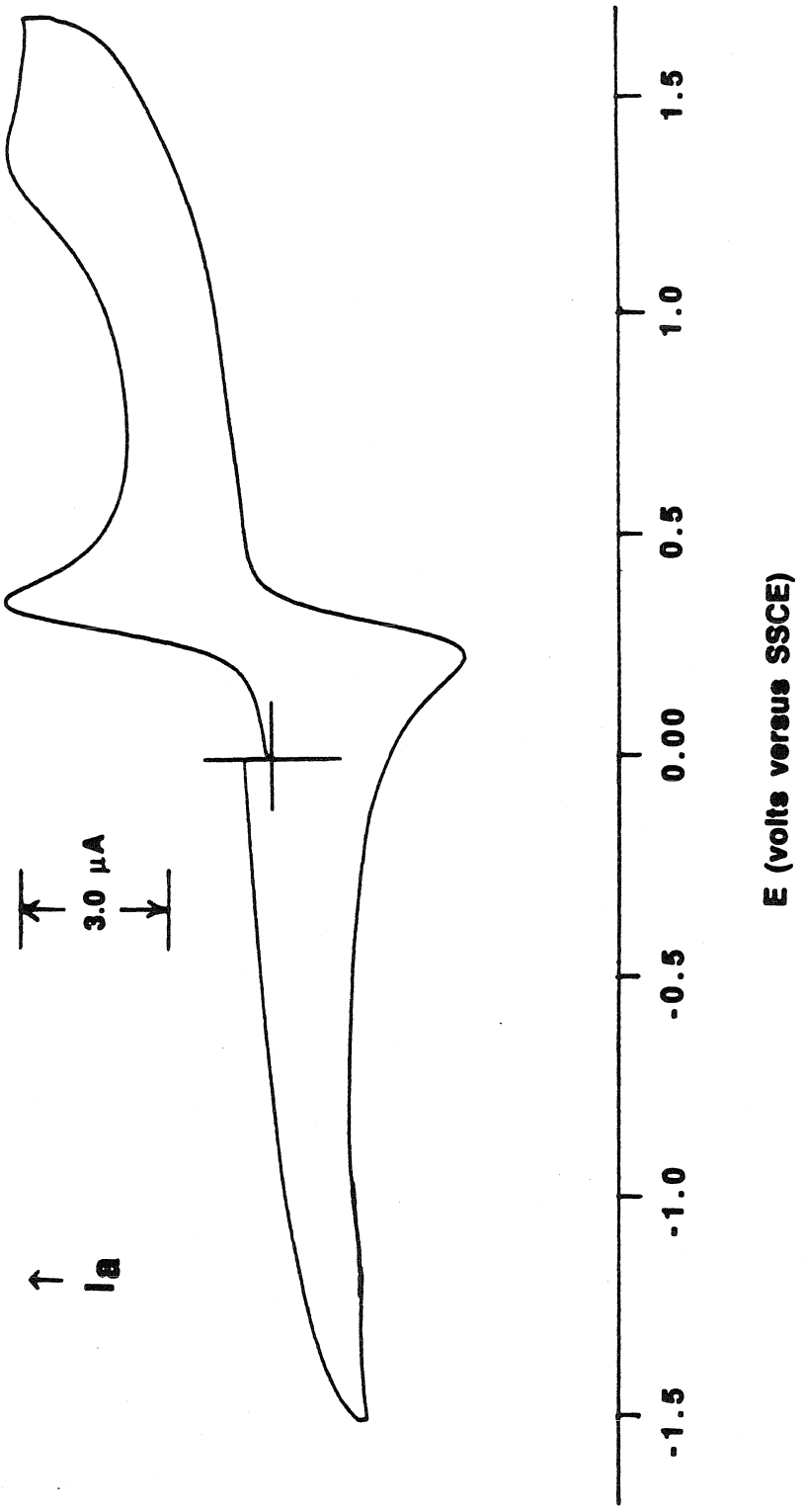
3.0 μA
i_a
-1.5
-1.0
-0.5
0.00
0.5
1.0
1.5
E (volts versus SSCE)

Figure 3.10. Cyclic voltammogram of $Ir_2(Pz^*)_2(CO)_2(Ph_2POCH_2CH_3)_2$ following bulk electrolysis at E_{app}=0.6 volts. $Ir_2(Pz^*)_2(CO)_2(Ph_2POCH_2CH_3)_2^+$ is not chemically stable on a bulk electrolysis time scale and reacts to form two unidentified products E_{pc}=-0.23 and E_{pc}=-1.0 volts.

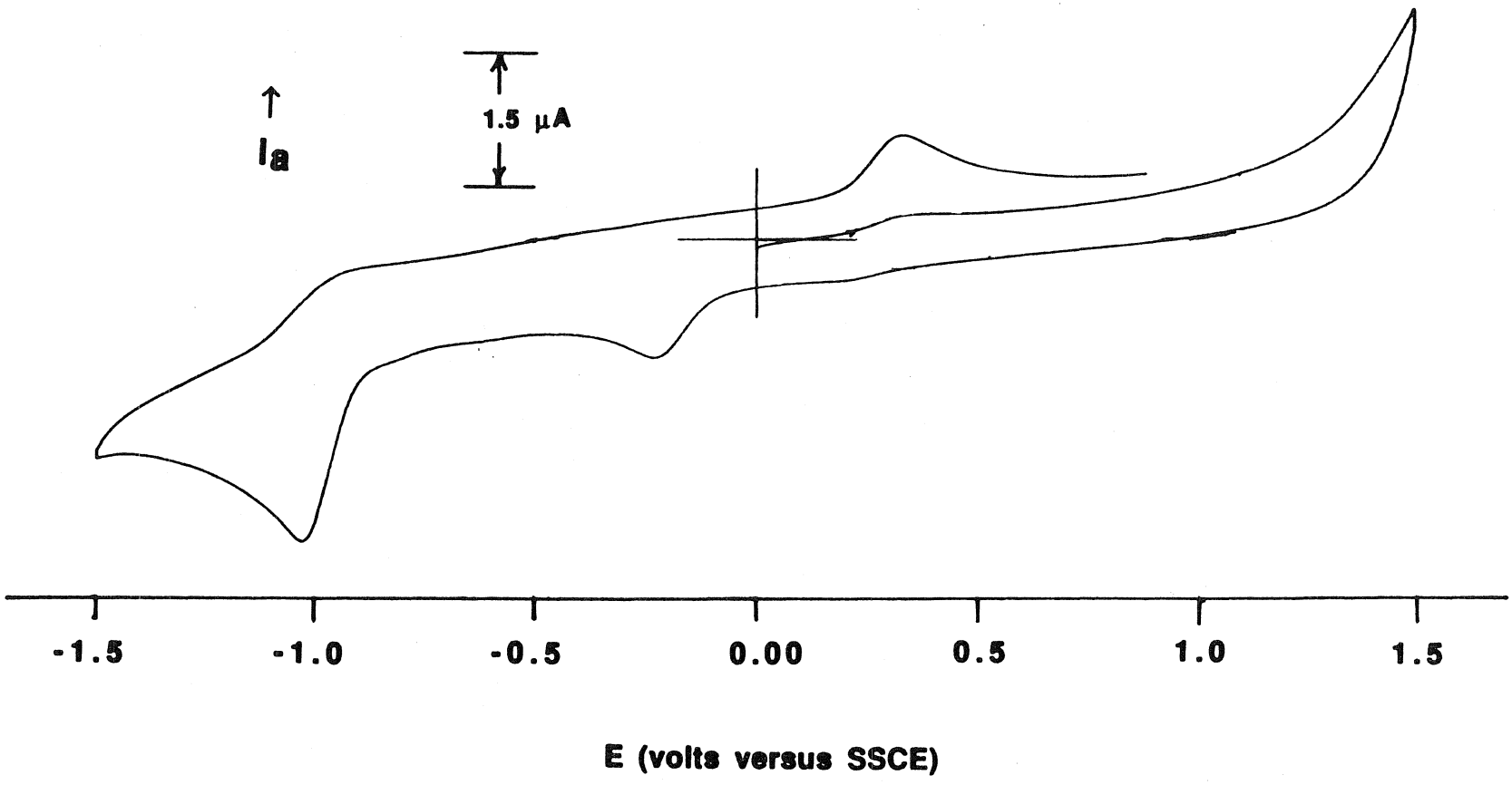
1.5 μA
I_a
-1.5
-1.0
-0.5
0.00
0.5
1.0
1.5
E (volts versus SSCE)

this complex following bulk electrolysis. Electrochemical oxidation of $Ir_2(Pz^*)_2(CO)_2(Ph_2POCH_2CH_3)_2$ at a pyrolytic graphite electrode (E_{app}= +0.6 volts) produces a color change from orange/red to light yellow. The intense visible absorption bands characteristic of the starting material decrease in intensity over the course of the experiment and are replaced by a higher energy absorption feature at λ_{max}=376 nm. Cyclic voltammograms of the electrolysis products are substantially different from CVs of $Ir_2(Pz^*)_2(CO)_2(Ph_2POCH_2CH_3)_2$. As seen in figure 3.10, in addition to the quasireversible couple at $E_{1/2}$=+0.30 volts discussed earlier, CVs of the electrolysis products show two irreversible couples at E_{pc}=-0.23 volts and E_{pc}=-1.0 volts. Scanning cathodically over either of these couples in CV experiments leads to the formation of $Ir_2(Pz^*)_2(CO)_2(Ph_2POCH_2CH_3)_2$ as indicated by the appearance of its oxidation wave at 0.3 volts. Bulk electrolysis of product solutions at potentials greater than -1.0 volts regenerates $Ir_2(Pz^*)_2(CO)_2(Ph_2POCH_2CH_3)_2$ in almost quantitative yield. These data show that the reactions associated with the oxidation of $Ir_2(Pz^*)_2(CO)_2(Ph_2POCH_2CH_3)_2$ are chemically reversible and that both electrolysis products are related to their d^8-d^8 precursor via what is presumed to be a one electron reduction. Specifically, they indicate that the metal-metal unit in the oxidized complex remains intact. If $Ir_2(Pz^*)_2(CO)_2(Ph_2POCH_2CH_3)_2^+$ fragmented into its corresponding monomers, it is not likely that electrochemically reducing these monomers would efficiently regenerate $Ir_2(Pz^*)_2(CO)_2(Ph_2POCH_2CH_3)_2$. In addition, the absence of either the -0.23 or -1.0 volt electrode couples in CVs of $Ir_2(Pz^*)_2(CO)_2(Ph_2POCH_2CH_3)_2$ supports the premise that the one electron oxidation of this complex can be characterized by an "ECE type" mechanism where the following chemical step does not significantly perturb the reversible electrode process.[23]

Figure 3.11. Infrared spectra of $Ir_2(Pz^*)_2(CO)_2(Ph_2POCH_2CH_3)_2$ in methylene chloride, a) before and b) following bulk electrolysis at E_{app}=0.6 volts. Asterisks in part b) label bands due to the solvent. The single CO band in the reactants splits into two separate bands in the products which are assigned to the symmetric and asymmetric CO modes. The stronger interaction between these two modes in spectrum b is consistent with the formation of a partial metal-metal bond in the electrolysis products.

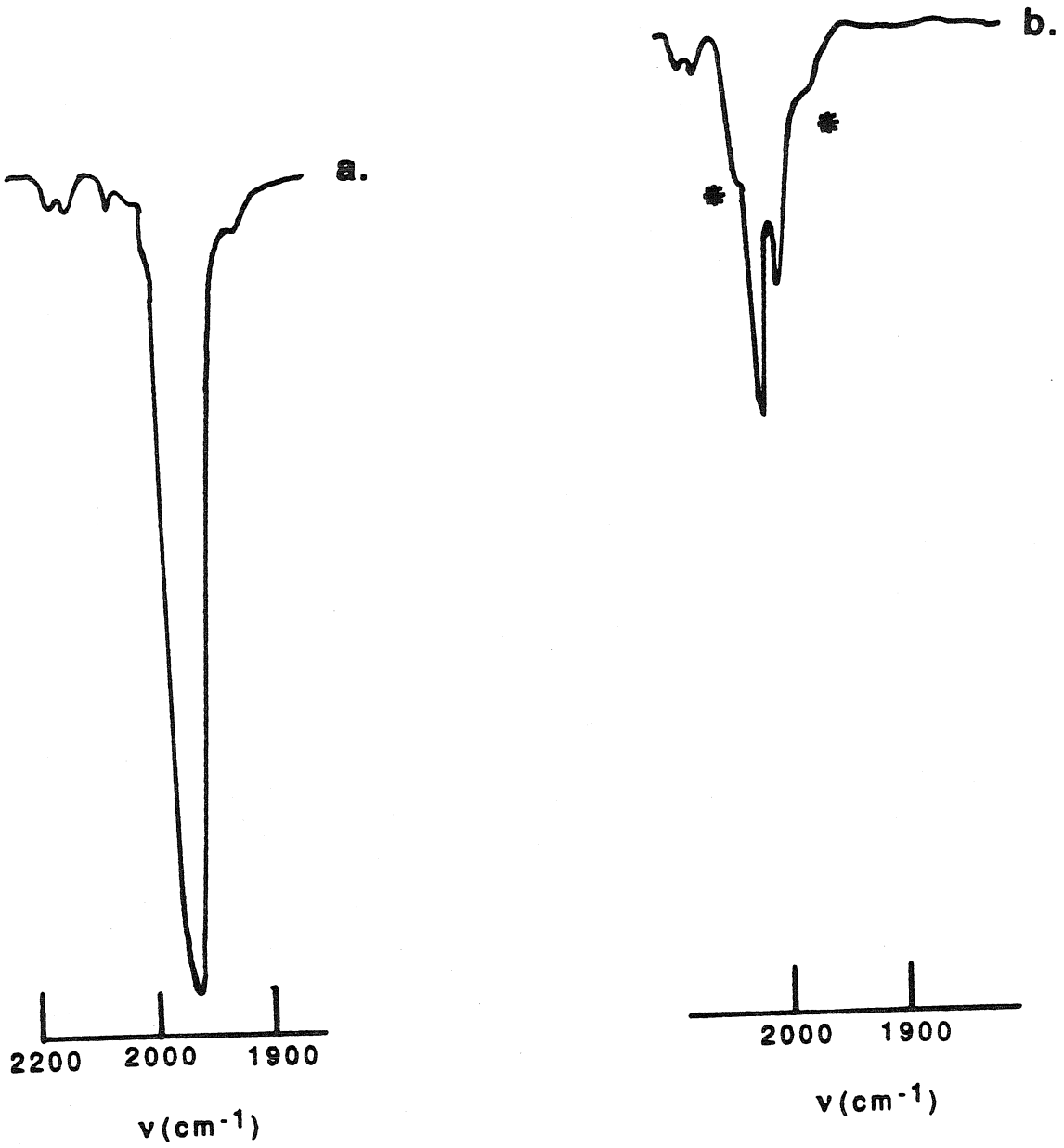
a.
2200
2000
1900
ν(cm-1)
b.
2000
1900
ν(cm-1)

Solution IR spectra of $Ir_2(Pz^*)_2(CO)_2(Ph_2POCH_2CH_3)_2$ and its electrolysis products show features that are consistent with the oxidation of the compound's iridium metal centers. As seen in figure 3.11, the broad band at ν=1960 cm^{-1}, attributed to overlapping symmetric and asymmetric CO vibrational modes in $Ir_2(Pz^*)_2(CO)_2(Ph_2POCH_2CH_3)_2$, shifts to higher frequency in spectra of the electrolysis products and splits into two well resolved bands with maxima at 2,150 cm^{-1} and 2,000 cm^{-1}. These bands are assigned to the symmetric (ν_A=2,150 cm^{-1}) and asymmetric (ν_B=2,000 cm^{-1}) CO vibrations in the products.[24,41] In addition, the larger splitting between the symmetric and asymmetric CO bands in the product is consistent with an increase in the metal-metal bond order that would accompany the oxidation of $Ir_2(Pz^*)_2(CO)_2(Ph_2POCH_2CH_3)_2$.[21f]

Unfortunately, these data say very little concerning the structures of the two electrolysis products. Several possibilities can be offered based on related d^8-d^8 systems. One plausible reaction, which could follow the oxidation of $Ir_2(Pz^*)_2(CO)_2(Ph_2POCH_2CH_3)_2$, is the sequential coordination of PF_6^- counter ions to the dimer's axial coordination sites. The coordination of weak field ligands to d^8-d^7 systems has been previously reported in studies involving $Rh(Dimen)_4^{2+}$ and a series of different counter ions (PF_6< ClO_4 < Cl).[21d] A more remote possibility would involve the oligomerization of the oxidized metal dimers. A similar dimerization reaction is known to occur in solutions of $Rh_2(Bridge)_4^{3+}$.[25] It is clear, however, that the nature of the electrolysis products formed from $Ir_2(Pz^*)_2(CO)_2(Ph_2POCH_2CH_3)_2$ is an area that is open to speculation and to further detailed investigations.

Donor-Acceptor Complexes: Cyclic voltammograms of the donor-acceptor compounds were, in general, qualitatively similar. Features common to all of these complexes are exemplified by the CVs of

Figure 3.12. Cyclic voltammograms of $Ir_2(Pz^*)_2(CO)_2(Ph_2POCH_2CH_2$-$246Me_3Py^+)_2$ in 0.1 M $TBAPF_6/CH_2Cl_2$ solutions. Part a shows all of the redox couples seen in CVs of the donor-acceptor complexes between ±1.5 volts. Part b shows that a return wave for the couple at E_{pa}=0.5 volts can be observed if the potential scan direction is reversed at the foot of the tetraphenylborate wave.

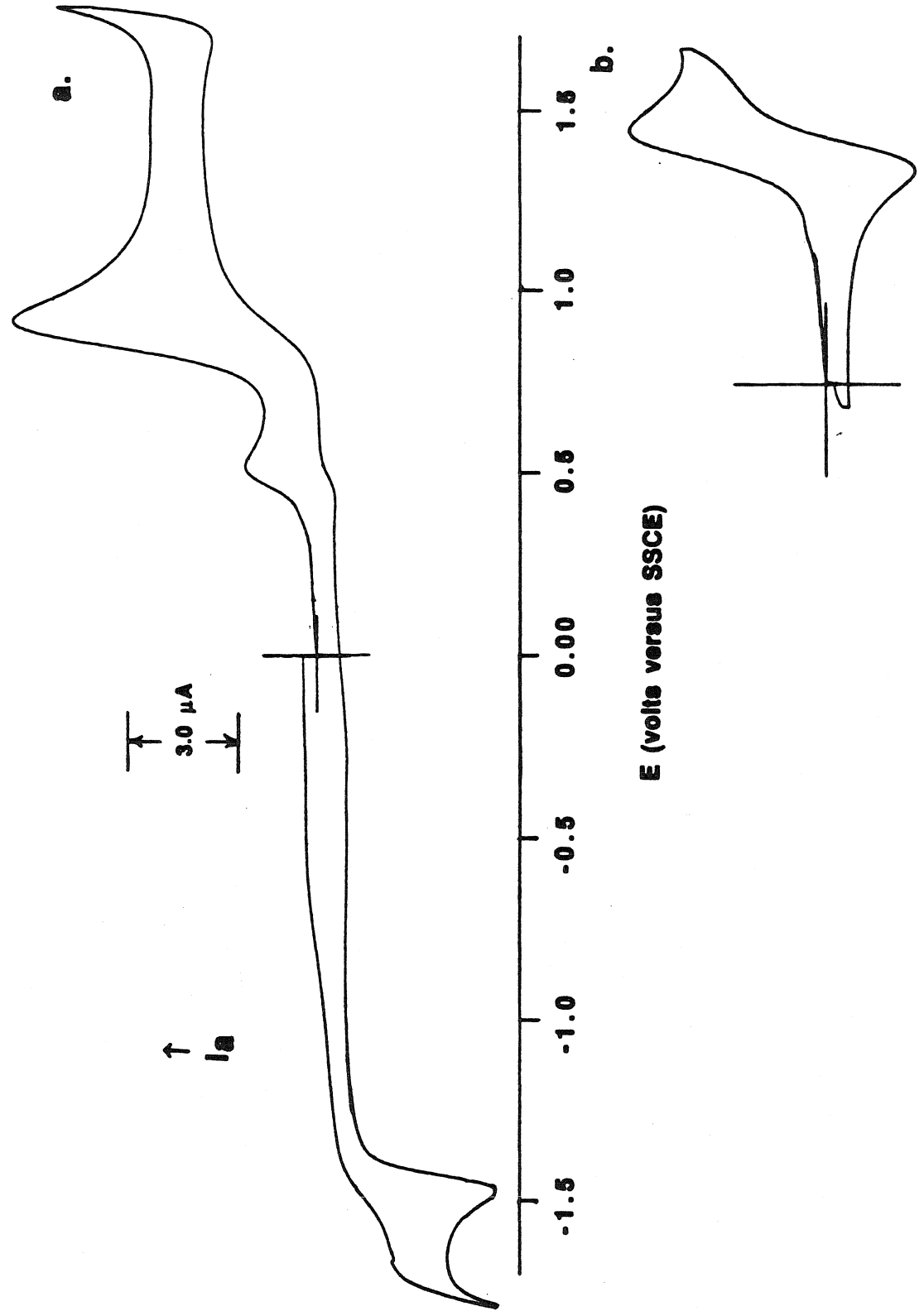
a.
b.
3.0 μA
i_a
1.5
1.0
0.5
0.00
-0.5
-1.0
-1.5
E (volts versus SSCE)

$Ir_2(Pz^*)_2(CO)_2(Ph_2POCH_2CH_2\text{-}Me_3Py^+)_2(Ph_4B)_2$ seen in figure 3.12. Final electrochemical parameters for these compounds are summarized in table 3.8. In contrast to $Ir_2(Pz^*)_2(CO)_2(Ph_2POCH_2CH_3)_2$, CVs of the donor-acceptor compounds show three electrochemical couples in the potential range between +1.5 and -1.5 volts versus SSCE. The two anodic couples, found at E_{pa}=0.5 volts and E_{pa}=0.95 volts, appear at approximately the same peak potentials in all the donor-acceptor complexes and were observed in CVs of $Ir_2(Pz^*)_2(CO)_2(Ph_2POCH_2CH_2\text{-}NEt_3^+)_2(Ph_4B)_2$ as well. The peak potentials of the cathodic couple, found at E_{pc}=-1.47 volts in figure 3.12a, varied as a function of the pyridinium cation in the donor-acceptor complexes and was absent in CVs of $Ir_2(Pz^*)_2(CO)_2(Ph_2POCH_2CH_2\text{-}NEt_3^+)_2$. This couple is assigned to the one electron reduction of the two covalently bound pyridinium cations in the donor-acceptor systems. The irreversible nature of this electrode process can be attributed to the rapid dimerization reactions of pyridyl radicals.[26] Control experiments involving CVs of $(Ph_2POCH_2CH_2\text{-}Me_3Py^+)(Ph_4B)$ and $TBA(Ph_4B)$ verified that the irreversible couple at E_{pa}=0.95 volts is due to the electrochemical oxidation of Ph_4B^-. If the scan direction was reversed at the foot of this wave, a return wave was observed for the couple at E_{pa}=0.5 volts (figure 3.11b). Scan rate dependence studies in a potential window between 0.0 and 0.6 volts indicated that the values of E_{pa}, E_{pc}, ΔE, and $E_{1/2}$ for this couple were scan rate independent for ν=20 to 500 mv/sec. Bulk electrolysis experiments regarding this oxidation process were precluded in the donor-acceptor compounds by its proximity to the oxidation of Ph_4B^-. However, as seen in figure 3.13, CVs of $Ir_2(Pz^*)_2(CO)_2(Ph_2POCH_2CH_2\text{-}NEt_3^+)_2(PF_6)_2$ contain an identical quasireversible electrochemical couple. Bulk electrolysis of this complex at a pyrolytic graphite electrode(E_{app}=+0.7 volts) yielded a value of n=1 for this electrode process. Reduction of the electrolysis products at E_{app}=-1.0 volts regenerated $Ir_2(Pz^*)_2(CO)_2(Ph_2POCH_2CH_2\text{-}NEt_3^+)_2$ in close to quantitative yield. These data

Figure 3.13. Cyclic voltammograms of $Ir_2(Pz^*)_2(CO)_2(Ph_2POCH_2CH_2NEt_3^+)_2(PF_6^-)_2$ in 0.1 M $TBAPF_6/CH_2Cl_2$.

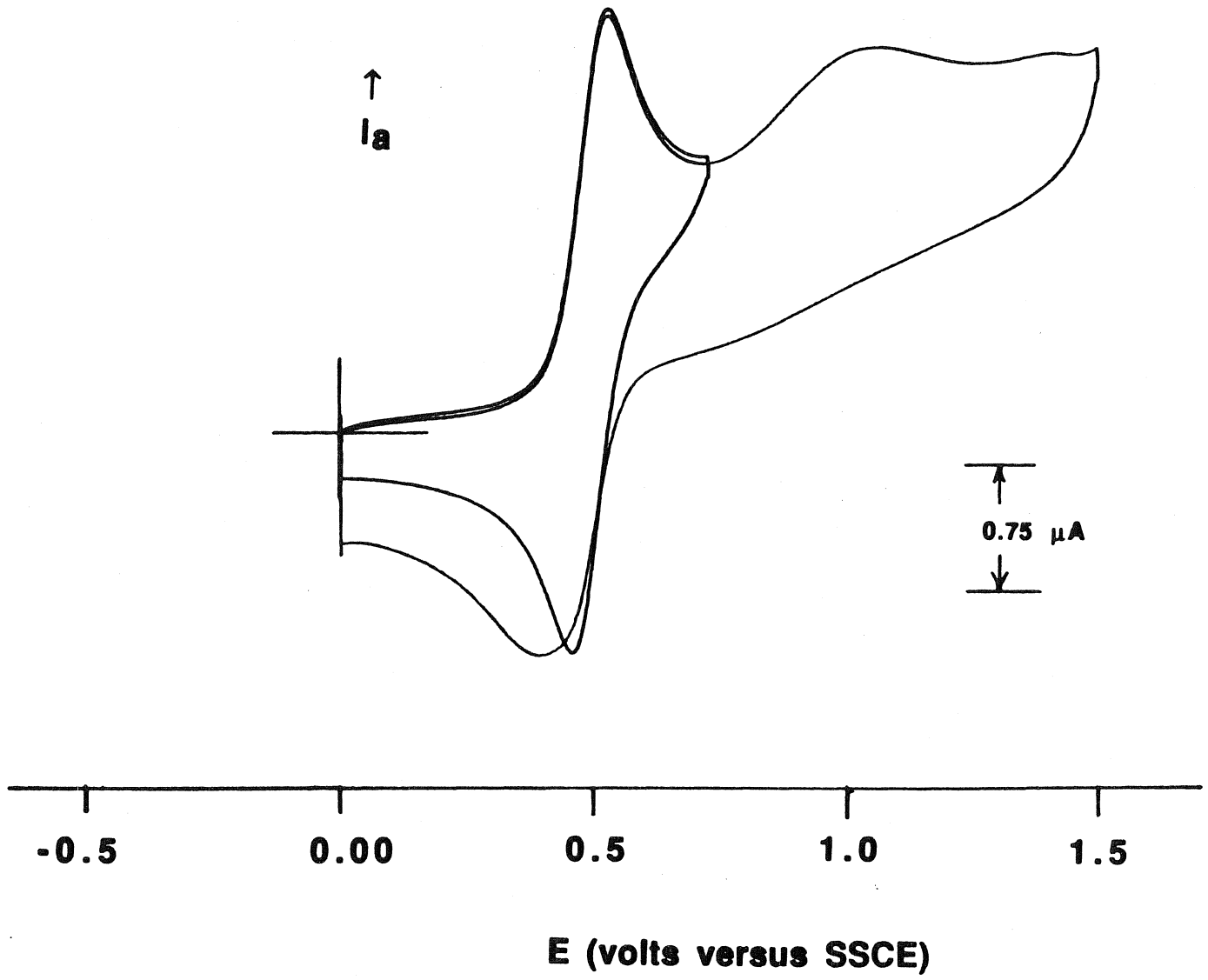
↑
Ia
0.75 µA
-0.5
0.00
0.5
1.0
1.5
E (volts versus SSCE)

indicate that this electrochemical couple in CVs of $Ir_2(Pz^*)_2(CO)_2(Ph_2POCH_2CH_2$-$Me_3Py^+)_2$ and $Ir_2(Pz^*)_2(CO)_2(Ph_2POCH_2CH_2$-$NEt_3^+)_2$ corresponds to the one electron oxidation of their iridium metal centers. Analogous quasireversible waves were seen in CVs of $Ir_2(Pz^{**})_2(CO)_2(Ph_2POCH_2CH_2$-$4MePy^+)_2$, $Ir_2(Pz^{**})_2(CO)_2(Ph_2POCH_2CH_2$-$Py^+)_2$, and $Ir_2(Pz^{**})_2(CO)_2(Ph_2POCH_2CH_2$-$4PhPy^+)_2$ at $E_{1/2} \cong 0.42$ volts. The 50 mv difference between the oxidation potential of these compounds and $Ir_2(Pz^*)_2(CO)_2(Ph_2POCH_2CH_2$-$Me_3Py^+)_2$ can be attributed to their more electron donating 3,5-dimethyl-4-isobutylpyrazole ligands. Similar trends have been observed in the photoelectron spectra of a series of $[Ir_2(Pz)_2(CO)_4]$ complexes (Pz=pyrazole, 3-methylpyrazole, and 3,5-dimethylpyrazole).[27]

A careful examination of the redox potentials for the donor-acceptor complexes and model compounds reveals an important trend in their electrochemical properties. As seen in table 3.8, the oxidation potentials of the donor-acceptor complexes lie approximately 150 mv anodic of the oxidation potential of $Ir_2(Pz^*)_2(CO)_2(Ph_2POCH_2CH_3)_2$. In addition, the oxidation potentials of $Ir_2(Pz^*)_2(CO)_2(Ph_2POCH_2CH_2$-$NEt_3^+)_2$ and $Ir_2(Pz^*)_2(CO)_2(Ph_2POCH_2CH_2$-$Me_3Py^+)_2$ are the same within experimental error. These findings indicate that the donor-acceptor compounds and $Ir_2(Pz^*)_2(CO)_2(Ph_2POCH_2CH_2$-$NEt_3^+)_2$ are more difficult to oxidize due to their overall 2+ charge. Our data show little evidence for ground state electronic interactions between the iridium metal centers and pyridinium cations in the donor-acceptor complexes.

$[Ir_2(Pz^*)_2(CO)_2(Ph_3P)_2]$: Cyclic voltammograms of $Ir_2(Pz^*)_2(CO)_2(Ph_3P)_2$ show two anodic electrode processes at $E_{pa}^{(1)}=0.2$ volts and $E_{pa}^{(2)}=1.3$ volts, which are qualitatively similar to the electrochemical couples observed in CVs of $Ir_2(Pz^*)_2(CO)_2(Ph_2POCH_2CH_3)_2$. Values of E_{pa}, E_{pc}, $E_{1/2}$, and ΔE for the first electrode process were independent of scan rate and $I_{pa}/I_{pc}=1.0$ for $\nu=20$ to 500

Table 3.8: Electrochemical Potentials for the Iridium Dimer Complexes.[a]

	$Ir_2 \rightarrow Ir_2^+ + e^-$				$e^- + Py^+ \rightarrow Py$
Complex	E_{pa}	E_{pc}	ΔE	$E_{1/2}$	E_{pc}
$Ir_2(Pz)_2(CO)_2L_2$	V	V	mv	V	V[c]
$Ph_2OCH_2CH_2$-$NEt_3(Ph_4B)$	0.52	0.43	90	0.48	- -
$Ph_2OCH_2CH_2$-$NEt_3(PF_6)$	0.53	0.43	100	0.48	- -
$Ph_2OCH_2CH_3$	0.35	0.26	90	0.30	- -
$Ph_2OCH_2CH_2$-Me_3Py	0.52	0.42	110	0.47	-1.49
$Ph_2OCH_2CH_2$-4MePy[b]	0.47	0.37	100	0.42	-1.32
$Ph_2OCH_2CH_2$-Py[b]	0.44	0.36	80	0.40	-1.17
$Ph_2OCH_2CH_2$-4PhPy[b]	0.47	0.37	100	0.42	-1.10

a. Measured in 0.1 M $TBAPF_6/CH_2Cl_2$ versus SSCE.

b. Potentials were measured using a 4-isobutyl-3,5-dimethylpyrazole derivative due to the poor solubility of the 3,5-dimethylpyrazole derviative in CH_2Cl_2.

c. Peak potentials measured at a sweep rate of 100 mv/sec.

mv/sec. These data indicated that $Ir_2(Pz^*)_2(CO)_2(Ph_3P)_2$ was a suitable system for electrochemically generating and characterizing a stable d^8-d^7 A-frame complex. Bulk electrolysis of this complex, in 0.1 M $TBAPF_6/CH_2Cl_2$ solutions at a platinum basket electrode (E_{app}=0.4 volts), produced a color change from red/orange to light yellow and yielded a value of n=1 for this redox process. The intense d $\rightarrow$ p transitions attributed to the starting material decrease in intensity during the electrolysis experiment and are replaced by absorption bands characteristic of the electrolysis products. As seen in figure 3.14, CVs of the electrolysis products are nearly identical to CVs of $Ir_2(Pz^*)_2(CO)_2(Ph_3P)_2$. Thus, in contrast to $[Ir_2(Pz^*)_2(CO)_2(Ph_2POCH_2CH_3)_2]^+$, $[Ir_2(Pz^*)_2(CO)_2(Ph_3P)_2]^+$ is a chemically stable species under the prevailing reaction conditions. IR spectra of this d^8-d^7 complex were similar to those seen earlier for the $[Ir_2(Pz^*)_2(CO)_2(Ph_2POCH_2CH_3)_2]^{0/+}$ system. As in IR spectra of $Ir_2(Pz^*)_2(CO)_2(Ph_2POCH_2CH_3)_2$ and its corresponding cations, ν_{CO} for $[Ir_2(Pz^*)_2(CO)_2(Ph_3P)_3]^+$ is greater than ν_{CO} for $Ir_2(Pz^*)_2(CO)_2(Ph_3P)_2$ (figure 3.15 ν_A=1990 cm^{-1}; ν_B=1980 cm^{-1}). Electronic absorption spectra of $[Ir_2(Pz^*)_2(CO)_2(Ph_3P)_2]^+$ show four bands with maxima at 373 nm, 460 nm, 500 nm,and 770 nm (figure 3.16). Extinction coefficients for these transitions were estimated from the known concentration of $Ir_2(Pz^*)_2(CO)_2(Ph_3P)_2$ in the electrolysis experiment. The intense band at 373 nm is assigned to a $^2B \rightarrow {}^2A$ ($d\sigma \rightarrow d\sigma^*$) electronic transition by analogy to a similar spectroscopic feature found in spectra of $Rh_2(Bridge)_4^{2+}$.[28] The weaker bands at 460 nm and 500 nm are tentatively assigned to ligand field transitions ($d_{xz}, d_{yz} \rightarrow d\sigma^*$). The broad low energy transition at 770 nm is not assigned.[29]

Figure 3.14. Cyclic voltammograms of $Ir_2(Pz^*)_2(CO)_2(Ph_3P)_2$ a) before and b) following bulk electrolysis at E_{app}=0.4 volts. CVs of the reactant and product of this reaction are identical, indicating that $Ir_2(Pz^*)_2(CO)_2(Ph_3P)_2^+$ is a chemically stable species.

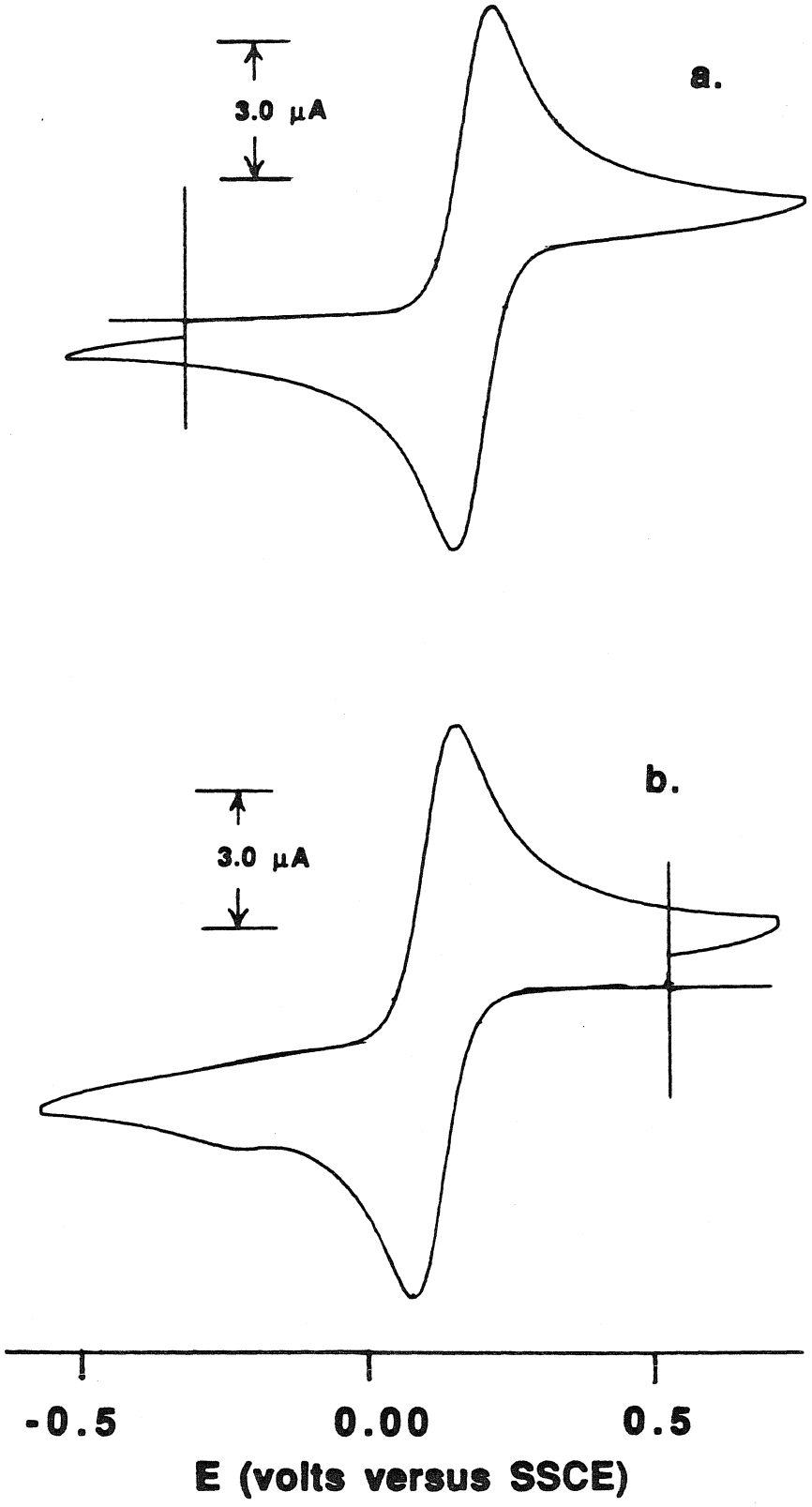
a.
3.0 μA
b.
3.0 μA
-0.5
0.00
0.5
E (volts versus SSCE)

Figure 3.15. Infrared spectra of $Ir_2(Pz^*)_2(CO)_2(Ph_3P)_2$ in methylene chloride a)before and b) following bulk electrolysis.

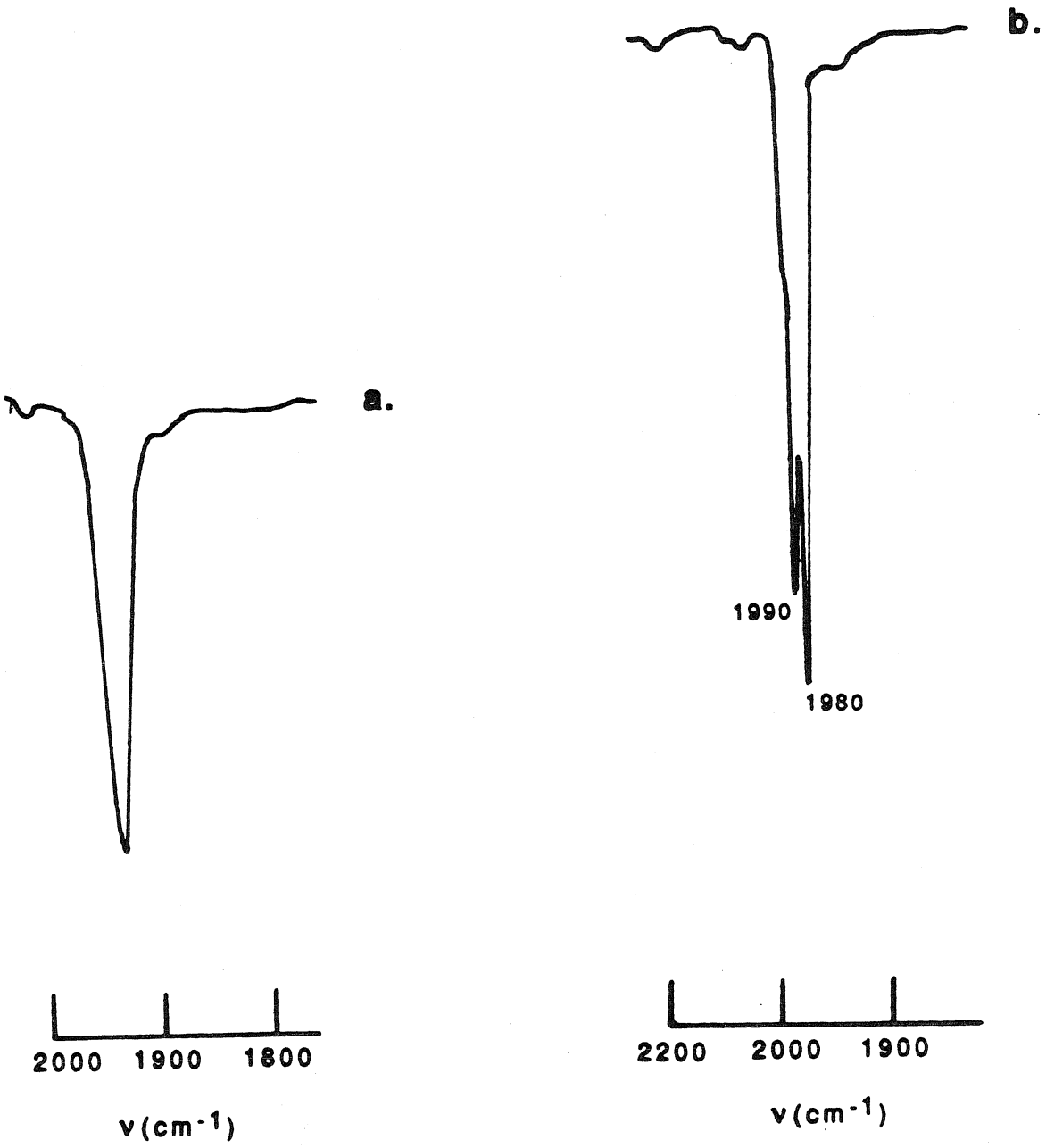
a.
2000
1900
1800
ν(cm-1)
b.
1990
1980
2200
2000
1900
ν(cm-1)

Figure 3.16. Electronic absorption spectra of $Ir_2(Pz^*)_2(CO)_2(Ph_3P)_2$ a) before and b) following bulk electrolysis. During the electrolysis experiment the $^1A \rightarrow {}^1B$ ($d\sigma^* \rightarrow p\sigma$) absorption band of the reactants disappears and is replaced by an intense feature at 377 nm which is assigned to a $^2B \rightarrow {}^2A(d\sigma \rightarrow d\sigma^*)$ transition.

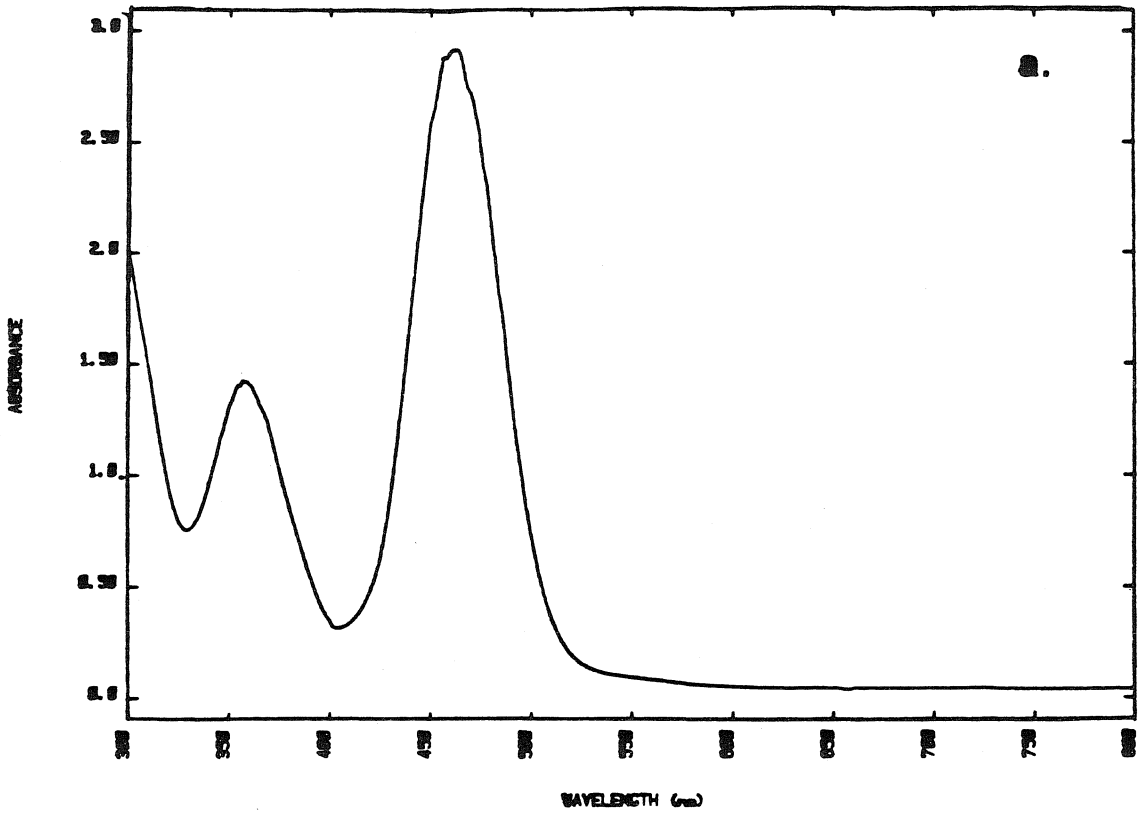
a.
ABSORBANCE
WAVELENGTH (nm)

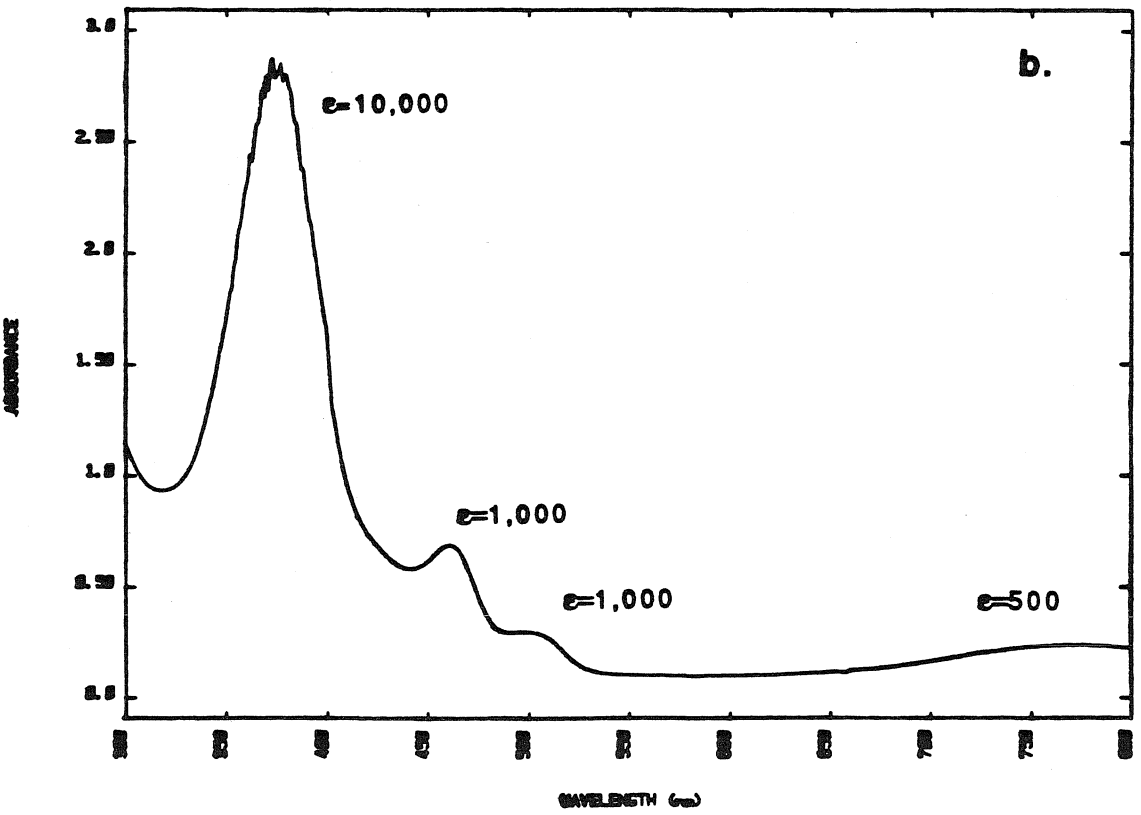
b.
ε=10,000
ε=1,000
ε=1,000
ε=500
ABSORBANCE
WAVELENGTH (nm)

Excited State Energetics

A central objective of our studies, regarding the electrochemical and spectroscopic properties of the donor-acceptor compounds, was to determine estimates for electron-transfer driving forces. This type of information is important from several stand points. First, reaction exoergicity is known to be a fundamental kinetic parameter in electron-transfer reactions.[30] The driving force dependence is an important characteristic of an electron-transfer process, because exoergicity, along with inner-sphere and outer-sphere reorganization energies, determines the thermal barriers to electron transfer. Secondly, in contrast to a bimolecular ET system, the charge separated state in the donor-acceptor complexes can be thought of as an additional molecular electronic state. Characterizing the relative energies of the metal localized (^{1}B and ^{3}B) and charge-transfer (CT) states in the donor-acceptor systems is important to understanding their photophysical properties.

The reaction exoergicities in the donor-acceptor complexes can be estimated from the one electron oxidation and reduction potentials of their ^{1}B and ^{3}B excited states, and pyridinium cations using the spectroscopic and electrochemical data presented in this chapter.[31,32] The oxidation potential of the ^{1}B and ^{3}B excited states are given by equations 3.3a and b.

$$E^\circ(Ir_2;{}^1B/Ir_2^+) = E_{oo}({}^1B) - E_{1/2}(Ir_2/Ir_2^+) \qquad \text{eq. 3.3a}$$

$$E^\circ(Ir_2;{}^3B/Ir_2^+) = E_{oo}({}^3B) - E_{1/2}(Ir_2/Ir_2^+) \qquad \text{eq. 3.3b}$$

These equations are essentially electrochemical analogs of Förster's equations for excited state acid-base reactions as discussed by Grabowski *et al.*[33] They assume that $\Delta H(M^*/M^+) - \Delta H(M/M^+) = E_{oo}(M^*)$ and $\Delta S(M^*/M^+) - \Delta S(M^*/M^+) \cong 0$. The former assumption is reasonable for condensed phase reactions at 1 atm. The validity of the

latter assumption depends on the nature M and M*. Differences in the entropy of the ground and excited states of a molecule can arise from several different effects: 1) changes in dipole moment that lead to changes in solvation, 2) changes in internal degrees of freedom, and 3) changes in orbital and spin degeneracies. This last factor can usually be neglected, because it amounts to about 0.03 eV at 25° C.[31] Changes in solvation are not likely to contribute to $\Delta\Delta S$ in the donor-acceptor systems due to the low polarity of the ^1B and ^3B metal localized excited states. Entropy effects due to changes in a chromophore's internal degrees of freedom are difficult to predict. However, a good estimate of $\Delta\Delta S$ can be obtained from the Stoke's shift between a compound's absorption and emission maxima; larger Stoke's shifts are associated with larger entropy changes. Previous studies have indicated that the triplet state oxidation potentials for $[Ir_2(Pz)_2(COD)_2]$, obtained from equation 3b and from bimolecular quenching studies are the same within experimental error; this compound's Stoke's shift is approximately 2500 cm^{-1}.[8] Considering that the Stoke's shift for the donor-acceptor complexes is a factor of two greater than this value suggests that $\Delta\Delta S$ contributions in these complexes are negligible as well. Thus, a knowledge of E_{oo} and $E_{1/2}$ is required to estimate the excited state redox potentials of the ^1B and ^3B excited states in these complexes. Values of $E_{oo}(^1B)$ and $E_{oo}(^3B)$ were estimated from the arithmetic mean of their corresponding emission and absorption maxima. This procedure yields exact values of E_{oo} provided that the ground and excited state vibrational frequencies for the complexes are the same.[34] However, the ground and excited state metal-metal vibrational frequencies in d^8-d^8 complexes are known to differ by as much as 100 cm^{-1}.The error incurred by using this approximation was found to be about $\pm$150 cm^{-1} by carrying out similar calculations on $Pt_2(P_2O_5H_2)_4^{2-}$ and $Rh_2(Bridge)_4^{2+}$. The oxidation potential of the iridium dimer chromophore is approximated as the average of the oxidation potential for $Ir_2(Pz^*)_2(CO)_2(Ph_2POCH_2CH_3)_2$ and $Ir_2(Pz^*)_2(CO)_2(Ph_2POCH_2CH_2\text{-}NEt_3^+)_2$ based on the following argument. In contrast

to a bimolecular ET reaction, charge in a donor-acceptor system is redistributed with a single molecular unit, rather than transferred from one molecule to another. As seen in equation 3.4, the electron-transfer reactions in the $Ir_2(Pz^*)_2(CO)_2(Ph_2POCH_2CH_2\text{-}Q^+)_2$ systems can be formally characterized by the redistribution of a positive charge from a single pyridinium cation (Q^+) to a pair of iridium metal centers.

$$Q^+\text{--}Ir_2\text{--}Q^+ \xrightarrow{h\nu} Q^+\text{--}Ir_2^+\text{--}Q \quad \text{eq. 3.4}$$

Within this formalism the oxidation half reaction for the donor-acceptor complexes is represented by the one electron oxidation of their iridium metal centers under the influence of a single pyridinium cation (equation 3.5.).

$$R\text{--}Ir_2\text{--}Q^+ \longrightarrow R\text{--}Ir_2^+\text{--}Q^+ + e^- \quad \text{eq. 3.5}$$

The redox potential for this half reaction could be easily determined using a complex that contains one neutral and one charged phosphinite ligand. However, asymmetrically substituted compounds are not readily prepared. It was shown in the previous section that the pyridinium cations alter the oxidation potentials of the donor-acceptor complexes by acting as inert electrostatic charges. Assuming that these effects are additive, a good estimate for the redox potential of reaction 5 is the mean value of the oxidation potential of $Ir_2(Pz^*)_2(CO)_2(Ph_2POCH_2CH_3)_2$ and $Ir_2(Pz^*)_2(CO)_2(Ph_2POCH_2CH_2\text{-}NEt_3^+)_2$.

Determining reduction potentials for the pyridinium cations in the donor-acceptor complexes is complicated by the dimerization reactions of pyridyl radical, which distort the pyridinium CV waves.[26] Earlier studies have established that pyridyl radicals exist in solution in equilibrium with their "4,4'-dihydrobipyridine like" counter parts (equation 3.6.).[35]

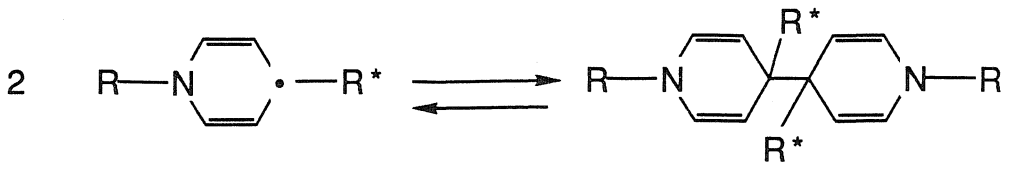

eq. 3.6

At room temperature these reactions take place at approximately 10^8 $M^{-1}s^{-1}$, favoring the dihydrobipyridine adduct. When R is an electron withdrawing substituent, such as CN or a carbomethoxy group, K_{eq} is approximately 10^5 M^{-1}; For R*= alkyl or H, K_{eq} is greater than 10^{11} M^{-1}. Electrochemical EC mechanisms, involving dimerization reactions such as those surrounding pyridyl radicals, have been discussed in detail by Saveant *et al.*[36] According to the kinetic analysis reported by these authors, the characteristics of an EC electrochemical couple are a function of the sweep rate (ν), substrate concentration (C_o), and equilibrium constant and rate constant for the dimerization reaction. The dimerization rates for the type of pyridinium cations employed in the donor-acceptor complexes place their electrochemical couples in the pure kinetic region of a logλ versus logχ plot. Under these conditions, the value of $E_{1/2}$ for their one electron reduction is related to their peak potentials through equation 3.7;

$$E_{1/2} = E_{pc} + 0.058 - 0.0197 Log\left[\frac{kC_o}{\upsilon}\right] \quad \text{eq. 3.7.}$$

where k is the dimerization rate constant. Reduction potentials for the pyridinium cations in the donor-acceptor complexes were calculated from their peak potentials using equation 3.7 and are summarized in table 3.9. This analysis assumes that the dimerization rate constants for pyridyl radicals bound to the donor-acceptor compounds can be approximated by rate constants for free pyridyl radicals.

Using the spectroscopic and electrochemical data found in table 3.9, an approximate state diagram for the donor-acceptor systems can be constructed. As seen

in figure 3.17, in addition to their ^1B and ^3B metal localized excited states, each of the donor-acceptor complexes possesses a charge-transfer state whose energy varies with the reduction potential of the compound's covalently attached pyridinium cation. Notably, the charge-transfer states in the complexes are all well below the ^3B excited state; However, no evidence for direct electronic transitions between these CT states and the ^1A ground state was found in the electronic absorption and emission spectra of the compounds. Such transitions might be loosely thought of as analogs of the MLCT transitions associated with $M(CO)_5(Py\text{-}R)$ (M=W, R=CN ,Ph, Cl, etc.) or $M(Bipy)_3^{3+}$ (M=Ru or Os) complexes[39]. Absorption bands corresponding to a direct optical charge-transfer process must be low enough in intensity in the donor-acceptor complexes that they are not detected with our instrumentation. Based on the photophysical data presented in table 3.7, k_r for the $^3B \rightarrow {}^1A$ transition in these compounds is approximately 10^4 sec^{-1}. The absence of $^1A \rightarrow$ CT absorption bands in their electronic spectra suggests that k_r for this process is less than 10^4 sec^{-1}. In the following chapter we will see that the excited state lifetimes of the CT state in the donor-acceptor compounds ranges from 100 ps to 10 ns. These relatively short lifetimes must correspond to rapid nonradiative charge recombination reactions, which return these systems to their ground states. Thus, charge separation in our donor-acceptor systems occurs via excited state electron transfer, involving the ^1B and ^3B excited states of their iridium dimer redox chromophores, and charge recombination occurs by a primarily nonradiative process.

Figure 3.17. A state diagram for the donor-acceptor systems, constructed from the spectroscopic and electrochemical data found in table 3.9. While the charge-transfer states in these complexes are energetic enough to have absorption bands in the visible and near IR, such absorption features were not observed.

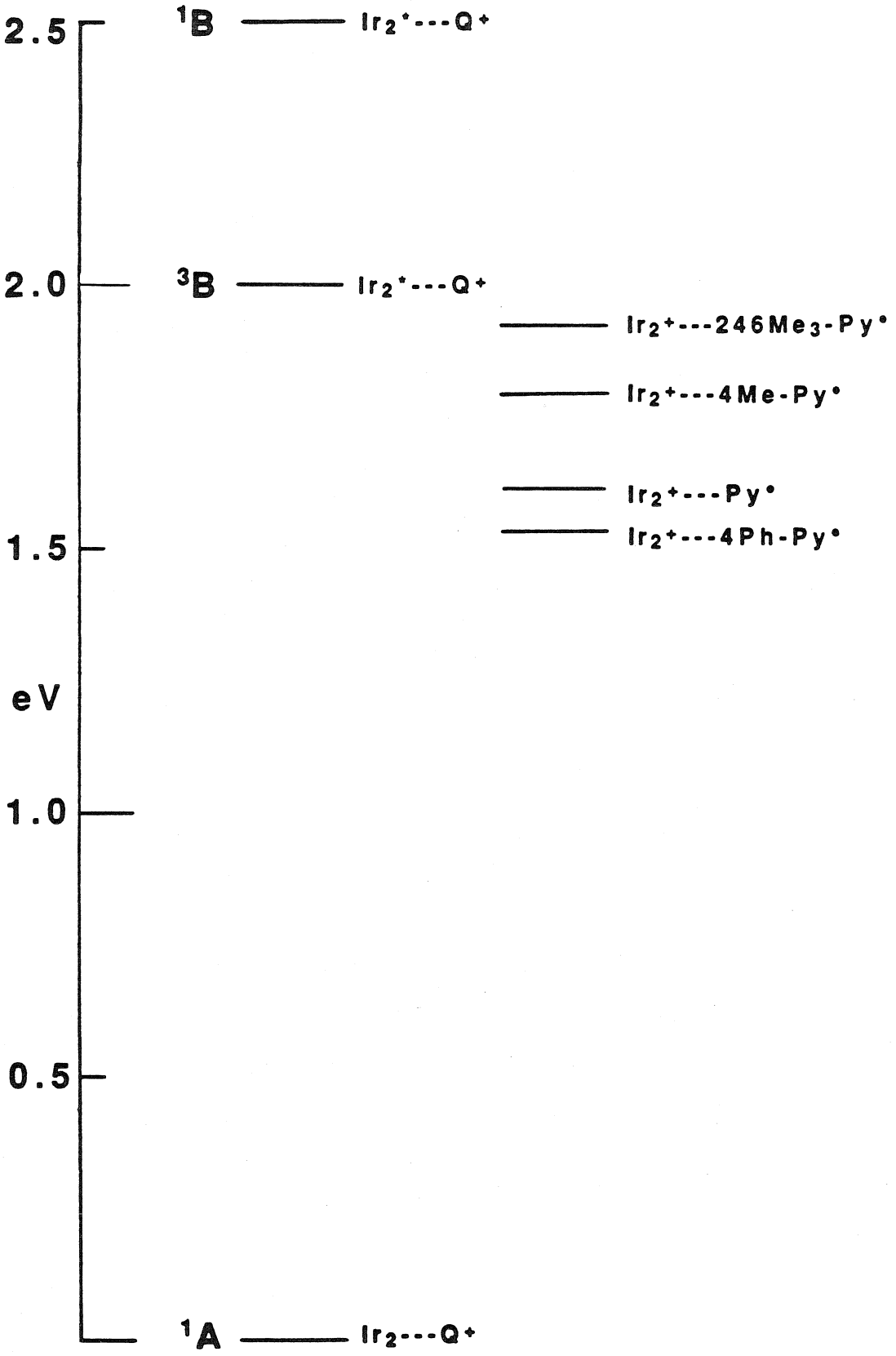
2.5
2.0
1.5
eV
1.0
0.5
^1B —— Ir_2^*---Q^+
^3B —— Ir_2^*---Q^+
—— Ir_2^+---246Me_3-Py$^\bullet$
—— Ir_2^+---4Me-Py$^\bullet$
—— Ir_2^+---Py$^\bullet$
—— Ir_2^+---4Ph-Py$^\bullet$
^1A —— Ir_2---Q^+

Table 3.9: Final Energetic Parameters for the Donor-Acceptor Complexes.

Transition	E(ev)	σ
$^1A \rightarrow {}^1B$	2.5	±0.02
$^1A \rightarrow {}^3B$	2.0	±0.02
$Ir_2 \rightarrow Ir_2^+ + e^-$	0.39	±0.03
$Ir_2(^1B) \rightarrow Ir_2^+ + e^-$	2.11	±0.04
$Ir_2(^3B) \rightarrow Ir_2^+ + e^-$	1.61	±0.04
$e^- + 246Me_3\text{-}Py^+ \rightarrow 246Me_3\text{-}Py$	-1.53	±0.05
$e^- + 4Me\text{-}Py^+ \rightarrow 4Me\text{–}Py$	-1.40	±0.05
$e^- + Py^+ \rightarrow Py$	-1.22	±0.05
$e^- + 4Ph\text{-}Py^+ \rightarrow 4Ph\text{-}Py$	-1.14	±0.05

References

1a. Zipp, A. P., *Coord. Chem. Rev.*, **1988**, *84*, 47-83.

b. Marshall, J, L.; Stiegman, A. E.; Gray, H. B., *ACS Symp. Ser.*, **1986**, *307*, 166-176.

c. Roundhill, D. M., *J. Amer. Chem. Soc.*, **1985**, *107*, 4354-4356.

d. Che, C.-M.; Lee, W.-M., *J. Chem. Soc. Chem. Comm.*, **1986**, 512-513.

e. Alexander, K. A.; Stein, P.; Hedden, D. B.; Roundhill, D. M., *Polyhedron*, **1983**, 1389-1392.

f. Roundhill, D. M.; Atherton, S. F., *submitted for publication.*

g. Roundhill, D. M.; Atherton, S. J.; Shen, Z.-P, *J. Amer. Chem. Soc.*, **1987**, *109*, 6076-6079.

2. Caspar, J. V.; Gray, H. B., *J. Amer. Chem. Soc.*, **1984**, *106*, 3029-3030.

3a. Vlcek, A.; Gray, H. B, *Inorg. Chem.*, **1987**, *26*, 1997-2001.

b. Harvey. E. L.; Stiegman, A. E.; Vlcek, A.; Gray, H. B., *J. Amer. Chem. Soc.*, **1987**, *109*, 5233-5235.

c. Vlcek, A.; Gray, H. B., *J. Amer. Chem. Soc.*, **1987**, *109*, 286-287.

d. Harvey, P. D.; Gray, H. B, *Nouv. J. Chem.*, **1987**, *11*, 595-596.

4a. Che, C.-M.; Butler, L. G.; Gray, H. B., *J. Amer. Chem. Soc.*, **1981**, *103*, 7796-7797.

b. Che, C.-M., Cho, K.-C.; Chan, W.-S.; Gray, H. B., *Inorg. Chem..*, **1986**, *25*, 4906-4909.

c. Milder, S. J.; Goldbeck, R. A.; Kliger, D. S.; Gray. H. B., *J. Amer. Chem. Soc.*, **1980**, *102*, 6761-6764.

d. Marshall, J, L.; Stobart, S. R.; Gray, H. B., *J. Amer. Chem. Soc.*, **1984**, *106*, 3027-3029.

5a. Rice, S. F., Ph.D. Dissertation, California Institute of Technology, Pasadena, CA, 1982.

b. Fordyce, W. A.; Brummer, J. G.; Crosby, G. A., *J. Amer. Chem. Soc.*, **1981**, *103*, 7061-7064.

c. Rice, S. F.; Miskowski, V. M.; Gray, H. B., *Inorg. Chem..*, **1988**, *manuscript in press.*

d. Balch, A., *J. Amer. Chem. Soc.*, **1976**, *98*, 8049-8054.

e. Isci, H.; Mason, W. R., *Inorg. Chem..*, **1985**, *24*, 1761-1765.

f. Rice, S. F.; Gray, H. B., *J. Amer. Chem. Soc.*, **1981**, *103*, 1593-1595.

g. Rice, S. F.; Gray, H. B., *J. Amer. Chem. Soc.*, **1983**, *105*, 4571-4575.

h. Mann, K. R.; Thich, J. A.; Bell, R. A.; Coyle, C. A.; Gray, H. B.,*Inorg. Chem..*, **1980**, *19*, 2462-2468.

i. Stiegman, A. E.; Rice, S. F.; Gray, H,. B.; Miskowski, V. M., *Inorg. Chem.*, **1987**, *109*, 1112-1116.

6. Smith, T. P., Ph.D. Dissertation, California Institute of Technology, Pasadena, CA, 1982.

7. Che, C.-M.; Butler, L. G.; Gray, H. B.; Crooks, R. M.; Woodruff, W. H., *J. Amer. Chem. Soc.*, **1983**, *105*, 5492-5494.

8. Marshall, J. L., Ph. D. Dissertation, California Institute of Technology, Pasadena, CA, 1987.

9a. Rodman, G. S.; Mann, K. R., *Inorg. Chem..*, **1985**, *24*, 3507-3508.

b. Kenney, M. I. S.; Kenny, J. W.; Crosby, G. A., *Inorg. Chem..*, **1986**, *25*, 1506-1508.

c. Rodman, G. S.; Daws, C. A.; Mann, K. R., *Inorg. Chem..*, **1988**, *27*, 3347-3353.

10a. Brady, R.; Plynn, B. R.; Geoffroy, G. L.; Gray, H. B.; Peonne, J.; Vaska, L., *Inorg. Chem.*, **1976**, *15*, 1485-1488.

b. Bandini, A. L.; Banditelli, G.; Bonati, F.; Minghetti, G.; Demartin, F.; Manasuro, M., *J. Organomet. Chem.*, **1984**, *269*, 91-105.

c. The compound reported in reference b is a monohapto Ir(I) pyrazole complex, which might serve as a suitable monomer system for investigating the higher lying excited states of iridium pyrazolate bridge complexes.

11. King, K. A.; Spellane, P. J.; Watts, R. J., *J. Amer. Chem. Soc.*, **1985**, *107*, 1431-1432.

12. Geoffroy, G.; Isci, H.; Mason, W. R., *Inorg. Chem.*, **1977**, *16*, 1950-1955.

13a. The spin-orbit coupling constant for iridium is approximately 4000 cm^{-1}.

b. Milder, S. J.; Kliger, D. S., *J. Phys. Chem.*, **1985**, *89*, 4170-4171.

14. V. M. Miskowski, private communication.

15a. Wrighton, M.; Morse, D. L., *J. Amer. Chem. Soc.*, **1974**, *96*, 998-1003.

b. Giordano, P. J.; Redericks, S. M.; Wrighton, M. S.; Morse, D. L., *J. Amer. Chem. Soc.*, **1978**, *100*, 2257-2259.

c. Barigelletti, F.; Belser, P.; Zelewsky, A.; Juris, A.; Balzani V., *J. Phys. Chem.*, **1985**, *89*, 3680-3684.

d. Servaas, P. C.; Dijk, H. K.; Snocek, T. L.; Sterfkens, D. J.; Oskam, A., *Inorg. Chem.*, **1985**, *24*, 4494-4498.

16a. Dellinger, B.; Kasha, M., *Chem. Phys. Lett.*, **1975**, *36*, 410-414.

b. Dellinger, B.; Kasha, M., *Chem. Phys. Lett.*, **1976**, *38*, 9-14.

c. Gardner, D. J.; Kasha, M., *J. Chem. Phys.*, **1969**, *50*, 1543-1552.

17a. Bushnell, G. W.; Fjeldsted, D. O. K.; Stobart, S. R.; Zaworotko, M. J.; Knox, S. A. R.; Macpherson, K. A., *Organomet.*, **1985**, *4*, 1107-1114.

b. Coleman, A. W.; Eadie, D. T.; Stobart, S. R., *J. Amer. Chem. Soc.*, **1982**, *104*, 922-923.

c. Beveridge, K. A.; Bushnell, G. W.; Dixon, K, R.; Eadie, D. T.; Stobart, S. R., *J. Amer. Chem. Soc.*, **1982**, *104*, 920-922.

18. Hopkins, M. D., Ph.D. Dissertation, California Institute of Technology, Pasadena, CA, 1986.

19a. Engleman, R.; Jortner, J., *J. Mol. Phys.*, **1970**, *18*, 145-164.

b. Freed, K. F.; Jortner, J., *J. Chem. Phys.*, **1970**, *52*, 6272-6291.

20a. Balzani, V.; Moggi, L.; Manfrin, M. F.; Bolletta, F.; Laurrence, G. S., *Coord. Chem. Rev.*, **1975**, *15*, 321-433.

b. Kemp, T. J., *Prog. React. Kinet.*, **1980**, *10*, 301-398.

21a. Mann, K. R.; Parkinson, B. A., *Inorg. Chem.*, **1981**, *20*, 1921-1924.

b. Enlow, P. D.; Woods, C., *Inorg. Chem.*, **1985**, *24*, 1273-1274.

c. Womack, D. R.; Enlow, P. D.; Woods, C., *Inorg. Chem.*, **1983**, *22*, 2653-2656.

d. Rhodes, M. R.; Mann, K. R., *Inorg. Chem.*, **1984**, *23*, 2053-2058.

e. Boyd, D. C.; Matsch, P. A.; Mixa, M. M.; Mann, K. R., *Inorg. Chem.*, **1986**, *25*, 3331-3333.

f. Bullock, J. P.; Boyd, D. C.; Mann, K. R., *Inorg. Chem.*, **1987**, *26*, 3084-3086.

g. Boyd, D. C.; Rodman, G. S.; Mann, K. R., *J. Amer. Chem. Soc.*, **1986**, *108*, 1779-1784.

22. Smith, D. C., Ph.D. Dissertation, California Institute of Technology, Pasadena, CA, 1989.

23a. Bard, A. J.; Faulkner, L. R., *"Electrochemical Methods, Fundamentals and Applications,"* Chapter 11, Wiley, 1980.

b. Nicholson, R. S.; Shain, I., *Anal. Chem.*, **1964**, *36*, 706-723.

24. Cotton, F. A.; Wilkinson, G., *"Advanced Inorganic Chemistry ,"* Wiley-Interscience, **1980**, page 1070 and references therein.

25. Miskowski, V. M.; Sigal, I. S.; Mann. K. R.; Gray, H. B.; Milder, S. J.; Hammond, G. S.; Ryason, P. R., *J. Amer. Chem. Soc.*, **1979**, *101*, 4383-4385.

26a. Volke, J.; Naarova, M., *Coll. Chzech. Chem. Comm.*, **1972**, *37*, 3361-3375.

b. Raghavan, R.; Iwamoto, R. T., *J. Electroanal. Chem.*, **1978**, *92*, 101-114.

c. Gandiello, J. G.; Larkin, D.; Rason, J. D.; Sosnowski, J. J.; Bancroft, E. E.; Blount, H. N., *J. Electroanal. Chem.*, **1982**, *131*, 203-214.

d. Yu, F. R.; Wang, Y. Y.; Wan, C. C., *Electrochem. Acta*, **1985**, *30*, 1693-1701.

27. Lichtenberger, D. L.; Copenhaver, A. S.; Gray, H. B.; Marshall, J. L.; Hopkins, M. D., *submitted for publication to Inorg. Chem.*

28. Milder, S. J.; Kliger, D. S.; Butler, L. G.; Gray, H. B., *J. Phys. Chem.*, **1986**, *90*, 5567-5570.

29. This transition has been observed in spectra of several d^8-d^7 compounds. Its assignment remains an area of controversy in the literature.

30a. Marcus, R. A.; Sutin, N., *Biochim. Biophys. Acta*, **1985**, *811*, 265-322.

b. Guarr. T.; McLendon, G., *Coord. Chem. Rev.*, **1985**, *68*, 1-52.

c. Sutin, N., *Prog. Inorg. Chem.*, **1983**, *30*, 441-498.

d. Newton, M. D.; Sutin, N., *Ann. Rev. Phys. Chem.*, **1984**, *35*, 437-480.

e. Meyer, T. J., *Prog. Inorg. Chem.*, **1983**, *30*, 389-440.

f. Sutin, N., *Acc. Chem. Res.*, **1982**, *15*, 275-282.

31. Balzani, V.; Bolletta, F.; Gandolfi, M. T.; Maestri, M., *Top. Curr. Chem.*, **1978**, *75*, 1-64.

32. Chanon, M.; Julliard, M., *Chem. Rev.*, **1983**, *83*, 425-506.

33a. Grabowski, Z. R.; Grabowski, A., *Z. Phys. Chem. Neue Folge*, **1976**, *101*, 197-208.

b. Grabowski, Z. R.; Rubaszewska, W., *J. Chem. Soc. Faraday Trans. I*, **1977**, *73*, 11-28.

34. Marcus, R. A., *manuscript in preparation.*

35a. Ikegami, Y., *Rev. Chem. Intermed.*, **1986**, *7*, 91-109.

b. Akiyama, K.; Kubota, S.; Ikegami, Y., *Chem. Lett.*, **1981**, 469-472.

c. Tero-Kubota, S.; Sano, Y.; Ikegami, Y., *J. Amer. Chem. Soc.*, **1982**, *104*, 3711-3714.

d. Akiyama, K.; Tero-Kubota, S.; Ikegami, Y., *J. Amer. Chem. Soc.*, **1983**, *105*, 3601-3604.

e. Akiyama, K.; Ishi, T.; Tero-Kubota, S.; Ikegami, Y., *Bull. Chem. Soc. Jpn.*, **1985**, *38*, 3535-3539.

f. Akiyama, K.; Tero-Kubota, S.; Ikegami, Y.; Ikenone, T., *J. Phys. Chem.*, **1985**, *89*, 339-342.

36. Andrieux, C. P.; Nadjo, L.; Saveant, J. M., *J. Electroanal. Chem. Interfacial Electrochem.*, **1970**, *26*, 147-186.

37. Demas, J. N.; Crosby, G. A., *J. Phys. Chem.*, **1971**, *75*, 991-1024.

38. Caspar, J. V.; Meyer, T. J., *J. Amer. Chem. Soc.*, **1983**, *105*, 5583-5590.

39. Wrighton, M. S.; Geoffroy, G. L.; *"Organometallic Photochemistry,"* Wiley Interscience.

40. Note that the emission spectrum of $Ir_2(Pz^*)_2(CO)_2(Ph_2POCH_2CH_2\text{-}NEt_3)_2^{2+}$ has been reduced by a factor of five so that all four spectra could be plotted on the same intensity scale. $Ir_2(Pz^*)_2(CO)_2(Ph_2POCH_2CH_2\text{-}4PhPy)_2^{2+}$ has been omitted in this figure because its low emission quantum yield ($< 10^{-5}$) precluded measuring its emission spectrum. The weak feature at approximately 500 nm in spectra of the donor-acceptor complexes is an artifact due to scattered light from the excitation source.

41. This interpretation is suggested by the similar changes seen in the triphenylphosphine complex.

42. Che, C.-M.; Wong, K.-Y., Anson, F. C., *J. Electroanal. Chem.*, **1987**, *226*, 211-226.

43. Electrochemical couples corresponding to the one electron reduction of $Ir_2(Pz^*)_2(CO)_2(Ph_2POCH_2CH_3)_2$ were not observed.

Chapter 4

Time-resolved Experiments

Introduction

The steady-state spectroscopic results presented in chapter 3 clearly establish that a quenching process involving both singlet and triplet ($d\sigma^*p\sigma$) excited states is active in the donor-acceptor complexes. We have proposed that the decrease in the emission intensities from both these states is due to excited state electron transfer. This chapter deals with characterizing the charge transfer reactions of the singlet, triplet, and CT excited states in our intramolecular redox systems using picosecond time-resolved absorption and emission techniques. Results from these experiments provide direct kinetic and spectroscopic information regarding the rates of the charge separation and the charge recombination reactions involving these three excited states. In particular the transient absorption data obtained in this phase of our research conclusively assigns the singlet and triplet quenching processes in our compounds to excited state ET by spectroscopically identifying the charge transfer products. In the discussion section of this chapter the electron transfer rate data are evaluated in terms of their dependence on reaction driving force. Clear evidence for inverted behavior is seen in the charge recombination reactions in our systems. Finally, the photophysical properties of these iridium d^8-d^8 donor-acceptor complexes are examined with regard to designing directional charge-transfer.systems

Experimental

General Procedures: All manipulations involving the iridium dimer complexes were carried out using standard Schlenk and high vacuum techniques. Solvents used in spectroscopic experiments were reagent grade or better in quality. They were purified as indicated, subjected to a minimum of five freeze/pump/thaw cycles, and stored in a round bottom storage flask fitted with a Kontes Teflon stopcock. 2-

Methyltetrahydrofuran was purified by distillation from a 0.5% (w/w) suspension of cuprous chloride, followed by distillation from CaH_2 and finally from sodium/benzophenone. It was stored under vacuum over sodium/benzophenone as an indicator. Acetonitrile was distilled from CaH_2 under nitrogen and stored in vacuo.

Kinetics and Spectral Measurements

Difference spectra and kinetics as well as emission lifetimes were recorded using two types of laser systems depending on the time scale required for a particular measurement. Both instruments have been fully described elsewhere,[1,2] and only their highlights are reported here. Phosphorescence lifetimes were recorded using a nanosecond laser system built at Caltech. The excitation source was a Quanta Ray DCR-1 Q-switched Nd:YAG laser, which was frequency doubled and tripled with a Quanta Ray HG-1 harmonic generator (KDP). Doubled and tripled 8 ns (fwhm) laser pulses were separated from the YAG fundamental using a Quanta Ray PHS-1 prism harmonic separator. Light emitted by the sample was collimated at 90° to the excitation beam and focused through a Corning 3483 sharp cut filter onto the entrance slit of a MacPherson 0.35 m monochromator. Luminescence was detected using a Hamamatsu R955 photomultiplier tube, and the signal was amplified with a LeCroy VV101ATM amplifier. Signals were digitized with a Biomation 6500 waveform recorder and transferred to a Digital PDP11/103-L computer. Data sets were analyzed on an IBM-AT PC using kinetics software developed in-house by Dr. Michael Albin. Samples were prepared under vacuum as acetonitrile solutions in an NMR tube which, was attached to a Kontes Teflon stopcock.

Picosecond time-resolved absorption and emission experiments were conducted at Brookhaven National Laboratory in collaboration with Dr. Jay R. Winkler. Figure 4.1 shows a schematic representation of the mode-locked Nd:YAG laser used in these experiments. A train of 30 ps (fwhm) pulses was generated in an actively-passively

Figure 4.1. Schematic representation of the picosecond laser system used in time-resolved emission and absorption measurements. A train of picosecond pulses is generated in an active-passive mode-locked Nd:YAG laser cavity (aml, osc, pml). A single pulse is selected using a pulse extraction device (pe) and amplified by two single pass YAG amplifiers (amp1, amp2). The amplified pulse is split into two components; one is amplified and used as an excitation source and the other component is used as a probe beam. Probe light is generated by passing the focused probe beam (either 532 nm or 355 nm) through a 10 cm pathlength cell containing 80:20 D_2O/H_2O.

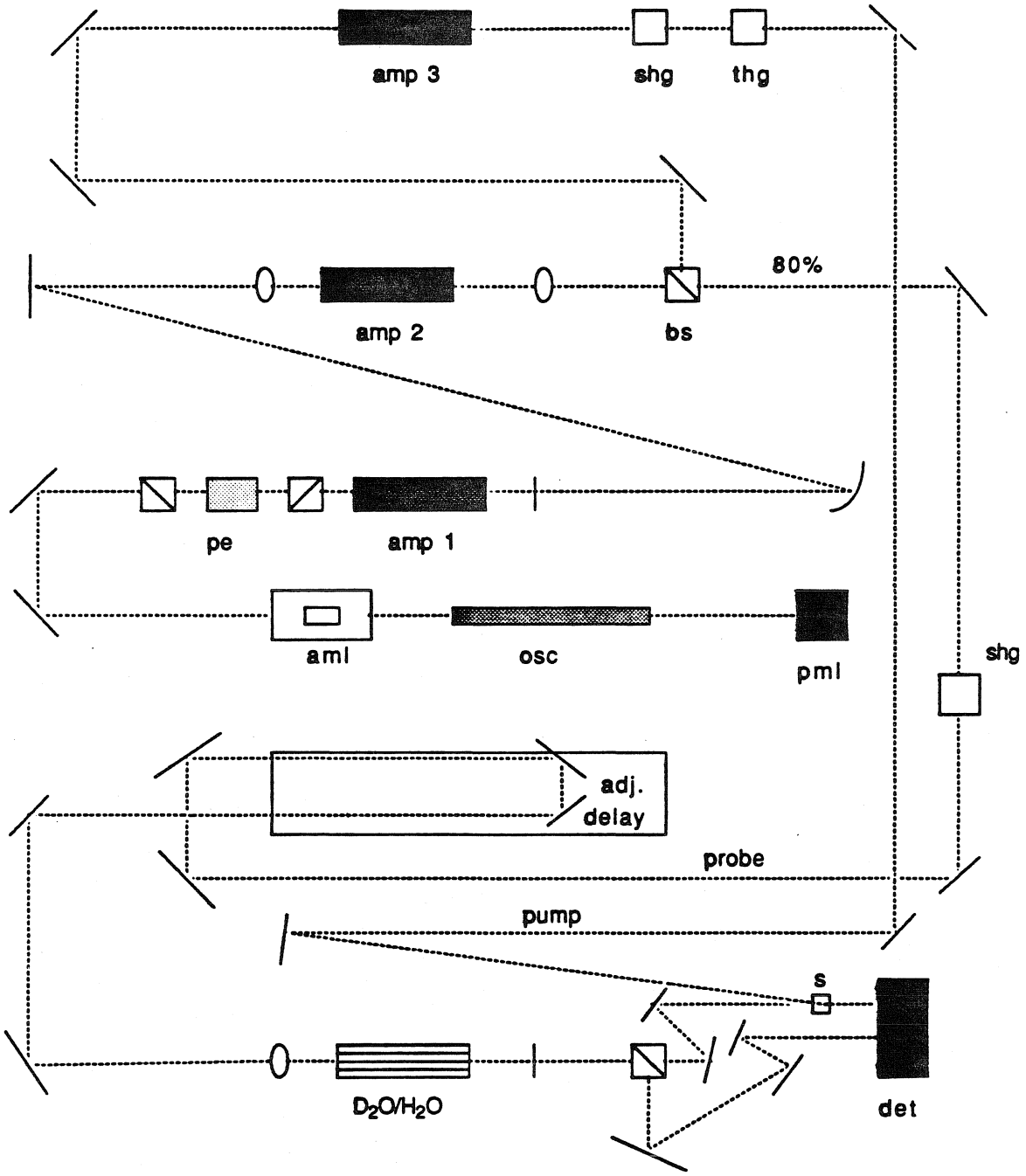
amp 3
shg
thg
80%
amp 2
bs
pe
amp 1
aml
osc
pml
shg
adj.
delay
probe
pump
s
D_2O/H_2O
det

mode-locked laser cavity (osc). A single pulse was removed from the pulse train using a Quantel SPS411 Pulse Selector (pe) and amplified twice by two Quantel single pass Nd:YAG amplifiers. The pulse was split into two components; 20% was passed through a third single pass amplifier and frequency doubled or tripled (KDP) for use as a pump beam. The remaining 80% of the pulse intensity was frequency doubled and used to generate picosecond probe light. The probe beam was passed through a series of mirrors and a translation stage to provide time delays between the pump beam and probe. Probe light was generated by focusing the probe beam into a 10 cm quartz cell containing an 80:20 by volume mixture of D_2O/H_2O and was focused onto a 400 μm-diameter aperture in contact with a sand blasted glass slide. Light from this aperture was collected and transferred to a beam splitter; one third of its intensity was reflected around the sample and used as a reference beam. The probe and reference beams were passed to the entrance slit of a DMC monochromator and then to two photomultiplier tubes. For each delay time and wavelength 100 laser shots were used. Fifty ratios of the probe and reference beams were measured without sample excitation and fifty ratios were measured with sample excitation. The log of the ratio of these ratios is equal to ΔA. Picosecond time-resolved emission experiments were conducted using this same laser system except that the sample luminescence was recorded using a Hamamatsu streak camera. Data were transferred to a PDP 11/23 computer and analyzed using kinetics software developed at BNL. Picosecond time-resolved emission data were analyzed using a deconvolution software package developed at Caltech-JPL by Dr. David Brinza.

Samples were prepared under vacuum as acetonitrile solutions and were held under argon in the flow cell seen in figure 4.2. Stirring in the main reservoir causes the solution to flow through the 2 mm optical glass cuvette at the bottom of the cell. This procedure assures that a fresh portion of solution is explored in each measurement. Samples were stable to laser radiation under these conditions for several weeks.

Figure 4.2. Inert atmosphere cell used in picosecond absorption measurements. The sample is contained under nitrogen in a 250 ml reservoir. When the solution is stirred, the hydrodynamic force created by the stirring action draws the solution through the optical cell. This procedure ensures that each laser shot interrogates a fresh and identical sample solution.

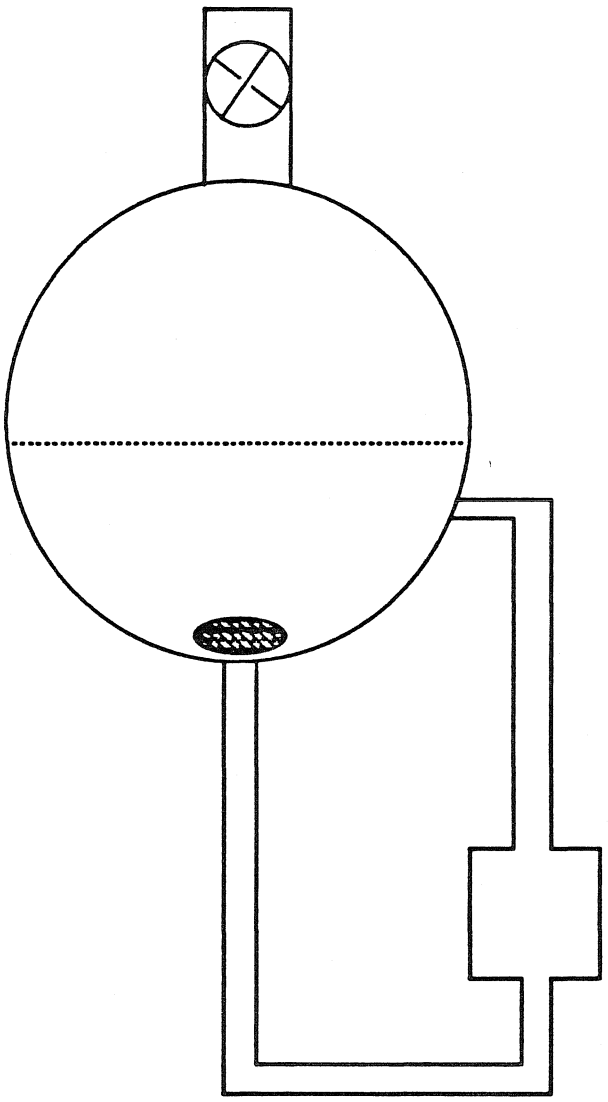

Results

Kinetic and Spectral Data

Model Complexes $Ir_2(Pz^*)_2(CO)_2(Ph_2POCH_2CH_3)_2$ and $Ir_2(Pz^*)_2(CO)_2(Ph_2POCH_2CH_2\text{-}NEt_3^+)_2$: Figures 4.3a-d show spectral and kinetic results for the two model compounds, $Ir_2(Pz^*)_2(CO)_2(Ph_2POCH_2CH_3)_2$ and $Ir_2(Pz^*)_2(CO)_2(Ph_2POCH_2CH_2\text{-}NEt_3^+)_2$, in acetonitrile solutions after a 30 ps laser pulse at 355 nm. Both compounds exhibit a biphasic transient absorption signal, which rises with the laser pulse and returns to baseline at long delay times (t> 10 μs). The shorter component decays with a lifetime of approximately τ_1 =100 ps; the second transient is much longer lived and decays on a microsecond timescale (τ_2 =1.2 μs). Kinetic results for both complexes were independent of λ_{ex} (either 355 nm or 532 nm) and λ_{obs}. Emission lifetimes for the ^1B and ^3B excited states in these molecules were determined independently to be $\tau(^1B)$ =100 ps and $\tau(^3B)$ =1.3 μs via time-resolved emission measurements. Thus, the two transients seen in difference spectra of $Ir_2(Pz^*)_2(CO)_2(Ph_2POCH_2CH_3)_2$ and $Ir_2(Pz^*)_2(CO)_2(Ph_2POCH_2CH_2\text{-}NEt_3^+)_2$ are logically attributed to their singlet and triplet ($d\sigma^*p\sigma$) excited states. Figures 4.3a and d show spectral data for the compounds in the wavelength range between 300 nm and 500 nm at delay times immediately following and well after the laser pulse. In addition to a ground state bleach at 450 nm both compounds exhibit a single transient absorption feature at approximately 400 nm. Data for $Ir_2(Pz^*)_2(CO)_2(Ph_2POCH_2CH_3)_2$ were obtained at probe wavelengths below 380 nm by exciting this complex at 532 nm and generating probe pulses with the 355 nm laser line. Unfortunately, higher energy excited state transitions were not observed in these experiments. Adequate UV probe light could only be generated up to 310 nm and spectral data above 500 nm could not be

Figure 4.3. Difference spectra and kinetics of the model compounds. a) Transient spectrum of $Ir_2(Pz^*)_2(CO)_2(Ph_2POCH_2CH_2\text{-}NEt_3^+)_2$ in acetonitrile (λ_{ex}=355 nm, 0: t=0.0 ps, Δ: t=12.35 ns). b) Kinetics for $Ir_2(Pz^*)_2(CO)_2(Ph_2POCH_2CH_2\text{-}NEt_3^+)_2$ (λ_{ex}=355 nm, λ_{obs}=420 nm, τ_{fit}=93 ps). c) Kinetics for $Ir_2(Pz^*)_2(CO)_2(Ph_2POCH_2CH_2\text{-}NEt_3^+)_2$ (λ_{ex}=355 nm, λ_{obs}=400 nm, τ_{fit}=1.26 μs). d) Transient spectrum of $Ir_2(Pz^*)_2(CO)_2(Ph_2POCH_2CH_3)_2$ (λ_{ex}=532 nm, 0: t=0.0 ps, Δ: t=5.0 ns).

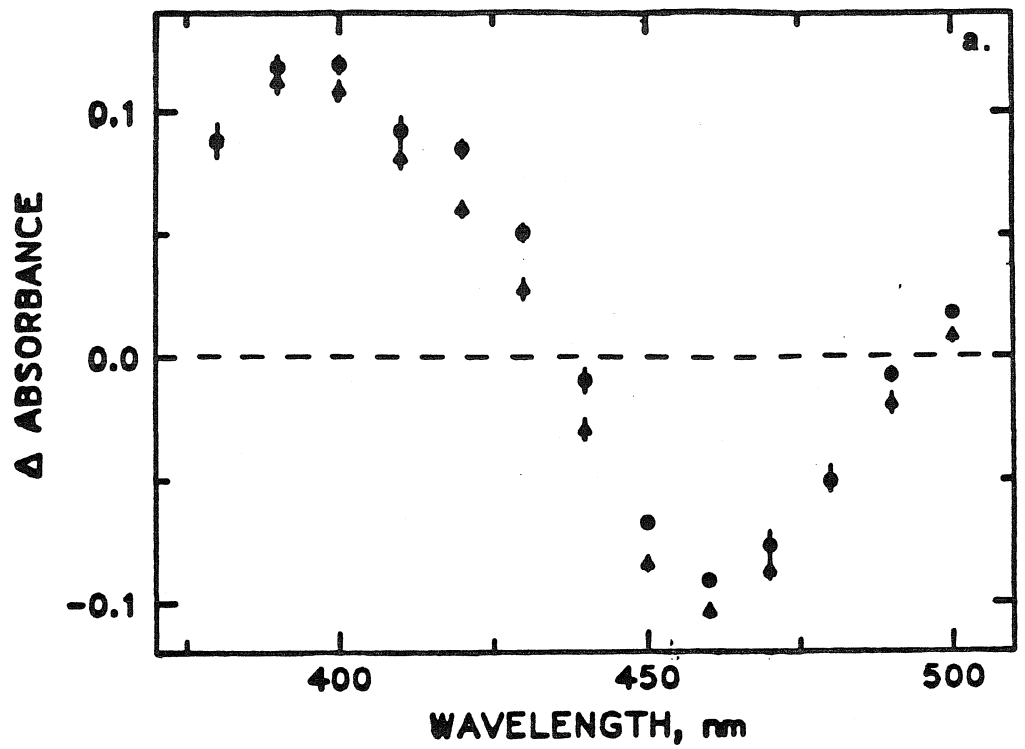
a.
0.1
0.0
-0.1
Δ ABSORBANCE
400
450
500
WAVELENGTH, nm

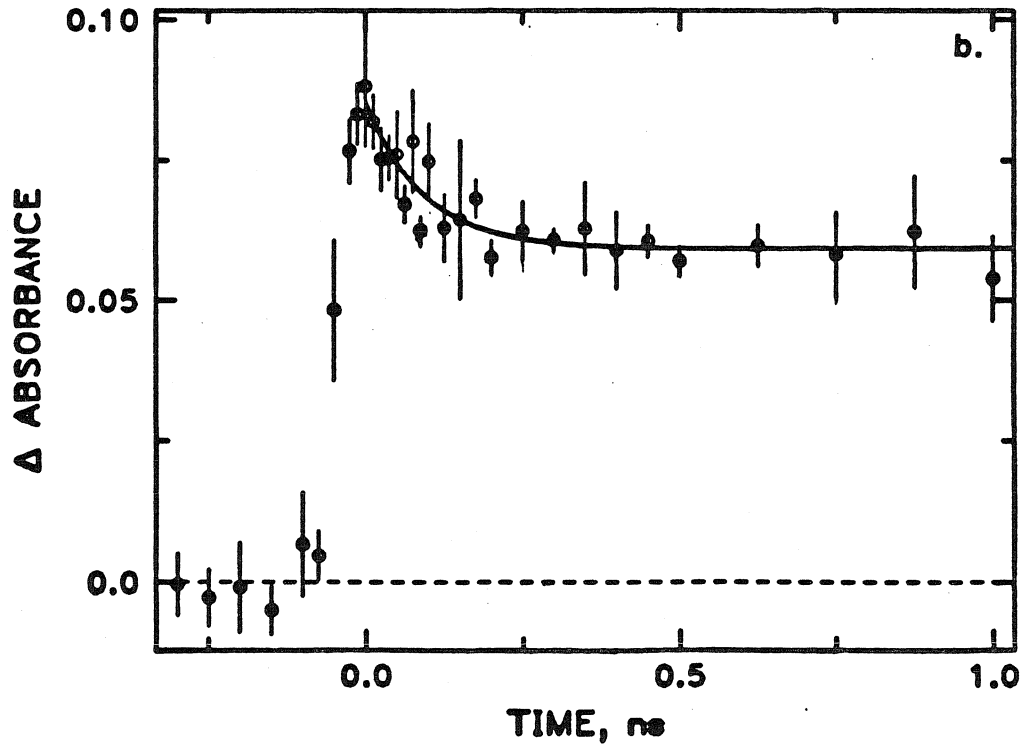
b.
0.10
0.05
0.0
Δ ABSORBANCE
0.0
0.5
1.0
TIME, ns

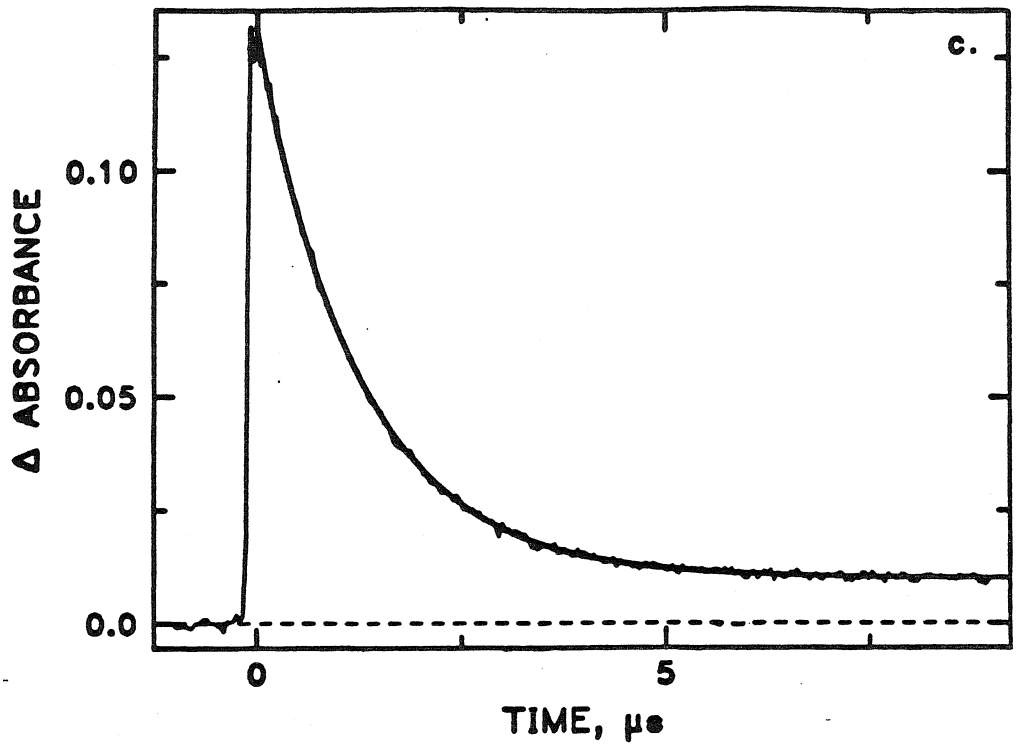
c.
0.10
0.05
0.0
Δ ABSORBANCE
0
5
TIME, μs

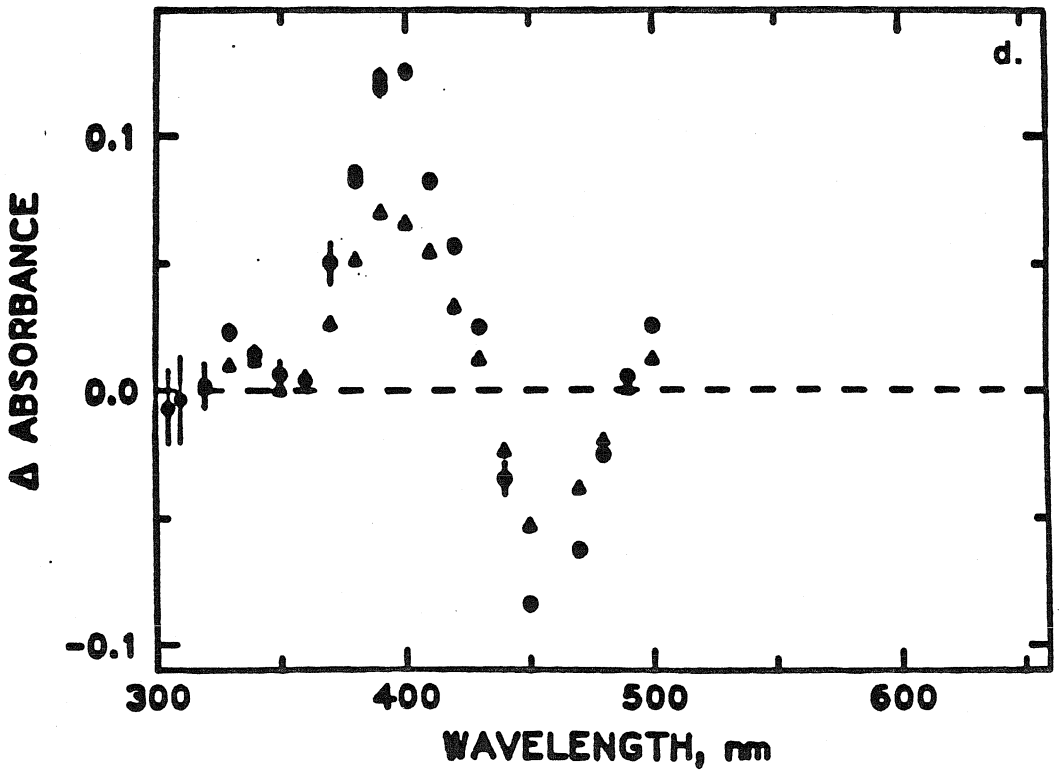
d.
0.1
0.0
-0.1
Δ ABSORBANCE
300
400
500
600
WAVELENGTH, nm

recorded due to luminescence backgrounds. Additional excited state transitions may occur in these complexes, but must lie outside the spectral range available in our experiments.

The excited state spectra and kinetics of $Ir_2(Pz^*)_2(CO)_2(Ph_2POCH_2CH_3)_2$ and $Ir_2(Pz^*)_2(CO)_2(Ph_2POCH_2CH_2\text{-}NEt_3^+)_2$ are interesting not only as points of reference for investigating electron transfer in the donor-acceptor complexes, but also with regard to the photophysical and excited state properties of d^8-d^8 A-frame chromophores. The excited state spectra and kinetics of d^8-d^8 compounds have been the focus of several previous studies.[3] In compounds such as $Rh_2(Bridge)_4^{2+}$ and $Rh_2(TMB)_4^{2+}$, the $^1A_{2u}$ and $^3A_{2u}$ ($d\sigma^*p\sigma$) excited states are easily differentiated by their transient absorption bands.[3c] The former excited states show an intense $^1A_{2u} \rightarrow {}^1A_{1g}$ ($d\sigma^*p\sigma \rightarrow p\sigma^2$) (ca. 450 nm) band in their transient spectrum. This transition is formally spin forbidden from a $^3A_{2u}$ excited state and is too weak to observe in transient difference spectra. The longer lived triplet state characteristically exhibits two transient absorption features which, in $Rh_2(Bridge)_4^{2+}$ and $Rh_2(TMB)_4^{2+}$ have been assigned to $^3A_{2u} \rightarrow {}^3A_{1g}$ ($d\sigma^*p\sigma \rightarrow d\sigma p\sigma$) (ca. 470 nm) and $^3A_{2u} \rightarrow {}^3E_{2g}(d\pi \rightarrow p\sigma)$ (ca. 420 nm) electronic transitions. Prior to this study, the only d^8-d^8 A-frame complex that had been examined using time-resolved spectroscopy was $[Ir_2(Pz)_2(COD)_2]$.[3a] In this particular system, only spectra of the ^3B excited state could be recorded due to its prohibitively short singlet lifetime (τ<30 ps). Thus, the data reported here provide the first opportunity for comparing the spectroscopic properties of the ^1B and ^3B excited states in a d^8-d^8 A-frame complex. In contrast to the transient spectra of $[Rh_2(Bridge)_4]^{2+}$ and $[Rh_2(TMB)_4]^{2+}$, the singlet and triplet excited state spectra in $Ir_2(Pz^*)_2(CO)_2(Ph_2POCH_2CH_3)_2$ and $Ir_2(Pz^*)_2(CO)_2(Ph_2POCH_2CH_2\text{-}NEt_3^+)_2$ are remarkably similar. Both states are characterized by an apparently identical absorption feature. At present it is difficult to assign these transitions with any degree of certainty. However, it can be safely

concluded that this band does not correspond to a ($d\sigma^*p\sigma \rightarrow p\sigma^2$) transition in the triplet spectra of these compounds. Further, based on the transient absorption spectra of $[Rh_2(Bridge)_4]^{2+}$ and $[Rh_2(TMB)_4]^{2+}$, it is unlikely that this transition in the singlet spectrum of $Ir_2(Pz^*)_2(CO)_2(Ph_2POCH_2CH_3)_2$ or $Ir_2(Pz^*)_2(CO)_2(Ph_2POCH_2CH_2$-$NEt_3^+)_2$ would be isoenergetic with either the ($d\sigma^*p\sigma \rightarrow d\sigma p\sigma$) or ($d\pi \rightarrow p\sigma$) transition originating from its triplet excited state. One plausible explanation for this behavior is that the ($d\sigma^*p\sigma \rightarrow p\sigma^2$) transitions in these complexes are near in energy to their ($d\sigma^* \rightarrow p\sigma$) transitions and are obscured in the bleach region of their transient difference spectra. Under this assumption the two bands at 400 nm are tentatively assigned to ($d\pi \rightarrow p\sigma$) and ($d\sigma \rightarrow d\sigma^*$) transitions by analogy to assignments made in spectra of $Rh_2(Bridge)_4^{2+}$ and $Rh_2(TMB)_4^{2+}$. Further studies directed toward measuring the extinction coefficients and polarizations of these bands will be necessary to conclusively assign them to specific transitions.

With regard to their photophysical properties, $Ir_2(Pz^*)_2(CO)_2(Ph_2POCH_2CH_3)_2$ and $Ir_2(Pz^*)_2(CO)_2(Ph_2POCH_2CH_2$-$NEt_3^+)_2$ have some of the longest lived singlet and triplet excited states found in A-frame complexes. We propose that the longer lifetimes in these compounds result from their smaller nonradiative decay rates. As seen in table 4.1, while the radiative rates for a series of different d^8-d^8 A-frame complexes are essentially the same, the quantum yields and emission lifetimes of these compounds vary as a function of their terminal and bridging ligands. These trends are indicative of variations in the nonradiative deactivation rates for their ($d\sigma^*p\sigma$) excited states due to differences in their coordination environments. While theoretical models for nonradiative decay processes are available,[4] the specific molecular parameters, which control these processes in large inorganic complexes are poorly understood. Thus, cause-effect relationships between molecular structure, and nonradiative rate constants in our metal dimers are difficult to evaluate. However, we

Table 4.1: Quantum Yield and Lifetime Data for Selected A-Frame Complexes.

Complex	$\phi(^1B)$	$\phi(^3B)$	$\tau(^1B)$ ns	$\tau(^3B)$ ns
$[Ir_2(Pz)_2(COD)_2]$[a]	0.0001	0.0078	<0.03	250
$[Ir_2(Pz^*)_2(COD)_2]$[a]	0.0001	0.0038	<0.03	80
$[Ir_2(Pz)_2(CO)_2(Ph_3P)_2]$[b]	- -	- -	- -	<8
$[Ir_2(Pz^*)_2(CO)_2(Ph_3P)_2]$	0.0003	0.0015	<0.03	60
$[Ir_2(Pz^*)_2(CO)_2$ $(Ph_2POCH_2CH_2NEt_3)_2]$	0.0015	0.039	0.09	1200
$[Ir_2(Pz^*)_2(CO)_2(Ph_2POCH_2CH_3)_2]$	0.0023	0.0250	0.1	1100

Complex	$k_r(^1B)$ sec^{-1}	$k_r(^3B)$ sec^{-1}
$[Ir_2(Pz)_2(COD)_2]$[a]	$3.0x10^6>$	$3.0x10^4$
$[Ir_2(Pz^*)_2(COD)_2]$[a]	$3.0x10^6>$	$4.75x10^4$
$[Ir_2(Pz^*)_2(CO)_2(Ph_3P)_2]$	$1.0x10^7>$	$2.5x10^4$
$[Ir_2(Pz^*)_2(CO)_2$ $(Ph_2POCH_2CH_2NEt_3)_2]$	$1.7x10^7$	$3.25x10^4$
$[Ir_2(Pz^*)_2(CO)_2(Ph_2POCH_2CH_3)_2]$	$2.3x10^7$	$2.3x10^4$

a. Marshall, J. L., Ph. D. Dissertation, Caltech, 1987.
b. Smith, T. J., Ph. D. Dissertation, Caltech, 1982.

can conclude from the data in table 4.1 that the nonradiative rates in d^8-d^8 A-frame complexes are strongly affected by the electronic and steric properties of their terminal and bridging ligands.

$Ir_2(Pz^*)_2(CO)_2(Ph_2POCH_2CH_2$-4PhPy$^+)_2$: Figure 4.4 shows spectral and kinetic data for $Ir_2(Pz^*)_2(CO)_2(Ph_2POCH_2CH_2$-4PhPy$^+)_2$ in acetonitrile solutions after a 30 ps laser pulse at 532 nm. This particular complex was excited using the frequency doubled Nd:YAG laser line, because strong fluorescence backgrounds from 4Ph-Py$^+$ localized excited states complicated the analysis of spectra obtained with 355 nm excitation. Kinetics measured at 380 nm and in the bleach region were characteristic of a single transient species whose concentration rises on the time scale of the laser pulse and returns to zero at long delay times (t> 500 ps). The kinetic data for this compound were fit to a single exponential intensity function yielding a lifetime of 50 ps for its long lived excited state. Figure 4.4b shows spectral data in the wavelength range between 340 nm and 650nm immediately after the laser pulse. In this case spectroscopic data were readily obtained at wavelengths greater than 500 nm due to this compound's low fluorescence and phosphorescence quantum yields. The spectroscopic properties of $Ir_2(Pz^*)_2(CO)_2(Ph_2POCH_2CH_2$-4PhPy$^+)_2$ differ substantially from those found in $Ir_2(Pz^*)_2(CO)_2(Ph_2POCH_2CH_3)_2$ and $Ir_2(Pz^*)_2(CO)_2(Ph_2POCH_2CH_2$-NEt$_3^+)_2$. Its difference spectra show two prominent absorption features at 350 nm and 525 nm. These bands can be assigned to transitions localized on a 4-phenyl pyridyl radical, based on previous spectroscopic studies.[5] Our data indicate that the marked luminescence quenching seen in emission spectra of the donor-acceptor complexes can be attributed to an electron-transfer process. Further, electron transfer to form a charge separated state in this particular complex occurs on a timescale equal to or less than the duration of the laser pulse. This conclusion is in line with its low emission quantum yields. An upper limit of 1 ps for its ^{1}B lifetime can be estimated from its fluorescence

Figure 4.4. Difference spectra and kinetics of $Ir_2(Pz^*)_2(CO)_2(Ph_2POCH_2CH_2\text{-}4PhPy^+)_2$ in acetonitrile solutions. a) Kinetics (λ_{ex}=532 nm, λ_{obs}=380 nm, τ_{fit}=50 ps). b) Difference spectrum at t=0.0 ps.

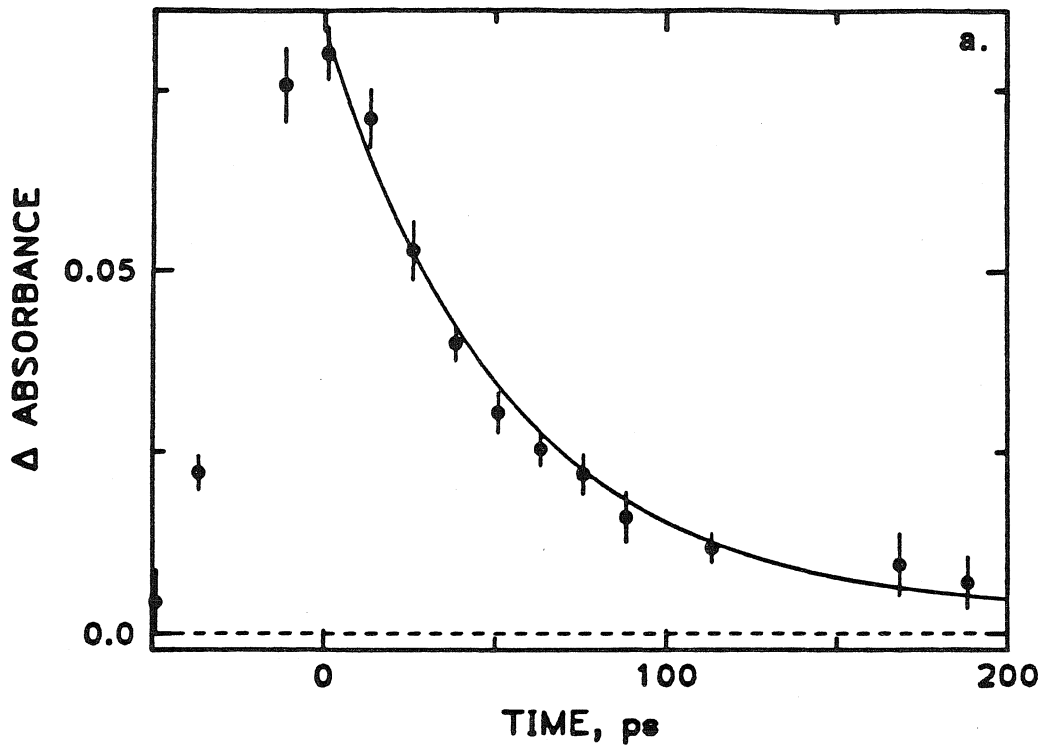
a.
Δ ABSORBANCE
0.05
0.0
0
100
200
TIME, ps

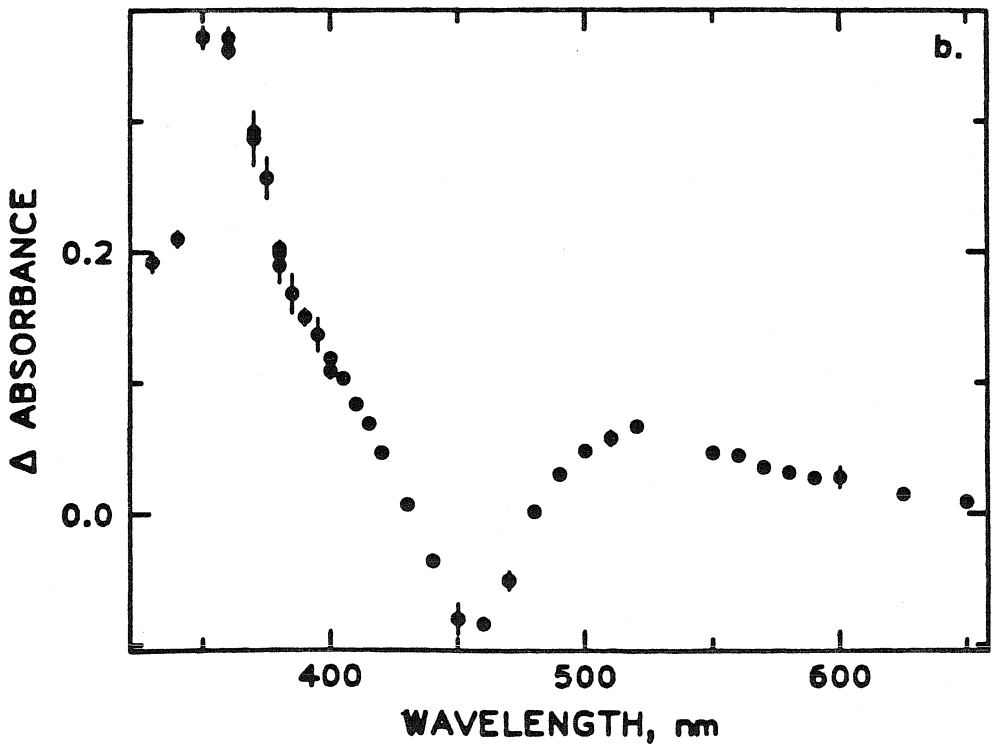
b.
Δ ABSORBANCE
0.2
0.0
400
500
600
WAVELENGTH, nm

quantum yield and the quantum yield and singlet lifetime of $Ir_2(Pz^*)_2(CO)_2(Ph_2POCH_2CH_3)_2$. Thus, the measured $2.0x10^{10}$ sec^{-1} rate constant in this complex corresponds to electron-hole recombination.

$Ir_2(Pz^*)_2(CO)_2(Ph_2POCH_2CH_2$-$Py^+)_2$: Figure 4.5 summarizes kinetic and spectral data for $Ir_2(Pz^*)_2(CO)_2(Ph_2POCH_2CH_2$-$Py^+)_2$ in acetonitrile solutions after an excitation pulse at 355 nm. The fluorescence backgrounds that necessitated exciting $Ir_2(Pz^*)_2(CO)_2(Ph_2POCH_2CH_2$-$4PhPy^+)_2$ at 532 nm were not observed in experiments involving $Ir_2(Pz^*)_2(CO)_2(Ph_2POCH_2CH_2$-$Py^+)_2$ and this complex was excited at higher energies where it has a larger absorption cross section. Kinetic results for λ_{ex}=532 nm and λ_{ex}=355 nm were the same within experimental error making comparisons between results for this complex and $Ir_2(Pz^*)_2(CO)_2(Ph_2POCH_2CH_2$-$4PhPy^+)_2$ possible. Kinetics measured at 400 nm and in the bleach region (450 nm) exhibited a single transient species whose concentration rises on the time scale of the laser pulse and returns to baseline at long delay times (t> 500 ps). The kinetic data for this complex were adequately modeled by an exponential intensity function with a time constant of 150 ps. Figure 4.5b shows a transient difference spectrum between 310 nm and 800 nm. In contrast to $Ir_2(Pz^*)_2(CO)_2(Ph_2POCH_2CH_2$-$4PhPy^+)_2$, $Ir_2(Pz^*)_2(CO)_2(Ph_2POCH_2CH_2$-$Py^+)_2$ exhibits a single absorption feature at 390 nm. The apparent bleach feature at 620 nm can be attributed to Raman scattering from the probe light generation process. Because N-alkyl pyridyl radicals lack strong absorption bands in the 310 nm to 700 nm spectral region, this 390 nm band cannot be ascribed to this particular chromophore.[6] Notably, it is very similar to the strong high energy absorption features characteristic of an iridium dimer cation. Recall from chapter 3 that $[Ir_2(Pz^*)_2(CO)_2(Ph_3P)_3]^+$ has an intense band at approximately 380 nm. However, this transient absorption feature is also very similar to transitions ascribed to the metal localized ^1B and ^3B excited states

Figure 4.5. Difference spectra and kinetics of $Ir_2(Pz^*)_2(CO)_2(Ph_2POCH_2CH_2Py^+)_2$ in acetonitrile solutions. a) Kinetics (λ_{ex}=355 nm, λ_{obs}=400 nm, τ_{fit}=150 ps). b) Difference spectrum at t=25 ps (λ_{ex}=532 nm).

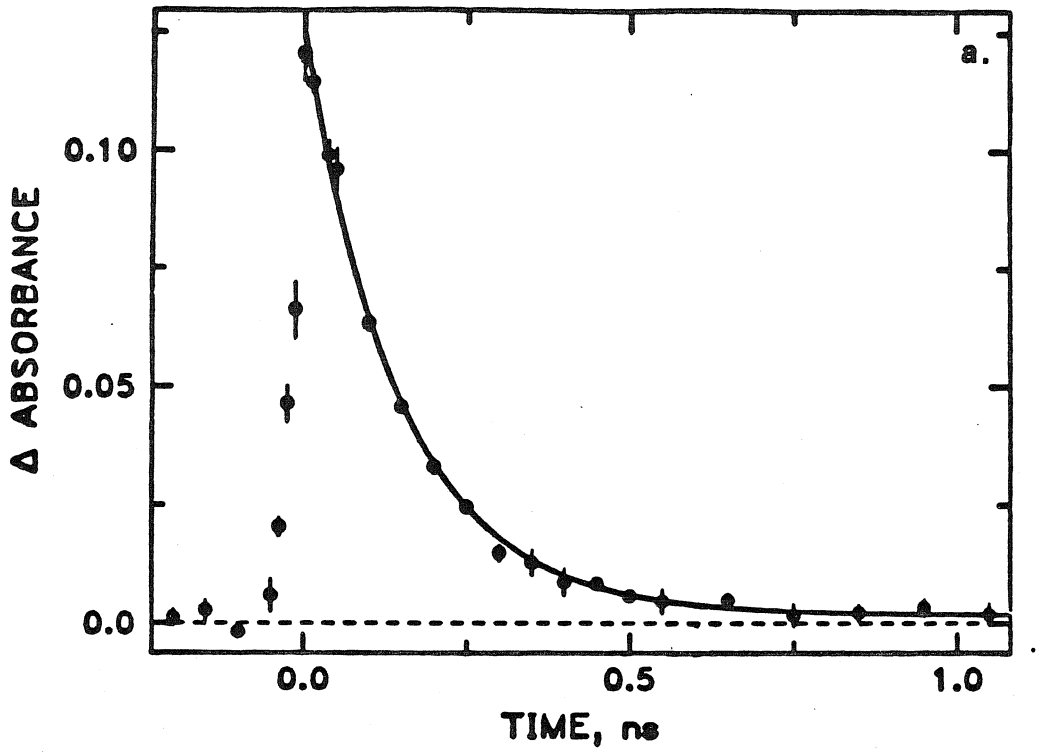
a.
0.10
0.05
0.0
Δ ABSORBANCE
0.0
0.5
1.0
TIME, ns

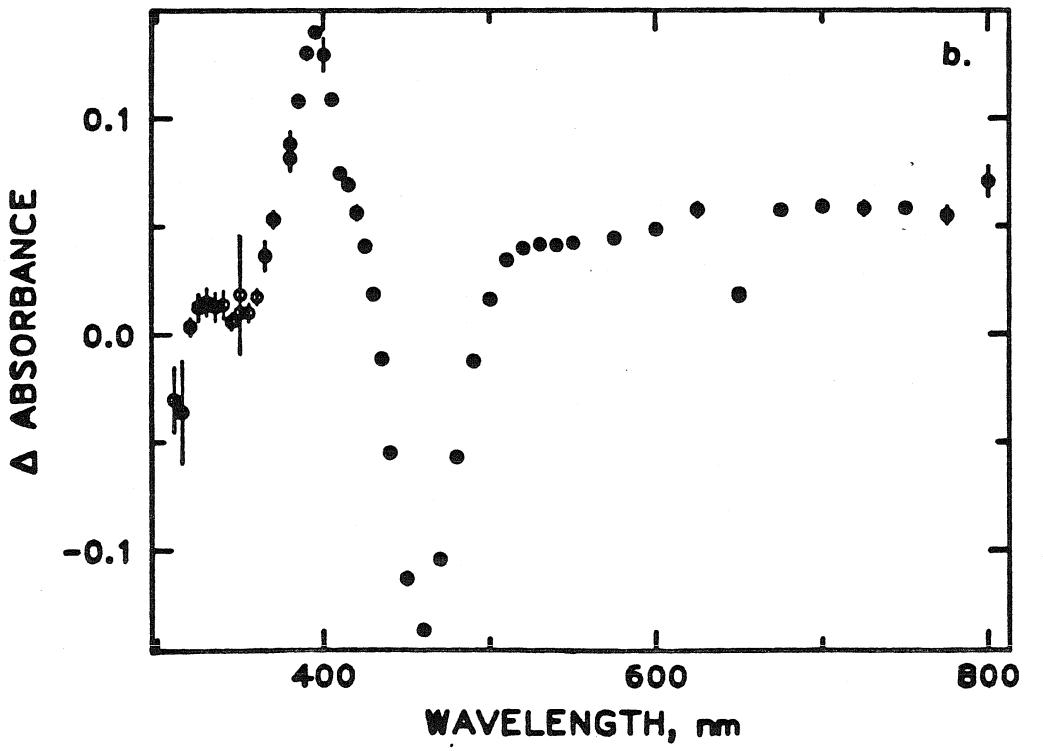
b.
0.1
0.0
-0.1
Δ ABSORBANCE
400
600
800
WAVELENGTH, nm

in the model complexes. Thus, additional information is required to assign this band to a particular excited state species. A ^1B excited state lifetime of 2 ps for this complex can be estimated from its fluorescence quantum yield and the quantum yield and singlet lifetime of $Ir_2(Pz^*)_2(CO)_2(Ph_2POCH_2CH_3)_2$. This analysis indicates that, as for $Ir_2(Pz^*)_2(CO)_2(Ph_2POCH_2CH_2\text{-}4PhPy^+)_2$, charge transfer from the ^1B state in this complex occurs on a timescale that is shorter than the laser pulse. $Ir_2(Pz^*)_2(CO)_2(Ph_2POCH_2CH_2\text{-}Py^+)_2$ has a triplet quantum yield that is less than or equal to 10^{-5}. Thus, the t=0 yield of formation of its ^3B excited state should be reduced relative to the yield of formation of the ^3B state in a model complex. However, under identical experimental conditions, the yield of formation of the triplet state in $Ir_2(Pz^*)_2(CO)_2(Ph_2POCH_2CH_3)_2$ and the 390 nm transient in $Ir_2(Pz^*)_2(CO)_2(Ph_2POCH_2CH_2\text{-}Py^+)_2$ were the same within experimental error. These data support the conclusion that this absorption feature is due to transitions associated with a transient iridium dimer cation species and can be attributed to the charge separated state in $Ir_2(Pz^*)_2(CO)_2(Ph_2POCH_2CH_2\text{-}Py^+)_2$. The measured $6.7x10^9$ sec^{-1} rate constant in this complex corresponds to a hole-electron charge recombination process.

$Ir_2(Pz^*)_2(CO)_2(Ph_2POCH_2CH_2\text{-}4MePy^+)_2$: Figure 4.6 shows kinetic and spectral data for $Ir_2(Pz^*)_2(CO)_2(Ph_2POCH_2CH_2\text{-}4MePy^+)_2$ in acetonitrile solutions. Flash photolysis of this complex with a 30 ps laser pulse at 355 nm leads to a ground state bleach at 450 nm and the formation of a transient absorption feature at 390 nm, which is similar to the absorption band seen in spectra of $Ir_2(Pz^*)_2(CO)_2(Ph_2POCH_2CH_2\text{-}Py^+)_2$. This transient is formed on a timescale that is equivalent to or less than that of the laser pulse and returns to baseline at long delay times (t>1 ns). Kinetic data for this compound fit well to a biexponential intensity function with time constants of τ_1=300 ps and τ_2=3.0 ns. As with

Figure 4.6. Difference spectra and kinetics of $Ir_2(Pz^*)_2(CO)_2(Ph_2POCH_2CH_2\text{-}4MePy^+)_2$ in acetonitrile solutions. a) Kinetics (λ_{ex}=355 nm, λ_{obs}=400 nm, τ_{fit1}=300 ps, τ_{fit2}=3 ns). b) Difference spectrum at t=1.25 ns (λ_{ex}=355 nm).

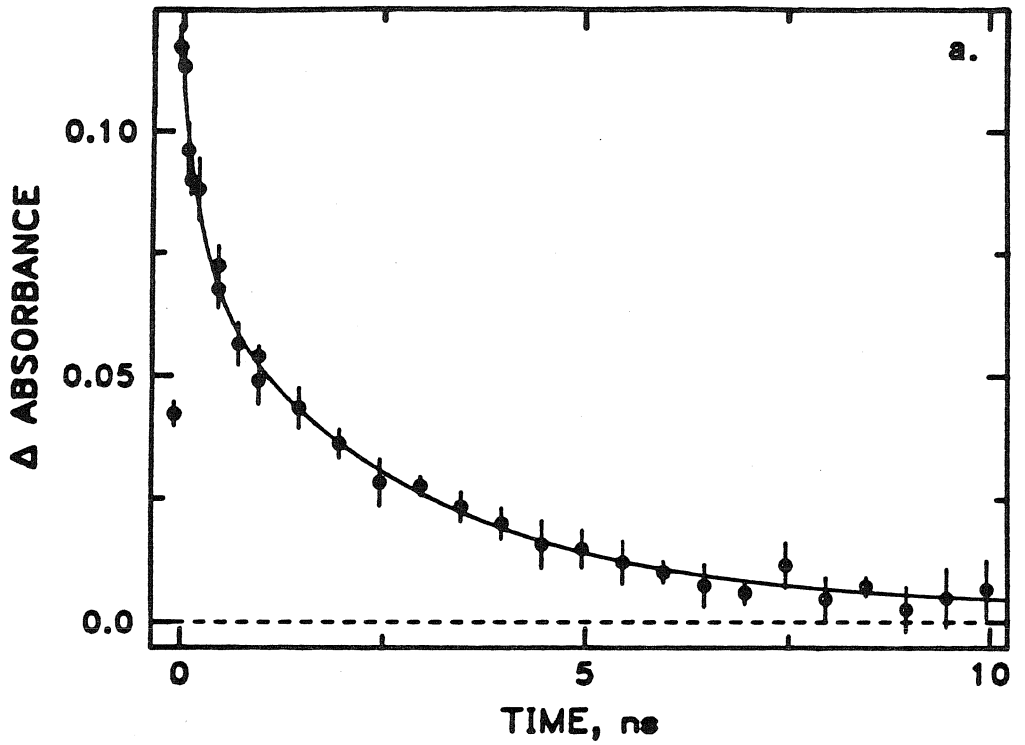
a.
0.10
0.05
0.0
Δ ABSORBANCE
0
5
10
TIME, ns

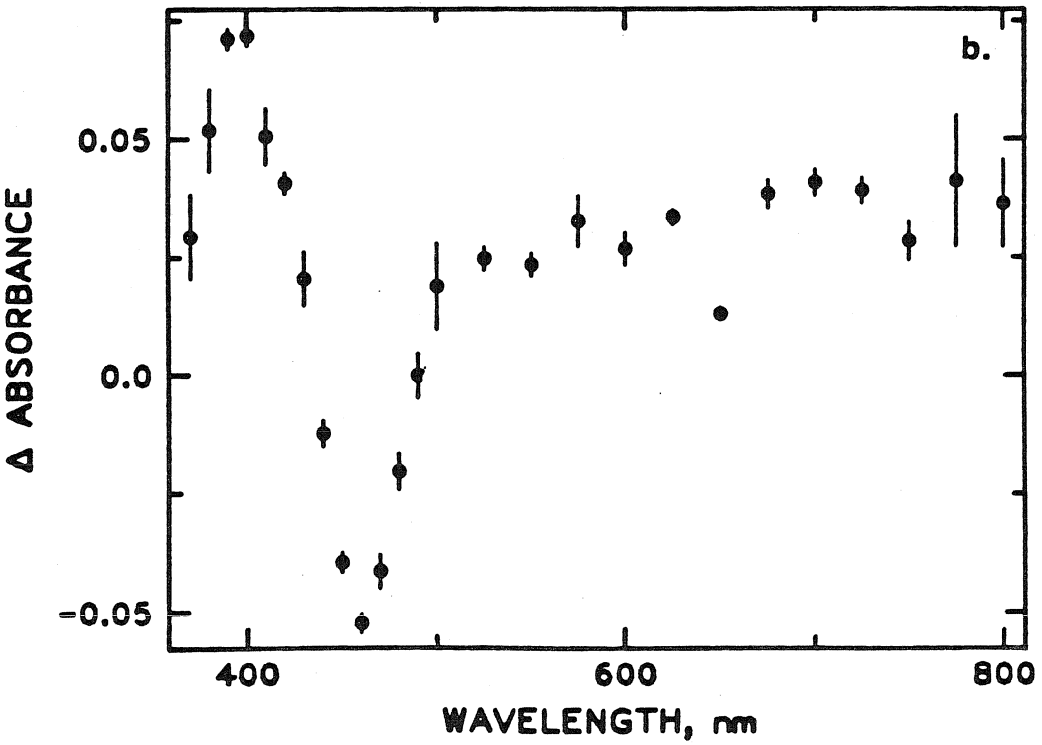
b.
0.05
0.0
-0.05
Δ ABSORBANCE
400
600
800
WAVELENGTH, nm

$Ir_2(Pz^*)_2(CO)_2(Ph_2POCH_2CH_2\text{-}Py^+)_2$ and $Ir_2(Pz^*)_2(CO)_2(Ph_2POCH_2CH_2\text{-}4PhPy^+)_2$, the singlet lifetime ($\tau_1$=2 ps) for this complex is much too short for its 390 nm absorption band to be assigned to a singlet excited state. Its phosphorescence lifetime was found to be 3.0 ns from transient emission measurements. Thus, the longer lived component in transient absorption spectra of $Ir_2(Pz^*)_2(CO)_2(Ph_2POCH_2CH_2\text{-}4MePy^+)_2$ can be assigned to its ^3B excited state; the shorter lived component is logically assigned to a charge recombination process involving its CT excited state.

$Ir_2(Pz^*)_2(CO)_2(Ph_2POCH_2CH_2\text{-}Me_3Py^+)_2$: Figures 4.7 a through j summarize the kinetic and spectral data for $Ir_2(Pz^*)_2(CO)_2(Ph_2POCH_2CH_2\text{-}Me_3Py^+)_2$ in acetonitrile solutions after a 30 ps excitation pulse at 355 nm. Flash photolysis of this complex leads to a ground state bleach at 450 nm and the formation of a transient absorption feature at 390 nm, which is similar to the absorption bands seen in difference spectra of $Ir_2(Pz^*)_2(CO)_2(Ph_2POCH_2CH_2\text{-}Py^+)_2$ and $Ir_2(Pz^*)_2(CO)_2(Ph_2POCH_2CH_2\text{-}4MePy^+)_2$. This transient is formed on a timescale equivalent to or less than the duration of the laser pulse and returns to baseline for delay times greater than 500 ns. On a picosecond timescale (figure 4.7b) kinetic data for this complex are adequately modeled using a biexponential intensity function, yielding time constants of 11 ns and 65 ps. The later time constant should be viewed as an upper limit, due to the relative intensities of the short and long lived absorption components. Kinetic data recorded on a nanosecond timescale (figure 4.7i) also fit well to a biexponential decay function with time constants of 14 ns and 144 ns. The former time constant is the same as the 11 ns lifetime found from analyzing the data in figure 4.7b. Thus, the 390 nm transient in this compound's difference spectrum represents three kinetically resolvable processes with time constants of approximately 65 ps, 12 ns, and 144 ns. As with $Ir_2(Pz^*)_2(CO)_2(Ph_2POCH_2CH_2\text{-}Py^+)_2$ and

Figure 4.7. Difference spectra and kinetics for $Ir_2(Pz^*)_2(CO)_2(Ph_2POCH_2CH_2$-$246Me_3Py^+)_2$ in acetonitrile solutions. a) Difference spectra (λ_{ex}=355 nm, 0: t=0.0 ps, Δ: t=5 ns). b) Picosecond kinetics (λ_{ex}=355 nm, λ_{obs}=400 nm, τ_{fit1}=65 ps, τ_{fit2}=11 ns). c) and d) Streak camera data showing the temporal and spectral response of the compound's fluorescence after a 30ps (fwhm) laser pulse at 355 nm. e) Response function for our laser system determined by scattering laser pulses from neat acetonitrile. f) Time-resolved emission profile of $Ir_2(Pz^*)_2(CO)_2(Ph_2POCH_2CH_2$-$246Me_3Py^+)_2$.

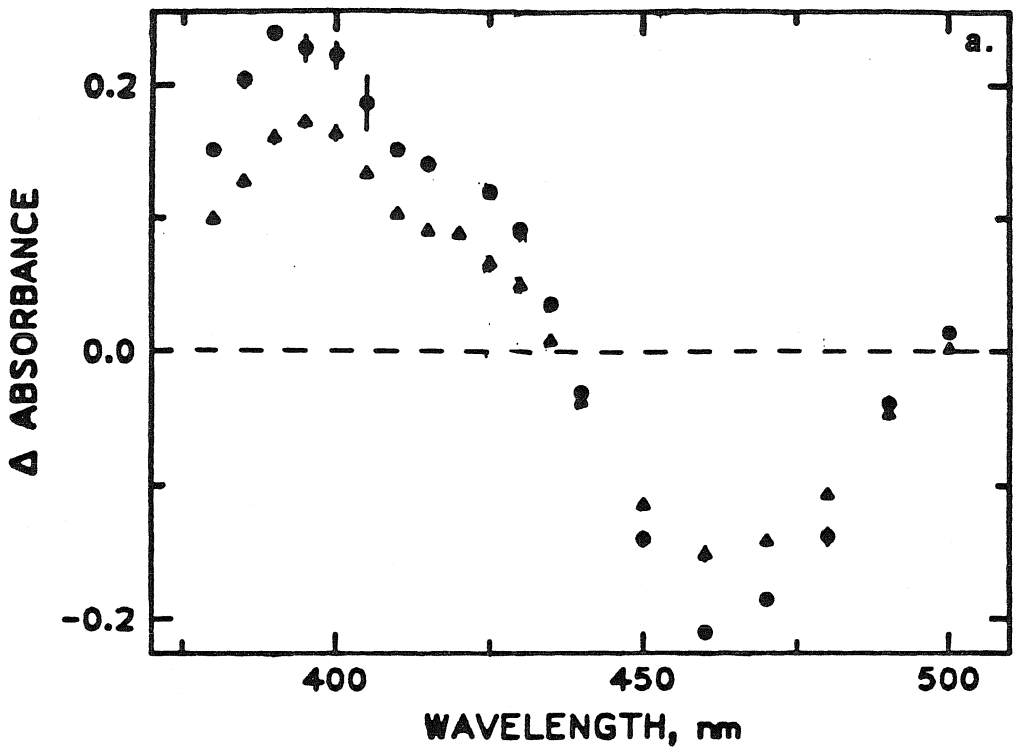
a.
0.2
0.0
-0.2
Δ ABSORBANCE
400
450
500
WAVELENGTH, nm

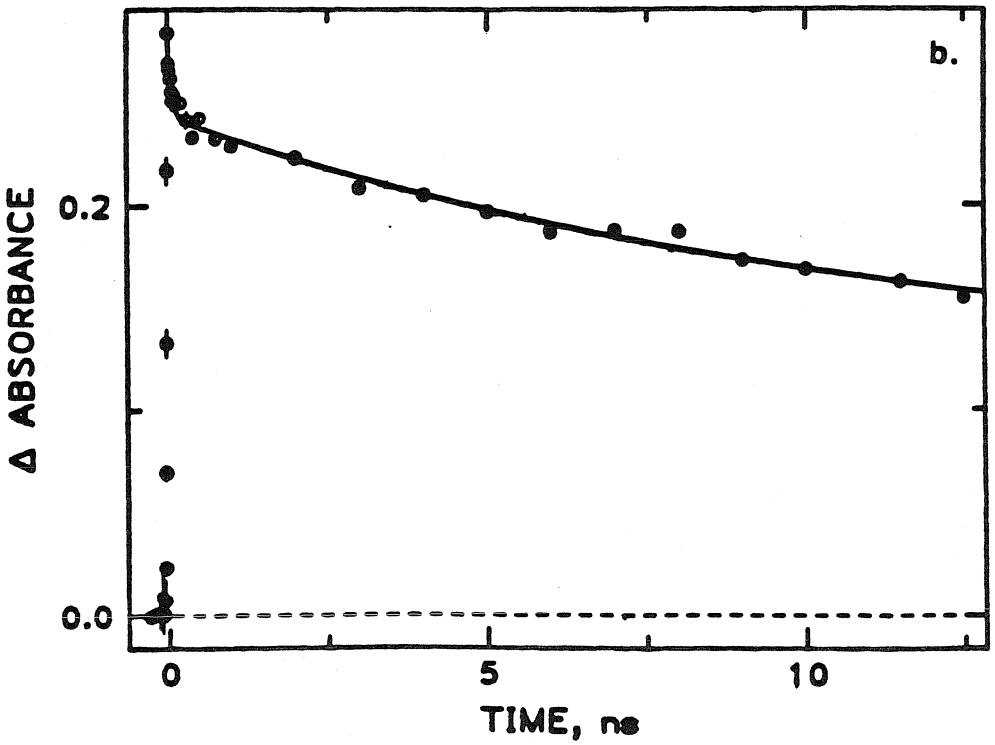
b.
0.2
0.0
Δ ABSORBANCE
0
5
10
TIME, ns

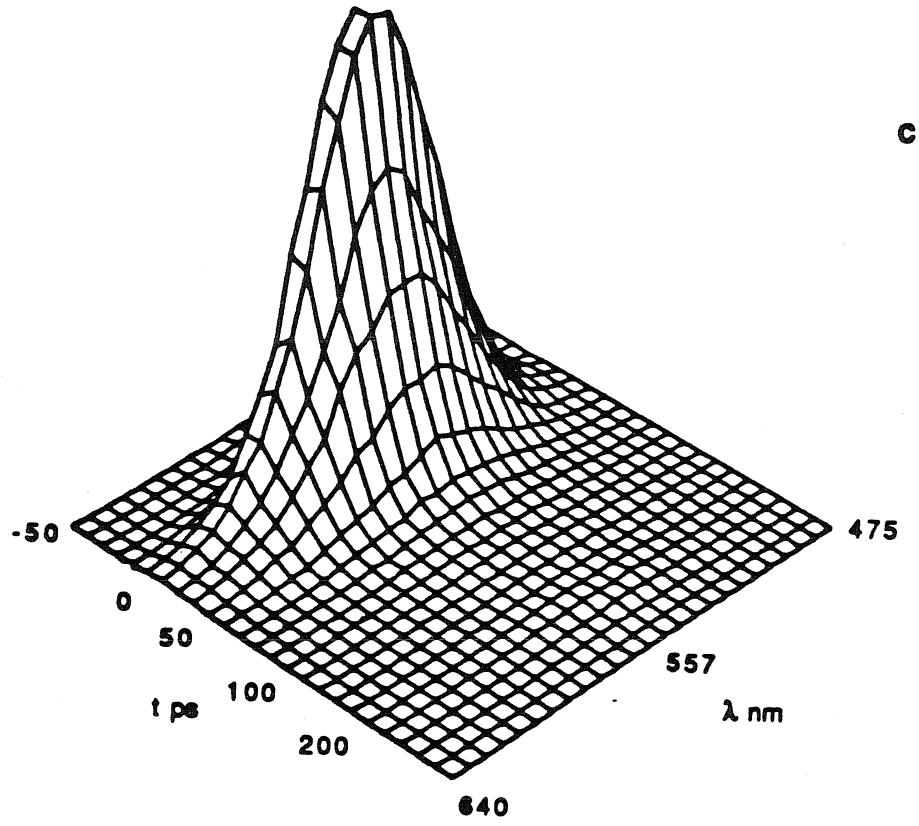
c.
-50
0
50
100
200
t ps
475
557
λ nm
640

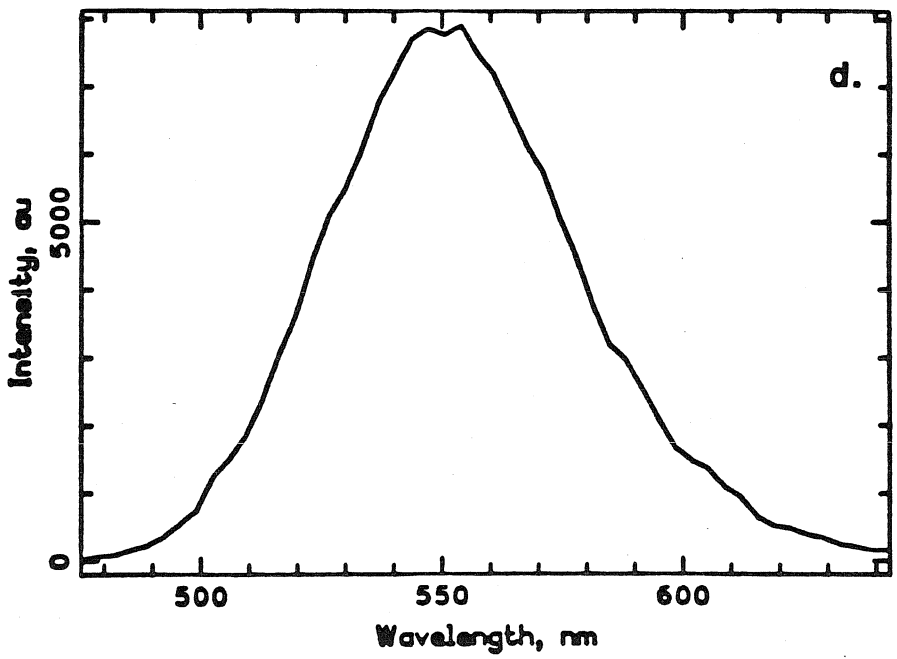
d.
Intensity, au
5000
0
500
550
600
Wavelength, nm

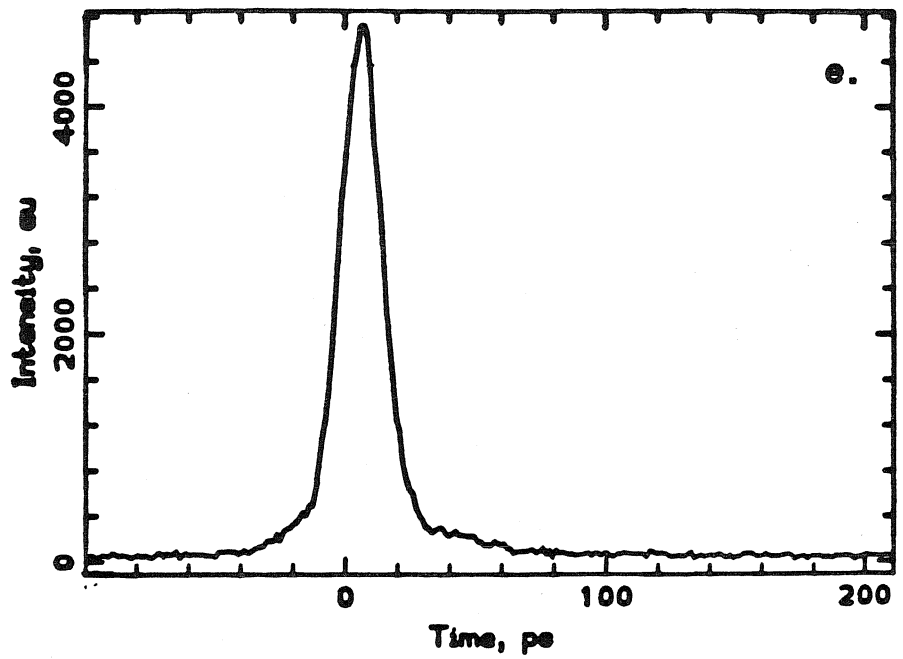
e.
Intensity, au
4000
2000
0
0
100
200
Time, ps

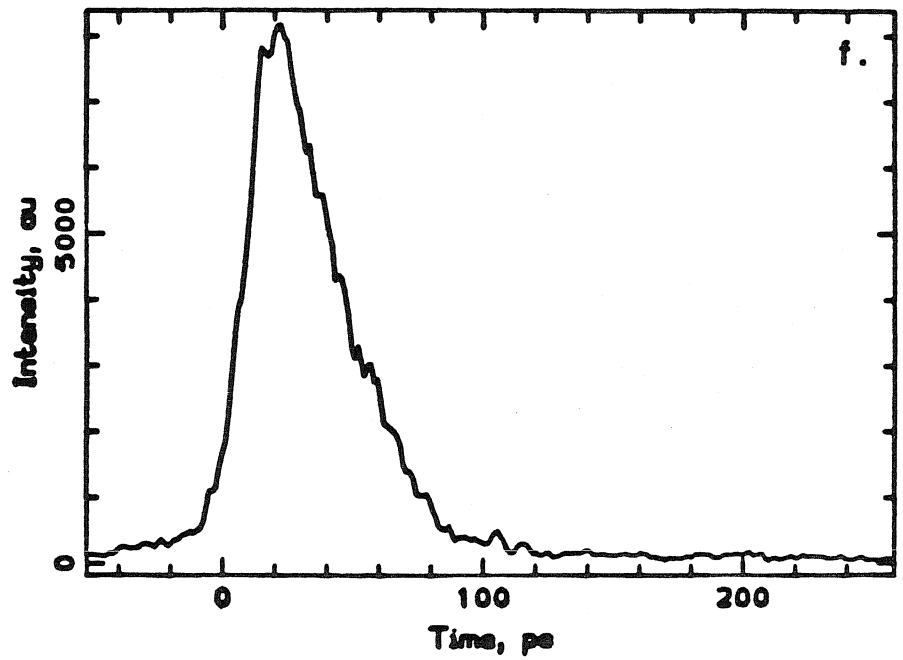
f.
Intensity, au
5000
0
0
100
200
Time, ps

$Ir_2(Pz^*)_2(CO)_2(Ph_2POCH_2CH_2\text{-}4MePy^+)_2$ transient absorption features, which distinguish the ^1B, ^3B, and CT excited states in this complex were not observed. Therefore, time-resolved emission studies were conducted to assign these time constants to specific excited state species.

In contrast to the donor-acceptor complexes discussed earlier, $Ir_2(Pz^*)_2(CO)_2(Ph_2POCH_2CH_2\text{-}Me_3Py^+)_2$ exhibited a fluorescence lifetime, which was long enough to be directly determined from piccosecond time-resolved emission measurements. As seen in figures 4.7 c and d, the time-resolved fluorescence spectrum of this complex is identical to its steady-state emission spectrum; thus, its ^1B excited state thermally equilibrates on a subpicosecond timescale. Figures 4.7e and f show the response function of our laser system, measured by scattering its 355 nm line from neat acetonitrile, and time-resolved emission data for $Ir_2(Pz^*)_2(CO)_2(Ph_2POCH_2CH_2\text{-}Me_3Py^+)_2$ (λ_{ex}=355 nm ; λ_{em}=550 nm). The emission profile in figure 4.7e is broadened with respect to the temporal width of our system response function, indicating that this compound's singlet excited state decays on a timescale commensurate with the duration of the laser pulse. A fluorescence lifetime of 25 ps was determined by fitting the experimental data to an emission intensity function, constructed from the convolution of our system response function with an exponentially decaying fluorescence intensity. The experimental and theoretical emission profiles are compared in figures 4.7g and h. This analysis indicates that the nominal 65 ps process found in the transient difference spectrum of $Ir_2(Pz^*)_2(CO)_2(Ph_2POCH_2CH_2\text{-}Me_3Py^+)_2$ can be attributed to its ^1B excited state.

As seen in figure 4.7 j, $Ir_2(Pz^*)_2(CO)_2(Ph_2POCH_2CH_2\text{-}Me_3Py^+)_2$ exhibits a biphasic phosphorescence profile (λ_{em}=750 nm) with lifetimes of 140 ns and 10 ns. This type of nonexponential behavior indicates that the phosphorescence from this complex is tied to at least two individual molecular species or states. Because the emission

Figure 4.7. Difference spectra and kinetics for $Ir_2(Pz^*)_2(CO)_2(Ph_2POCH_2CH_2$-$246Me_3Py^+)_2$ in acetonitrile solutions. g) and h) These two figures compare the experimental fluorescence data (g) with a theoretical curve (h) generated by convoluting the system response function with an exponential emission function; τ_f=25 ps. i) Kinetics measured at a longer delay time (λ_{ex}=355 nm, λ_{obs}=400 nm, τ_{fit1}=14 ns, τ_{fit2}=144 ns). j) Time-resolved emission profiles measured at longer delay times (λ_{ex}=355 nm, λ_{obs}=700 nm, τ_{fit1}=10 ns, τ_{fit2}=139 ns).

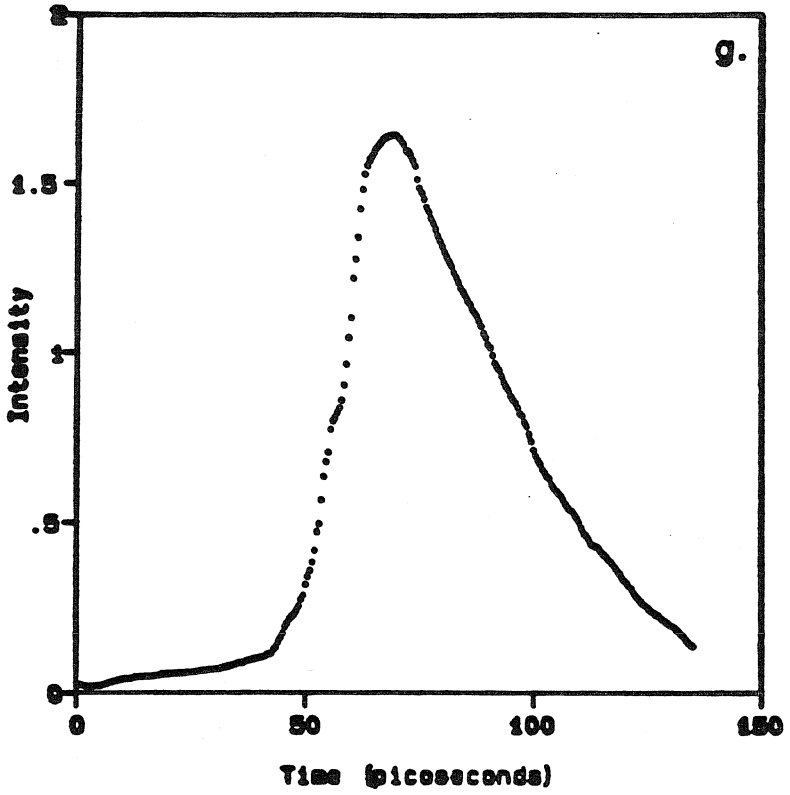
g.
Intensity
0
.5
1
1.5
2
0
50
100
150
Time (picoseconds)

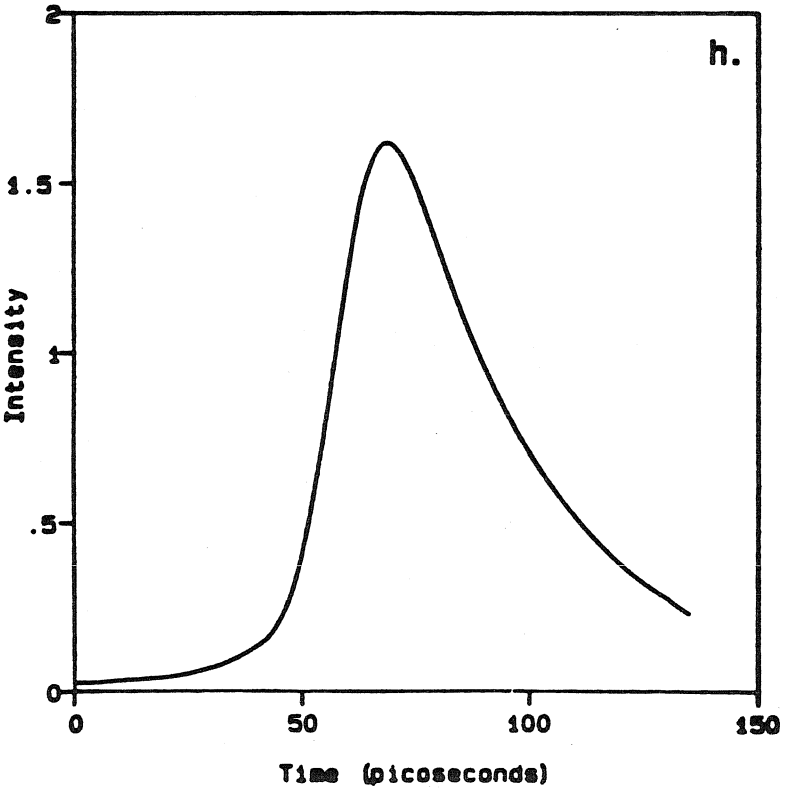
h.
Intensity
0
.5
1
1.5
2
0
50
100
150
Time (picoseconds)

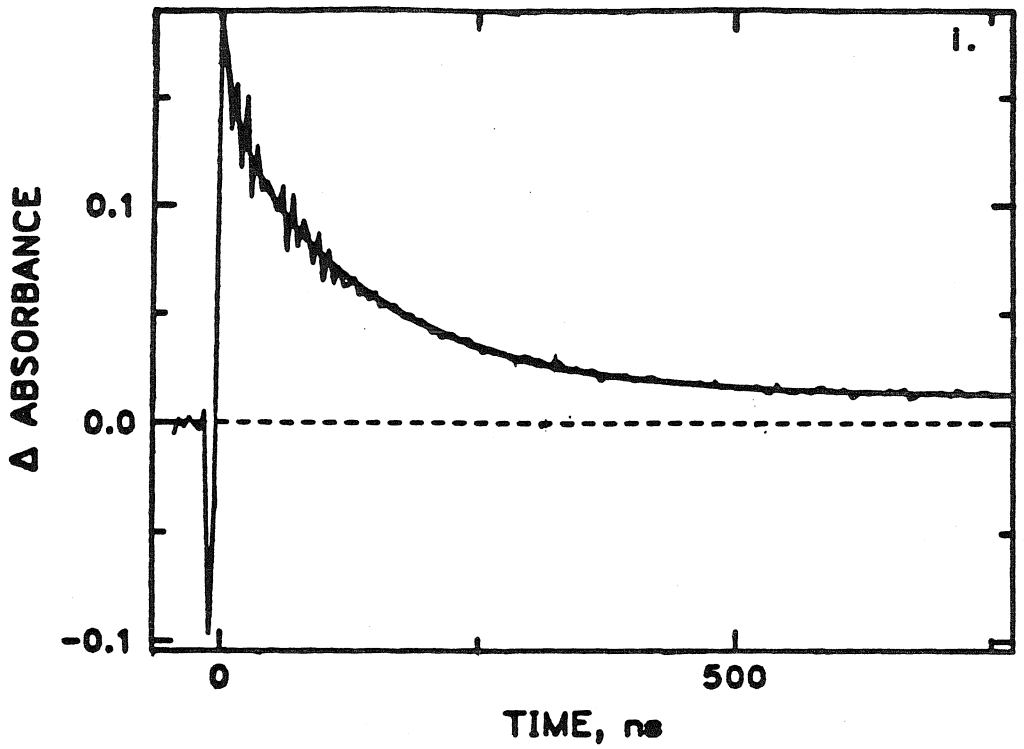
i.
Δ ABSORBANCE
0.1
0.0
-0.1
0
500
TIME, ns

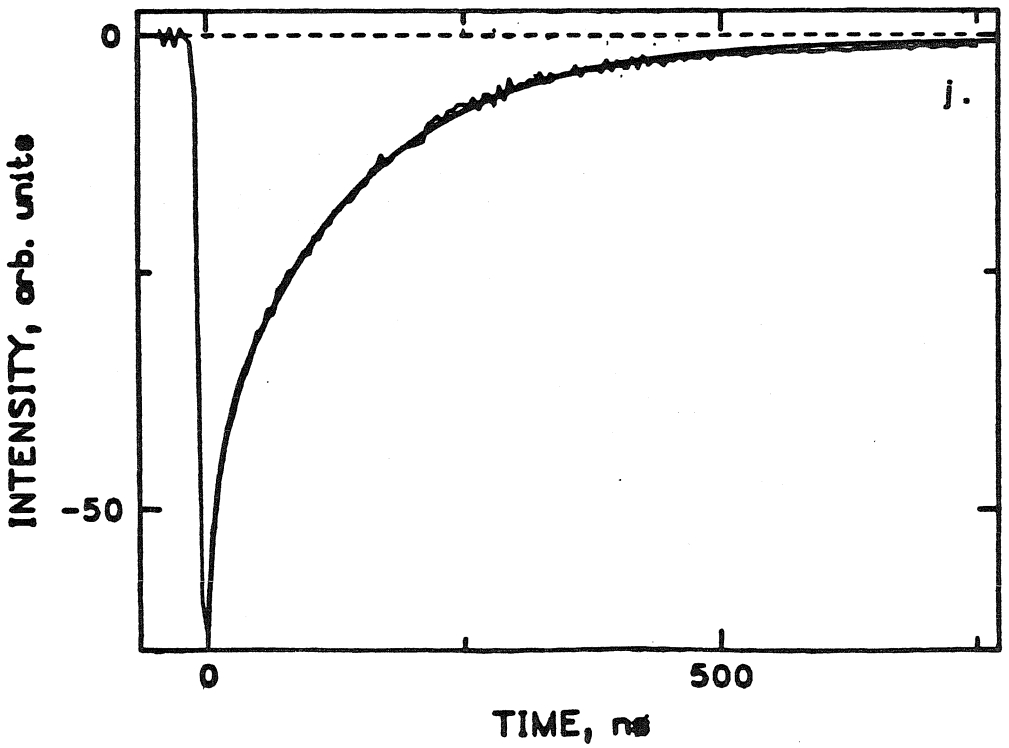
j.
INTENSITY, arb. units
0
-50
0
500
TIME, ns

bandshapes and maxima for $Ir_2(Pz^*)_2(CO)_2(Ph_2POCH_2CH_2\text{-}Me_3Py^+)_2$ are identical to those of the model compounds, its biexponential phosphorescence profiles cannot be attributed to two electronically distinct triplet states. One plausible explanation for this behavior is that two non-interconverting populations of this donor-acceptor molecule with substantially different triplet electron-transfer rates exist in fluid solution. The differences in k_{ET} for these two isomers could result from significant differences in their donor-acceptor separations and orientations. Leland and coworkers have recently observed nonexponential emission behavior in a porphyrin-quinone ET system in low temperature matrices.[7] At 77° K the solvent matrix restricts rotations about the system's three-fold axis and leads to the resolution of kinetically distinct ET processes. Lindsey[8] and Bolton[9] have observed multiexponential fluorescence decays in porphyrin-quinone systems at room temperature in fluid solutions. In both studies, multiple solution conformers were invoked to explain this behavior and were identified in the electronic and NMR spectra of the compounds. While a similar interpretation for $Ir_2(Pz^*)_2(CO)_2(Ph_2POCH_2CH_2\text{-}Me_3Py^+)_2$ in room temperature acetonitrile solutions is conceptually attractive, it is at odds with the known conformational variability of the redox ligands in this complex. Recall from chapter 2 of this thesis that intramolecular rotations about the Ir-P and linker group single bonds make a distribution of donor-acceptor separations and orientations available to the iridium dimer compounds in fluid solution. Further, based on the structural similarities between $Ir_2(Pz^*)_2(CO)_2(Ph_2POCH_2CH_2\text{-}Me_3Py^+)_2$ and $Ir_2(Pz^*)_2(CO)_2(Ph_2POCH_2CH_2\text{-}4MePy^+)_2$, it is difficult to rationalize profound differences in the distribution of solution conformations available to their redox ligands. Yet as seen earlier, the time resolved emission data for the former compound were readily modeled by a single exponential intensity function. These considerations indicate that a model involving two non-interconverting donor-acceptor complexes is not reasonable for explaining the biphasic emission behavior associated with this complex.

A more plausible model, which accounts for the nonexponential emission decays found in $Ir_2(Pz^*)_2(CO)_2(Ph_2POCH_2CH_2\text{-}Me_3Py^+)_2$, involves the equilibration of this compound's ^3B and CT states on a timescale commensurate with their excited state lifetimes (figure 4.8). This kinetic scheme is based on an analogous model for the biphasic emission decays found in exciplex donor-acceptor systems and is in line with the approximate 80 mv separation between the ^3B and CT states in this complex reported in chapter 3.[10] Because of this added complication, rates for triplet state electron transfer and charge recombination must be extracted from a detailed analysis of the time resolved emission data in figure 4.7j. To simplify a derivation for the time dependent concentrations of the ^3B and CT excited states in $Ir_2(Pz^*)_2(CO)_2(Ph_2POCH_2CH_2\text{-}Me_3Py^+)_2$, we make several fundamental assumptions. The first of these is that electron transfer does not take place from any of the higher-lying excited states in the donor-acceptor complexes. This assumption is necessary because the time-resolved emission data for this complex were recorded using 355 nm excitation pulses which populate the compound's higher-lying ($d\pi p\sigma$) states. It will greatly simplify expressions for the yield of formation of triplet and CT state from these higher lying electronic levels, which will play an important role in interpreting the results of our kinetic analysis. This premise is reasonable because a lower limit for k_{ic} in these complexes is 10^{13} sec^{-1} and their activationless ET rate is approximately two orders of magnitude slower (vida infra).[11] Further, order of magnitude estimates for the reaction driving force from these ($d\pi p\sigma$) states indicate that k_{et} for these reactions would be well below this activationless limit.[12] A second assumption underlying our kinetic model is that the ^3B and CT states are populated on a timescale that is shorter than their excited state lifetimes. This assumption is valid based on the rapid rates of internal conversion and ^1B electron transfer in this complex. With these assumptions in place, the kinetic scheme in figure 4.8 indicates that the rate of disappearance of the ^3B and CT states in

Figure 4.8. A kinetic scheme for $Ir_2(Pz^*)_2(CO)_2(Ph_2POCH_2CH_2\text{-}246Me_3Py^+)_2$ that includes back electron transfer from the CT to triplet state (T_1). Similar models have been used to describe biphasic emission profiles in exciplex donor-acceptor systems (S_1=lowest energy singlet state, T_1=lowest energy triplet state, CT=charge transfer state, S_n=higher energy singlet state being pumped by the laser pulse).

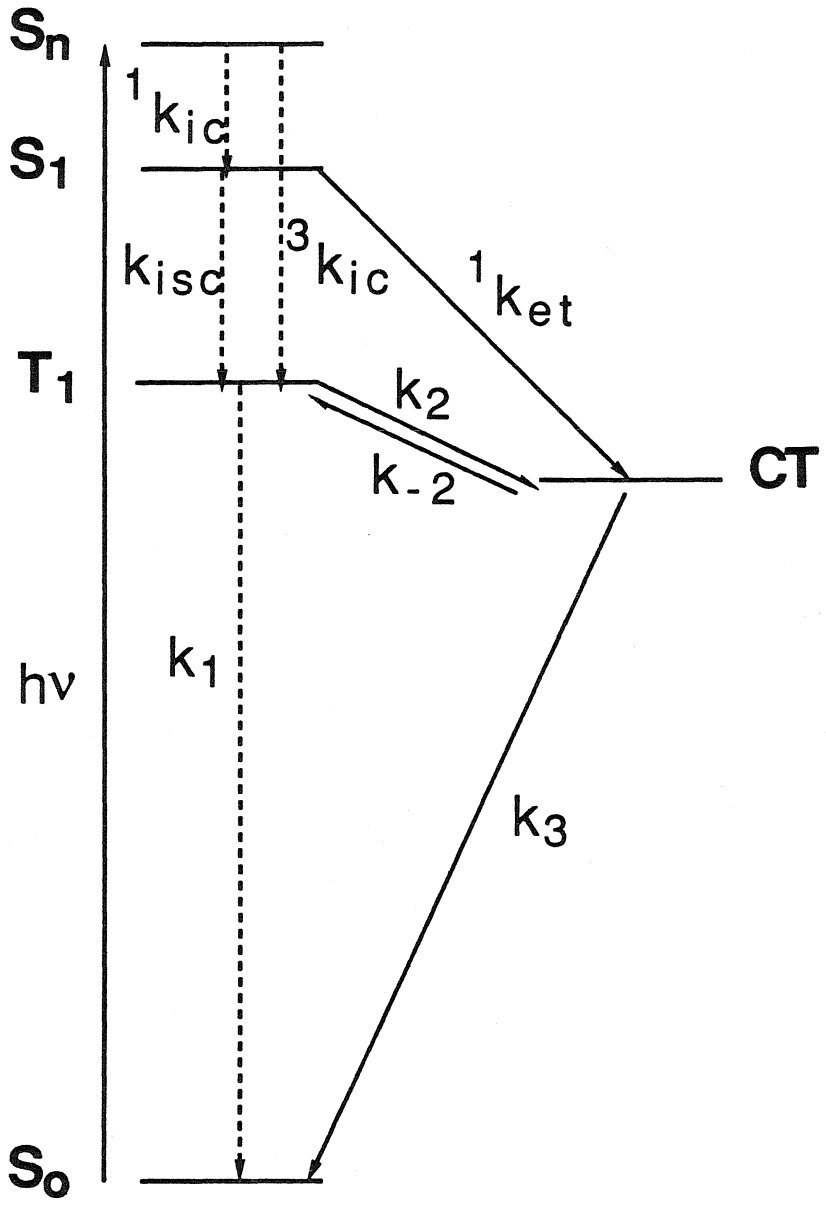
Sn
S1
T1
So
hν
1kic
kisc
3kic
1ket
k2
k-2
CT
k1
k3

this complex can be written in differential form as seen in equations 4.1 and 4.2.

$$\frac{-d[T_1]}{dt} = (k_1 + k_2)[T_1] - k_{-2}[CT] \qquad \text{eq. 4.1}$$

$$\frac{-d[CT]}{dt} = (k_3 + k_{-2})[CT] - k_2[T_1] \qquad \text{eq. 4.2}$$

Here k_1 represents the sum of radiative and nonradiative rates for the triplet state in a model compound. Equations 4.1 and 4.2 are a system of homogeneous first order differential equations with constant coefficients and can be solved using standard techniques.[13] Substituting the general exponential functions in 4.3 and 4.4 for the concentration terms in 4.1 and 4.2 leads to a matrix equation relating the fundamental rate constants and emission lifetimes (equation 4.5);

$$[T_1] = T_1^0 \exp(-\lambda t) \qquad \text{eq. 4.3}$$

$$[CT] = CT^0 \exp(-\lambda t) \qquad \text{eq. 4.4}$$

$$\begin{bmatrix} k_A - \lambda & -k_{-2} \\ -k_2 & k_B - \lambda \end{bmatrix} \begin{pmatrix} T_1^0 \\ CT^0 \end{pmatrix} = 0 \qquad \text{eq. 4.5}$$

where $k_A = k_1 + k_2$ and $k_B = k_3 + k_{-2}$. Solving equation 4.5 by requiring that its determinant equal zero produces a Characteristic Equation whose roots are

$$\lambda_{1,2} = \frac{(k_A + k_B) \pm \sqrt{(k_A - k_B)^2 + 4k_2k_{-2}}}{2} \qquad \text{eq. 4.6.}$$

It is interesting to note that as $k_{-2} \rightarrow 0$, $\lambda_1 \rightarrow k_1+k_2$ and the triplet emission profile becomes monophasic. Thus, the eigenvalues in equation 4.6 tend to their proper limits as the energy gap between T_1 and CT increases. Eigenvectors for λ_1 and λ_2 can be found by substituting each of these eigenvalues into equation 4.5 and solving for T_1^o in terms CT^o. This procedure yields general equations for the time dependent concentrations of T_1 and CT (4.7 and 4.8).

$$[T_1] = k_{-2}\left\{\frac{C_1}{k_A - \lambda_1}\exp(-\lambda_1 t) + \frac{C_2}{k_A - \lambda_2}\exp(-\lambda_2 t)\right\} \qquad \text{eq. 4.7}$$

$$[CT] = C_1\exp(-\lambda_1 t) + C_2\exp(-\lambda_2 t) \qquad \text{eq. 4.8}$$

The coefficients C_1 and C_2 are determined by the boundary conditions found in equations 4.9 and 4.10.

$$[T_1]_{t=0} = t_o \qquad \text{eq. 4.9}$$

$$[CT]_{t=0} = p_o \qquad \text{eq. 4.10}$$

In contrast to exciplex systems where $[CT]_{t=o}=0$, in our particular case the t=0 populations of the triplet and CT states are not readily determined.[10] This situation arises because these states are populated from higher-lying levels rather than by direct excitation and because they cannot be spectroscopically differentiated in transient absorption data. We will deal with this problem later using order of magnitude arguments regarding the yields of formation of T_1 and CT from upper excited states. Applying these general boundary conditions and solving for C_1 and C_2 leads to equations 4.11 and 4.12.

$$C_1 = \frac{p_o k_{-2} - t_o(k_A - \lambda_2)}{k_{-2}(\lambda_2 - \lambda_1)}(k_A - \lambda_1) \qquad \text{eq. 4.11}$$

$$C_2 = \frac{t_o(k_A - \lambda_1) - p_o k_{-2}}{k_{-2}(\lambda_2 - \lambda_1)}(k_A - \lambda_2) \qquad \text{eq. 4.12}$$

These relationships can be further simplified by requiring that the total number of excited molecules at t=0 (I_o) be equal to the sum of the t=0 triplet and CT state populations.

$$t_o + p_o = I_o$$
$$\phi_1 = \frac{t_o}{I_o}$$
$$\phi_2 = \frac{p_o}{I_0}$$
$$\phi_1 + \phi_2 = 1 \qquad \text{eq. 4.13}$$

Replacing t_o and p_o in 4.11 and 4.12 by their corresponding fractional populations, ϕ_1 and $1-\phi_1$, leads to 4.14 and 4.15.

$$C_1^* = \frac{(1-\phi_1)k_{-2} - \phi_1(k_A - \lambda_2)}{(\lambda_2 - \lambda_1)k_{-2}}(k_A - \lambda_1)I_o \qquad \text{eq. 4.14}$$

$$C_2^* = \frac{\phi_1(k_A - \lambda_1) - (1-\phi_1)k_{-2}}{(\lambda_2 - \lambda_1)k_{-2}}(k_A - \lambda_2)I_o \qquad \text{eq. 4.15}$$

Thus, the time dependent concentration of $T_1$is,

$$[T_1] = I_o\left\{\left[\frac{(1-\phi_1)k_{-2} - \phi_1(k_A - \lambda_2)}{\lambda_2 - \lambda_1}\right]\exp(-\lambda_1 t) + \left[\frac{\phi_1(k_A - \lambda_1) - k_{-2}(1-\phi_1)}{\lambda_2 - \lambda_1}\right]\exp(-\lambda_2 t)\right\}$$

.

Values for k_2, k_{-2}, k_3, and ϕ_1 can be determined from the two time constants (λ_1 and λ_2), the integrated intensities of the two emission components, and the equilibrium constant k_{-2}/k_2 using equations 4.16 through 4.19.

$$\lambda_1 + \lambda_2 = k_A + k_B \quad \text{eq. 4.16}$$

$$\lambda_1\lambda_2 = k_A k_B - k_2 k_{-2} \quad \text{eq. 4.17}$$

$$\frac{k_{-2}}{k_2} = \exp(-\Delta E) = 0.04384 \quad \text{eq. 4.18}$$

$$\frac{I_1}{I_2} = \frac{(1-\phi_1)k_{-2} - \phi_1(k_A - \lambda_2)}{\phi_1(k_A - \lambda_1) - k_{-2}(1-\phi_1)} \quad \text{eq. 4.19}$$

Solving equations 4.16, 4.17, and 4.18 leads to an equation, which is quadratic in k_2; its solution yields two positive roots, $k_2^a = 6.5 \times 10^7$ sec^{-1} and $k_2^b = 7.0 \times 10^6$ sec^{-1}. Sequential substitution of these values into equations 4.16, 4.17, 4.18, and 4.19 produces values for k_{-2}, k_3, and ϕ_1. ϕ_2 can be determined from equation 4.13. Numerical values for these fundamental kinetic parameters from each of the roots in k_2 are summarized in table 4.2.

Table 4.2: Kinetic Parameters for the 2,4,6-Me_3Py Complex.

Root	k_2 sec^{-1}	k_{-2} sec^{-1}	k_3 sec^{-1}	ϕ_1	ϕ_2
a	6.5×10^7	2.8×10^6	3.9×10^6	0.046	0.95
b	7.0×10^6	3.1×10^5	6.4×10^7	0.67	0.33

Two sets of rate constants, describing different kinetic scenarios, arise from this analysis because the boundary conditions in equations 4.9 and 4.10 are not uniquely determined. For $k_2=k_2^a$, $k_2>k_3$ and the initial populations of the triplet and CT states are close to their equilibrium values. This situation can be contrasted with a second case where $k_2<k_3$ and the initial populations of T_1 and CT lie in favor of the triplet state. Because these two cases are readily differentiated by their substantially different values of ϕ_1 and ϕ_2, additional information regarding the relative yields of formation of T_1 and CT will identify the correct set of rate constants for the $Ir_2(Pz^*)_2(CO)_2(Ph_2POCH_2CH_2\text{-}Me_3Py^+)_2$ system.

Recall that the luminescence data for $Ir_2(Pz^*)_2(CO)_2(Ph_2POCH_2CH_2\text{-}Me_3Py^+)_2$ were obtained by exciting this complex at 355 nm. Electronic transitions at this wavelength populate one of its higher-lying $^1(d\pi p\sigma)$ excited states. According to the Jablonski diagram in figure 4.8 and our initial assumptions, this state rapidly relaxes to form a distribution of ^1B and ^3B excited states. The singlet states in this initial distribution are subsequently converted to triplet and CT states via intersystem crossing and electron transfer, respectively. Thus, a knowledge of the $^1(d\pi p\sigma)$ to ^1B and ^3B internal conversion and intersystem crossing efficiencies, and the ^1B to ^3B intersystem crossing efficiency in this complex is required to fully characterize the initial yields of its triplet and CT states. Information regarding the former two quantities can be obtained by analyzing the excitation spectra of $Ir_2(Pz^*)_2(CO)_2(Ph_2POCH_2CH_3)_2$ (figure 4.9) using equations 4.20 and 4.21.

$$\frac{I_{355}}{I_{460}} = \frac{\epsilon_{355}}{\epsilon_{460}}\phi_{ic}^{singlet} \qquad \text{eq. 4.20.}$$

$$\frac{I_{355}}{I_{460}} = \frac{\epsilon_{355}}{\epsilon_{460}}\left[\phi_{ic}^{singlet} + \phi_{ic}^{triplet}\right] \qquad \text{eq. 4.21.}$$

From these relationships, if the conversion efficiencies between the $^1(d\pi p\sigma)$ and $^{1,3}(d\sigma^* p\sigma)$ excited states in d^8-d^8 A-frame complexes are close to unity, then the ratio of the excitation band intensities for these states should be equal to the ratio of their extinction coefficients. As seen in figure 4.9a, in triplet excitation spectra of $Ir_2(Pz^*)_2(CO)_2(Ph_2POCH_2CH_3)_2$ I_{355}/I_{460} is equal to the ratio of extinction coefficients at these wavelengths. This implies that $\phi_{ic}^{singlet} + \phi_{isc}^{triplet}=1$. In contrast I_{355}/I_{460} in its singlet excitation spectrum is much less than $\varepsilon_{355}/\varepsilon_{460}$ (figure 4.9b); thus, $\phi_{ic}^{singlet}=0.15$ and $\phi_{isc}^{triplet}=0.85$. These results indicate that $^1(d\pi p\sigma)$ to ^3B intersystem crossing in d^8-d^8 A-frame complexes is more efficient than internal conversion to their lowest-lying singlet states. Similar results have been reported for $Rh_2(Bridge)_4^{2+}$ and ascribed to the substantial spin-orbit coupling associated with this chromophore's metal centers.[11] An analogous effect must also play a role in the relaxation of the upper excited states in iridium A-frame compounds. The ^1B to ^3B intersystem crossing efficiency in $Ir_2(Pz^*)_2(CO)_2(Ph_2POCH_2CH_2\text{-}Me_3Py^+)_2$ can be estimated from equation 4.22;

$$\frac{\tau}{\tau^o}\phi^o_{isc} = \phi_{isc} \quad \text{eq. 4.22}$$

where τ^o and τ are the fluorescence lifetimes of a model complex and $Ir_2(Pz^*)_2(CO)_2(Ph_2POCH_2CH_2\text{-}Me_3Py^+)_2$, respectively. Here, we assume that k_{isc} is the same for the donor-acceptor and model compounds; a reasonable premise because k_{isc} is a quantity associated with the iridium dimer chromophore. For iridium d^8-d^8 complexes ϕ^o_{isc} is close to unity.[3b,e] Thus, ϕ_{isc} is approximately 0.25 in $Ir_2(Pz^*)_2(CO)_2(Ph_2POCH_2CH_2\text{-}Me_3Py^+)_2$. Using these values for the internal

Figure 4.9. Electronic excitation spectra of $Ir_2(Pz^*)_2(CO)_2(Ph_2POCH_2CH_3)_2$ in 2-methyltetrahydrofuran. a) Room temperature triplet spectrum. b) Room temperature singlet spectrum.

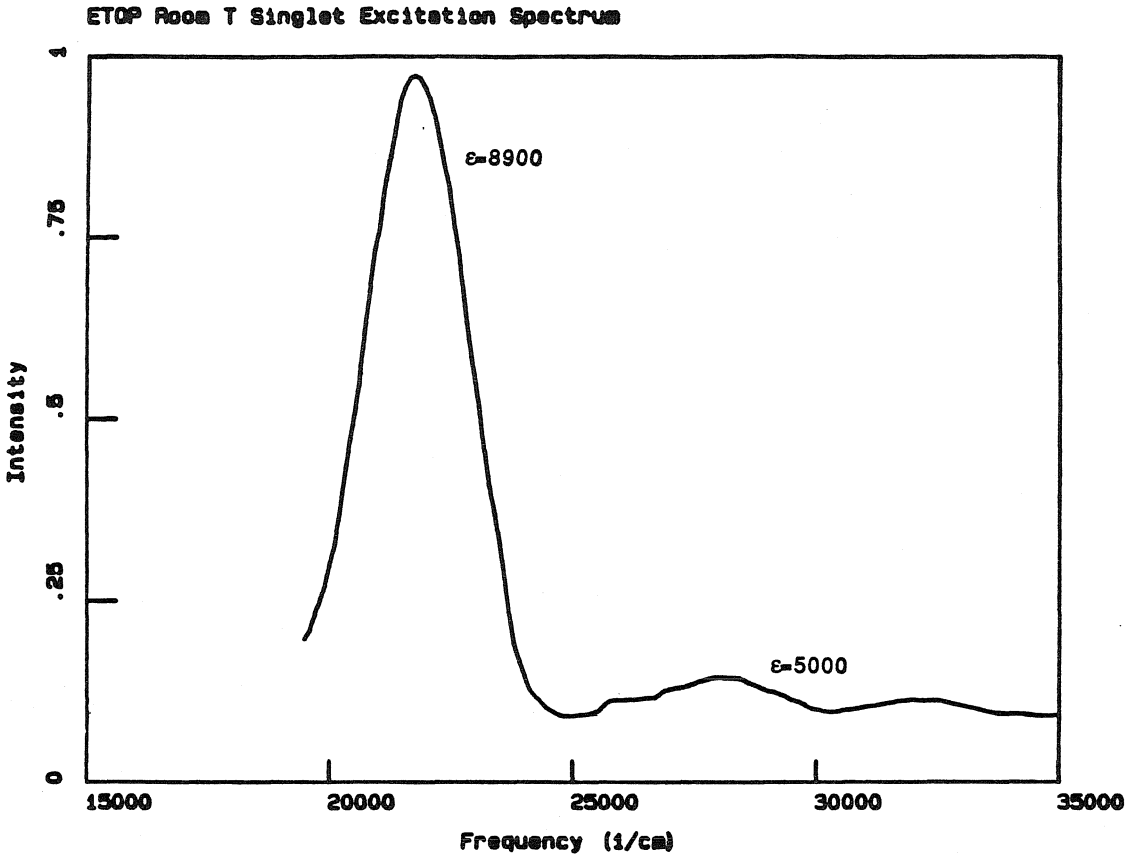
ETOP Room T Singlet Excitation Spectrum
Intensity
0
.25
.5
.75
1
ε=8900
ε=5000
15000
20000
25000
30000
35000
Frequency (1/cm)

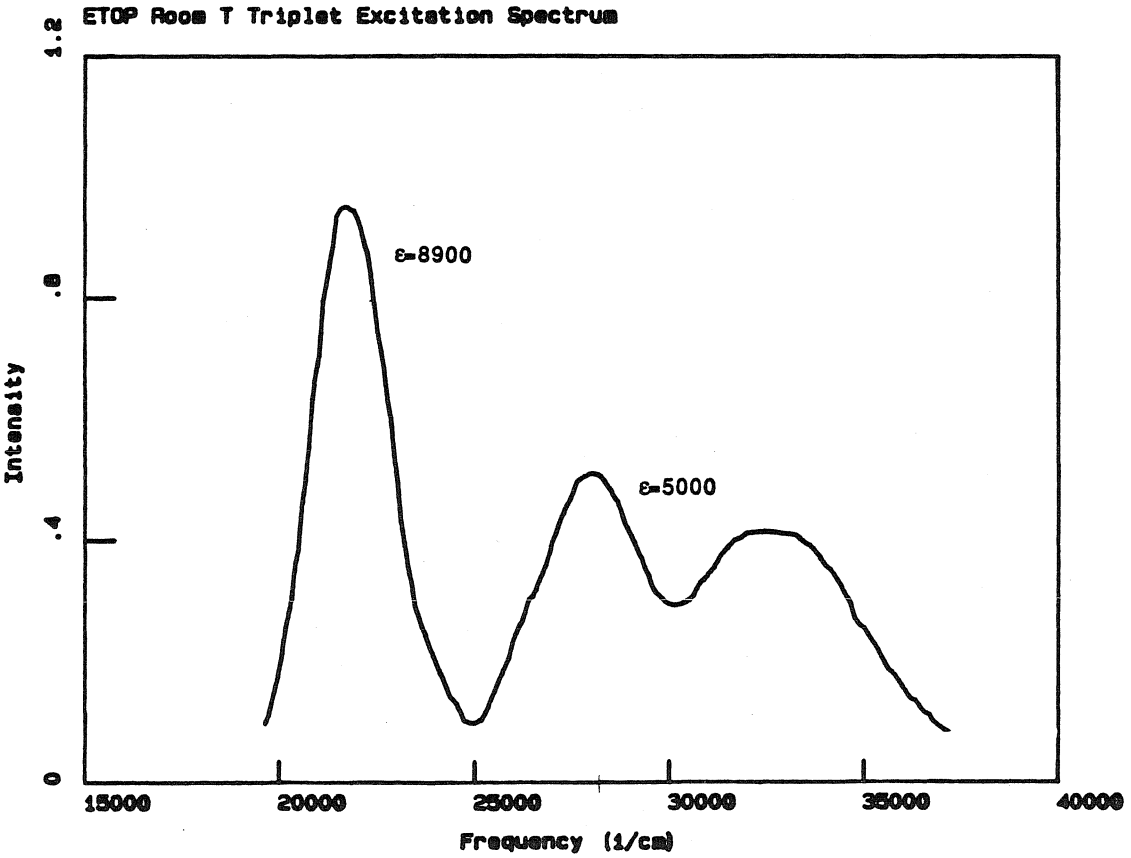
ETOP Room T Triplet Excitation Spectrum
Intensity
0
.4
.8
1.2
ε=8900
ε=5000
15000
20000
25000
30000
35000
40000
Frequency (1/cm)

conversion and intersystem crossing efficiencies, the yields of formation of the ^3B and CT excited states are found to be $\eta_{triplet}=0.88$ and $\eta_{CT}=0.12$. The ratio of these two quantities ($\eta_{CT}/\eta_{triplet}=0.14$) compares most favorably with $\phi_2{}^b/\phi_1{}^b=0.49$ calculated from the kinetic data in table 4.2. These results indicate that $k_2{}^b$,$k_{-2}{}^b$, and $k_3{}^b$ are the correct electron-transfer rate constants for this complex and that at t=0 the populations of its triplet and charge-transfer states lie in favor of the ^3B state; a situation that is primarily due to efficient intersystem between its $^1(d\pi p\sigma)$ and ^3B excited states.

Discussion

Driving Force Dependence: Previous experimental[14] and theoretical[15] studies have established reaction exoergicity as a fundamental kinetic parameter in electron-transfer reactions. Together with the inner-sphere and outer-sphere reorganization energies, reaction driving force determines the thermal barriers to electron transfer. In the classical theory for outer-sphere electron transfer, first developed by Marcus,[16] the reaction rate and activation free energy are described by equations 4.23 to 4.28,

$$k_{et} = \kappa A\sigma^2 \exp\left[-\frac{\Delta G^*}{RT}\right] \quad \text{eq. 4.23}$$

$$\Delta G^* = \frac{(\lambda + \Delta G^{o'})^2}{4\lambda} \quad \text{eq. 4.24}$$

$$\Delta G^{o'} = \Delta G^o + w^r + w^p \quad \text{eq. 4.25}$$

$$\lambda = \lambda_i + \lambda_o \quad \text{eq. 4.26}$$

$$\lambda_i = \sum_j \frac{f^r_j f^p_j}{f^r_j + f^p_j}(\Delta q_j)^2 \quad \text{eq. 4.27}$$

$$\lambda_o = (\Delta e)^2\left[\frac{1}{2a_1} + \frac{1}{2a_2} - \frac{1}{r}\right]\left[\frac{1}{n^2} - \frac{1}{\varepsilon}\right] \quad \text{eq. 4.28}$$

where $A\sigma^2$ is an effective solution collision frequency, discussed in detail elsewhere. σ is the average center-to-center distance between the two redox partners in an encounter complex and κ is the electronic transmission coefficient. The latter quantity represents

the probability that charge transfer will take place once the reactants have reached the transition state. In the Landau-Zener formalism κ is related to the electronic interaction between the reactants and their rate of passage through the transition state region.[15a,c] When $\kappa=1$, charge transfer takes place with unit efficiency and the reaction is termed adiabatic. A $\kappa<1$ is associated with a less efficient nonadiabatic charge transfer process. The intrinsic thermal barrier (λ) is composed of two reorganization components. The inner-sphere component (λ_i) describes the energy required to adjust the molecular bond lengths and angles in the two redox partners to their transition state configurations, while λ_o refers to the energy needed to reorient solvent molecules in the surrounding medium. Both are treated classically in the Marcus model as seen in equations 4.26 and 4.27, where f_j^r and f_j^p are the normal mode force constants for the jth vibration in the reactants and products, respectively, Δq_j is the change in the jth normal coordinate, a_1 and a_2 are the hard-sphere radii of the two reactants, and r is their center-to-center separation. w^r and w^p are the free energies required to bring the reactants and products from $r=\infty$ to $r=\sigma$. According to equation 4.24 the free energy of activation should vary quadratically as a function of the reaction driving force. When the driving force is small compared to the reorganization energy (i.e., the normal region), the reaction rate should increase as a function of $\Delta G^{o'}$ and maximize at $\Delta G^{o'}=\lambda$; for $\Delta G^{o'}>\lambda$ the reaction rate decreases as a function of driving force into what has been termed "the inverted region." Fundamentally, this model asserts that the total activation free energy for electron transfer is a function of the free energy change of the reaction and the energy required to rearrange the reactant normal coordinates into their transition state configurations. In the normal region the system must extract energy from its surroundings to reach the transition state. As $\Delta G^{o'}$ increases, the thermal barrier to electron transfer decreases until at $-\Delta G^{o'}=\lambda$ the reaction proceeds at its quantum mechanical rate (effectively $k=A\sigma^2\kappa$). In the inverted region the system must

Figure 4.10. Schematic potential energy surfaces illustrating the origin of the normal and invert driving force regions in the Marcus model for electron transfer. Increasing the reaction driving force decreases the energy of the crossing point between the reactant and product surfaces along the reaction coordinate until at $\Delta G^{o'}=\lambda$ there is no thermal barrier to electron transfer. As the reaction driving force increases further, the reactant and product surfaces cross at larger energies and the rate of electron transfer decreases into the inverted region.

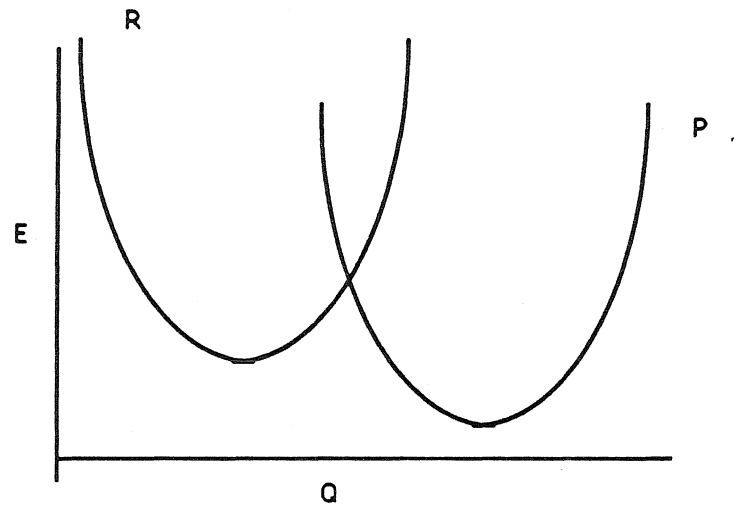
R
P
E
Q

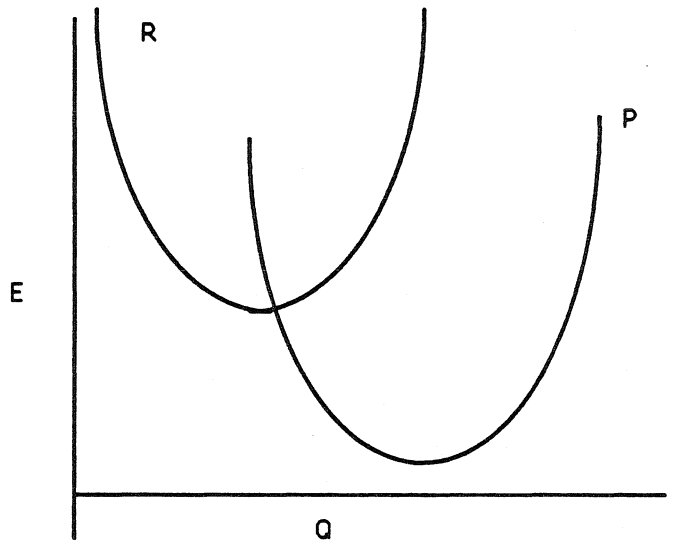
R
P
E
Q

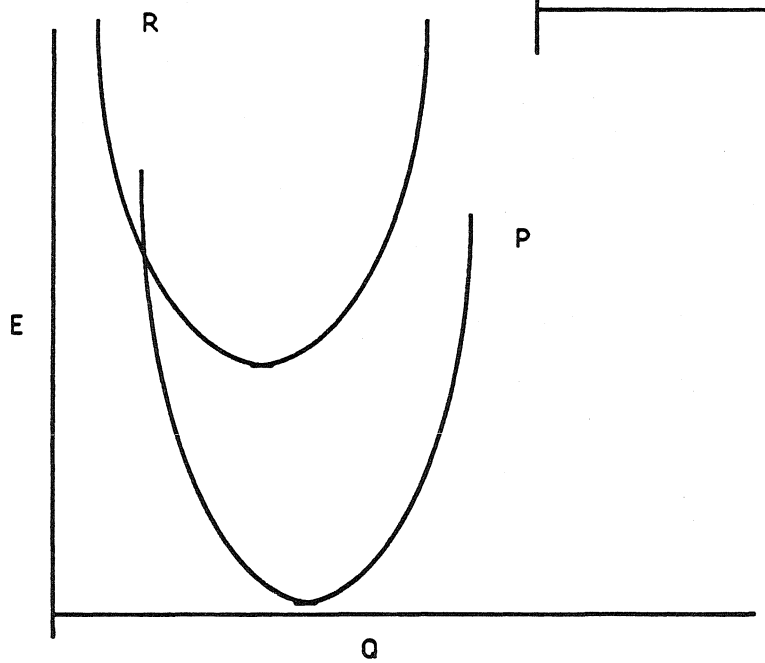
R
P
E
Q

release excess energy into its surroundings to relax from a transition state configuration to one associated with the products and a thermal barrier once again controls the rate of electron transfer. These concepts are pictorially illustrated in figure 4.10. Experimental evidence, collected over the past two decades, has indicated that the Marcus model embodies most of the fundamental principles required to describe adiabatic electron-transfer reactions.[15a] In particular, the Marcus equations in conjunction with the Marcus Cross Relation have proven to be powerful relationships for predicting electron-transfer rates in a normal driving force regime. Several models, based on quantum mechanical and semiclassical descriptions,[16] have appeared for interpreting ET kinetics at low temperature and in the inverted region; however, these relationships reduce to the classical Marcus equations on going to a high temperature limit.

While the driving force dependence of electron transfer in the normal region is for the most part well understood, reactions in the inverted region have remained largely unexplored. This situation has arisen primarily because until recently, evidence for inverted behavior had not been observed. Failure to observe inverted behavior at high reaction driving forces has been attributed to a number of experimental difficulties including rate limiting effects due to bimolecular diffusion[17] and the formation of electronically excited products at driving forces associated with the inverted region.[18] In addition, theoretical studies have indicated that the driving force dependence found in the inverted region is more gradual than predicted by the Marcus equations due to nuclear tunneling effects. As seen in equation 4.29, developed by Jortner and coworkers,[16a,b] for $h\nu >> kT$ the rate of electron transfer at high driving force will be enhanced in comparison to the rate predicted by classical theories due to the formation of vibrationally excited normal modes in the products. This leads to less pronounced variations in k_{ET} as a function $\Delta G^{o'}$ in the inverted region.

$$k_{et} = \left(\frac{\pi}{\hbar^2 \lambda_s k_b T}\right)^{1/2} |V|^2 \sum_{w=0}^{\infty} \left(e^{-S} S^w / w!\right) \exp\left\{\frac{(\lambda_s + \Delta G + w h\nu)^2}{4 \lambda_s k_b T}\right\} \quad \text{eq. 4.29}$$

$$S = \frac{\lambda_v}{h\nu} \quad \text{eq. 4.30}$$

More recently, Mataga and coworkers[19] have proposed that the lack of inverted behavior seen in photoinduced charge separation reactions can be attributed to differences in the librational frequencies of solvent molecules surrounding the neutral (charged) reactants and charged (neutral) products. This model challenges the dielectric continuum model for solvent reorganization by suggesting that partial dielectric saturation around charged redox partners is responsible for mitigating inverted behavior. Considering the mechanistic complexity of electron-transfer processes, it is not likely that any single factor controls the driving force behavior of highly exothermic reactions. A greater understanding of the roles played by nuclear tunneling, solvent motion, and electronic excited states in determining the rates of electron-transfer reactions in the inverted region will develop as additional examples of inverted behavior are discovered.

In a previous bimolecular study we examined the driving force dependence of triplet electron transfer in $[Ir_2(Pz)_2(COD)_2]$ for $\Delta G^{o\prime}$=0.13 to 1.1 eV.[14a] Plots of $RT\ln(k_{et})$ versus $\Delta G^{o\prime}$ showed a driving force dependent region, where $\ln(k_{et})$ increased as a function of $\Delta G^{o\prime}$, and a plateau region where no further driving force dependence was observed. We, like others, have speculated that our failure to observe inverted behavior in this study is tied to the limitations placed on rapid bimolecular electron transfer reactions by diffusion. Our current intramolecular electron-transfer systems have allowed use to measure electron-transfer rates, which are well above the diffusion limit and at driving forces in excess of 1.0 eV.

Table 4.3 summarizes the photophysical data for the donor-acceptor complexes and model compounds obtained from the time-resolved spectroscopic experiments discussed in this chapter and from measurements reported in chapter 3. With the exception of the fluorescence lifetimes of $Ir_2(Pz^*)_2(CO)_2(Ph_2POCH_2CH_2\text{-}4MePy^+)_2$, $Ir_2(Pz^*)_2(CO)_2(Ph_2POCH_2CH_2\text{-}Py^+)_2$, and $Ir_2(Pz^*)_2(CO)_2(Ph_2POCH_2CH_2\text{-}4PhPy^+)_2$, all of the excited state lifetimes reported here were determined using time-resolved spectroscopic techniques. The three former parameters were calculated from the fluorescence quantum yields of the complexes, and the fluorescence quantum yield and lifetime of $Ir_2(Pz^*)_2(CO)_2(Ph_2POCH_2CH_3)_2$ using equation 4.31.

$$\frac{\Phi}{\Phi^\circ}\tau^\circ = \tau \qquad \text{eq. 4.31.}$$

While this procedure is expected to introduce a larger degree of uncertainty in these quantities, similar calculations involving $Ir_2(Pz^*)_2(CO)_2(Ph_2POCH_2CH_2\text{-}Me_3Py^+)_2$ indicated that reasonable values of τ_f can be obtained using this approach; τ_f^{calc} for $Ir_2(Pz^*)_2(CO)_2(Ph_2POCH_2CH_2\text{-}Me_3Py^+)_2$ is 7.5 ps as compared with its measured 25 ps fluorescence lifetime. These lifetimes carry an accuracy of ±30% based on the uncertainties in their corresponding fluorescence quantum yields. Values of ϕ_{isc} for the donor-acceptor complexes were estimated from equation 4.22, assuming that intersystem crossing in the model complexes occurs with near unit efficiency.[3b,e] The fluorescence lifetime and intersystem crossing efficiency for $Ir_2(Pz^*)_2(CO)_2(Ph_2POCH_2CH_2\text{-}4PhPy^+)_2$ are reported as upper limits due to its negligible emission quantum yields. Electron-transfer rate constants and electrochemical driving forces for the complexes are given in table 4.4. Rate constants

Table 4.3: Photophysical Parameters for the Iridium Dimer Complexes.[a]

Complex $Ir_2(Pz^*)_2(CO)_2L_2$	Φ_f	Φ_p	τ_f ps	τ_p[g] μs	Φ_{isc}
$Ph_2OCH_2CH_2$-NEt_3[b]	0.0015	0.032	95[g]	1.2	1.0
$Ph_2OCH_2CH_3$	0.0023	0.025	100[g]	1.1	1.0
Ph_2OCH_3	0.0027	0.040	100[f]	1.2	1.0
$Ph_2O(CH_2)_3CH_3$	0.0025	0.030	100[f]	1.1	1.0
$Ph_2OCH_2CH_2$-Me_3Py[c]	0.00017	0.0013	25[g]	0.012 0.144	0.25
$Ph_2OCH_2CH_2$-4MePy	0.00006	0.0004	2.6[e]	0.003	0.06
$Ph_2OCH_2CH_2$-Py	0.00003	--[d]	1.3[e]	- -	0.03
$Ph_2OCH_2CH_2$-4PhPy	--[d]	- -	≤1.0[e]	- -	≤0.02

a. Quantum yields taken from spectra measured in acetonitrile solutions at room temperature using $Ru(Bipy)_3^{2+}$ as a standard; l_{ex}=436 nm.
b. Singlet quantum yields for the model compounds are accurate to ±10%; triplet quantum yields are accurate to ±30%.
c. Singlet quantum yields for the donor-acceptor compounds are accurate to ±30%; triplet quantum yields are accurate to ±80%.
d. Emission too weak to measure.
e. Estimated using quantum yields and the singlet lifetime of $Ir_2(Pz^*)_2(CO)_2(Ph_2POCH_2CH_3)_2$; accurate to ±30%.
f. Estimated using quantum yields and the singlet lifetime of $Ir_2(Pz^*)_2(CO)_2(Ph_2POCH_2CH_3)_2$; accurate to ±10%.
g. Determined from time-resolved emission measurements; accurate to ±10%.

Table 4.4: Driving Force and Rate Data.

	Donor	Acceptor	ΔE (eV)[a]	$k_{ET}(sec^{-1})$
1	$^3Ir_2$	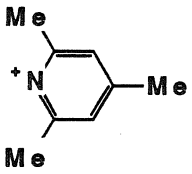	-0.08	[b] 3.5×10^6
2	$^3Ir_2$	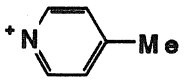	-0.21	[b] 1.7×10^8
3	$^1Ir_2$	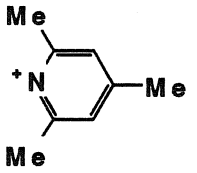	-0.58	[b] 2.0×10^{10}
4	$^1Ir_2$	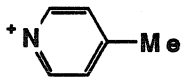	-0.71	[c] 1.5×10^{11}
5	$^1Ir_2$	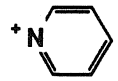	-0.89	[c] 3.2×10^{11}
6	$^1Ir_2$	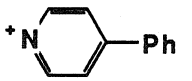	-0.97	[d] 5.0×10^{11}
7	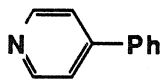	$^+Ir_2$	-1.53	[b] 2.0×10^{10}
8		$^+Ir_2$	-1.61	[b] 6.7×10^9
9	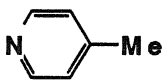	$^+Ir_2$	-1.79	[b] 3.3×10^9
10	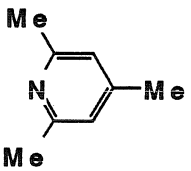	$^+Ir_2$	-1.92	[b] 6.7×10^7

a. Potentials are accurate to ±100 mv versus SSCE in 0.1 M $TBAPF_6/CH_2Cl_2$.
b. Accurate to ±10%. c. Accurate to ±30%. d. Lower limit.

for the photoinduced charge separation reactions (#2-6) were determined from equation 4.32,

$$k_{et} = 1/2\left(\frac{1}{\tau} + \frac{1}{\tau_o}\right) \quad \text{eq. 4.32}$$

assuming that the radiative and nonradiative rates intrinsic to the d^8-d^8 chromophores are not perturbed by the pyridinium cations. This premise is firmly substantiated by the spectroscopic and photophysical data presented in chapter 3 (see tables 3.1, 3.2, and 3.7). The factor of 1/2 in this equation is required by the 1:2 donor-acceptor stoichiometry in these redox systems; it assumes that motions of the quenchers with respect to the iridium dimer chromophores are not correlated. Rate constants for the charge recombination reactions (#7-10) are the reciprocals of the charge transfer state lifetimes.[31] The driving forces found in table 4.4 are taken from the electrochemical data discussed in chapter 3. Peak potentials for the pyridinium reduction waves and iridium dimer oxidation waves are the same in methylene chloride and acetonitrile. However, electrochemical oxidation of the iridium dimer complexes in acetonitrile is an irreversible two electron process, making its one electron oxidation potential less certain in this solvent. Thus, the driving forces in table 4.4 are accurate to only ±100 mv.

Figure 4.11 shows a plot of $\log(k_{et})$ versus $\Delta G^{o\prime}$ for the triplet and singlet charge separation reactions and the charge recombination reactions in our systems. The rate of photoinduced charge separation (#1-6) increases as a function of driving force and maximizes near $\Delta G^{o\prime}$=1.0 eV, consistent with previous estimates for the total reorganization energy associated with iridium dimer/pyridinium redox systems.[20] In contrast, rates for the charge recombination processes, which return these compounds

Figure 4.11. Plot of Log(k_{et}) versus $\Delta G^{o'}$ for the charge separation (#1-6) and charge recombination (#7-10) reactions in the donor-acceptor complexes. Driving forces are accurate to ±100 mv; log values are accurate to ±0.05 log units.

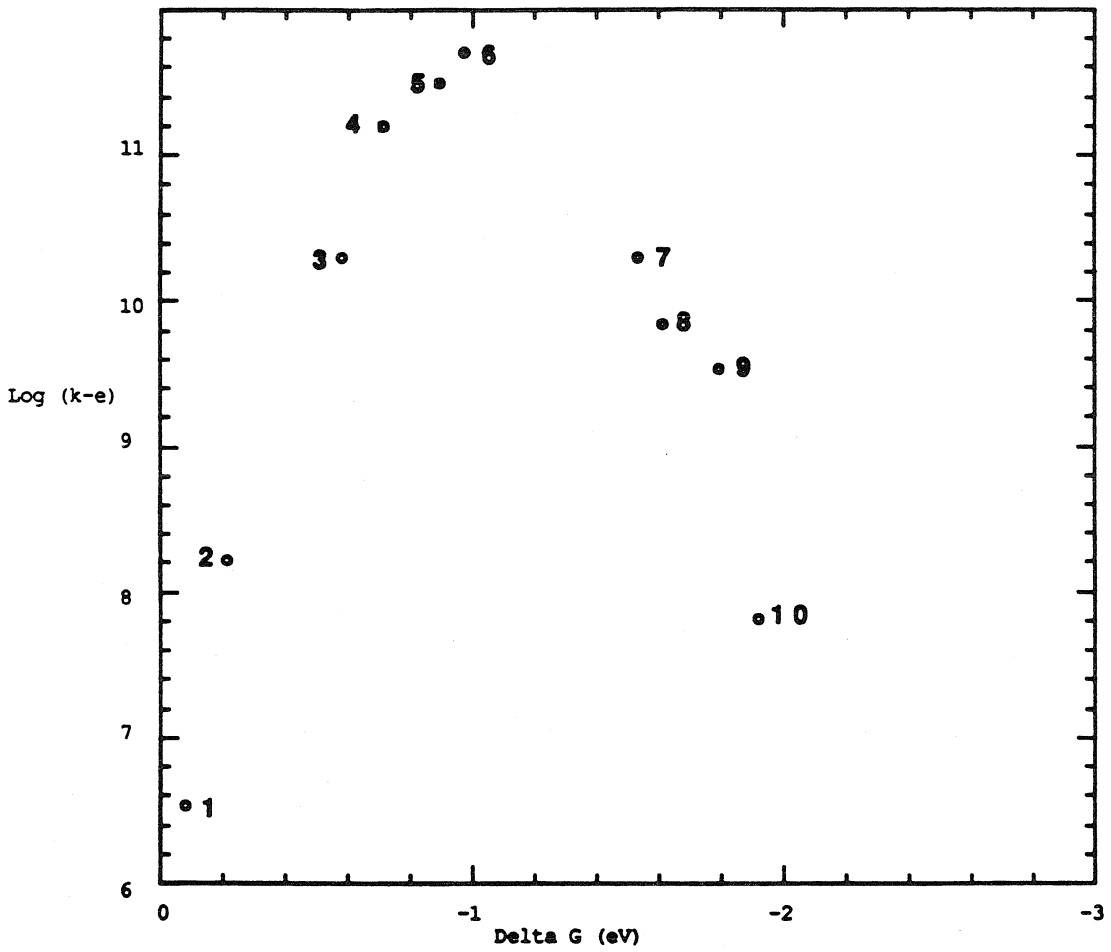
Log (k-e)
11
10
9
8
7
6
0
-1
-2
-3
Delta G (eV)
1
2
3
4
5
6
7
8
9
10

to their electronic ground states (#7-10), decrease by over two orders of magnitude in the driving force range 1.5 to 2.0 eV. This large decrease in k_{et} can be attributed to the inverted behavior predicted by classical Marcus theory and by more recent semiclassical and quantum mechanical electron-transfer models. Inverted effects have been observed in a number of different bimolecular[14b,f,21] and donor-acceptor redox systems.[14e,h] Indications of inverted behavior have also been observed in biological donor-acceptor molecules[14g] including the photosynthetic reaction center.[14c] One common feature found among these chemically diverse systems is that they all have been studied at driving forces well above 1.0 eV. Thus, a principal criterion for observing inverted behavior may be that the redox system probe exoergicities approaching 2.0 eV. This conclusion is borne out in our results as well.

Figures 4.12 to 4.14 summarize results from the analysis of our driving force dependence data using the classical and semiclassical models for electron transfer found in equations 4.23 and 4.29.[33] Figure 4.12 shows a fit of our data to a classical Marcus relationship. Recalling that the estimated standard error along the potential axis in this plot is ±100 mv, the data are adequately approximated by this model, with the exception of point #1. This analysis yields a total reorganization energy of 1.0 eV and an electronic coupling matrix element of 35 cm^{-1}. Our value of λ is strikingly similar to the reorganization energies determined in several recent driving force dependence studies on a variety of organic and biological donor-acceptor molecules.[14b,c,e,f,g,h] It is not likely that λ_i would be the same for our compounds and systems based solely on organic donors and acceptors. Therefore, the similarity between our reorganization energy and values found in the literature suggests that $\lambda \cong \lambda_o$ in redox systems whose donors and acceptors are exposed to the solvent. Our value of H_{ab} is comparable to values obtained by Closs and Miller[14e] for reactions at substantially longer donor-acceptor separations. Because the Closs-Miller systems are known to transfer electrons

Figure 4.12. Driving force data fit to a classical Marcus model (solid curve). λ=1.0 eV, H_{ab}=35 cm^{-1}.

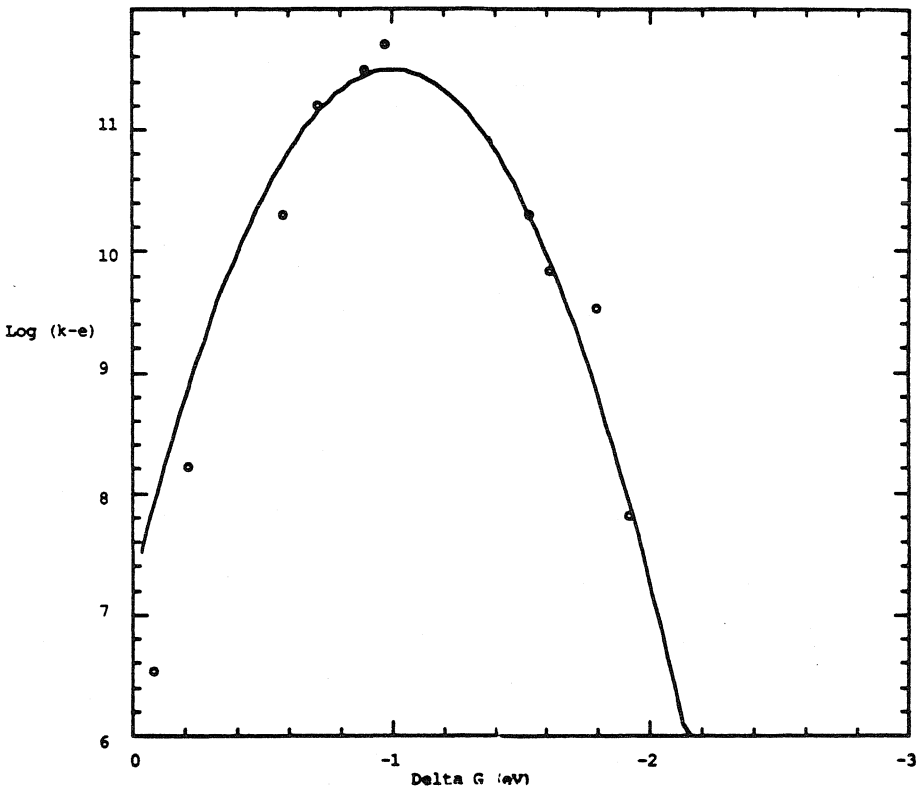
Log (k-e)
11
10
9
8
7
6
0
-1
-2
-3
Delta G (eV)

via a through bond mechanism, this comparison suggests that electron transfer in our compounds does not involve through bond pathways. This conclusion is in line with the absence of ICT bands in the electronic spectra of the iridium dimer complexes.[22] Figures 4.13 and 4.14 show results from the analysis of our data using the semiclassical model for electron-transfer found in equation 4.29. This equation includes effects due to nuclear tunneling of high frequency modes in the donor and acceptor by using an average frequency (ν) for the tunneling coordinate and by representing the solvent as a dielectric continuum. Closs and Miller,[14e,f] Dutton and coworkers,[14c] and Farid *et al.*[14b] have observed significant nuclear tunneling effects in their driving force dependence studies and have successfully utilized this relationship in analyzing their data. In figures 4.13 and 4.14, we have fixed H_{ab}^2=35 cm^{-1} and λ=1.0 eV in accord with our findings using equation 4.23. λ_o, λ_i, and ν were allowed to vary to determine how changes in the tunneling frequency and inner-sphere and outer-sphere reorganization energies affect the shapes of driving force curves predicted by this model. As seen in figures 4.13a-d for constant values of the inner-sphere and outer-sphere reorganization energies, as ν increases from 300 cm^{-1} to 1000 cm^{-1}, the theoretical driving force curves (solid line) drastically depart from the experimental data; when ν=1000 cm^{-1} variations in λ_o, λ_i, and H_{ab}^2 do not improve the fit between the model and data. In comparison to the results presented in figure 4.11, the data appear to be better represented by the semiclassical equations when ν=300 to 400 cm^{-1}. It is well known that oxidation of d^8-d^8 metal complexes leads to significant rearrangement of their metal-metal and metal ligand bond lengths.[23] A tunneling frequency of 400 cm^{-1} would be consistent with a nuclear tunneling mechanism involving the metal ligand modes in the donor-acceptor compounds.[24] Figures 4.14a-h show how emphasizing either λ_o or λ_i in the total reorganization energy changes the shape of the theoretical driving force curves for several different tunneling frequencies. Here again, good correlations between the model and data are obtained for smaller values of ν or larger values of λ_o.

Due to the 100 mv esds in our values of $\Delta G^{o'}$, it is difficult to differentiate between a classical or semiclassical kinetic model as being more appropriate for describing electron transfer in the iridium dimer complexes. These results do, however, indicate that in contrast to many of the organic donor-acceptor systems found in the literature, our complexes do not exhibit substantial nuclear tunneling contributions from modes associated with their pyridinium electron acceptors.[14b,e,f,h]

Figure 4.13. Driving force data fit to the semiclassical model of Jortner *et al.* showing changes in the theoretical curves as a function of the tunneling frequency ω for λ=1.0 eV and H_{ab}=35. a) ω=300 cm^{-1}. b) ω=400 cm^{-1}. c) ω=500 cm^{-1}. d) ω=1000 cm^{-1}.

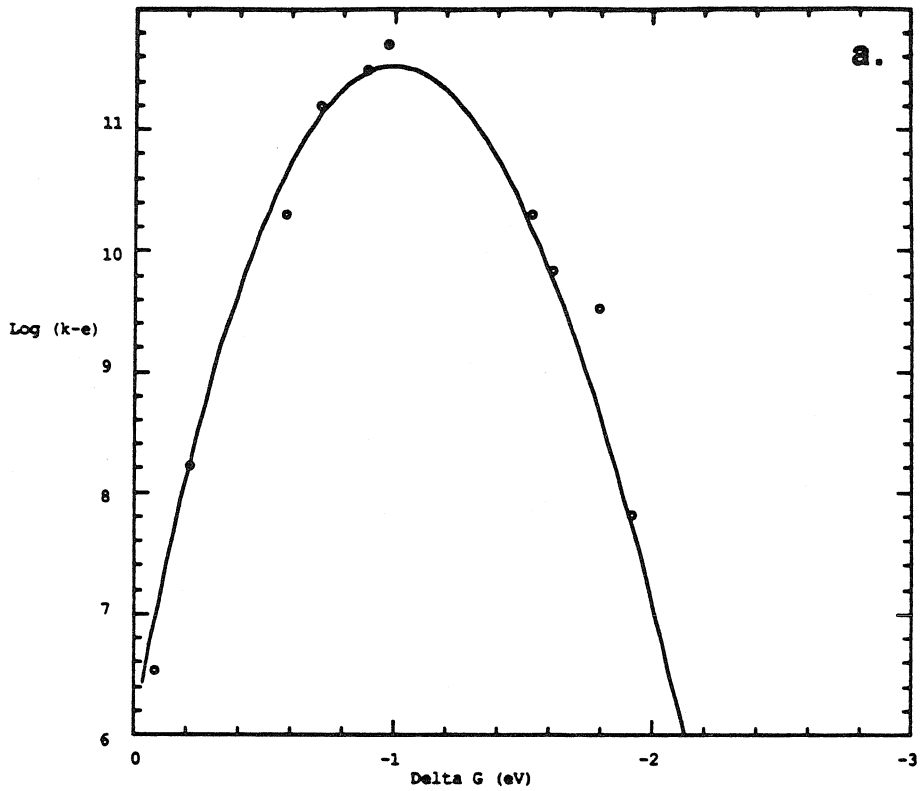
a.
Log (k-e)
11
10
9
8
7
6
0
-1
-2
-3
Delta G (eV)

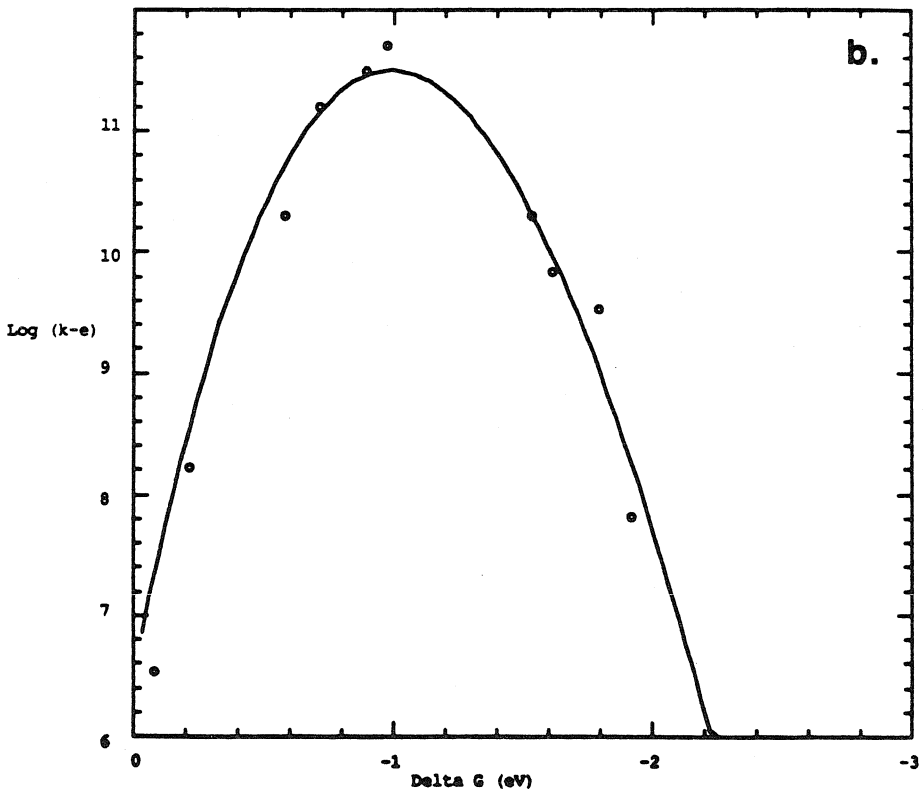
b.
Log (k-e)
11
10
9
8
7
6
0
-1
-2
-3
Delta G (eV)

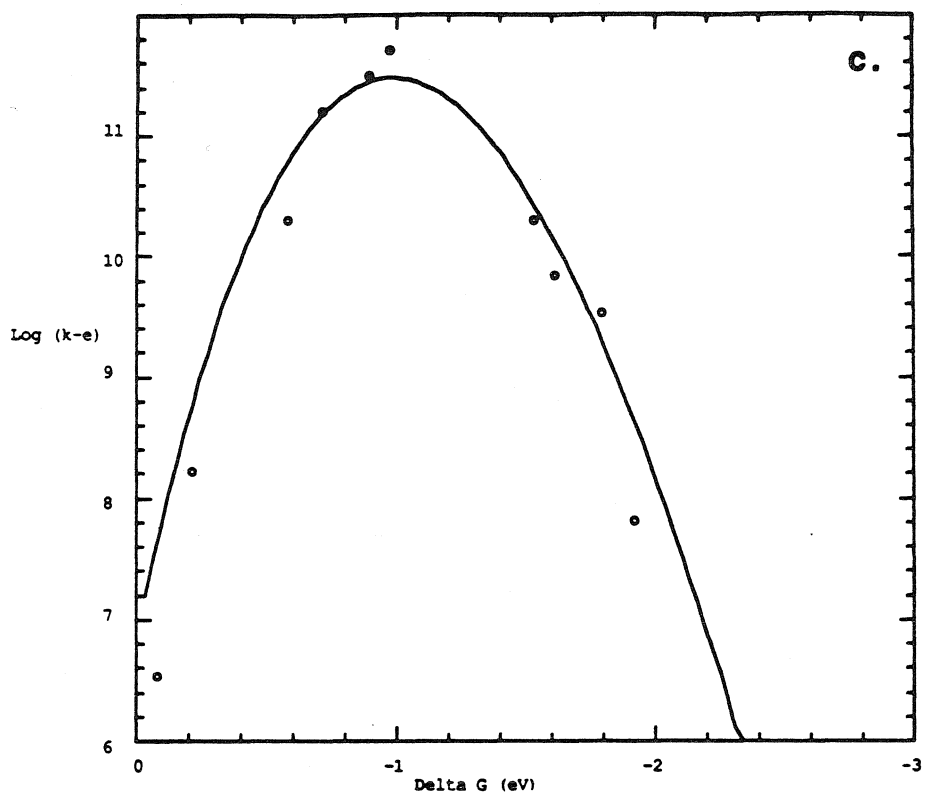
c.
Log (k-e)
11
10
9
8
7
6
0
-1
-2
-3
Delta G (eV)

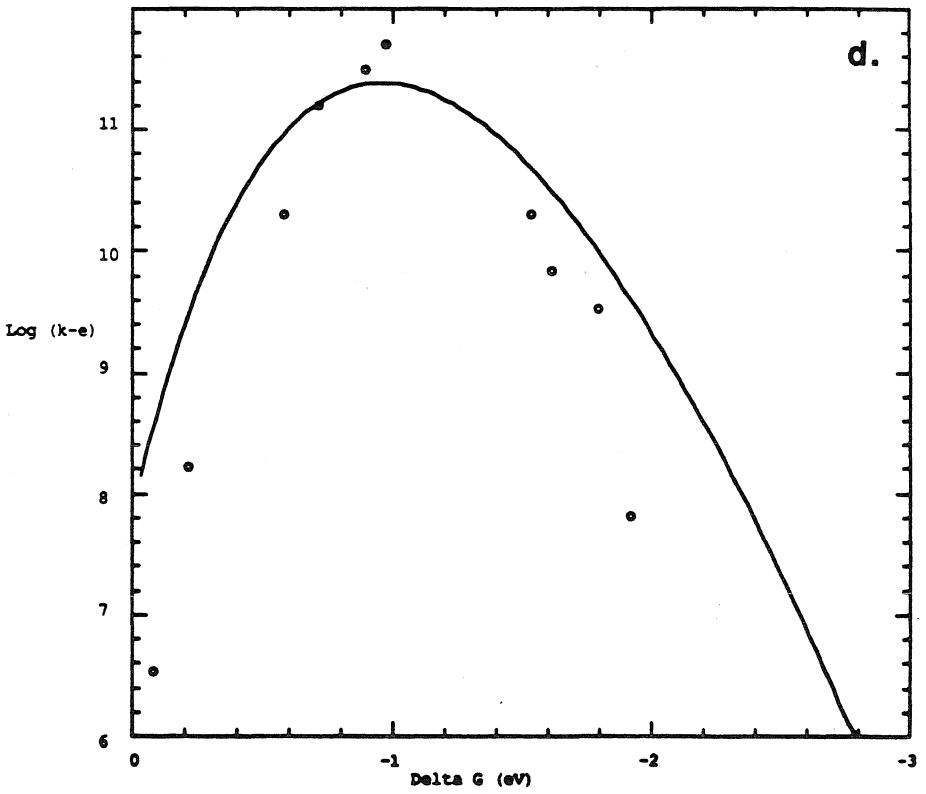
d.
Log (k-e)
11
10
9
8
7
6
0
-1
-2
-3
Delta G (eV)

Figure 4.14. Driving force data fit to the semiclassical model of Jortner *et al.* showing changes in the theoretical curves as a function of λ_i and λ_o for λ=1.0 eV and H_{ab}=35. a) ω= 300 cm^{-1}, λ_i= 0.2 eV, λ_o= 0.8 eV. b) ω= 300 cm^{-1}, λ_i=0.8 eV, λ_o= 0.2 eV. c) ω= 400 cm^{-1}, λ_i=0.2 eV, λ_o= 0.8 eV. d) ω=500 cm^{-1}, λ_i=0.80 eV, λ_o=0.20 eV. e) ω=500 cm^{-1}, λ_i=0.2 eV, λ_o=0.8 eV. f) ω=500 cm^{-1}, λ_i=0.8 eV, λ_o=0.2 eV. g) ω=1000 cm^{-1}, λ_i=0.2 eV, λ_o=0.8 eV. h) ω=1000 cm^{-1}, λ_i=0.8 eV, λ_o=0.2 eV.

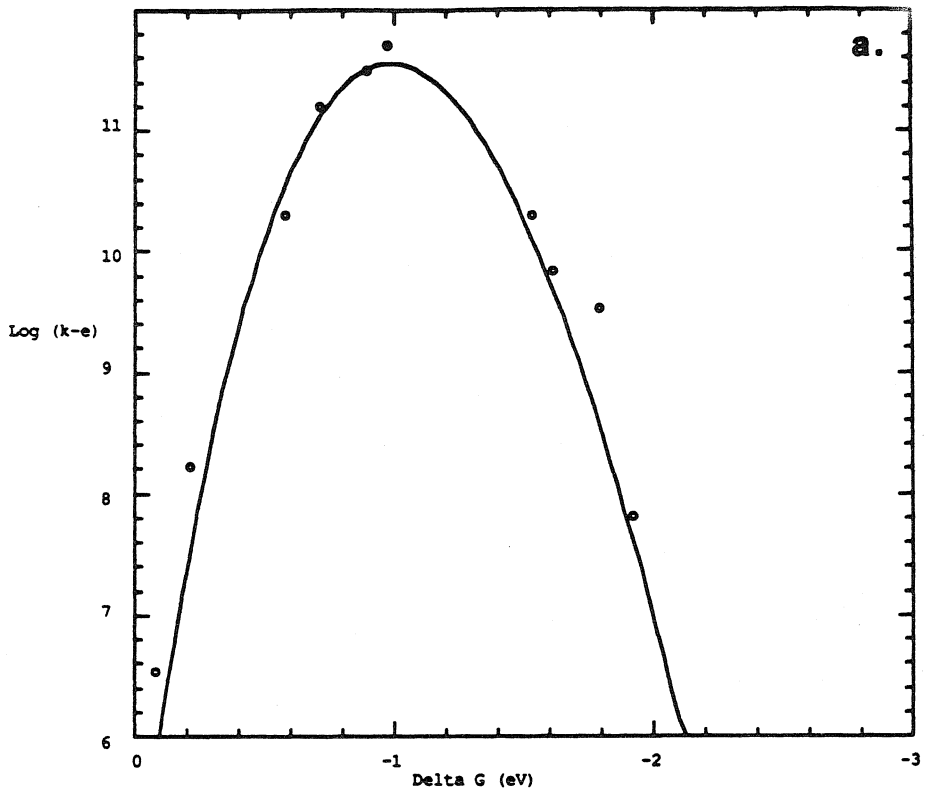
a.
Log (k-e)
11
10
9
8
7
6
0
-1
-2
-3
Delta G (eV)

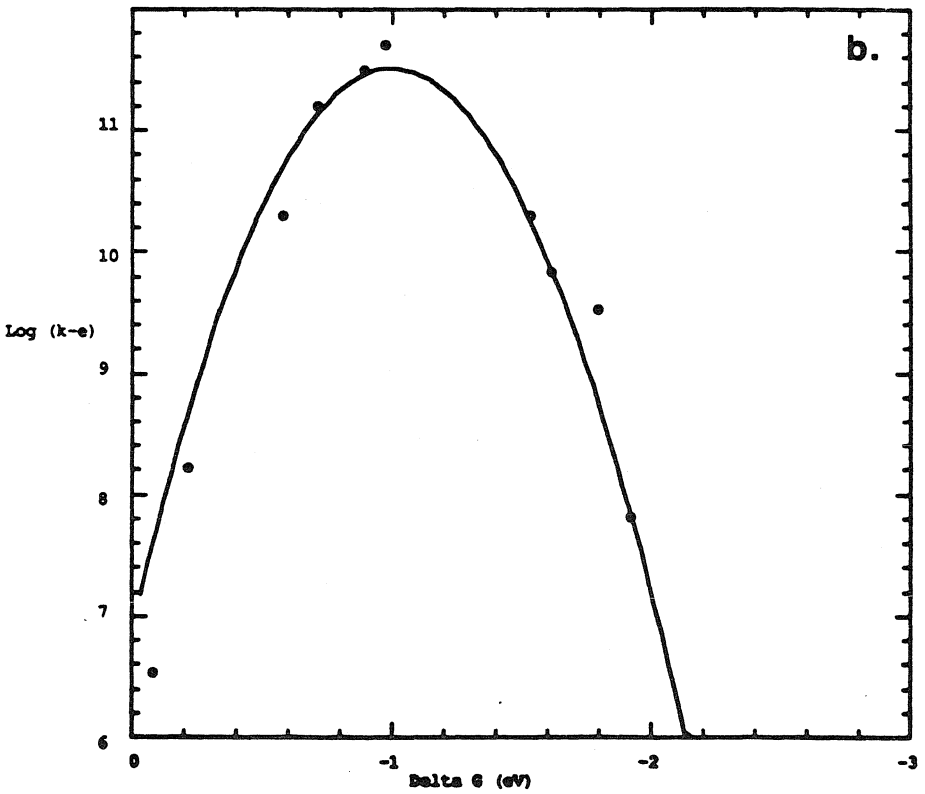
b.
Log (k-e)
11
10
9
8
7
6
0
-1
-2
-3
Delta G (eV)

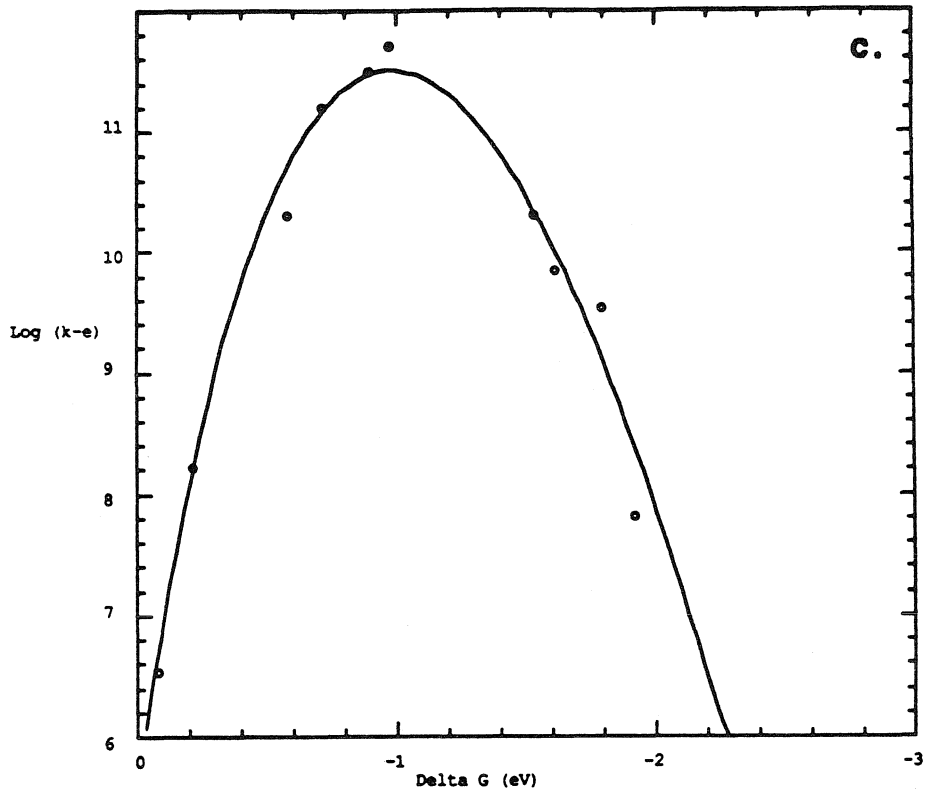
c.
Log (k-e)
11
10
9
8
7
6
0
-1
-2
-3
Delta G (eV)

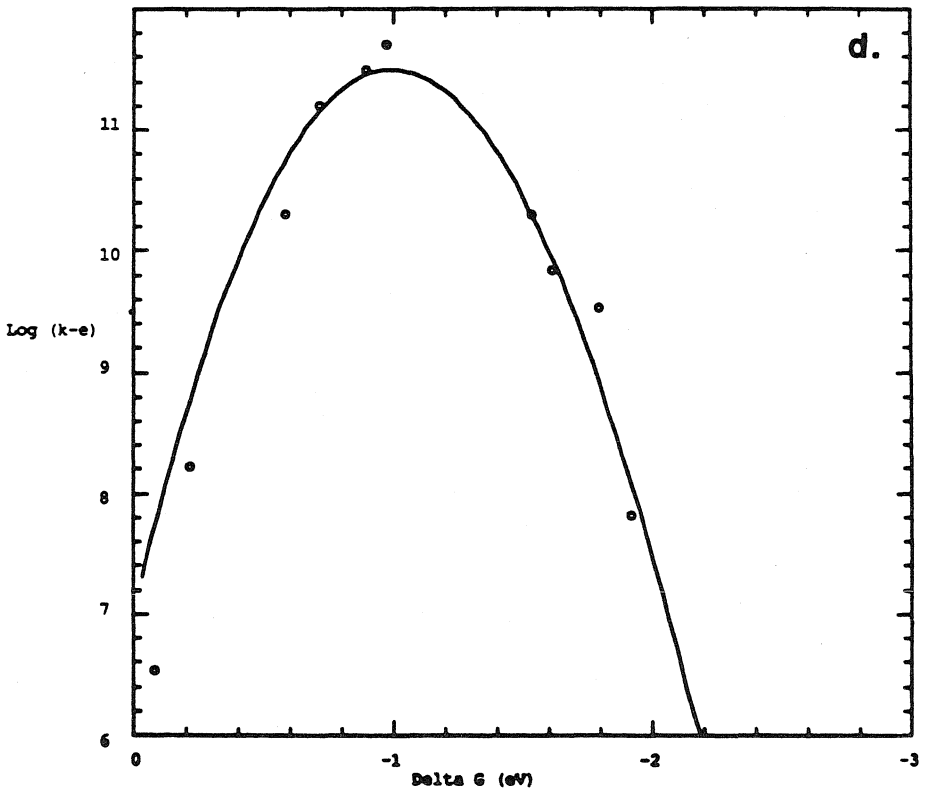
d.
Log (k-e)
11
10
9
8
7
6
0
-1
-2
-3
Delta G (eV)

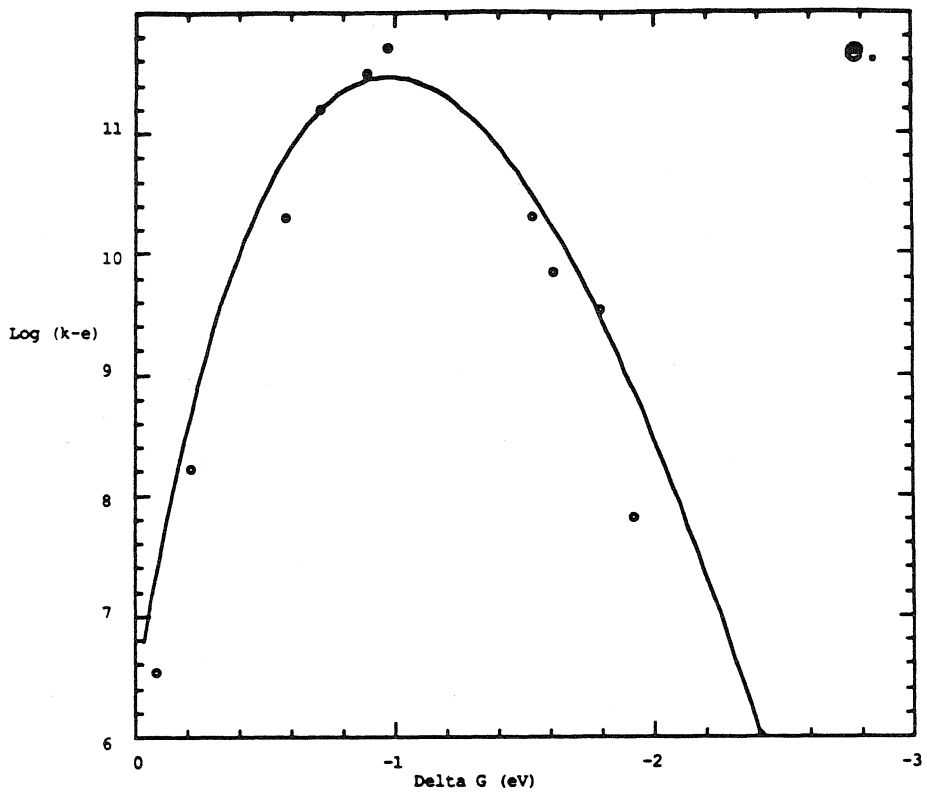
e.
11
10
9
8
7
6
Log (k-e)
0
-1
-2
-3
Delta G (eV)

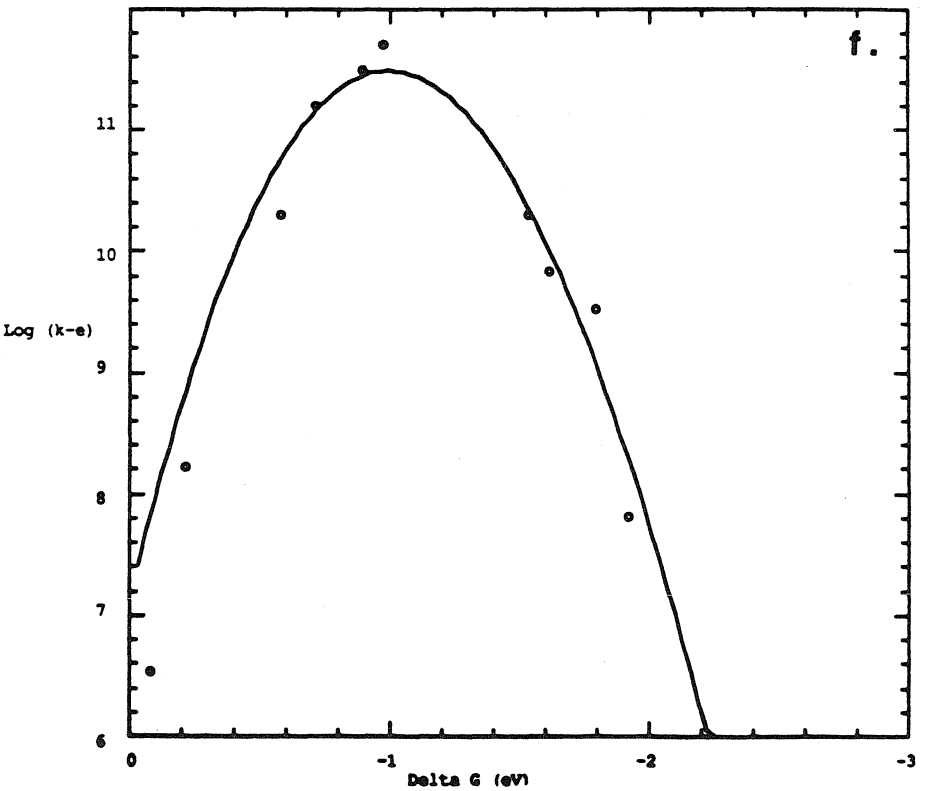
f.
11
10
9
8
7
6
Log (k-e)
0
-1
-2
-3
Delta G (eV)

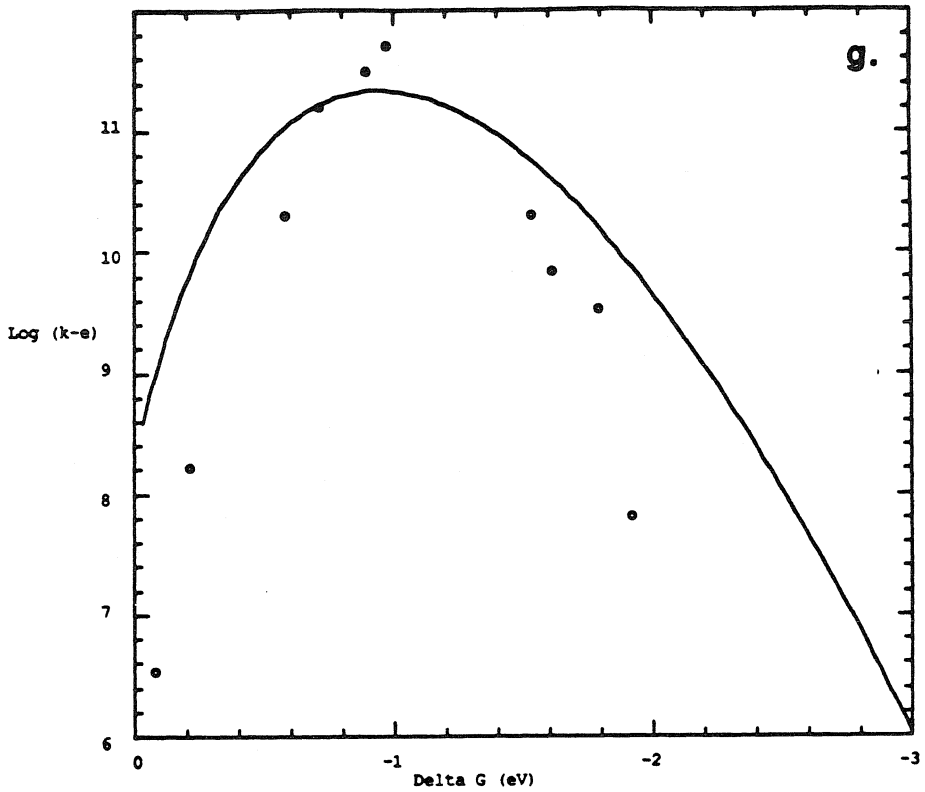
g.
Log (k-e)
11
10
9
8
7
6
0
-1
-2
-3
Delta G (eV)

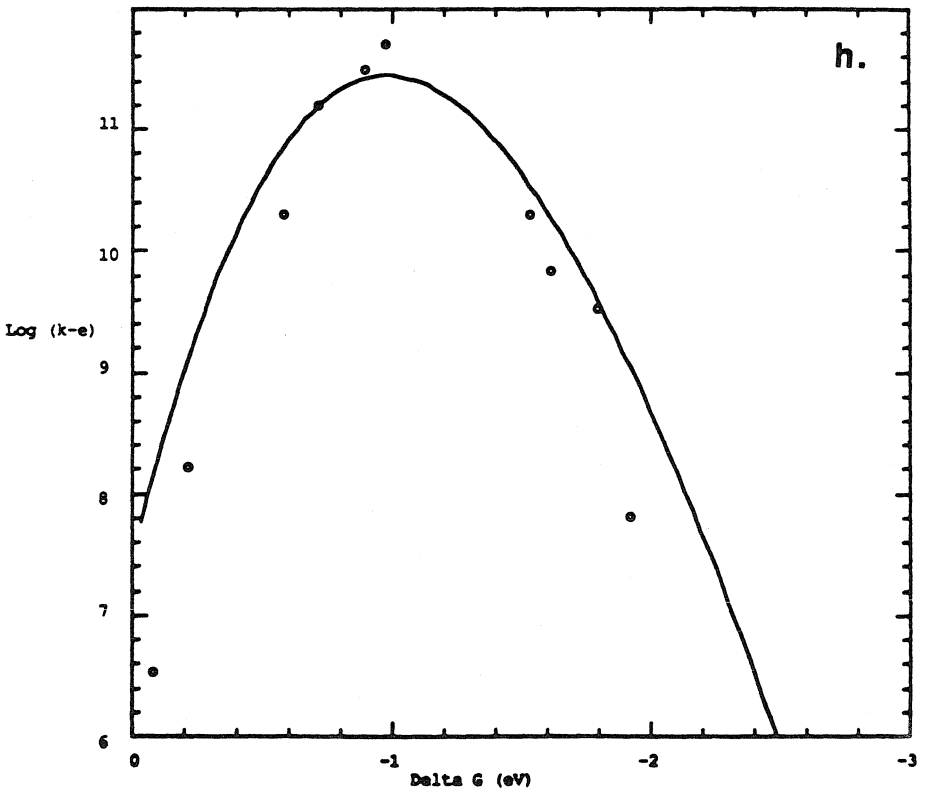
h.
Log (k-e)
11
10
9
8
7
6
0
-1
-2
-3
Delta G (eV)

Our driving force analysis assumes that the reorganization energies and electronic coupling factors for charge separation and charge recombination in these systems are the same. The validity of this assumption is currently an area of significant interest in electron-transfer research.[13d,14h,25] Available data regarding this issue from biological and synthetic donor-acceptor systems suggest that the driving force dependence for charge separation and recombination reactions can be described by the same thermal and electronic barriers; however, further investigation will be necessary to resolve these issues. In this light, the correlations between the experimental data and theoretical models in figures 4.12 to 4.14 are remarkable. From these plots it appears that rate data for the triplet and singlet photoinduced electron transfer reactions and charge recombination reactions in our molecules are adequately represented by the same electronic coupling and reorganization parameters.[32] At present we are particularly intrigued by the premise that the charge separation and recombination reactions in photoredox molecules may be controlled by different reorganization energies, electronic coupling matrix elements, and spin selection rules. An understanding of these factors is clearly important for designing redox systems that perform vectorial photoinduced charge separation. Experiments designed to address these issues are currently in progress in our laboratories.

Photophysics and Vectorial Electron Transfer: In addition to providing further evidence for inverted behavior, the quantum yield and lifetime data presented in this chapter also differentiate the photophyscial properties of bimolecular and intramolecular photoredox systems based on iridium d^8-d^8 complexes and pyridinium electron acceptors. Much like photoredox systems based on porphyrin electron donors, our iridium donor-acceptor compounds possess a low lying singlet and triplet redox active excited state. Due to the moderate rates for intersystem crossing in the porphyrin based compounds,[27] their primary photoredox reactions occur from their singlet excited states. This preferred singlet reactivity is found in synthetic donor-

acceptor systems and also in the photosynthetic reaction center. In contrast photoinduced electron transfer in redox systems based on inorganic chromophores largely involves their lowest lying high spin excited states. This apparent change in the excited state reactivities of the spin allowed and spin forbidden states is a direct consequence of the decreased fluorescence lifetimes and increased intersystem crossing rates characteristic of inorganic chromophores. In our earlier bimolecular electron transfer studies, we found that charge transfer occurred solely from the ^3B excited states of iridium A-frame complexes.[20,14a] However, much like photoredox systems containing porphyrin electron donors, photoinduced electron transfer in our intramolecular ET complexes is primarily a ^1B process. As seen in table 4.3, the intersystem crossing efficiencies for the donor-acceptor compounds are ≤0.25; for $Ir_2(Pz^*)_2(CO)_2(Ph_2POCH_2CH_2\text{-}4PhPy^+)_2$ intersystem crossing is essentially a negligible singlet deactivation pathway. Thus the initial charge separation reactions in these compounds occur with close to unit efficiency. The recent findings of Closs and Miller[14e], Wasielewski,[14h] Gust,[28] Dervan,[7] and Bolton[9] have suggested that one of the primary motives for linking two redox partners into a single molecular unit is to remove diffusion as the rate limiting step in electron transfer. Our results expand upon this notion by indicating that a covalent linkage between donor and acceptor can also allow higher energy, shorter lived excited states to be efficiently intercepted by rapid electron transfer processes. This concept clearly has implications with regard to photochemical energy storage and is discussed in this context below.

A second aspect of the photophysical behavior of the donor-acceptor complexes, which differentiates them from their bimolecular analogues, concerns charge recombination to form electronic excited states of the iridium dimer chromophore. In our bimolecular ET studies involving $[Ir_2(Pz)_2(COD)_2]$ no evidence for back electron transfer to form its triplet excited state was observed. In particular, values of k_{et}, determined from quantum yield and lifetime quenching experiments, were the same

within experimental error, indicating that charge recombination formed exclusively ground state iridium dimer products. In contrast, back electron transfer to form a ^3B d^8-d^8 excited state occurs in $Ir_2(Pz^*)_2(CO)_2(Ph_2POCH_2CH_2\text{-}Me_3Py^+)_2$. It is well known that in some reactions where $\Delta G^{o'}$ is greater than the energy of an electronic transition associated with the donor or acceptor, electron transfer leads to the formation of electronically excited products. For example, electrogenerated chemiluminescence has been observed in a number of inorganic redox systems,[29] most notably $Ru(Bipy)_3^{2+}$. In addition, back electron transfer to the special pair triplet state is a well characterized process in photosynthetic reaction centers that are missing their ubiquinone electron acceptors.[27] This particular process was most likely not observed in our bimolecular studies involving $[Ir_2(Pz)_2(COD)_2]$ because the charge transfer state, $[Ir_2(Pz)_2(COD)_2]^+/Py^{\bullet}$, is not energetically within k_bT of the triplet state.

In a highly efficient photochemical energy storage system a photoinduced charge separation must take place with a minimum loss of the captured photon energy and the charge separated state must be maintained long enough to allow bond forming reactions to occur. The realization of well defined molecular systems that execute vectorial charge transfer reactions is an extremely challenging area of current research. In the photosynthetic reaction centers of green plants, transmembrane electron transfer takes place on a picosecond timescale creating an excited state whose energy can be harnessed into chemical bonds (figure 4.15).[27] When all of the intermediate redox partners are in place, directional charge transfer occurs with near unit efficiency. An important kinetic feature of photosynthesis is that it achieves this high charge separation efficiency by sequentially coupling two very rapid electron-transfer processes. A primary photoredox reaction occurs directly from the excited special pair yielding a charge separated state ($^+P^-IQ_AQ_B$) that is approximately 950 cm^{-1} above the special pair triplet state. This transient CT state is transformed by a second rapid reaction into

Figure 4.15. A photophysical scheme for the photosynthetic reaction center in *Rhodopseudamonas viridis.* White arrows correspond to the charge separation pathway in this photoredox system.

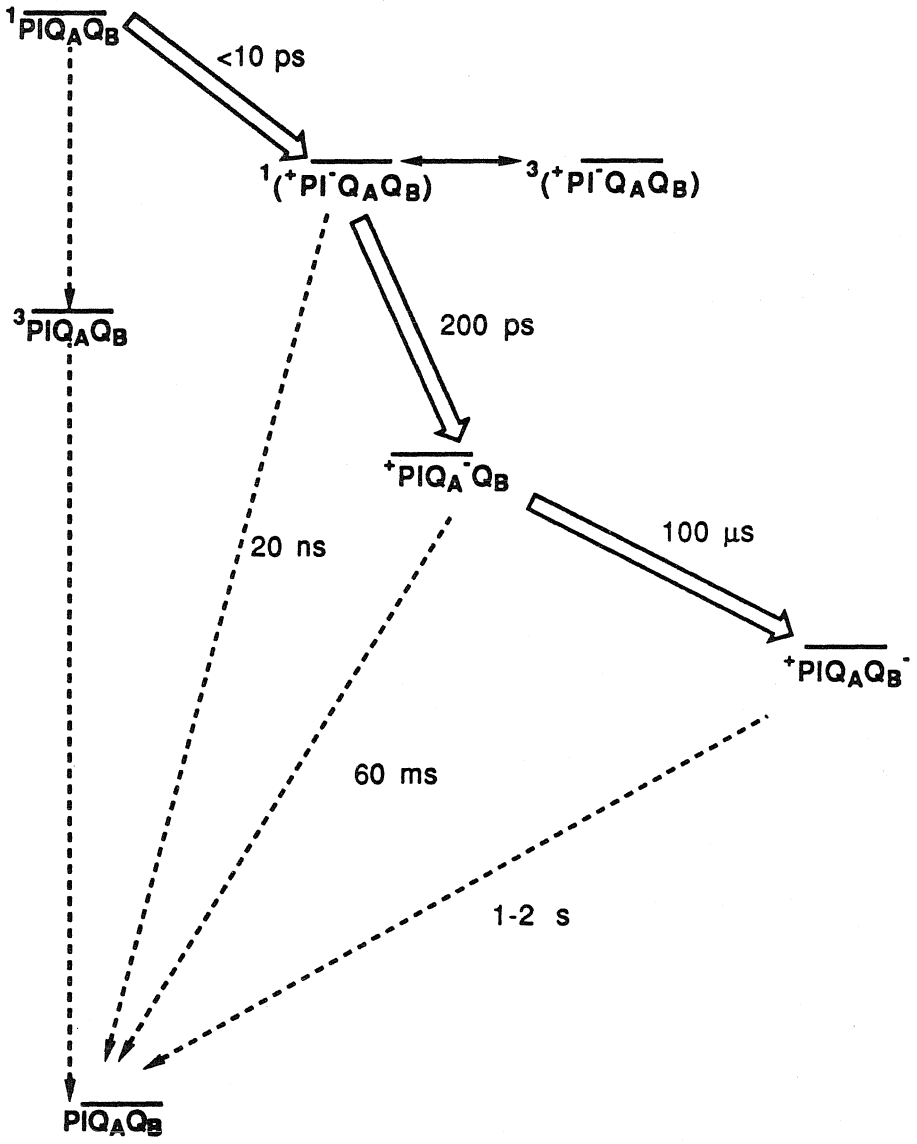
$^1\overline{PIQ_AQ_B}$
<10 ps
$^1(^+PI^-Q_AQ_B)$
$^3(^+PI^-Q_AQ_B)$
$^3\overline{PIQ_AQ_B}$
200 ps
$^+\overline{PIQ_A^-Q_B}$
20 ns
100 µs
$^+\overline{PIQ_AQ_B^-}$
60 ms
1-2 s
$\overline{PIQ_AQ_B}$

lower energy states that can interact with reaction center redox enzymes. An analogous two step approach has recently been employed by Gust and coworkers to produce long lived charge separated states in synthetic redox triads.[28] The large conversion efficiencies found in these naturally occurring and synthetic photoredox systems can be traced to their ability to rapidly create a substantial spatial separation between a hole and an electron. However, they utilize close to 50% of the total energy made available by their initial donor localized excited states to affect this separation .

It is intriguing to consider designing a synthetic photoredox system where a single high energy charge-transfer state is created and then directly utilized to drive bond forming chemical reactions. If efficient, such a system might surpass the photosynthetic reaction center as a light energy conversion device. To our knowledge this issue has not been directly addressed in any of the recent studies concerning synthetic donor-acceptor compounds. The iridium d^8-d^8 complexes reported here possess two important characteristics, which suggest that they might be utilized in this capacity. As mentioned earlier, the covalent linkage between the metal complex and pyridinium electron acceptors in these systems allows their more potent singlet excited states to be intercepted by rapid electron-transfer reactions. In addition, we have seen that due to the inverted behavior associated with their charge recombination reactions, these systems possess charge separation and recombination rates, which differ by close to three orders of magnitude. If these two features can be profitably combined, then a CT state with enhanced reactivity relative to the ^3B state in these systems might be available for subsequent bond forming reactions.

Rate constants for the charge separation (k_f) and charge recombination steps (k_{b1} and k_{b2}) in figure 4.16 were calculated as a function of the CT state energy (ΔG_{b2}) using λ=1.0 eV and H_{ab}=35 cm^{-1}. Results from these calculations reveal several important trends (table 4.5). First, the lifetime of the CT state increases slightly as a function of ΔG_{b2} and then decreases to near 100 ps. This trend arises from competition

between the parallel recombination processes k_{b1} and k_{b2}. If charge recombination to form the triplet state were not an active excited state process, the lifetime of the CT state would increase as a function of ΔG_{b2} to hundreds of nanoseconds, based on the values of k_{b2} predicted by our calculations. However, back electron transfer to form the ^3B state is known to be important in the photophysics of these complexes from earlier discussions regarding the emission properties of $Ir_2(Pz^*)_2(CO)_2(Ph_2POCH_2CH_2\text{-}Me_3Py^+)_2$ and will clearly decrease the lifetime of a high energy CT state. A second and somewhat more limiting trend concerns the lifetime of the ^1B state. As the driving force for singlet electron transfer decreases from 0.5 to 0.3 eV, the rate constant for this process decreases to well below the rate of intersystem crossing (10^{10} sec^{-1}). These changes in k_f are paralleled by a substantial decrease in the yield of formation of the CT state. From our calculations, the CT state systems cannot be generated efficiently from the metal localized ^1B state when $E_{CT}>0.1 + E_{triplet}$.

This analysis indicates that a single high energy, long lived CT state in our donor-acceptor complexes cannot be generated and maintained on the basis of driving force effects alone. Designing a photoredox system with a CT state between the triplet and singlet donor states will require the manipulation of additional electron-transfer parameters. Clearly, one possible avenue of investigation would be to utilize electronic coupling as a second means of controlling the rates of charge separation and recombination in these systems. We are currently investigating the factors that govern through bond ET reactions in these complexes. Our preliminary studies indicate that the singlet and triplet electron-transfer reactions in systems utilizing rigid aromatic spacers have very different distance dependencies. Research along these lines may lead to more efficient photoredox systems.[30]

Figure 4.16. A Kinetic scheme showing the rate processes important to directional electron transfer in the iridium d^8-d^8 donor-acceptor complexes.

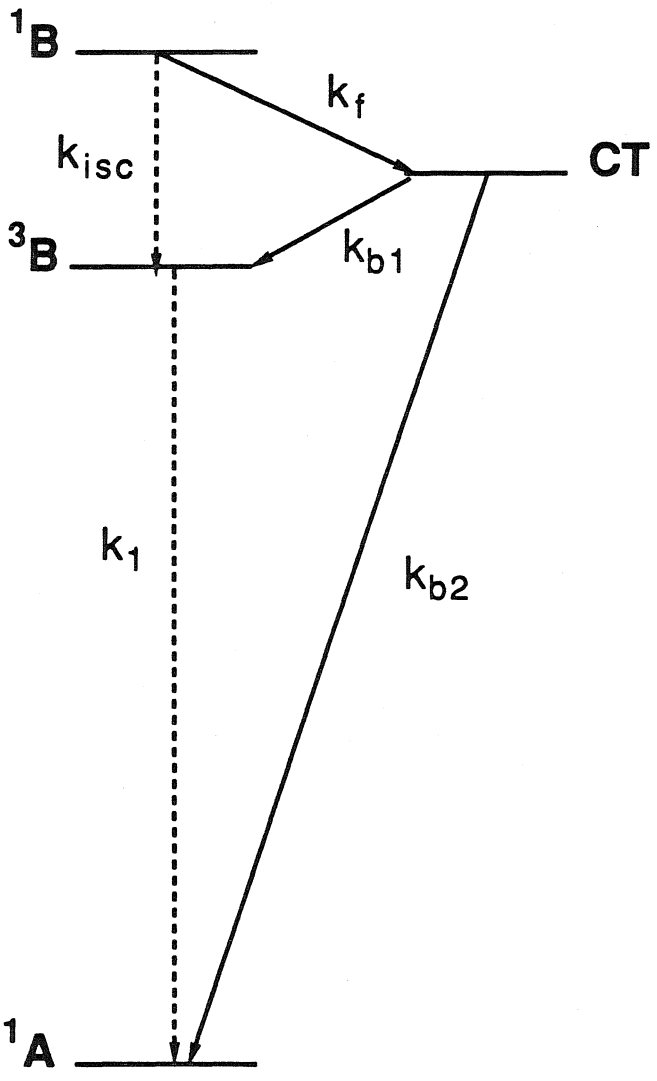
^1B
k_f
k_{isc}
CT
^3B
k_{b1}
k_1
k_{b2}
^1A

Table 4.5: Predicted Electron-Transfer Rates and Photophysical Parameters.

ΔG_f	ΔG_{b1}	ΔG_{b2}	k_f	k_{b1}	k_{b2}	τ_f	τ_{CT}	ϕ_{CT}
eV	eV	eV	sec^{-1} $x10^{10}$	sec^{-1} $x10^{9}$	sec^{-1} $x10^{7}$	ps	ns	-
-0.5	0	-2.0	2.4	0.003	5.7	30	17	0.70
-0.4	-0.1	-2.1	0.72	0.036	0.97	58	22	0.42
-0.3	-0.2	-2.2	0.16	0.28	0.16	86	3.6	0.14
-0.2	-0.3	-2.3	0.028	1.6	0.025	97	0.6	0.03
-0.1	-0.4	-2.4	0.004	7.2	0.003	100	0.1	0

Calculated for λ_i=0.5 eV, λ_o=0.5 eV, ω=400 cm^{-1}.

References

1. Nocera, D. G.; Winkler, J. R.; Yocom, K. M.; Bordignon, E.; Gray, H. B., *J. Amer. Chem. Soc.*, **1984**, *106*, 5145-5150.

2a. Winkler, J. R.; Netzel, T. L.; Creutz, C.; Sutin, N., *J. Amer. Chem. Soc.*, **1987**, *109*, 2381-2392.

b. Winkler, J. R.; Nocera, D. G.; Netzel, T. L., *J. Amer. Chem. Soc.*, **1986**, *108*, 4451-4458.

3a. Winkler, J. R.; Marshall, J. L.; Netzel, T. L.; Gray, H. B., *J. Amer. Chem. Soc.*, **1986**, *108*, 2263-2266.

b. Miskowski, V. M.; Nobinger, G. L.; Kliger, D. S.; Hammond, G. S.; Lewis N. S.; Mann, K. R.; Gray, H. B. , *J. Amer. Chem. Soc.*, **1978**, *100*, 485-488.

c. Milder, S. J.; Kliger, D. S.; Butler, L. G.; Gray, H. B., *J. Phys. Chem.*, **1986**, *90*, 5567-5570.

d. Che., C.-M.; Butler, L. G.; Gray, H. B., *J. Amer. Chem. Soc.*, **1981**, *103*, 7796-7797.

e. Dallinger, R. F.; Miskowski, V. M.; Gray, H. B.; Woodruff, W. H., *J. Amer. Chem. Soc.*, **1981**, *103*, 1595-1596.

f. Che. C.-M.; Butler, L. G.; Gray, H. B.; Crooks, R. M.; Woodruff, W. H., *J. Amer. Chem. Soc.*, **1983**, *105*, 5492-5494.

4a. Freed, K. F.; Jortner, J., *J. Chem. Phys.*, **1970**, *52*, 6272-6291.

b. Englman, R.; Jortner, J., *J. Mol. Phys.*, **1970**, *18*, 145-164.

5. Akiyama, K.; Kubota, S.; Ikegami, Y., *Chem. Lett.*, **1981**, 469-472.

6. Kosower, E. D.; Land, E. J.; Swallow, A. J., *J. Amer. Chem. Soc.*, **1972**, *94*, 986-987.

7. Leland, B. A.; Joran, A. H. D.; Felker, P. M.; Hopfield, J. J.; Zewail, A. H.; Dervan, P. B., *J. Phys. Chem.*, **1985**, *89*, 5571-5573.

8a. Lindsey, J. S.; Delany, J. K.; Manzerall, D. C.; Linschitz, H., *J. Amer. Chem. Soc.*, **1988**, *110*, 3610-3620.

b. Lisecki, M. A.; Mishra, P. K.; Bothner-By, A. A.; Lindsey, J. S., *J. Phys. Chem.*, **1988**, *92*, 3400-3403.

9. Siemiarczuk, A.; McIntosh, A. R.; Ho, T.F.; Stillman, M. J.; Roach, K. J.; Weedon, A. C.; Bolton, J. R.; Connolly, J. S., *J. Amer. Chem. Soc.*, **1983**, *105*, 7224-7230.

10a. Memming, R.; Hobs, K. J., *J. Phys. Chem.*, **1981**, *85*, 2771-2777.

b. Evers, F.; Memming, R.; Kobs, K.; Terrill, D. R., *J. Amer. Chem. Soc.*, **1983**, *105*, 5988-5995.

c. Birckner, E.; Partzold, R.; Kozmenko, M. V.; Kregmin, M. G., *Chem. Phys. Lett.*, **1983**, *96*, 38-42.

d. Karstens, T.; Kobs, K.; Memming, R.; Schroppel, F., *Chem. Phys. Lett.*, **1977**, *V*, 540-544.

11. Milder, S. J.; Kliger, D. S., *J. Phys. Chem.*, **1985**, *89*, 4170-4171.

12. Driving forces for ($d\pi p\sigma$) electron transfer would be greater than 2.0 eV in this complex making k_{et} approximately 10^8 sec^{-1}.

13. Zill, D. G., *"A First Course in Differential Equations with Applications"*, **1980**, Prindle, Weber, Schmidt, Boston, Mass.

14a. Gould, I. R.; Ege, D.; Mattes, S. L; Farid, S., *J. Amer. Chem. Soc.*, **1987**, *89*, 3675-3679.

b. Snadrini, D.; Maestri, M.; Belser, P.; von Zelewsky, A.; Balzani, V., *J. Phys. Chem.*, **1985**, *89*, 3675-3679.

c. Gunner, M. R.; Robertson, D. E.; Dutton, P. L., *J. Phys. Chem.*, **1986**, *90*, 3783-3795.

d. Meade, T. J.; Gray, H. B.; Winkler, J. R., *manuscript in preparation.*

e. Closs, G. L.; Miller, J. R., *Science*, **1988**, *240*, 440-447.

f. Miller, J. R.; Beitz, J. V.; Huddleston, R. K., *J. Amer. Chem. Soc.*, **1984**, *106*, 5057-5068.

g. McLendon, G., *Acc. Chem. Res.*, **1988**, *21*, 160-167.

h. Wasieleski, M. R.; Niemczyk, M. R.; Svec, W. A.; Pewitt, E. B., *J. Amer. Chem. Soc.*, **1985**, *107*, 1080-1082.

i. Elias, H.; Chou, M. H.; Winkler, J. R., *J. Amer. Chem. Soc.*, **1988**, *110*, P.

j. Meyer, T. J., *Prog. Inorg. Chem.*, **1984**, *30*, 389-440.

15a. Marcus, R. A.; Sutin, N., *Biochim. Biophys. Acta*, **1985**, *811*, 265-322.

b. Newton, M. D.; Sutin, N., *Ann. Rev. Phys. Chem.*, **1984**, *35*, 437-480.

c. Sutin, N., *Prog. Inorg. Chem.*, **1984**, *30*, 441-498.

d. Jortner, J., *Biochim. Biophys. Acta*, **1980**, *594*, 193-230.

16a. Marcus, R. A., *J. Chem. Phys.*, **1956**, *24*, 966-978.

b. Marcus, R. A., *J. Chem. Phys.*, **1957**, *26*, 867-871.

c. Marcus, R. A., *J. Chem. Phys.*, **1957**, *26*, 872-877.

d. Kestner, N. R.; Logan, J.; Jortner, J., *J. Phys. Chem.*, **1984**, *78*, 2148-2166.

e. Jortner, J., *J. Chem. Phys.*, **1976**, *64*, 4860-4867.

f. Efrima, S.; Bixon, M., *Chem. Phys.*, **1976**, *13*, 447-460.

g. Van Duyne, R. P.; Fischer, S. F., M., *Chem. Phys.*, **1974**, *5*, 183-197.

h. Jortner, J., *J. Amer. Chem. Soc.*, **1980**, *102*, 6676-6686.

17. Marcus, R. A.; Siders, P., *J. Phys. Chem.*, **1982**, *86*, 622-630.

18. Siders, P.; Marcus, R. A., *J. Amer. Chem. Soc.*, **1981**, *103*, 748-752.

19a. Kakitani, T.; Mataga, N., *Chem. Phys.*, **1985**, *93*, 381-397.

b. Kakitani, T.; Mataga, N., *J. Phys. Chem.*, **1985**, *89*, 4752-4757.

c. Kakitani, T.; Mataga, N., *J. Phys. Chem.*, **1985**, *89*, 8-10.

d. Kakitani, T.; Mataga, N., *J. Phys. Chem.*, **1986**, *90*, 993-995.

e. Kakitani, T.; Mataga, N., *J. Phys. Chem.*, **1985**, *91*, 6277-6285.

f. Hatano, Y.; Saito, M.; Kakitani, T.; Mataga, N., *J. Phys. Chem.*, **1988**, *92*, 1008-1010.

20. Marshall, J. L., *Ph. D. Dissertation*, **1987**, California Institute of Technology, Pasadena, California.

21a. Ohno, T.; Yoshimura, A.; Shioyama, H.; Mataga, N., *J. Phys. Chem.*, **1987**, *91*, 4365-4370.

b. Ohno, T.; Yoshimura, A.; Mataga, N., *J. Phys. Chem.*, **1986**, *90*, 3295-3297.

22a. Verhoven, J. W., *Pure & Appl. Chem.*, **1986**, *58*, 1285-1290.

b. Stiegman, A. E.; Miskowski, V. M.; Perry, J. W.; Coulter, D. R., *J. Amer. Chem. Soc.*, **1087**, *109*, 5884-5886.

23a. Brost, R. D.; Harrison, D. G.; Fjeldsted, D. O. K.; Stobart, S. R.; *submitted for publication.*

b. Coleman. A. W.; Eadie, D. T.; Stobart, S. R., *J. Amer. Chem. Soc.*, **1982**, *104*, 922-923.

c. Atwood, J. L.; Beveridge, K. A.; Bushnell, G. W.; Dixon, K. R.; Eadie, D. T.; Stobart, S. R.; Zaworotko, M. J., *J. Amer. Chem. Soc.*, **1984**, *23*, 4050-4057.

24. Nakamoto, K., *"Infrared and Raman Spectra of Inorganic Coordination Compounds,"* **1980**, John Wiley and Sons, New York.

25. Schmidt, J. A.; McIntosh, A. R.; Weedon, A. C.; Bolton, J. R.; Connolly, J. S.; Hurly, J. K.; Wasielewski, M. R., *J. Amer. Chem. Soc.*, **1988**, *110*, 1733-1740.

26. Kikuchi, K.; Kurabayashi, Y,; Kokubun, H.; Kaizer, Y.; Kobayashi, H., *J. Photochem. Photobio. A:Chem.*, **1988**, *45*, 261-263 and references therein.

27. Boxer, S. G., *Biochem. Biophys. Acta*, **1983**, *726*, 265-292.

28.a. Gust, D.; Moore, T. A.; Makings, L. R.; Liddell, P. A.; Nemeth, G. A.; Moore, A. L., *J. Amer. Chem. Soc.*, 1986, 108, 8028-8031.

b. Gust, D.; Moore, T. A.; Liddell, P. A.; Nemeth, G. A.; Makings, L. R. ;Moore, A. L.; Barrett, D.; Pessiki, P. J.; Bensasson, R. V.; Ronger, M.; Chachaty, C; De Schyver, F. C.;

Van der Anwerau, M.; Holzwarth, A. R.; Connolly, J. S., *J. Amer. Chem. Soc.*, 1987, 109, 846-856.

c. Moore, T. A.; Gust, D.; Mathis, P.; Mialocq, J.-C.; Chachaty, C.; Bensasson R. V.; Land, E. J.; Doizi, D.; Lidell, P. A.; Lehman, W. R.; Nemeth, G. A.; Moore, A. L., *Science*, **1984**, *307*, 630-632.

d. Liddel, P. A.; Barrett, D.; Makings, L. R.; Pessiki, P. J.; Gust, D.; Moore, T. A., *J. Amer. Chem. Soc.*, **1986**, *108*, 5350-5352.

e. Gust, A.; Moore, T. A.; Moore, A. L.; Makings, L. R.; Gilbert, R. S.; Ma, X.; Trier, T. T.; Gao, F., *J. Amer. Chem. Soc.*, **1988**, *110*, 7567-7569.

29. Kalyanasundaram, K., *Coord. Chem. Rev.*, **1982**, *46*, 159-244.

30. Farid, R. S.; Larson, W.; Gray, H. B., *research in progress.*

31. Rigorously, τ=0.7/k. However, making this minor correction does not change our values of k_{et} outside their experimental uncertainties.

32. This result suggests that electron transfer must occur by a predominantly through space mechanism. Based on current theories, H_{ab}^{f} should not equal H_{ab}^{b} if a through bond mechanism is active.

33. Kinetic data were fit to classical and semiclassical models for k_{et} on a Macintosh Plus PC using the program "INVERT" developed by Samir Farid and Ian Gould at the Eastman Kodak Company.

Appendix

Structure Factor Tables

Data appears in the following format:

h k

l F_{obs} F_{calc} $\Delta F^2/\sigma_{F2}$

-11 0 l

2	982	975	2
4	-317	-53	-25
6	902	-872	8
8	1433	1447	-4
10	1798	-1801	0
12	1758	1767	-3
14	1522	-1536	-4
16	1222	1262	-13
18	582	-590	-1
20	498	-516	-3

-10 0 l

2	1664	-1588	26
4	-186	-287	-29
6	1247	1285	-13
8	374	-299	11
10	1193	1214	-7
12	1419	-1402	5
14	551	513	8
16	851	-824	7
18	-228	143	-17
20	374	462	-16
22	499	-469	6
24	1120	1135	-4
26	593	-563	6

-9 0 l

2	-225	-182	-23
4	972	-956	5
6	1895	1883	4
8	2585	-2550	11
10	2704	2687	5
12	2144	-2194	-17
14	1415	1443	-10
16	554	-633	-20
18	383	-314	11
20	1305	1309	-1
22	1858	-1889	-11
24	2188	2125	20
26	2034	-1969	21
28	1276	1262	4
30	665	-715	-12
32	-214	75	-10

-8 0 l

2	399	519	-30
4	1521	1603	-34
6	1488	-1634	-61
8	3000	2930	21
10	3226	-3167	17
12	1332	1345	-4
14	971	-937	12
16	970	-1019	-18
18	1541	1556	-5
20	1971	-2014	-15
22	2018	1985	11
24	1341	-1358	-6
26	526	627	-24
28	1078	-1205	-43
30	257	434	-26
32	-256	248	-28
34	390	-599	39

-7 0 l

2	676	-681	-1
4	1835	1800	14
6	2166	-2230	-25
8	2230	2285	-21
10	2183	-2177	2
12	1488	1480	3
14	551	-606	-17
16	237	-388	-28
18	1660	1672	-4
20	2155	-2192	-13
22	1953	1975	-8
24	1795	-1818	-8
26	1449	1492	-15
28	326	-469	-25
30	613	-585	6
32	1113	1124	-3
34	1307	-1387	-26
36	1544	1586	-13
38	1582	-1590	-2

-6 0 l

2	511	566	-20
4	855	-886	-14
6	3234	3198	11
8	2426	-2433	-2
10	4002	3924	20
12	2096	-1946	58
14	387	-439	-14
16	2307	2291	6
18	1873	-1982	-45
20	3639	3641	0
22	2354	-2459	-38
24	2449	2470	-7
26	546	-582	-9
28	1210	-1201	3
30	498	649	-36
32	1089	-1182	-32
34	1394	1488	-32
36	1334	-1229	32
38	1197	1233	-11
40	1674	-1628	13

-5 0 l

2	811	874	-34
4	1667	-1704	-17
6	2416	2438	-8
8	2332	-2378	-18
10	1321	1331	-4
12	-136	182	-23
14	959	-1049	-44
16	1365	1363	1
18	2259	-2271	-4
20	2706	2719	-4
22	2008	-2003	1
24	1206	1183	8
26	756	-778	-6
28	-271	-37	-19
30	1097	1081	5
32	1404	-1533	-46
34	1377	1455	-26
36	1197	-1188	2
38	868	839	7
40	-15	-430	-35
42	-400	-27	-30

-4 0 l

2	3242	-3265	-7
4	3014	2950	21
6	3699	-3590	31
8	466	467	0
10	1643	-1633	4
12	232	-192	7
14	969	954	7
16	5837	-5725	21
18	4236	4306	-23
20	1614	-1776	-74
22	2600	2686	-30
24	1591	-1601	-4
26	217	-348	-20
28	1856	1839	6
30	2239	-2355	-40
32	2452	2400	16
34	1847	-1727	38
36	1478	1493	-4
38	1540	-1485	17
40	1139	1113	7
42	-232	346	-31

-3 0 l

2	501	612	-62
4	463	-506	-21
6	118	-113	0
8	1238	1261	-13
10	1042	-1059	-9
12	427	-431	-1
14	1317	1339	-11
16	1237	-1273	-18
18	1303	1325	-10
20	1299	-1306	-3
22	940	910	11
24	300	-320	-3
26	388	-472	-19
28	1245	1220	9
30	1486	-1497	-3
32	1329	1321	2
34	1054	-1081	-8
36	924	893	8
38	665	-662	0
40	-436	203	-46
42	-388	72	-30
44	256	-568	-43

-2 0 l

2	5531	5521	2
4	2593	-2508	35
6	1028	974	37
8	4677	-4593	20
10	2577	-2479	38
12	1031	1002	15
14	2223	-2197	10
16	4586	4548	9
18	4823	-4815	1
20	3921	3872	12
22	1870	-1800	27
24	527	550	-6
26	1457	1490	-13
28	4766	-4646	25
30	4217	4143	17
32	3887	-3683	49
34	1651	1626	8
36	1134	-1253	-37
38	-317	-285	-36
40	-366	70	-27
42	694	-604	17
44	1749	1742	2

-1 0 l

4	618	-686	-62
6	258	320	-36
8	128	-5	13
10	140	54	10
12	84	176	-11
14	949	-875	34
16	1324	1231	42
18	703	-713	-3
20	-188	245	-33
22	-101	-74	-5
24	-248	-80	-20
26	366	447	-16
28	931	-897	10
30	1343	1219	41
32	639	-678	-9
34	-256	261	-28
36	-318	175	-27
38	-234	-164	-16
40	403	312	11
42	525	-517	1
44	319	362	-4

0 0 l

6	3516	-3428	30
8	4868	-4867	0
10	4826	4686	35
12	4228	-4088	39
14	5793	5678	24
16	5075	-4950	30
18	2808	2806	0
20	602	-662	-29
22	1160	1076	44
24	899	974	-40
26	2592	-2578	5
28	4854	4841	3
30	2937	-2829	38
32	3141	3033	36
34	1220	-1352	-60
36	449	-686	-69
38	810	815	-1
40	2168	-2027	53
42	2394	2474	-30
44	1707	-1579	48

1 0 l

4	665	-725	-53
6	785	843	-45
8	559	-554	3
10	-113	112	-13
12	250	155	15
14	138	-128	0
16	-179	120	-16
18	279	-338	-11
20	84	335	-34
22	208	-341	-21
24	-339	160	-42
26	-413	94	-51
28	-388	-161	-45
30	-237	-217	-23
32	-359	-73	-30
34	-316	234	-32
36	-423	-40	-38
38	-408	79	-35
40	-349	11	-24
42	-291	-127	-18

2 0 l

0	5874	-5905	-6
2	3163	3135	9
4	656	-634	16
6	5307	-5258	10
8	3226	3232	-1
10	3419	-3504	-26
12	4981	5013	-7
14	4248	-4186	15
16	2980	2955	8
18	362	-328	7
20	1186	-1075	45
22	2150	2156	-2
24	1084	-1145	-23
26	2229	2178	17
28	2871	-2855	4
30	2644	2700	-17
32	1516	-1561	-14
34	411	-228	-46
36	173	413	-26
38	2326	-2242	24
40	2750	2775	-6
42	1629	-1517	32

3 0 l

0	928	-1015	-56
2	605	675	-40
4	146	245	-22

6	285	-359	-24	24	2158	-2087	23	4	1766	-1655	36	20	435	-453	-3				
8	449	-411	14	26	922	953	-9	6	1524	1380	46	21	695	799	-30				
10	1253	1246	3	28	280	-539	-43	8	619	-650	-7	22	675	683	-1				
12	1377	-1367	5	30	-205	-274	-24	10	-315	122	-26	23	371	-530	-31				
14	1172	1170	0	32	-217	340	-32					24	526	-540	-3				
16	942	-956	-6	34	1308	-1267	11		-11	1	1	25	1166	1130	12				
18	218	179	5									26	209	232	-2				
20	-273	-37	-27		7	0	1	1	1045	-1158	-38	27	928	-948	-6				
22	572	-584	-3					2	125	43	3	28	155	-339	-20				
24	888	838	17	0	350	-341	2	3	586	568	4	29	-49	350	-27				
26	678	-627	13	2	866	889	-9	4	-235	-84	-15	30	-218	-64	-11				
28	-213	302	-31	4	1435	-1471	-15	5	199	326	-15	31	600	-721	-28				
30	-421	-63	-41	6	2035	2180	-58	6	-273	80	-20	32	-61	341	-24				
32	-70	-263	-14	8	2493	-2498	-1	7	553	-583	-6								
34	-95	362	-26	10	1777	1759	6	8	-84	-204	-11		-8	1	1				
36	131	-206	-4	12	838	-866	-10	9	817	820	0								
38	-71	364	-25	14	-334	116	-37	10	177	7	7	1	-190	264	-32				
40	271	-352	-8	16	517	583	-17	11	1058	-1067	-2	2	-154	-245	-25				
				18	1133	-1143	-3	12	-260	-114	-19	3	952	998	-19				
	4	0	1	20	1290	1320	-7	13	476	484	-1	4	457	485	-7				
				22	1620	-1605	5	14	-64	-14	0	5	1957	-1947	3				
0	4975	4795	39	24	1360	1344	5	15	477	-692	-51	6	551	-485	17				
2	589	-551	17	26	822	-977	-46	16	132	-159	-1	7	2474	2446	9				
4	1574	-1604	-15	28	244	524	-44	17	111	298	-16	8	743	600	43				
6	2022	1997	10	30	-353	94	-28	18	-154	12	-5	9	2495	-2510	-5				
8	4291	-4336	-11	32	274	-354	-9	19	-110	66	-3	10	853	-728	41				
10	5116	5004	24									11	1968	1986	-6				
12	4903	-4953	-11		8	0	1		-10	1	1	12	589	630	-12				
14	358	91	45									13	1133	-1158	-9				
16	3352	-3365	-4	0	961	-978	-6	1	1074	-1068	1	14	304	-389	-16				
18	1719	-1653	26	2	410	491	-20	2	-116	-126	-7	15	385	404	-3				
20	1611	1643	-13	4	1406	-1419	-4	3	-272	129	-23	16	-286	84	-26				
22	2594	-2567	9	6	2579	2503	25	4	-169	-31	-7	17	325	443	-23				
24	2865	2795	21	8	1671	-1683	-4	5	1105	1084	7	18	220	138	7				
26	2113	-2226	-40	10	1292	1268	9	6	276	306	-4	19	1410	-1421	-4				
28	2011	1990	7	12	832	-864	-10	7	1615	-1641	-9	20	485	-294	34				
30	1624	-1717	-31	14	-310	-209	-37	8	703	-559	36	21	2020	2034	-4				
32	452	625	-34	16	439	449	-2	9	1790	1837	-17	22	628	428	44				
34	-196	321	-27	18	1260	-1266	-2	10	937	775	47	23	1900	-1946	-16				
36	1590	-1627	-11	20	1581	1572	2	11	2166	-2116	16	24	688	-501	44				
38	2108	2072	10	22	1902	-1856	15	12	1050	-834	65	25	1512	1510	0				
				24	2043	2033	3	13	1840	1812	9	26	523	500	4				
	5	0	1	26	507	-714	-47	14	725	624	26	27	1145	-1143	0				
				28	-402	-88	-36	15	1235	-1183	17	28	250	-145	9				
0	-132	-155	-20					16	273	-377	-15	29	687	664	5				
2	336	-401	-21		9	0	1	17	421	501	-16	30	-337	-51	-27				
4	726	751	-12					18	-147	114	-8	31	-291	123	-23				
6	1460	-1487	-13	0	1217	1185	12	19	448	482	-6	32	-404	67	-39				
8	1778	1819	-18	2	1742	-1746	-1	20	248	245	0	33	866	-940	-21				
10	1406	-1410	-1	4	1957	1926	11	21	1247	-1268	-7	34	458	-150	35				
12	1126	1159	-15	6	1899	-1906	-2	22	583	-470	23	35	1346	1381	-11				
14	-116	-306	-40	8	1534	1535	0	23	1662	1674	-3								
16	-182	164	-21	10	859	-873	-4	24	778	565	49		-7	1	1				
18	428	450	-5	12	-312	-45	-25	25	1887	-1832	17								
20	902	-920	-6	14	648	638	2	26	783	-557	50	1	555	-625	-24				
22	1431	1479	-18	16	909	-986	-25	27	1777	1735	13	2	760	757	1				
24	1630	-1659	-10	18	1363	1407	-14					3	1426	-1371	23				
26	1455	1491	-12	20	1515	-1525	-3		-9	1	1	4	1205	-1147	24				
28	815	-863	-13	22	1326	1233	28					5	2011	2060	-19				
30	-300	299	-39	24	810	-798	3	1	1414	1367	17	6	1427	1499	-32				
32	-377	183	-37					2	-303	152	-33	7	2715	-2743	-9				
34	455	-650	-38		10	0	1	3	158	336	-23	8	1092	-1040	21				
36	767	872	-25					4	681	676	1	9	2822	2887	-22				
				0	1017	929	28	5	803	-793	3	10	486	381	27				
	6	0	1	2	1544	-1608	-23	6	553	-550	0	11	2668	-2711	-14				
				4	1381	1359	7	7	2010	2033	-8	12	116	175	-5				
0	1094	-1129	-16	6	1067	-1153	-30	8	508	525	-3	13	782	839	-22				
2	749	-658	40	8	585	625	-9	9	1994	-1988	2	14	79	-195	-10				
4	1182	1196	-6	10	290	-405	-18	10	265	-59	17	15	314	-263	8				
6	1051	-1092	-19	12	483	-635	-34	11	1522	1507	5	16	446	424	5				
8	3555	3592	-10	14	-119	411	-42	12	324	279	6	17	1274	-1291	-6				
10	2467	-2512	-16	16	442	-490	-8	13	154	-244	-9	18	282	-292	-1				
12	2936	2923	4	18	1130	1178	-14	14	-65	-291	-23	19	2529	2592	-21				
14	1130	-1170	-16					15	-294	-72	-24	20	901	890	3				
16	503	-506	0		11	0	1	16	-302	-103	-27	21	2077	-2093	-5				
18	2277	2314	-12					17	-348	159	-39	22	709	-745	-11				
20	1494	-1516	-8	0	1461	-1460	0	18	-225	35	-13	23	1580	1654	-28				
22	3494	3559	-17	2	1722	1675	15	19	867	-844	6	24	530	576	-11				

25	1230	-1304	-27
26	183	-188	0
27	829	840	-3
28	-149	283	-24
29	63	270	-16
30	-314	-54	-24
31	-71	-298	-21
32	384	-449	-11
33	301	453	-23
34	422	562	-27
35	823	-821	0
36	511	-601	-18
37	1663	1633	9
38	508	315	27

-6 1 1

1	765	807	-19
2	679	702	-10
3	1613	-1646	-15
4	961	-1008	-23
5	1945	2026	-35
6	859	840	9
7	2023	-2081	-24
8	649	-579	27
9	1807	1870	-27
10	411	325	22
11	1147	-1154	-3
12	-126	-26	-6
13	-112	82	-7
14	-158	-50	-10
15	790	812	-9
16	236	233	0
17	1290	-1353	-27
18	677	-666	3
19	1747	1790	-17
20	937	790	52
21	2156	-2135	7
22	823	-715	35
23	2117	2095	8
24	644	552	24
25	1221	-1253	-12
26	566	-536	7
27	-236	206	-25
28	226	294	-8
29	400	520	-24
30	76	256	-13
31	922	-978	-17
32	473	-334	22
33	1203	1236	-10
34	508	312	30
35	1470	-1482	-4
36	594	-433	29
37	1297	1295	0
38	489	382	16
39	971	-989	-4
40	-117	-192	-9

-5 1 1

1	2102	-2032	29
2	772	-693	37
3	2953	2969	-5
4	1036	988	24
5	2030	-1989	17
6	1622	-1634	-5
7	2855	2934	-28
8	551	539	4
9	3096	-3094	0
10	635	-578	23
11	1440	1393	22
12	627	-500	48
13	930	839	41
14	259	225	6
15	1594	-1525	30
16	1020	-980	18
17	1226	1340	-54
18	1097	1065	14
19	4258	-4308	-12
20	798	-656	50
21	3384	3433	-14
22	994	950	17
23	1471	-1527	-23
24	836	-822	4
25	1227	1220	2
26	-191	-79	-11
27	229	-381	-23
28	-266	-33	-19
29	1938	-1836	35
30	380	-320	9
31	1470	1524	-19
32	713	777	-17
33	1583	-1620	-12
34	918	-940	-6
35	1449	1508	-19
36	961	932	8
37	1371	-1482	-36
38	386	-397	-1
39	1067	1122	-16
40	-244	34	-11
41	476	-630	-28
42	315	461	-19

-4 1 1

1	1089	-1086	2
2	1456	-1517	-33
3	1580	1590	-5
4	1079	1136	-33
5	1654	-1728	-38
6	517	-588	-32
7	1078	1138	-33
8	147	168	-3
9	452	-475	-9
10	128	197	-10
11	-247	94	-35
12	638	-671	-16
13	552	582	-12
14	756	770	-6
15	1516	-1532	-7
16	379	-208	39
17	2088	2098	-3
18	316	241	15
19	1702	-1793	-40
20	578	-530	16
21	1238	1241	-1
22	237	215	3
23	884	-876	3
24	-89	-117	-6
25	465	520	-14
26	-247	142	-23
27	455	487	-7
28	-105	-66	-4
29	1168	-1166	0
30	392	1	34
31	1393	1448	-19
32	456	280	26
33	1305	-1349	-15
34	461	-339	18
35	1115	1082	10
36	581	524	11
37	867	-885	-4
38	415	-484	-11
39	477	578	-18
40	-348	118	-26
41	-378	-97	-29
42	-513	-47	-51
43	285	-505	-28

-3 1 1

1	7362	7334	4
2	1150	-1094	33
3	2908	-2861	17
4	1723	-1740	-9
5	550	335	89
6	1478	1483	-2
7	1863	-1900	-18
8	1264	-1244	11
9	3102	3052	17
10	1003	-967	19
11	1563	-1483	39
12	842	819	11
13	2512	-2396	44
14	76	-78	0
15	3294	3300	-1
16	2223	2189	13
17	2745	-2798	-18
18	968	-979	-5
19	5364	5359	1
20	480	531	-17
21	2685	-2750	-22
22	523	-498	7
23	3033	2914	36
24	366	-424	-13
25	-193	-302	-40
26	299	227	10
27	1914	-1863	18
28	817	-737	24
29	2984	2987	0
30	1229	982	76
31	2875	-2830	13
32	1304	-1243	20
33	2574	2556	5
34	1125	1144	-6
35	1821	-1842	-6
36	974	-937	10
37	1526	1456	21
38	278	307	-3
39	1220	-1154	18
40	-320	81	-20
41	-264	-229	-22
42	-364	-454	-64
43	785	896	-26
44	465	432	3

-2 1 1

1	1056	1191	-107
2	196	110	26
3	952	-1083	-105
4	128	111	3
5	794	889	-74
6	516	-557	-27
7	698	-790	-67
8	341	293	18
9	-240	2	-34
10	294	327	-10
11	566	601	-17
12	161	-223	-11
13	491	-599	-45
14	129	-170	-5
15	815	815	0
16	381	354	7
17	1338	-1354	-7
18	372	-385	-3
19	1039	1101	-29
20	405	357	12
21	882	-877	2
22	323	-397	-16
23	223	280	-8
24	-192	127	-16
25	-128	223	-19
26	-194	-58	-11
27	771	-788	-5
28	258	-110	13
29	1248	1269	-7
30	318	237	9
31	1262	-1247	4
32	471	-323	22
33	914	911	0
34	425	585	-30
35	-101	-331	-23
36	273	-467	-27
37	-395	-81	-33
38	-143	436	-40
39	-300	120	-20
40	-416	-40	-34
41	169	-345	-16
42	-156	-263	-17
43	-249	405	-41
44	-449	67	-39

-1 1 1

1	6402	-6548	26
2	1031	-995	28
3	5421	5390	6
4	1876	1904	-15
5	2024	-1966	29
6	2456	-2450	2
7	803	-808	-3
8	2875	2920	-17
9	478	456	11
10	1273	1258	8
11	313	-222	21
12	1917	-1886	14
13	3749	3617	36
14	432	439	-2
15	6916	-6717	32
16	1529	-1534	-2
17	4236	4157	19
18	2131	2098	13
19	3011	-3008	0
20	883	-797	33
21	1737	1755	-7
22	512	522	-2
23	638	-703	-21
24	680	666	4
25	1580	-1559	8
26	927	-803	41
27	3059	2921	40
28	1686	1528	115
29	4487	-4409	17
30	1437	-958	138
31	4865	4809	11
32	1030	639	97
33	2261	-2241	6
34	651	-697	-10
35	580	757	-41
36	-421	386	-69
37	-256	-351	-37
38	359	471	-16
39	1445	-1463	-5
40	572	-527	36
41	2187	2075	32
42	691	666	5
43	1447	-1471	-7
44	797	-753	9

0 1 1

4	66	-17	4
5	215	210	2
6	471	-479	-6
7	266	-241	12
8	531	551	-15
9	364	351	6
10	326	-254	27
11	527	-508	9
12	-219	144	-39
13	331	306	7
14	-171	80	-18
15	354	-299	16
16	8	-289	-39
17	-270	8	-36
18	469	531	-25
19	-296	42	-44
20	410	-500	-34
21	-261	-54	-33
22	-248	194	-45
23	-359	45	-60

24	-369	-76	-63	7	117	103	1	39	2335	-2245	25	29	941	1008	-20
25	-318	-138	-50	8	549	-613	-32	40	939	-654	59	30	-283	96	-19
26	-299	1	-35	9	296	349	-16	41	2282	2258	7	31	-358	-231	-39
27	329	402	-18	10	473	509	-14					32	-338	18	-24
28	-251	77	-24	11	379	-456	-26		4	1	1	33	-214	-345	-33
29	423	-533	-32	12	243	-306	-14					34	-320	-251	-33
30	290	-486	-46	13	916	928	-5	0	846	-898	-29	35	750	787	-8
31	321	451	-29	14	323	398	-20	1	-173	36	-16	36	361	381	-2
32	180	384	-34	15	707	-726	-7	2	251	-337	-23	37	1854	-1704	43
33	-319	-160	-39	16	-234	-81	-25	3	635	635	0				
34	-237	-324	-47	17	571	628	-21	4	911	983	-40		6	1	1
35	-414	40	-52	18	-211	-150	-25	5	918	-944	-13				
36	126	449	-51	19	525	-573	-15	6	1089	-1155	-36	0	-195	13	-16
37	-343	211	-46	20	-56	222	-17	7	960	970	-5	1	182	287	-20
38	-300	-27	-25	21	-283	134	-33	8	730	792	-31	2	676	702	-10
39	-105	-427	-52	22	-199	-278	-37	9	1294	-1320	-13	3	1204	-1208	-2
40	-340	-100	-35	23	-267	309	-51	10	619	-647	-12	4	1138	-1126	5
41	-366	202	-48	24	-348	-117	-40	11	1299	1265	16	5	1620	1638	-7
42	-291	76	-24	25	279	-429	-27	12	484	508	-8	6	1188	1221	-15
43	-119	-287	-24	26	-137	262	-22	13	952	955	-1	7	1989	-1992	-1
44	-254	-201	-26	27	291	387	-14	14	115	-119	0	8	976	-916	26
				28	-386	-47	-36	15	658	673	-6	9	1959	1952	2
	1	1	1	29	-347	-208	-37	16	-88	-23	-3	10	463	458	1
				30	-346	30	-26	17	-146	-252	-31	11	1531	-1551	-8
0	2438	-2460	-10	31	-388	25	-33	18	604	662	-20	12	419	-374	10
1	7055	7184	-21	32	-466	-200	-57	19	454	-452	0	13	1173	1189	-6
2	568	543	20	33	-402	172	-40	20	921	-958	-15	14	-201	-23	-13
3	5000	-5076	-17	34	-349	90	-26	21	802	786	5	15	232	-331	-16
4	2626	-2746	-51	35	-373	105	-30	22	815	792	7	16	450	495	-11
5	1492	1567	-47	36	-474	138	-51	23	1039	-1074	-13	17	296	-377	-14
6	878	878	0	37	-375	119	-31	24	488	-558	-16	18	442	-563	-30
7	961	-970	-5	38	-282	63	-16	25	1089	1143	-19	19	722	724	0
8	1422	-1390	18	39	-237	-104	-12	26	277	265	1	20	525	506	4
9	6548	-6683	-23	40	-410	56	-34	27	781	-824	-12	21	1461	-1454	2
10	1456	-1459	-1	41	-269	75	-14	28	-338	9	-26	22	653	-611	10
11	2531	2540	-3	42	-479	-147	-49	29	258	391	-18	23	1605	1605	0
12	1235	1198	18					30	-348	-134	-30	24	434	356	13
13	5533	-5587	-10		3	1	1	31	-463	16	-48	25	1499	-1498	0
14	678	-651	10					32	-211	344	-33	26	201	-255	-5
15	2498	2527	-10	0	895	-940	-28	33	-228	-303	-28	27	992	1070	-24
16	1871	1832	16	1	1969	-1852	55	34	465	-569	-19	28	164	265	-9
17	1809	-1861	-22	2	253	-211	11	35	408	498	-14	29	489	-609	-25
18	474	-564	-28	3	2034	1978	26	36	292	446	-20	30	-367	-114	-32
19	650	782	-50	4	184	-190	-1	37	400	-495	-14	31	-397	-68	-35
20	393	505	-29	5	1598	1627	-15	38	165	-271	-8	32	-436	-7	-41
21	256	-222	4	6	623	-681	-30	39	452	414	5	33	414	524	-18
22	-269	-93	-25	7	1135	-1152	-9					34	-251	222	-21
23	426	-582	-41	8	1225	-1195	15		5	1	1	35	820	-789	7
24	471	-421	11	9	5804	5879	-14								
25	1882	1846	12	10	1515	1506	4	0	311	309	0		7	1	1
26	659	673	-3	11	2244	-2297	-22	1	1685	1595	41				
27	2117	-2209	-32	12	1844	-1832	5	2	846	-860	-6	0	96	169	-7
28	1320	-1179	47	13	4758	4750	1	3	1013	-1021	-4	1	964	945	8
29	3266	3307	-11	14	413	444	-9	4	473	466	2	2	138	338	-33
30	809	183	107	15	3504	-3314	54	5	1791	-1836	-20	3	1528	-1506	9
31	3130	-3175	-12	16	1029	-1003	11	6	655	-687	-14	4	380	-343	8
32	710	-649	14	17	447	508	-19	7	3879	3797	22	5	1305	1364	-25
33	873	999	-37	18	136	361	-39	8	1052	1023	13	6	826	855	-11
34	417	392	3	19	476	598	-39	9	5223	-5037	50	7	2470	-2401	24
35	242	-510	-38	20	385	377	1	10	1010	-982	13	8	851	-828	8
36	-235	235	-22	21	843	-951	-43	11	2622	2580	14	9	2657	2604	17
37	1493	-1581	-28	22	1028	-1061	-13	12	1518	1524	-2	10	414	434	-4
38	422	-88	30	23	2741	2719	7	13	3002	-2991	3	11	1471	-1506	-14
39	1817	1821	-1	24	800	810	-3	14	346	282	13	12	510	-587	-21
40	799	808	-2	25	2879	-2783	29	15	1244	1243	0	13	827	863	-12
41	1960	-1958	0	26	1152	-1013	45	16	856	816	15	14	134	-181	-4
42	876	-764	25	27	2692	2628	19	17	569	695	-43	15	364	-484	-26
43	1996	2052	-16	28	761	610	37	18	-175	357	-51	16	-40	393	-42
				29	2192	-2124	22	19	1592	-1596	-1	17	1247	-1221	9
	2	1	1	30	-151	-275	-21	20	368	-367	0	18	553	-527	6
				31	1620	1576	14	21	2837	2894	-18	19	1787	1696	31
0	152	-31	22	32	-316	-92	-22	22	666	716	-14	20	708	655	14
1	874	-961	-70	33	184	-434	-29	23	2218	-2193	8	21	3289	-3242	13
2	108	98	1	34	-325	125	-24	24	996	-1008	-3	22	740	-657	21
3	732	792	-47	35	618	-743	-27	25	2527	2489	12	23	2405	2306	31
4	663	-726	-46	36	405	-220	20	26	702	660	10	24	809	705	27
5	153	-107	9	37	2091	2109	-5	27	1226	-1238	-3	25	1756	-1691	21
6	1030	1104	-49	38	884	668	46	28	370	-372	0	26	315	-370	-7

27	-262	174	-21
28	-242	152	-17
29	-149	285	-21
30	-324	232	-33
31	1350	-1312	11
32	-160	-211	-13

8 1 1

0	-317	130	-37
1	923	-907	6
2	283	-332	-8
3	1533	1498	13
4	572	512	15
5	2068	-2075	-2
6	673	-567	30
7	1938	1965	-9
8	675	527	39
9	1408	-1452	-17
10	390	-366	4
11	775	859	-28
12	156	96	3
13	-316	-14	-27
14	-155	120	-9
15	726	-773	-14
16	409	-397	2
17	1378	1323	19
18	615	583	7
19	1576	-1522	18
20	605	-443	33
21	1552	1556	-1
22	456	311	22
23	1171	-1197	-8
24	178	-318	-14
25	743	755	-3
26	-382	182	-40
27	-357	-55	-28
28	-456	-15	-46

9 1 1

0	196	303	-14
1	1470	-1467	1
2	456	-452	0
3	1441	1484	-16
4	658	694	-10
5	1280	-1216	23
6	830	-860	-9
7	1125	1200	-28
8	518	556	-9
9	1035	-1113	-27
10	515	-552	-8
11	348	365	-2
12	-283	176	-28
13	-324	61	-27
14	-228	43	-13
15	837	-833	1
16	-87	-131	-5
17	1059	1071	-4
18	360	389	-4
19	990	-1018	-9
20	406	-342	9
21	1769	1827	-19
22	182	174	0
23	688	-794	-26
24	499	-547	-9

10 1 1

0	441	-295	24
1	1405	1391	4
2	631	462	37
3	1662	-1674	-4
4	629	-510	27
5	1792	1788	1
6	703	561	34
7	1356	-1398	-14
8	459	-377	14
9	923	859	19
10	62	194	-7
11	-107	-182	-10
12	-338	66	-29
13	474	-511	-7
14	108	-296	-17
15	965	959	1
16	462	320	22
17	1362	-1272	28
18	512	-369	23

11 1 1

0	176	-250	-7
1	872	911	-11
2	387	248	19
3	833	-880	-13
4	281	22	17
5	940	980	-12
6	338	337	0
7	-286	-158	-24
8	-233	-253	-27
9	-258	-114	-18
10	-311	167	-28

-11 2 1

1	766	-724	11
2	770	861	-26
3	388	401	-2
4	-237	-137	-18
5	-125	101	-6
6	483	-550	-14
7	485	-476	1
8	1042	1015	8
9	949	859	26
10	1398	-1408	-3
11	1246	-1154	30
12	1500	1462	12
13	1151	1064	26
14	1258	-1235	7
15	748	-758	-2
16	870	872	0
17	359	458	-16
18	287	-297	-1

-10 2 1

1	-56	163	-7
2	1166	-1085	27
3	164	294	-14
4	417	-399	3
5	57	-91	-1
6	1102	1128	-9
7	659	656	0
8	848	-949	-33
9	495	-459	7
10	1152	1160	-2
11	296	310	-2
12	984	-925	19
13	550	-554	0
14	425	459	-6
15	-272	64	-19
16	783	-705	21
17	155	163	0
18	-90	272	-19
19	-220	-102	-14
20	467	479	-2
21	970	969	0
22	382	-356	3
23	356	-430	-12
24	793	814	-5
25	113	282	-14
26	775	-741	8

-9 2 1

1	79	321	-25
2	-256	21	-18
3	-200	181	-20
4	774	-840	-21
5	794	-778	5
6	1424	1461	-14
7	1284	1273	4
8	1818	-1832	-5
9	1430	-1424	2
10	2010	1986	8
11	1466	1440	9
12	1605	-1560	16
13	1393	-1345	17
14	894	854	12
15	869	834	10
16	71	-280	-18
17	-237	-156	-20
18	431	-463	-6
19	396	-394	0
20	1241	1209	10
21	996	947	15
22	1528	-1526	0
23	1201	-1145	18
24	1675	1641	11
25	1146	993	46
26	1617	-1538	26
27	1163	-985	53
28	986	978	2
29	735	791	-14
30	283	-376	-12
31	139	-230	-6

-8 2 1

1	-334	204	-49
2	585	590	-1
3	1487	-1456	12
4	881	891	-3
5	918	963	-17
6	1935	-1963	-10
7	1455	-1453	0
8	2014	2021	-2
9	930	947	-6
10	2322	-2317	1
11	651	-649	0
12	1110	1089	8
13	-237	151	-23
14	290	-453	-32
15	167	-96	5
16	-238	-216	-29
17	302	-335	-5
18	856	878	-7
19	795	811	-5
20	1335	-1395	-22
21	954	-995	-14
22	1255	1317	-22
23	1056	1064	-2
24	727	-748	-6
25	1166	-1186	-6
26	419	540	-25
27	601	632	-7
28	425	-545	-24
29	-132	-26	-4
30	506	611	-23
31	-148	-289	-23
32	232	-209	2
33	722	742	-5
34	622	-605	3
35	799	-789	2

-7 2 1

1	-132	136	-13
2	1240	-1245	-2
3	618	-584	11
4	1850	1901	-20
5	890	899	-3
6	2003	-2038	-14
7	1149	-1160	-4
8	1897	1947	-20
9	1419	1403	7
10	1578	-1542	14
11	1257	-1243	5
12	852	837	5
13	715	760	-16
14	-273	22	-25
15	256	-241	2
16	843	-831	4
17	168	-184	-1
18	1424	1460	-14
19	701	643	17
20	1721	-1754	-12
21	1183	-1149	13
22	1613	1692	-30
23	1285	1233	18
24	1334	-1370	-13
25	867	-852	4
26	894	954	-19
27	529	580	-11
28	247	-332	-11
29	-53	-364	-31
30	-242	-258	-29
31	-150	-135	-9
32	521	616	-21
33	656	671	-3
34	964	-967	0
35	925	-899	6
36	1207	1181	7
37	912	794	29
38	1406	-1325	23

-6 2 1

1	219	-303	-17
2	795	815	-8
3	2380	2286	35
4	951	-918	14
5	1953	-2013	-25
6	2906	2894	3
7	1209	1148	20
8	3037	-2992	14
9	1018	-965	23
10	2428	2435	-2
11	267	328	-13
12	1251	-1215	16
13	364	362	0
14	257	250	1
15	199	-267	-11
16	1348	1287	25
17	931	892	15
18	1954	-2011	-22
19	1313	-1369	-23
20	2344	2384	-14
21	1128	1162	-13
22	2535	-2573	-13
23	736	-738	0
24	1861	1884	-8
25	950	996	-16
26	251	-334	-12
27	506	-610	-25
28	511	-436	15
29	376	-358	2
30	322	475	-26
31	825	888	-18
32	691	-728	-9
33	1211	-1262	-17
34	1080	1186	-33
35	1078	1066	3
36	1377	-1401	-7
37	1210	-1204	1
38	1131	1196	-19
39	566	516	9
40	1173	-1176	-1

-5 2 1

1	435	-451	-5

2	1216	1226	-5
3	781	822	-20
4	1357	-1357	0
5	960	-999	-20
6	1008	1056	-25
7	945	1005	-30
8	978	-1034	-28
9	913	-968	-28
10	604	646	-17
11	749	712	16
12	-137	112	-14
13	-31	-47	-1
14	634	-660	-10
15	877	-905	-12
16	1131	1094	16
17	1314	1269	20
18	1617	-1614	1
19	1264	-1194	29
20	1716	1744	-11
21	1249	1154	38
22	1229	-1241	-5
23	1292	-1257	13
24	687	702	-4
25	889	945	-20
26	-229	111	-17
27	-75	-339	-31
28	798	-838	-12
29	183	-89	6
30	1105	1129	-8
31	669	529	31
32	1260	-1252	2
33	846	-791	14
34	1268	1238	9
35	983	930	15
36	1137	-1103	10
37	951	-853	25
38	811	826	-3
39	556	602	-9
40	311	-469	-21
41	-317	-174	-24

-4 2 1

1	3213	3157	18
2	2072	-1931	60
3	2451	-2461	-4
4	3917	3789	34
5	1395	1406	-6
6	3103	-3107	-1
7	3202	-3152	15
8	1611	1674	-32
9	885	930	-23
10	2333	-2348	-5
11	604	629	-11
12	51	-158	-10
13	1359	-1407	-24
14	1165	1022	66
15	1786	1766	9
16	2687	-2659	9
17	1481	-1583	-48
18	3535	3595	-17
19	2418	2412	2
20	2883	-2943	-19
21	2106	-2061	17
22	2104	2121	-6
23	1241	1241	0
24	1660	-1583	30
25	-280	-138	-29
26	-287	24	-24
27	84	241	-13
28	1403	1408	-1
29	1312	1300	4
30	1867	-1847	7
31	1602	-1565	12
32	1928	1929	0
33	1531	1426	34
34	1710	-1708	0
35	1768	-1639	40
36	1463	1503	-13
37	1182	1085	27
38	923	-1040	-32
39	250	-423	-21
40	252	391	-16
41	-242	-277	-24
42	-40	366	-23

-3 2 1

1	431	-360	28
2	2905	-3087	-68
3	461	429	14
4	1804	1913	-56
5	264	-211	13
6	1084	-1197	-69
7	272	-272	0
8	287	288	0
9	130	54	6
10	487	545	-24
11	342	384	-13
12	1094	-1113	-10
13	269	-326	-14
14	1363	1355	3
15	621	612	4
16	1500	-1534	-16
17	1093	-1015	36
18	1259	1313	-26
19	849	830	7
20	1046	-1068	-9
21	512	-434	22
22	691	715	-8
23	-169	149	-17
24	-152	-111	-11
25	-272	-241	-41
26	405	-502	-22
27	-137	-123	-9
28	1154	1139	5
29	601	547	12
30	1163	-1172	-3
31	830	-774	15
32	913	940	-8
33	955	911	12
34	736	-750	-3
35	810	-829	-4
36	426	475	-7
37	656	717	-13
38	-201	-197	-15
39	-171	-367	-30
40	-319	-270	-33
41	-457	24	-37
42	235	561	-44
43	-176	219	-13

-2 2 1

1	1058	-1001	38
2	3521	3582	-19
3	4772	4821	-11
4	2206	-2139	30
5	831	-769	40
6	5131	5116	3
7	1521	-1465	31
8	3661	-3561	29
9	2478	-2452	10
10	1461	-1496	-19
11	1458	-1391	34
12	1150	1111	20
13	3199	3119	25
14	1016	-1020	-2
15	2743	-2734	3
16	3814	3770	11
17	2433	2525	-35
18	3240	-3319	-25
19	2519	-2557	-13
20	2826	2837	-3
21	139	-15	6
22	3148	-3038	33
23	220	9	15
24	930	870	22
25	977	-967	3
26	811	790	6
27	1699	1690	3
28	2759	-2726	10
29	2098	-1890	67
30	3124	3073	14
31	2167	2023	45
32	2813	-2712	29
33	1615	-1560	17
34	1837	1885	-15
35	1585	1501	26
36	558	-473	14
37	1027	-1118	-26
38	-346	-241	-35
39	-229	-179	-16
40	-325	336	-42
41	621	832	-48
42	1024	-1148	-35
43	1099	-1079	5
44	1213	1191	5

-1 2 1

1	427	-491	-51
2	827	927	-87
3	722	773	-43
4	327	-313	7
5	737	-797	-45
6	179	156	6
7	1352	1417	-40
8	364	-232	46
9	1164	-1182	-10
10	274	-249	6
11	511	451	22
12	382	356	7
13	97	-229	-17
14	391	-419	-8
15	41	220	-17
16	419	466	-13
17	386	400	-3
18	513	-559	-15
19	560	-617	-19
20	-150	209	-22
21	429	476	-12
22	-233	-43	-17
23	455	-519	-16
24	48	26	0
25	240	338	-15
26	472	515	-10
27	-257	84	-19
28	692	-689	0
29	199	-101	6
30	849	867	-5
31	257	111	11
32	401	-555	-29
33	226	-430	-26
34	-141	229	-14
35	279	550	-43
36	-210	239	-20
37	-205	-278	-23
38	602	-751	-33
39	221	312	-9
40	547	668	-24
41	23	-10	0
42	482	-615	-24
43	-432	-364	-61
44	235	458	-26

0 2 1

0	8446	8983	-75
1	2107	2135	-16
2	3423	-3341	29
3	4816	-4844	-7
4	1682	1561	76
5	2122	2026	50
6	175	-81	22
7	2569	-2542	11
8	861	-818	31
9	567	390	92
10	4084	4006	23
11	2135	2032	50
12	2884	-2754	51
13	1798	-1657	73
14	4656	4566	23
15	2568	2531	15
16	4312	-4145	46
17	3150	-3036	40
18	2007	1981	40
19	870	918	-26
20	1683	-1716	-17
21	583	-595	-5
22	764	727	17
23	302	-385	-22
24	1362	1355	3
25	1401	1360	20
26	2098	-2067	13
27	1266	-1244	10
28	3578	3413	50
29	1924	1817	46
30	3102	-3096	2
31	1656	-1607	21
32	2433	2470	-14
33	733	760	-9
34	1146	-1126	8
35	645	-699	-17
36	-284	409	-70
37	-124	-171	-12
38	735	790	-18
39	757	749	2
40	1619	-1676	-23
41	1213	-1237	-9
42	1639	1542	37
43	1272	1231	15

1 2 1

0	610	-663	-47
1	221	-208	5
2	461	498	-29
3	277	-305	-15
4	136	225	-29
5	307	343	-17
6	177	-127	10
7	336	-400	-27
8	230	-168	13
9	595	646	-24
10	288	271	4
11	228	-250	-4
12	-225	115	-25
13	-239	-55	-23
14	421	-428	-1
15	625	615	3
16	546	528	5
17	737	-784	-18
18	591	-568	7
19	414	555	-40
20	-249	58	-21
21	198	-299	-14
22	-180	73	-11
23	-345	-23	-36
24	-262	-230	-34
25	-324	262	-48
26	-219	159	-19
27	303	-340	-5
28	-334	0	-27
29	103	236	-9
30	-390	-13	-35
31	-276	-243	-29
32	-350	200	-35
33	-199	208	-17
34	-409	-29	-36
35	-146	-379	-32
36	-381	-143	-34

37	367	483	-17
38	-367	202	-35
39	-485	7	-49
40	-252	-426	-46
41	-314	-35	-19
42	-448	-15	-39
43	-254	50	-12

2 2 1

0	5772	-5765	1
1	2490	-2444	18
2	377	48	96
3	2438	2353	35
4	1801	-1796	2
5	1130	1097	19
6	723	-751	-15
7	3102	3027	25
8	3647	3681	-10
9	2953	2959	-2
10	3722	-3716	1
11	1747	-1804	-27
12	3608	3663	-16
13	3244	3297	-17
14	2959	-2909	16
15	3016	-2902	36
16	2299	2270	10
17	1551	1585	-15
18	449	-526	-23
19	1408	-1286	50
20	1240	-1252	-5
21	-133	176	-15
22	1640	1659	-7
23	1556	1590	-13
24	1984	-1942	15
25	1740	-1777	-13
26	2270	2308	-12
27	2079	1906	56
28	2435	-2403	10
29	1659	-1664	-1
30	2160	2062	31
31	723	685	8
32	1388	-1415	-8
33	-399	61	-34
34	-365	153	-32
35	-456	110	-46
36	668	707	-8
37	1311	1256	16
38	1763	-1559	59
39	1304	-1193	32
40	2139	2062	22
41	1449	1219	62
42	1639	-1668	-8

3 2 1

0	2869	3046	-66
1	332	-305	8
2	1307	-1335	-16
3	-174	-100	-22
4	84	-22	3
5	-157	-37	-13
6	749	835	-47
7	550	593	-19
8	989	-1071	-45
9	980	-1009	-15
10	757	807	-25
11	679	747	-31
12	734	-775	-20
13	630	-639	-3
14	701	683	7
15	285	374	-22
16	456	-410	13
17	-109	224	-23
18	-225	-164	-28
19	304	-376	-15
20	-255	66	-23
21	-191	215	-26
22	-76	-225	-16
23	366	-449	-17
24	429	406	4
25	446	453	-1
26	403	-552	-31
27	-184	-195	-16
28	305	436	-20
29	-380	63	-34
30	-215	-269	-25
31	-288	-11	-17
32	-361	350	-52
33	-95	-342	-24
34	-375	59	-28
35	472	551	-13
36	52	-190	-6
37	461	-624	-29
38	-250	-44	-12
39	230	412	-20
40	-162	-201	-11
41	207	-177	1

4 2 1

0	2594	2547	18
1	1332	-1383	-28
2	1933	-1856	34
3	498	-517	-7
4	546	-531	6
5	907	-863	22
6	1800	1803	-1
7	1772	1710	28
8	3841	-3849	-2
9	2083	-2055	12
10	4383	4231	37
11	1837	1828	4
12	3111	-3129	-5
13	2210	-2159	20
14	1357	1330	12
15	1085	1077	3
16	1159	-1146	5
17	201	-305	-18
18	1106	-1157	-21
19	407	-380	6
20	1110	1166	-22
21	1575	1421	57
22	2577	-2623	-15
23	1356	-1383	-10
24	2423	2371	17
25	2132	2100	11
26	1685	-1617	23
27	1719	-1749	-10
28	1229	1186	13
29	608	725	-28
30	1009	-1071	-18
31	32	-291	-17
32	331	364	-4
33	-327	-292	-39
34	-69	311	-19
35	723	812	-21
36	1137	-1032	27
37	1103	-1027	19
38	1787	1703	24
39	1145	1024	30

5 2 1

0	654	-673	-8
1	-107	178	-21
2	-210	-59	-23
3	642	-696	-24
4	785	733	23
5	1256	1297	-20
6	1116	-1137	-10
7	1716	-1768	-24
8	1362	1424	-30
9	1488	1509	-9
10	1140	-1169	-13
11	983	-1007	-10
12	1263	1271	-3
13	300	301	0
14	1062	-1116	-23
15	337	460	-31
16	472	527	-15
17	573	-618	-14
18	-242	113	-22
19	966	993	-10
20	457	-496	-9
21	1079	-1074	1
22	687	682	1
23	722	733	-3
24	764	-756	2
25	768	-750	5
26	959	912	14
27	400	524	-23
28	707	-715	-2
29	-263	-100	-17
30	75	394	-30
31	-263	-124	-17
32	-459	59	-46
33	-316	311	-40
34	-312	-248	-31
35	323	-503	-26
36	445	523	-12
37	420	528	-16

6 2 1

0	94	158	-6
1	-78	-21	-2
2	745	-776	-13
3	633	-624	3
4	602	619	-6
5	1073	1040	14
6	1673	-1680	-2
7	2050	-2063	-5
8	2712	2792	-28
9	1876	1817	23
10	2401	-2434	-12
11	1531	-1511	8
12	1877	1939	-25
13	1025	1019	2
14	641	-561	24
15	120	-253	-14
16	-163	-170	-16
17	-247	-119	-21
18	1850	1874	-9
19	336	313	3
20	1750	-1798	-18
21	1664	-1665	0
22	2399	2370	9
23	1177	1128	16
24	1752	-1746	2
25	1913	-1857	18
26	812	876	-18
27	725	917	-55
28	-213	31	-10
29	198	-462	-35
30	-403	-12	-36
31	-144	-301	-22
32	-245	269	-26
33	378	621	-43
34	749	-737	2
35	791	-704	18

7 2 1

0	153	257	-14
1	-177	-180	-23
2	619	621	0
3	854	807	18
4	1212	-1236	-10
5	1277	-1284	-3
6	1596	1593	1
7	1554	1529	10
8	1695	-1714	-7
9	1348	-1327	8
10	1493	1505	-4
11	634	666	-9
12	837	-856	-6
13	-253	-161	-26
14	-175	197	-19
15	-129	-272	-24
16	-80	220	-14
17	601	701	-28
18	909	-929	-6
19	888	-947	-19
20	1182	1168	4
21	1121	1118	0
22	1154	-1129	8
23	971	-884	25
24	986	1014	-8
25	681	595	20
26	765	-825	-16
27	-115	-302	-22
28	300	514	-34
29	-382	130	-35
30	-485	29	-52
31	-189	256	-19
32	386	-489	-16

8 2 1

0	736	-812	-26
1	681	-776	-32
2	850	931	-30
3	857	850	2
4	864	-919	-20
5	1071	-1051	7
6	1816	1760	21
7	1424	1442	-7
8	1415	-1358	21
9	1311	-1316	-2
10	1054	1131	-28
11	718	781	-19
12	810	-822	-3
13	-304	47	-25
14	-229	-221	-26
15	-237	-253	-30
16	286	414	-21
17	990	940	16
18	965	-1073	-36
19	678	-771	-25
20	1423	1335	29
21	1098	1086	3
22	1639	-1614	8
23	666	-691	-6
24	1239	1258	-6
25	605	665	-13
26	-148	-397	-37
27	-325	-72	-23
28	-434	-275	-57

9 2 1

0	787	797	-3
1	736	691	13
2	1310	-1350	-15
3	998	-997	0
4	1609	1569	14
5	1177	1187	-3
6	1653	-1643	3
7	1068	-1060	2
8	1401	1403	0
9	713	692	5
10	865	-861	1
11	-252	-98	-18
12	-300	172	-30
13	515	-482	6
14	490	516	-5
15	686	725	-10
16	1043	-1023	6
17	935	-922	3
18	1165	1193	-9
19	1006	903	30

20	1298	-1313	-4
21	790	-740	12
22	1161	1129	10
23	403	440	-6

10 2 1

0	1472	1465	2
1	562	557	1
2	1099	-1178	-28
3	345	-239	14
4	1180	1149	10
5	976	987	-3
6	469	-606	-31
7	1001	-918	25
8	32	134	-4
9	429	547	-24
10	-334	-181	-35
11	371	-471	-18
12	663	-667	0
13	-232	-139	-17
14	273	453	-28
15	629	746	-29
16	600	-681	-19
17	457	-460	0
18	950	1020	-20

11 2 1

0	1140	-1191	-17
1	941	-812	36
2	1394	1354	13
3	938	832	29
4	1534	-1419	37
5	988	-885	29
6	1214	1138	23
7	737	639	23
8	683	-645	8
9	-177	-130	-10

-11 3 1

1	933	-1018	-26
2	-237	-209	-23
3	298	276	2
4	-128	-125	-7
5	-205	119	-13
6	245	440	-29
7	21	-349	-27
8	252	-436	-28
9	297	425	-20
10	347	531	-34
11	481	-450	5
12	457	-606	-32
13	367	472	-18
14	127	418	-35
15	323	-434	-17
16	286	-304	-2
17	742	616	29

-10 3 1

1	573	-617	-10
2	586	-598	-2
3	190	168	1
4	-122	-123	-7
5	490	501	-2
6	961	964	0
7	940	-914	8
8	1532	-1518	5
9	1298	1234	22
10	1743	1716	9
11	1417	-1302	39
12	1869	-1752	39
13	1158	995	51
14	1463	1402	20
15	674	-590	20
16	812	-813	0
17	88	87	0
18	-257	140	-20
19	532	570	-8
20	756	722	8
21	1084	-1068	4
22	1505	-1421	27
23	1206	1136	21
24	1512	1468	14
25	1187	-1071	34

-9 3 1

1	1259	1292	-12
2	476	-473	0
3	226	-166	6
4	160	403	-35
5	621	-666	-12
6	876	-915	-13
7	1032	1106	-27
8	1130	1141	-4
9	1511	-1416	34
10	618	-719	-29
11	853	860	-2
12	1359	1375	-5
13	515	-608	-23
14	951	-955	-1
15	-108	181	-11
16	218	307	-11
17	-182	-202	-18
18	589	632	-10
19	220	-158	5
20	758	-894	-42
21	184	210	-2
22	1347	1375	-9
23	254	-138	10
24	1374	-1383	-3
25	674	546	29
26	713	834	-33
27	797	-808	-2
28	560	-623	-14
29	513	604	-19
30	-252	71	-14

-8 3 1

1	-308	-143	-35
2	324	-300	4
3	701	723	-7
4	1098	1092	2
5	1145	-1120	9
6	1588	-1610	-8
7	1332	1251	31
8	2003	1923	29
9	1400	-1291	41
10	2003	-1927	27
11	1013	958	19
12	1535	1553	-7
13	-55	-198	-11
14	763	-818	-18
15	210	-378	-26
16	-224	190	-23
17	786	840	-17
18	705	547	41
19	1361	-1341	7
20	1313	-1266	17
21	1381	1272	37
22	1667	1645	7
23	1243	-1145	33
24	1681	-1670	3
25	1085	915	51
26	1607	1487	40
27	495	-438	10
28	1032	-976	17
29	-216	91	-12
30	-266	223	-27
31	147	213	-5
32	167	381	-24
33	609	-588	4
34	876	-829	12

-7 3 1

1	645	-619	8
2	899	945	-19
3	416	-454	-10
4	2009	-2018	-3
5	1036	1001	14
6	1721	1691	12
7	1909	-1920	-4
8	1639	-1618	8
9	1825	1779	18
10	1499	1459	16
11	1622	-1689	-28
12	432	-427	1
13	814	880	-24
14	-200	63	-13
15	-332	-53	-36
16	403	483	-19
17	-118	-89	-6
18	1294	-1307	-5
19	1511	1506	1
20	1150	1124	9
21	1436	-1382	19
22	1518	-1649	-51
23	892	930	-12
24	1570	1581	-3
25	882	-914	-10
26	720	-790	-20
27	530	596	-15
28	360	552	-38
29	260	-279	-2
30	301	452	-24
31	180	5	7
32	1407	-1428	-7
33	225	46	10
34	1320	1316	1
35	731	-634	22
36	1198	-1220	-6
37	1043	1044	0

-6 3 1

1	949	992	-20
2	124	87	3
3	1028	-1016	5
4	983	-950	14
5	1067	978	40
6	1329	1360	-14
7	1356	-1347	4
8	1607	-1653	-20
9	1174	1154	9
10	1565	1579	-5
11	487	-463	7
12	995	-1008	-5
13	56	-136	-5
14	330	348	-4
15	667	690	-8
16	344	411	-15
17	1170	-1138	13
18	1214	-1251	-15
19	1366	1318	19
20	1685	1687	0
21	1169	-1111	22
22	1459	-1466	-2
23	731	750	-6
24	1255	1218	13
25	424	-419	0
26	916	-955	-13
27	-84	-101	-4
28	180	415	-32
29	494	608	-26
30	377	376	0
31	754	-703	12
32	1010	-980	8
33	803	754	12
34	1241	1194	14
35	948	-858	24
36	1193	-1202	-2
37	1040	989	14
38	1188	1070	32
39	845	-784	14

-5 3 1

1	1019	-1034	-7
2	2943	-2923	6
3	1361	1333	13
4	2885	2975	-31
5	1767	-1688	35
6	2644	-2676	-11
7	2145	2078	27
8	2490	2460	11
9	2626	-2633	-2
10	1604	-1613	-4
11	1066	1045	9
12	329	-326	0
13	154	-185	-4
14	682	743	-25
15	216	-208	1
16	2913	-2851	20
17	1074	1089	-6
18	2082	2246	-66
19	1757	-1766	-4
20	1716	-1772	-23
21	1870	1867	1
22	2193	2167	9
23	1543	-1597	-21
24	1099	-1077	8
25	900	978	-27
26	498	627	-33
27	-291	37	-22
28	-137	241	-19
29	457	-525	-14
30	1547	-1607	-21
31	641	669	-6
32	1734	1695	13
33	852	-822	8
34	1827	-1812	5
35	1126	1093	9
36	1580	1499	25
37	866	-840	6
38	1215	-1151	18
39	930	962	-8
40	137	333	-16
41	749	-760	-2

-4 3 1

1	1918	-2007	-41
2	520	-428	34
3	1575	1636	-31
4	555	529	10
5	1181	-1246	-35
6	854	-835	9
7	696	767	-37
8	673	679	-2
9	266	-429	-51
10	351	-439	-30
11	212	-179	5
12	30	-74	-2
13	924	904	9
14	649	600	19
15	1138	-1114	11
16	877	-863	6
17	988	991	-1
18	1237	1241	-1
19	934	-889	19
20	1429	-1443	-6
21	772	713	21
22	1145	1196	-21
23	-38	-119	-4
24	688	-756	-22
25	-163	-254	-25
26	-164	223	-20

27	605	638	-8
28	434	425	1
29	1146	-1084	20
30	1026	-967	19
31	1066	974	29
32	1226	1206	6
33	757	-689	16
34	1069	-1134	-20
35	486	463	3
36	999	1027	-8
37	203	-93	6
38	562	-709	-31
39	-365	-41	-26
40	-245	301	-28
41	-258	296	-27
42	-298	57	-16

-3 3 1

1	2402	2401	0
2	6733	6771	-6
3	2807	-2713	34
4	2537	-2559	-8
5	2203	2211	-3
6	3928	3877	14
7	1600	-1611	-5
8	2087	-2090	-1
9	1807	1750	26
10	1262	-1251	5
11	1245	-1314	-36
12	2684	2499	65
13	169	-245	-14
14	3243	-3177	20
15	1696	1634	27
16	3994	3948	12
17	2437	-2383	20
18	3482	-3515	-9
19	2882	2800	26
20	1244	1227	7
21	2843	-2841	0
22	885	-883	0
23	2307	2301	2
24	682	717	-11
25	517	-489	7
26	550	614	-17
27	791	-947	-52
28	1208	-1288	-29
29	1587	1564	8
30	2460	2410	16
31	1855	-1770	28
32	2247	-2209	12
33	1457	1295	49
34	2249	2129	36
35	965	-870	24
36	1244	-1211	9
37	773	892	-30
38	282	386	-12
39	68	-374	-24
40	-310	94	-19
41	-118	-247	-13
42	1274	-1213	16
43	864	699	34

-2 3 1

1	1447	1540	-55
2	1584	1769	-108
3	767	-769	-1
4	1720	-1851	-71
5	281	155	29
6	1233	1323	-54
7	245	178	14
8	1190	-1240	-28
9	571	-578	-3
10	924	946	-11
11	599	581	7
12	184	-206	-3
13	700	-703	-1
14	230	-320	-20
15	260	292	-6
16	615	689	-30
17	210	-123	11
18	937	-952	-6
19	-28	16	0
20	659	694	-12
21	-194	-82	-15
22	533	-522	3
23	31	248	-18
24	440	488	-11
25	92	345	-30
26	270	-310	-5
27	453	-570	-26
28	-254	-149	-21
29	517	519	0
30	474	555	-16
31	549	-621	-15
32	624	-686	-14
33	239	279	-4
34	556	623	-13
35	-293	-33	-17
36	645	-726	-18
37	-447	-35	-41
38	420	603	-32
39	-360	210	-33
40	-336	-146	-25
41	-125	-417	-34
42	210	-279	-5
43	254	353	-10

-1 3 1

1	3585	-3472	34
2	2743	-2856	-45
3	2077	1991	40
4	6051	6068	-3
5	444	385	26
6	1175	-1049	71
7	859	862	-2
8	1175	1165	5
9	218	205	2
10	1247	1159	44
11	2267	-2179	35
12	3787	-3731	15
13	1297	1230	30
14	3641	3544	27
15	3348	-3264	25
16	4321	-4233	21
17	3196	3088	32
18	1649	1681	-13
19	1332	-1386	-23
20	978	-960	7
21	1502	1516	-5
22	152	261	-13
23	854	-843	4
24	1295	1247	17
25	830	-693	40
26	1237	-1232	2
27	1300	1390	-32
28	2509	2470	12
29	2460	-2446	4
30	1980	-1994	-4
31	2681	2461	64
32	1876	1869	2
33	1643	-1622	6
34	1539	-1483	17
35	744	754	-2
36	914	896	4
37	-233	-44	-10
38	397	-562	-27
39	714	-686	5
40	729	-783	-12
41	1017	1076	-16
42	1306	1297	2
43	1275	-1304	-8

0 3 1

1	495	510	-13
2	298	-217	41
3	924	-908	13
4	385	294	47
5	881	828	39
6	384	-222	61
7	1004	-971	22
8	388	321	24
9	1078	1034	27
10	382	-240	41
11	728	-738	-6
12	102	-38	4
13	399	438	-13
14	245	227	3
15	664	-625	18
16	476	-515	-15
17	-150	95	-14
18	626	671	-21
19	-192	66	-19
20	308	-405	-28
21	-171	-133	-20
22	-56	371	-58
23	255	466	-58
24	375	-452	-22
25	560	-596	-13
26	-197	191	-27
27	502	542	-12
28	-388	0	-52
29	167	-351	-29
30	233	-294	-9
31	109	188	-6
32	185	327	-20
33	-353	161	-45
34	-210	-350	-47
35	364	-498	-30
36	-216	337	-44
37	412	414	0
38	-340	-151	-38
39	609	-609	0
40	-211	110	-15
41	597	748	-45
42	-258	185	-26
43	257	-466	-36

1 3 1

0	6565	-6558	1
1	2794	2799	-1
2	4300	4286	3
3	1464	-1410	31
4	1679	1647	17
5	310	334	-8
6	-85	50	-5
7	744	723	10
8	711	-714	-1
9	3497	-3495	0
10	1847	-1939	-43
11	2468	2417	19
12	3865	3914	-13
13	2160	-2139	8
14	3885	-3904	-5
15	3235	3184	15
16	4328	4241	21
17	623	-637	-4
18	3766	-3553	55
19	468	-330	30
20	589	-627	-11
21	350	-528	-42
22	794	854	-20
23	1432	-1405	10
24	1585	-1632	-17
25	1862	1773	31
26	2717	2682	11
27	1514	-1407	36
28	3031	-2880	43
29	2473	2457	5
30	1730	1688	13
31	2012	-2029	-5
32	1070	-986	25
33	940	920	5
34	652	734	-19
35	-205	-227	-18
36	346	460	-16
37	654	-736	-18
38	970	-1020	-13
39	1240	1270	-8
40	1384	1239	40
41	1279	-1298	-5
42	2121	-1962	45

2 3 1

0	779	881	-66
1	1400	-1521	-73
2	488	-497	-3
3	1804	1952	-78
4	359	280	25
5	1111	-1183	-43
6	-75	97	-7
7	520	530	-4
8	449	-350	32
9	-135	-70	-10
10	388	377	3
11	564	-615	-20
12	403	-412	-2
13	861	843	8
14	-169	142	-20
15	1100	-1066	15
16	82	47	1
17	1114	1103	5
18	141	205	-7
19	805	-808	-1
20	-308	28	-32
21	277	289	-1
22	187	-255	-8
23	-357	38	-38
24	-106	364	-38
25	158	-356	-24
26	168	-306	-15
27	848	884	-10
28	-59	159	-6
29	512	-671	-35
30	-397	27	-34
31	387	512	-21
32	-219	-235	-20
33	-171	-190	-12
34	246	365	-13
35	-297	112	-19
36	204	-498	-38
37	-107	-266	-15
38	352	585	-38
39	-335	-74	-22
40	-296	-319	-35
41	-340	-39	-21

3 3 1

0	3000	2987	4
1	2062	-1957	46
2	288	178	24
3	801	741	30
4	528	477	21
5	932	997	-36
6	1393	1445	-28
7	1670	-1636	16
8	2508	-2420	33
9	2806	2817	-3
10	3328	3324	1
11	2453	-2473	-7
12	3383	-3362	6
13	2772	2714	20
14	2334	2489	-61
15	1596	-1474	52
16	2461	-2514	-19
17	624	663	-13

18	-226	-158	-27
19	311	356	-9
20	772	820	-18
21	1074	-1187	-46
22	1884	-1806	28
23	1733	1681	19
24	2635	2587	15
25	1511	-1613	-38
26	2678	-2620	18
27	1706	1739	-11
28	2078	2056	7
29	1307	-1328	-7
30	944	-1039	-28
31	1169	1272	-33
32	629	690	-13
33	529	-580	-9
34	510	645	-26
35	-142	-242	-14
36	1191	-1234	-13
37	1132	1009	32
38	1433	1318	32
39	1601	-1541	17
40	1822	-1851	-8

4 3 1

0	264	-176	18
1	2168	2243	-32
2	71	-125	-5
3	1109	-1178	-37
4	406	450	-15
5	-109	174	-20
6	1109	-1135	-13
7	694	670	11
8	1597	1582	7
9	1360	-1350	4
10	1696	-1697	0
11	1390	1375	7
12	1140	1101	18
13	1184	-1114	31
14	357	-397	-10
15	699	697	0
16	-227	15	-19
17	546	-633	-28
18	370	424	-12
19	381	425	-10
20	629	-618	3
21	-303	-17	-27
22	715	785	-22
23	236	-251	-1
24	701	-766	-18
25	241	214	2
26	531	599	-15
27	613	-530	18
28	283	-376	-12
29	767	867	-27
30	-278	107	-18
31	226	-400	-21
32	-435	36	-40
33	-282	131	-19
34	-173	-342	-28
35	-377	-131	-31
36	77	505	-45
37	-95	-103	-3
38	453	-548	-15

5 3 1

0	557	-603	-19
1	1108	1075	16
2	912	-951	-19
3	273	-209	13
4	1442	1457	-7
5	236	67	21
6	1868	-1837	13
7	2013	1946	27
8	1799	1897	-43
9	2925	-2855	23
10	1896	-1908	-4
11	1756	1764	-3
12	2822	2711	36
13	1597	-1633	-15
14	508	-640	-44
15	267	244	3
16	869	867	0
17	383	413	-6
18	259	305	-7
19	1509	-1464	17
20	1340	-1437	-38
21	1547	1544	1
22	1628	1737	-41
23	1842	-1816	9
24	2172	-2157	5
25	1335	1268	22
26	2294	2290	1
27	379	-402	-3
28	1347	-1372	-8
29	-319	397	-56
30	199	512	-44
31	-481	41	-52
32	-301	201	-27
33	433	-457	-3
34	574	-732	-34
35	291	473	-24
36	1339	1401	-18

6 3 1

0	609	-633	-9
1	589	-572	6
2	961	906	24
3	188	161	3
4	1186	-1173	5
5	589	544	15
6	1625	1647	-9
7	1150	-1096	23
8	1842	-1873	-12
9	1314	1244	29
10	1312	1344	-13
11	910	-966	-22
12	764	-711	18
13	573	596	-7
14	-241	-8	-18
15	-132	-280	-28
16	570	598	-7
17	91	-171	-5
18	985	-966	6
19	312	295	2
20	1269	1285	-5
21	697	-615	21
22	1401	-1376	8
23	1024	916	33
24	1144	1082	19
25	710	-708	0
26	621	-529	19
27	387	433	-7
28	-347	120	-30
29	-238	-301	-31
30	-373	122	-33
31	-414	118	-40
32	207	-350	-15
33	177	404	-24
34	431	539	-17

7 3 1

0	291	289	0
1	879	971	-38
2	247	289	-7
3	97	-334	-33
4	1228	-1270	-17
5	1065	1031	13
6	1962	1942	7
7	1484	-1405	31
8	2143	-2050	33
9	1538	1475	24
10	2061	2150	-34
11	1337	-1285	19
12	861	-867	-2
13	794	803	-2
14	-224	99	-16
15	-248	8	-16
16	-291	52	-23
17	466	-525	-13
18	1039	-1026	4
19	1174	1132	14
20	1049	987	19
21	1735	-1736	0
22	1028	-1016	3
23	1920	1769	49
24	1359	1400	-13
25	887	-875	3
26	994	-1010	-4
27	-389	22	-34
28	611	719	-25
29	-343	347	-51
30	-454	-28	-44
31	605	-747	-31

8 3 1

0	479	525	-11
1	159	-260	-12
2	912	-945	-11
3	755	750	1
4	1454	1393	23
5	1486	-1462	9
6	1675	-1667	2
7	1655	1618	14
8	1346	1340	2
9	1114	-1160	-17
10	744	-800	-17
11	737	826	-28
12	-273	52	-20
13	-217	-265	-30
14	405	519	-24
15	442	-470	-5
16	947	-943	1
17	522	563	-9
18	1175	1119	19
19	696	-671	6
20	1109	-1150	-14
21	768	742	7
22	1010	1065	-17
23	578	-512	13
24	689	-727	-9
25	326	398	-10
26	-125	264	-17
27	-158	-174	-11

9 3 1

0	176	302	-15
1	1063	-1094	-10
2	1069	-1044	9
3	825	764	18
4	786	849	-20
5	552	-590	-9
6	1518	-1484	12
7	638	608	7
8	1396	1387	3
9	224	-177	4
10	936	-931	1
11	-183	119	-11
12	-205	-158	-16
13	383	327	8
14	24	265	-16
15	1170	-1127	14
16	650	-707	-14
17	615	620	-1
18	1038	1038	0
19	1047	-1020	8
20	933	-953	-5
21	1063	1012	14
22	979	955	6
23	377	-451	-11

10 3 1

0	1097	-1039	19
1	833	773	17
2	1362	1328	11
3	1153	-1076	25
4	1557	-1498	20
5	1218	1138	26
6	1476	1408	23
7	1024	-1034	-3
8	913	-866	14
9	712	721	-2
10	-119	188	-11
11	-282	-29	-19
12	369	439	-12
13	255	-402	-21
14	681	-752	-18
15	700	598	23
16	1024	972	14
17	1063	-971	26

11 3 1

0	524	-470	10
1	604	650	-11
2	584	613	-6
3	591	-631	-9
4	506	-582	-16
5	445	462	-3
6	824	883	-16
7	136	136	0

-11 4 1

1	1183	-1134	15
2	-72	230	-13
3	507	594	-18
4	-152	0	-5
5	142	170	-1
6	287	-325	-4
7	834	-802	8
8	652	523	28
9	1333	1348	-4
10	812	-666	36
11	1606	-1552	17
12	758	567	43
13	1578	1527	16
14	600	-420	34

-10 4 1

1	477	552	-16
2	1003	-862	44
3	240	-44	13
4	263	180	8
5	415	-504	-18
6	295	299	0
7	738	766	-7
8	347	-310	5
9	1344	-1357	-4
10	551	474	16
11	905	969	-20
12	485	-375	20
13	978	-1088	-36
14	699	672	7
15	453	458	0
16	672	-607	16
17	-121	63	-4
18	707	737	-7
19	663	-629	8
20	127	-299	-16
21	597	719	-30
22	203	181	1
23	1259	-1268	-2
24	243	-32	12

-9 4 1

1	644	697	-15
2	-278	-68	-22
3	-29	230	-14
4	10	-210	-11
5	1017	-1051	-12
6	454	406	9
7	1513	1551	-13
8	558	-397	33
9	1797	-1810	-4
10	646	471	40
11	1842	1823	6
12	455	-190	38
13	1632	-1588	15
14	171	109	4
15	1031	1009	7
16	-110	-1	-3
17	-148	-181	-13
18	387	-418	-5
19	682	-663	4
20	705	630	19
21	1410	1391	6
22	842	-618	56
23	1790	-1772	6
24	827	586	58
25	1874	1840	11
26	679	-386	56
27	1524	-1477	15
28	414	207	25
29	891	824	18

-8 4 1

1	158	-185	-2
2	637	631	1
3	1395	-1304	34
4	162	-64	6
5	1738	1729	3
6	687	-682	1
7	1256	-1212	16
8	1114	1054	22
9	1664	1709	-17
10	1423	-1369	20
11	1019	-1057	-14
12	570	592	-5
13	870	984	-40
14	199	-347	-21
15	-290	-29	-23
16	-215	129	-16
17	-254	106	-20
18	-158	71	-7
19	452	561	-25
20	317	-324	-1
21	2088	-2088	0
22	445	304	23
23	1202	1269	-23
24	374	-212	20
25	1582	-1531	17
26	648	641	1
27	1133	1143	-3
28	254	-434	-26
29	-293	130	-23
30	703	701	0
31	723	-751	-6
32	634	-633	0
33	906	862	11

-7 4 1

1	-60	-111	-5
2	871	-897	-10
3	1186	-1093	37
4	924	891	13
5	1967	1927	15
6	807	-775	11
7	2407	-2384	8
8	741	664	25
9	2096	2093	1
10	425	-304	24
11	1541	-1544	-1
12	280	-177	13
13	923	874	17
14	247	358	-19
15	-150	0	-6
16	513	-602	-24
17	852	-874	-7
18	818	813	1
19	1550	1583	-12
20	1091	-1045	16
21	1985	-1932	18
22	1121	911	67
23	2061	2016	15
24	739	-482	61
25	1661	-1685	-8
26	451	126	40
27	1120	1133	-4
28	275	321	-6
29	348	-323	3
30	403	-385	2
31	561	-580	-4
32	609	570	8
33	1114	1121	-2
34	864	-728	33
35	1457	-1397	18
36	1034	761	66

-6 4 1

1	2298	-2169	47
2	291	-150	22
3	3946	3895	13
4	416	-125	53
5	2430	-2413	6
6	946	950	-1
7	3254	3163	27
8	1897	-1840	23
9	2115	-2207	-36
10	1360	1352	3
11	851	805	18
12	1245	-1269	-10
13	-168	-107	-14
14	256	349	-17
15	744	-850	-40
16	297	269	4
17	1756	1726	11
18	503	-554	-13
19	1851	-1956	-41
20	756	759	0
21	1903	1964	-22
22	927	-927	0
23	1646	-1615	11
24	967	1040	-25
25	1957	1937	6
26	605	-588	4
27	302	-380	-12
28	128	172	-3
29	-276	31	-18
30	-137	-276	-21
31	1203	1221	-5
32	194	165	2
33	1580	-1613	-10
34	376	86	26
35	1743	1806	-20
36	634	-500	26
37	1201	-1285	-26
38	724	572	30

-5 4 1

1	623	-604	7
2	1461	1423	17
3	1310	1340	-14
4	900	-888	5
5	1403	-1419	-7
6	810	840	-14
7	1234	1203	14
8	860	-822	18
9	1438	-1442	-1
10	427	315	29
11	818	766	21
12	151	7	8
13	-91	-50	-4
14	385	-486	-29
15	446	-464	-5
16	870	928	-24
17	1237	1291	-23
18	959	-956	1
19	1758	-1777	-7
20	934	833	36
21	1604	1612	-3
22	851	-771	26
23	1228	-1193	13
24	297	290	1
25	763	737	7
26	264	275	-1
27	-200	-183	-18
28	761	-829	-20
29	714	-687	7
30	838	744	25
31	1347	1307	13
32	828	-692	34
33	1311	-1375	-21
34	723	621	23
35	1219	1248	-8
36	525	-231	39
37	1197	-1241	-13
38	207	34	7
39	787	822	-8
40	-284	77	-16

-4 4 1

1	1550	1658	-54
2	225	2	23
3	3789	-3774	4
4	980	920	29
5	4195	4240	-11
6	901	-795	50
7	2083	-2131	-20
8	1579	1627	-23
9	2034	2022	5
10	1917	-1916	0
11	469	-461	2
12	399	466	-22
13	1457	-1420	17
14	364	-265	22
15	2406	2486	-30
16	825	-818	2
17	3010	-3050	-13
18	1221	1124	40
19	2477	2555	-28
20	662	-737	-26
21	2632	-2529	34
22	962	1025	-24
23	1791	1697	35
24	906	-948	-15
25	946	-989	-16
26	503	529	-6
27	690	-745	-15
28	203	348	-18
29	1490	1352	46
30	467	-384	14
31	2491	-2506	-4
32	526	526	32
33	2314	2334	-6
34	767	-666	23
35	1685	-1685	0
36	796	628	37
37	1682	1745	-19
38	677	-696	-4
39	414	-579	-28
40	815	762	11
41	433	-575	-23

-3 4 1

1	2188	2302	-50
2	478	-409	25
3	2244	-2347	-44
4	491	500	-3
5	1714	1823	-54
6	194	-48	16
7	1396	-1436	-21
8	604	-658	-25
9	626	656	-13
10	855	873	-9
11	-136	-116	-15
12	1123	-1137	-6
13	396	-447	-16
14	1010	986	11
15	891	894	-1
16	906	-862	19
17	1196	-1211	-6
18	559	487	22
19	1188	1220	-14
20	229	233	0
21	924	-939	-5
22	408	-382	5
23	487	508	-5
24	232	449	-40
25	-109	-252	-20
26	754	-802	-14
27	-260	-59	-17
28	829	828	0
29	610	677	-16
30	529	-538	-2
31	1009	-990	5
32	405	243	20
33	1105	1218	-36
34	82	-18	1
35	963	-1017	-15
36	97	-229	-8
37	359	532	-27
38	291	426	-17
39	-283	-221	-24
40	-149	-403	-33
41	-166	-224	-13
42	94	445	-32

-2 4 1

1	6305	-6290	2
2	2103	1994	47
3	5301	5365	-13
4	748	-609	70
5	2266	-2222	18
6	937	926	5
7	2813	2746	23
8	1592	-1532	29
9	822	-845	-11
10	354	388	-10
11	2191	-2137	22
12	170	-129	5
13	3968	3791	46
14	1194	-1046	66
15	5225	-5067	32
16	2128	1916	80
17	3625	3699	-21
18	1368	-1287	34
19	3760	-3665	25
20	1065	1010	23
21	566	644	-25
22	1451	-1430	8
23	-323	45	-32
24	797	888	-31
25	-219	295	-35
26	205	295	-10
27	1655	1601	18
28	939	-796	40
29	2453	-2361	28

30	1539	1368	54
31	2534	2451	25
32	1325	-1143	55
33	2111	-2098	4
34	520	198	40
35	1881	1961	-25
36	137	-27	3
37	1298	-1263	10
38	-445	-94	-41
39	454	-492	-5
40	-251	169	-17
41	700	759	-12
42	604	-367	35

-1 4 1

1	357	352	1
2	1710	-1746	-19
3	483	403	32
4	1459	1475	-9
5	669	-654	7
6	731	-737	-2
7	770	770	0
8	364	334	8
9	1074	-1031	21
10	292	-289	0
11	604	589	5
12	62	129	-4
13	45	153	-8
14	-237	-126	-28
15	424	-489	-19
16	-93	152	-11
17	1037	1023	5
18	494	391	26
19	766	-783	-6
20	479	-523	-11
21	479	432	11
22	677	679	0
23	509	-557	-12
24	514	-572	-14
25	-223	175	-20
26	609	694	-22
27	92	162	-4
28	640	-745	-27
29	-94	-307	-22
30	293	450	-23
31	123	471	-42
32	-173	-177	-12
33	247	-409	-20
34	-303	-328	-40
35	220	391	-19
36	334	656	-57
37	-197	-299	-24
38	562	-602	-7
39	-424	160	-40
40	338	589	-40
41	-277	216	-23
42	170	-307	-11

0 4 1

0	3694	3572	35
1	2078	1967	58
2	2756	-2695	25
3	1665	-1630	21
4	208	22	26
5	2064	2026	19
6	1373	1310	38
7	1756	-1672	45
8	961	-954	4
9	1218	1186	19
10	2167	2076	42
11	4601	4304	76
12	1452	-1312	75
13	4186	-4218	-9
14	1383	1253	89
15	4230	4186	12
16	2299	-2132	72
17	4222	-4270	-13
18	416	-194	53
19	1609	1616	-3
20	-187	78	-17
21	310	333	-5
22	668	780	-50
23	658	-608	19
24	781	736	18
25	2114	2152	-16
26	624	-453	51
27	2649	-2624	9
28	1153	978	75
29	2778	2754	8
30	2011	-1867	58
31	2209	-2276	-27
32	1138	996	57
33	1627	1601	10
34	442	-581	-36
35	469	-613	-38
36	-276	104	-24
37	-344	-123	-37
38	397	552	-36
39	965	1023	-22
40	576	-595	-5
41	1282	-1364	-32
42	751	746	1

1 4 1

0	1903	1995	-46
1	736	823	-52
2	1295	-1391	-57
3	1027	-1100	-43
4	400	427	-10
5	787	867	-45
6	254	228	5
7	582	-621	-16
8	1016	-1026	-4
9	192	141	6
10	1304	1301	1
11	86	-40	2
12	1099	-1058	18
13	-229	44	-20
14	-181	171	-22
15	344	475	-34
16	150	160	-1
17	526	-535	-2
18	547	-629	-25
19	351	375	-4
20	1004	1009	-1
21	304	-327	-3
22	729	-758	-8
23	102	284	-18
24	356	497	-28
25	117	-340	-23
26	-225	-270	-28
27	-382	161	-40
28	-310	-4	-21
29	-282	-2	-17
30	268	418	-20
31	-261	-229	-25
32	487	-598	-21
33	-351	172	-31
34	495	593	-18
35	-350	31	-24
36	744	-795	-12
37	-240	136	-14
38	588	636	-9
39	-334	-131	-24
40	86	-384	-25
41	-416	-31	-33
42	-306	139	-20

2 4 1

0	1427	-1361	35
1	3534	-3519	4
2	1136	1096	22
3	2895	2899	-1
4	298	180	26
5	358	386	-9
6	1295	-1288	3
7	2051	-2032	8
8	1273	1244	14
9	2197	2236	-16
10	2056	-2023	14
11	3549	-3533	-24
12	1256	1208	22
13	4322	4252	17
14	2283	-2254	11
15	3257	-3282	-7
16	777	687	33
17	1866	1904	-15
18	625	683	-19
19	1210	-1161	19
20	-223	-318	-46
21	1059	-1130	-27
22	873	1000	-45
23	2118	2190	-25
24	955	-846	33
25	3056	-2919	39
26	885	554	79
27	3815	3707	26
28	1129	-948	52
29	2635	-2650	-4
30	1402	1380	7
31	1729	1697	10
32	962	-955	1
33	-277	-179	-21
34	-297	228	-27
35	-370	-187	-34
36	-381	-75	-29
37	1003	1035	-8
38	790	-693	20
39	2115	-2042	21
40	1043	898	35
41	1655	1660	-1

3 4 1

0	1355	1387	-16
1	964	1053	-50
2	1445	-1498	-27
3	-43	-194	-19
4	1420	1465	-23
5	401	-394	2
6	1217	-1284	-35
7	621	640	-8
8	177	341	-38
9	795	-837	-20
10	135	161	-3
11	834	821	6
12	557	-576	-7
13	600	-624	-8
14	762	851	-39
15	509	488	6
16	1126	-1148	-9
17	232	-223	1
18	1195	1268	-30
19	-187	81	-13
20	842	-897	-20
21	249	280	-4
22	258	373	-18
23	316	-439	-22
24	-306	87	-25
25	475	521	-9
26	497	-544	-9
27	600	-676	-18
28	630	692	-14
29	248	368	-14
30	506	-667	-34
31	-238	-305	-30
32	640	778	-32
33	-234	-110	-12
34	503	-623	-22
35	-209	284	-23
36	-233	97	-11
37	-187	-305	-23
38	-330	-272	-33
39	498	640	-25

4 4 1

0	950	907	21
1	2855	2842	4
2	-94	-76	-7
3	616	623	-2
4	251	80	25
5	1884	-1847	16
6	1019	988	15
7	2479	2549	-27
8	1578	-1531	21
9	3213	-3207	1
10	1231	1220	5
11	3261	3264	0
12	1249	-1266	-7
13	2664	-2730	-23
14	889	852	14
15	1890	1849	16
16	-150	-226	-25
17	1231	-1119	44
18	248	-428	-36
19	436	-482	-11
20	1003	1006	-1
21	1938	1898	14
22	1058	-1131	-26
23	2760	-2849	-28
24	996	949	15
25	2480	2425	17
26	419	-247	23
27	2668	-2600	20
28	297	140	14
29	1819	1867	-16
30	586	-580	1
31	236	-278	-4
32	-264	164	-19
33	441	-539	-16
34	-363	1	-26
35	784	831	-11
36	189	-333	-13
37	1937	-1958	-6
38	733	624	20

5 4 1

0	1313	-1307	2
1	90	147	-5
2	1190	1199	-4
3	835	-784	22
4	1171	-1136	16
5	980	985	-2
6	385	362	6
7	1355	-1338	7
8	346	176	31
9	1289	1344	-25
10	423	-348	18
11	1422	-1458	-15
12	499	432	18
13	1152	1113	16
14	648	-668	-6
15	302	-318	-2
16	472	593	-34
17	197	-339	-21
18	514	-524	-2
19	790	788	0
20	475	507	-7
21	1066	-1042	8
22	74	-127	-2
23	1164	1178	-4
24	358	-328	4
25	723	-722	0
26	737	589	34
27	451	400	8
28	212	-426	-28

29	143	-166	-1
30	193	447	-32
31	-188	-312	-26
32	-244	-164	-17
33	28	428	-34
34	-392	37	-31
35	382	-470	-12
36	-383	132	-30

6 4 1

0	1007	888	49
1	268	246	3
2	132	-64	4
3	1110	-1159	-21
4	99	30	3
5	2151	2247	-38
6	680	-504	55
7	3355	-3292	18
8	665	526	43
9	2440	2408	11
10	981	-951	11
11	1745	-1607	52
12	523	675	-47
13	871	897	-9
14	156	-413	-41
15	-238	-283	-39
16	384	-413	-5
17	407	-489	-18
18	884	887	-1
19	603	643	-10
20	955	-1001	-15
21	1830	-1753	26
22	1555	1494	21
23	2493	2391	31
24	828	-751	20
25	2051	-1967	27
26	249	23	12
27	1520	1581	-20
28	638	575	13
29	512	-578	-13
30	-278	-237	-27
31	-348	-15	-25
32	234	450	-27
33	810	799	2

7 4 1

0	849	885	-14
1	923	-977	-23
2	550	-570	-5
3	1514	1535	-9
4	336	-48	31
5	1724	-1788	-25
6	837	773	22
7	1599	1618	-7
8	1086	-1012	28
9	1480	-1376	39
10	995	968	10
11	925	925	0
12	684	-652	9
13	-196	-258	-28
14	286	372	-14
15	233	-280	-6
16	315	-551	-49
17	893	913	-6
18	-140	201	-14
19	1442	-1413	10
20	216	136	6
21	1592	1517	25
22	303	-164	14
23	1287	-1307	-6
24	411	296	16
25	881	964	-24
26	467	-578	-22
27	324	-361	-5
28	343	542	-34
29	-168	-316	-25
30	210	-240	-2

8 4 1

0	1016	-1060	-16
1	508	-457	12
2	482	641	-44
3	1385	1290	35
4	207	-230	-2
5	1815	-1872	-21
6	845	742	32
7	2200	2250	-17
8	259	-213	5
9	1140	-1108	11
10	-130	53	-5
11	832	832	0
12	-227	-297	-36
13	635	-754	-34
14	553	-535	4
15	1223	-1131	30
16	470	364	18
17	1022	983	12
18	490	-551	-13
19	1198	-1179	6
20	702	718	-4
21	1541	1572	-10
22	770	-804	-9
23	892	-908	-4
24	130	433	-35
25	809	683	30
26	-203	-32	-8

9 4 1

0	291	274	2
1	1522	1426	34
2	521	-464	12
3	1673	-1630	15
4	704	653	13
5	1631	1605	9
6	929	-896	10
7	1585	-1585	0
8	1031	1009	7
9	1149	1046	33
10	684	-641	11
11	298	-326	-4
12	104	177	-4
13	-202	-281	-28
14	217	177	3
15	973	907	19
16	403	-325	11
17	1285	-1233	16
18	433	393	6
19	1361	1333	9
20	772	-585	42
21	1257	-1158	29

10 4 1

0	1059	1058	0
1	650	729	-21
2	489	-539	-11
3	650	-699	-13
4	436	407	5
5	1236	1220	5
6	-125	-11	-3
7	1107	-1176	-23
8	398	-319	12
9	677	802	-34
10	174	242	-6
11	-211	-49	-10
12	394	-425	-5
13	299	-361	-8
14	347	503	-27
15	672	655	3

11 4 1

0	473	-311	25
1	1530	-1470	19
2	617	442	34
3	1648	1576	23
4	671	-514	33

-11 5 1

2	69	-79	0
3	597	602	-1
4	414	459	-8
5	516	-627	-24
6	393	471	-13
7	242	9	12

-10 5 1

1	-197	-52	-10
2	718	-684	9
3	-242	-25	-14
4	173	-115	3
5	-218	102	-14
6	839	860	-6
7	420	-207	29
8	1324	-1326	0
9	348	182	19
10	1513	1555	-14
11	491	-176	43
12	1628	-1591	12
13	455	91	41
14	1289	1348	-20
15	217	-3	10
16	707	-722	-3
17	-287	-105	-21
18	-166	-12	-6
19	453	396	9
20	767	774	-1
21	547	-411	24

-9 5 1

1	1115	958	50
2	166	-324	-19
3	611	-612	0
4	298	424	-21
5	389	373	2
6	702	-836	-41
7	295	313	-2
8	1045	1012	11
9	373	-319	8
10	1119	-1238	-44
11	567	475	20
12	1536	1462	26
13	312	-132	18
14	1090	-1054	11
15	385	322	9
16	942	967	-8
17	761	-736	6
18	595	598	0
19	261	363	-14
20	979	-928	15
21	491	-537	-9
22	1487	1433	18
23	548	472	15
24	1308	-1403	-32
25	662	331	59
26	1220	1215	1
27	431	-287	20

-8 5 1

1	501	-516	-3
2	-100	-57	-3
3	460	482	-5
4	940	1000	-22
5	463	-249	37
6	1644	-1628	6
7	526	47	65
8	1819	1765	19
9	416	82	41
10	1930	-1920	3
11	553	-392	35
12	1448	1410	14
13	673	648	6
14	619	-626	-2
15	815	-843	-8
16	-65	11	-1
17	469	559	-20
18	712	746	-10
19	526	-527	0
20	1515	-1547	-11
21	646	207	74
22	1982	2016	-11
23	580	49	67
24	1832	-1845	-4
25	621	-183	68
26	1521	1531	-3
27	660	490	36
28	1032	-981	15
29	628	-606	5
30	8	-113	-2
31	451	340	16
32	1013	954	16

-7 5 1

1	748	-767	-6
2	1144	1169	-10
3	1407	1373	13
4	2072	-2061	4
5	326	-140	24
6	2867	2788	25
7	533	-440	23
8	2229	-2227	0
9	797	808	-3
10	1676	1693	-6
11	640	-765	-41
12	1143	-1091	19
13	-146	253	-24
14	131	296	-19
15	982	-924	20
16	131	49	4
17	-210	-51	-12
18	1675	-1687	-4
19	208	13	11
20	952	948	1
21	514	462	11
22	2468	-2486	-5
23	750	596	39
24	1911	1897	4
25	295	175	12
26	1301	-1302	0
27	510	441	13
28	729	851	-34
29	369	-439	-11
30	265	372	-14
31	717	782	-17
32	1279	-1209	21
33	694	-713	-4
34	1396	1364	10
35	532	297	33

-6 5 1

1	759	780	-8
2	1525	1581	-24
3	820	-685	49
4	2100	-2049	19
5	773	657	41
6	2100	2066	12
7	604	-359	65
8	2257	-2266	-3
9	481	-241	50
10	1682	1614	27
11	449	400	12
12	705	-714	-3

13	540	-478	17
14	257	-366	-20
15	611	619	-2
16	1264	1267	-1
17	705	-608	28
18	1644	-1640	1
19	592	460	32
20	1843	1842	0
21	514	-116	58
22	1710	-1675	12
23	362	103	28
24	1431	1433	0
25	435	263	26
26	780	-834	-15
27	676	-656	5
28	193	28	8
29	616	678	-15
30	510	550	-8
31	568	-521	9
32	1263	-1295	-10
33	694	255	71
34	1621	1596	7
35	654	-198	65
36	1470	-1492	-6
37	557	-5	52

-5 5 1

1	1208	1151	25
2	4296	-4190	26
3	403	-101	55
4	3550	3517	9
5	1672	1749	-35
6	2485	-2481	1
7	824	818	2
8	3855	3928	-19
9	1683	-1678	2
10	1696	-1693	1
11	180	45	11
12	389	-478	-25
13	874	-958	-38
14	556	608	-17
15	175	79	8
16	1647	-1743	-40
17	328	-147	25
18	2625	2730	-36
19	252	-82	16
20	2319	-2369	-17
21	383	363	3
22	2242	2306	-22
23	745	-679	19
24	1531	-1492	14
25	409	382	4
26	802	860	-17
27	649	-686	-9
28	-160	34	-6
29	181	223	-3
30	1385	-1472	-30
31	449	-399	8
32	1432	1501	-23
33	312	350	-4
34	2003	-2059	-18
35	258	3	12
36	1740	1779	-12
37	585	-377	33
38	1633	-1545	25
39	651	532	21

-4 5 1

1	1231	-1214	8
2	1634	-1711	-36
3	1173	1155	9
4	2016	2128	-49
5	497	-416	27
6	1876	-1857	8
7	228	-6	22
8	1172	1190	-8
9	723	690	13
10	942	-901	19
11	1117	-1087	14
12	255	-55	23
13	1007	965	18
14	815	763	21
15	738	-726	4
16	1311	-1315	-1
17	484	408	20
18	1365	1349	6
19	265	85	19
20	1024	-1051	-10
21	565	-526	10
22	971	999	-10
23	646	613	9
24	572	-680	-30
25	691	-695	-1
26	203	192	1
27	692	816	-36
28	481	539	-12
29	449	-510	-12
30	871	-889	-5
31	368	230	16
32	1097	1123	-8
33	558	274	42
34	1106	-1128	-6
35	630	-380	42
36	1014	1002	3
37	498	498	0
38	478	-540	-10
39	463	-493	-4
40	-432	67	-35

-3 5 1

1	1403	1263	67
2	4530	4577	-11
3	1374	1414	-20
4	2602	-2698	-36
5	504	488	6
6	4807	4809	0
7	871	-784	43
8	1383	-1437	-27
9	1008	1043	-17
10	637	663	-11
11	1815	-1740	32
12	1565	1567	0
13	524	464	20
14	3112	-3176	-20
15	444	-273	40
16	3494	3527	-9
17	328	-22	35
18	2918	-3000	-27
19	322	-104	28
20	2678	2587	29
21	530	-526	0
22	1880	-1898	-6
23	661	726	-19
24	730	778	-14
25	-114	-275	-22
26	499	577	-18
27	276	308	-4
28	1339	-1250	29
29	445	96	38
30	2605	2504	30
31	540	255	41
32	2373	-2425	-16
33	618	189	58
34	2606	2589	5
35	389	124	24
36	903	-987	-22
37	334	-286	5
38	992	1074	-22
39	897	-878	4
40	424	474	-7
41	316	335	-2

-2 5 1

1	364	251	30
2	546	541	2
3	889	927	-20
4	651	-561	39
5	1455	-1490	-18
6	728	694	16
7	1502	1548	-23
8	822	-776	24
9	1505	-1521	-8
10	319	248	16
11	949	989	-19
12	284	243	8
13	703	-713	-4
14	571	-544	9
15	321	310	2
16	1069	1037	13
17	315	48	31
18	1199	-1177	9
19	407	-204	36
20	533	508	6
21	486	601	-32
22	147	-242	-10
23	610	-741	-39
24	-142	217	-17
25	409	606	-44
26	-193	55	-9
27	413	-532	-23
28	463	-401	10
29	-129	206	-12
30	455	576	-23
31	32	-23	0
32	670	-723	-12
33	179	-302	-11
34	685	710	-5
35	567	485	14
36	643	-701	-12
37	392	-610	-37
38	-345	314	-41
39	-253	415	-43
40	-376	4	-26
41	-298	-252	-27

-1 5 1

1	556	-308	83
2	6002	-5959	7
3	469	311	49
4	3850	3837	3
5	1354	1323	15
6	2035	-1962	30
7	345	-337	2
8	624	-472	54
9	76	139	-5
10	772	757	6
11	413	480	-20
12	3748	-3694	14
13	336	-32	38
14	4737	4725	2
15	749	-500	77
16	3701	-3753	-14
17	744	677	22
18	3642	3739	-26
19	1034	863	59
20	2051	-2044	2
21	441	538	-23
22	454	424	6
23	1056	-1117	-22
24	410	410	0
25	357	-256	13
26	2229	-2243	-4
27	530	32	53
28	2798	2782	4
29	592	-199	56
30	2312	-2394	-26
31	964	932	8
32	1980	1963	5
33	285	-171	9
34	1495	-1553	-18
35	487	-369	17
36	513	555	-7
37	-459	202	-50
38	173	-317	-12
39	-498	-8	-50
40	930	-944	-3
41	327	256	6

0 5 1

1	556	520	20
2	219	-8	29
3	1294	-1303	-6
4	348	148	53
5	1896	1877	10
6	503	-380	49
7	1576	-1576	0
8	484	428	21
9	1162	1155	4
10	248	-132	20
11	1006	-995	5
12	-220	0	-23
13	484	456	10
14	-100	168	-17
15	-200	-125	-24
16	626	-603	9
17	587	-536	19
18	737	707	13
19	1322	1293	14
20	624	-494	45
21	1351	-1299	25
22	339	-179	28
23	1236	1195	19
24	407	225	35
25	1339	-1299	18
26	497	-464	9
27	751	657	32
28	420	427	-1
29	-114	-264	-24
30	-228	-169	-23
31	-366	140	-45
32	-316	217	-42
33	-99	257	-20
34	-275	-24	-21
35	571	-596	-7
36	-154	-168	-13
37	607	701	-27
38	237	306	-9
39	579	-707	-37
40	-112	-254	-19
41	264	438	-29

1 5 1

0	3905	-3866	11
1	693	650	20
2	2957	2906	17
3	1164	-1110	27
4	1149	-1053	48
5	386	-445	-19
6	630	-714	-37
7	803	872	-32
8	1863	1803	25
9	1777	-1848	-31
10	2160	-2183	-9
11	169	-192	-3
12	3808	3876	-19
13	271	46	23
14	4323	-4344	-5
15	922	725	68
16	3889	3820	17
17	671	408	66
18	3061	-3027	10
19	1136	-1000	48
20	231	-276	-6
21	190	-332	-18
22	1022	1049	-9

23	450	27	43
24	2774	-2859	-26
25	801	-268	99
26	3402	3436	-9
27	1042	616	103
28	3239	-3156	22
29	950	533	92
30	2375	2403	-8
31	972	-936	9
32	1630	-1582	15
33	305	401	-12
34	444	465	-3
35	-254	-139	-16
36	256	445	-23
37	-272	-26	-14
38	828	-940	-28
39	119	-175	-2
40	1439	1453	-4
41	502	-42	39

2 5 1

0	275	101	30
1	1008	-985	12
2	87	-36	3
3	815	874	-31
4	65	-246	-26
5	1063	-1112	-26
6	335	388	-16
7	1139	1170	-15
8	403	-353	14
9	908	-891	8
10	442	465	-7
11	179	205	-3
12	621	-531	31
13	338	326	2
14	763	719	16
15	715	-706	3
16	291	-33	26
17	1350	1295	22
18	298	-146	19
19	1250	-1273	-9
20	421	342	15
21	1071	1157	-32
22	488	-418	14
23	617	-589	6
24	347	285	8
25	-336	57	-27
26	-113	-276	-19
27	411	410	0
28	297	251	4
29	466	-477	-2
30	67	-397	-29
31	645	641	0
32	-179	375	-32
33	866	-864	0
34	-298	-65	-18
35	739	833	-22
36	-306	83	-19
37	787	-767	4
38	-384	30	-28
39	186	463	-31
40	-291	-133	-18

3 5 1

0	4145	4195	-13
1	-47	-34	-1
2	391	-355	11
3	116	-162	-6
4	342	-357	-4
5	716	-630	37
6	1072	1013	29
7	1084	-1086	-1
8	3340	-3274	19
9	678	566	43
10	3892	3902	-2
11	358	46	46
12	3433	-3359	21
13	388	237	31
14	2915	2935	-6
15	250	-18	20
16	1930	-1901	11
17	-159	-102	-11
18	1097	1104	-2
19	545	681	-41
20	1065	1052	4
21	134	-288	-16
22	1551	-1589	-14
23	399	309	14
24	2870	2780	26
25	545	57	58
26	3124	-3171	-13
27	588	-523	13
28	2481	2561	-25
29	264	160	8
30	1314	-1330	-5
31	242	170	5
32	1137	1094	12
33	414	-594	-31
34	-391	133	-33
35	268	-342	-7
36	1294	-1353	-17
37	232	296	-5
38	1266	1152	30

4 5 1

0	1430	-1497	-33
1	1386	1420	-17
2	596	641	-19
3	990	-1022	-16
4	78	-83	0
5	375	415	-12
6	484	-451	10
7	406	-472	-20
8	779	745	14
9	297	310	-2
10	1178	-1173	2
11	183	75	10
12	1323	1360	-16
13	624	-628	-1
14	998	-995	1
15	748	760	-4
16	496	504	-2
17	766	-819	-18
18	-254	21	-19
19	398	560	-38
20	313	-369	-9
21	156	-425	-39
22	482	520	-8
23	99	127	-1
24	582	-685	-25
25	-159	221	-16
26	651	660	-2
27	353	-481	-21
28	696	-630	15
29	671	712	-9
30	-354	235	-37
31	499	-437	10
32	-334	-134	-26
33	-210	389	-37
34	-432	91	-39
35	-31	-567	-58
36	294	498	-27
37	-197	402	-34

5 5 1

0	422	-384	10
1	622	-585	13
2	175	-97	8
3	992	-977	6
4	1239	1184	24
5	1211	-1236	-11
6	3172	-3272	-31
7	422	328	23
8	2688	2699	-3
9	334	-166	27
10	2456	-2425	10
11	353	-303	10
12	1872	1865	2
13	144	202	-6
14	1586	-1573	5
15	305	-310	0
16	-220	234	-29
17	399	447	-10
18	594	566	7
19	734	-818	-26
20	1726	-1697	10
21	299	434	-23
22	2168	2144	8
23	404	211	25
24	2652	-2568	25
25	349	-144	21
26	2655	2511	42
27	967	866	28
28	1464	-1421	13
29	253	-456	-28
30	212	439	-28
31	-424	-47	-38
32	407	490	-13
33	-236	-124	-13
34	998	-1059	-16
35	355	-244	11

6 5 1

0	200	296	-16
1	494	-535	-12
2	546	577	-10
3	415	463	-12
4	1109	-1151	-17
5	380	-373	1
6	1372	1388	-6
7	355	247	19
8	1427	-1478	-21
9	252	187	8
10	1437	1448	-4
11	466	-406	13
12	1063	-1028	13
13	601	606	-1
14	579	575	1
15	561	-679	-33
16	219	279	-7
17	648	783	-40
18	938	-971	-10
19	656	-736	-22
20	1343	1340	1
21	398	300	15
22	1356	-1266	29
23	211	-6	9
24	1183	1086	30
25	277	-102	13
26	798	-756	10
27	482	472	1
28	-258	77	-15
29	482	-629	-29
30	-241	263	-25
31	265	414	-18
32	712	-673	8

7 5 1

0	774	747	9
1	788	744	14
2	917	869	17
3	213	-223	-1
4	1889	-1947	-22
5	315	165	19
6	2686	2653	10
7	363	101	32
8	2347	-2341	2
9	338	-66	28
10	2419	2487	-23
11	175	189	-1
12	117	23	3
13	488	-580	-22
14	496	-499	0
15	-206	-161	-17
16	-53	292	-21
17	57	-1	0
18	1422	-1387	12
19	774	756	4
20	1507	1476	10
21	559	-566	-1
22	1221	-1071	46
23	619	537	17
24	1153	1179	-8
25	58	178	-6
26	1141	-1216	-23
27	375	-419	-6
28	744	733	2
29	-282	228	-26

8 5 1

0	830	801	9
1	532	459	17
2	1500	-1492	2
3	523	-329	38
4	1788	1781	2
5	385	132	31
6	1884	-1878	2
7	364	-31	31
8	1347	1386	-14
9	451	-303	25
10	1043	-1049	-1
11	540	588	-11
12	606	616	-2
13	454	-467	-2
14	-223	117	-15
15	-247	67	-16
16	679	-607	17
17	235	-148	7
18	1037	963	22
19	384	241	18
20	1327	-1268	19
21	169	-177	0
22	1110	1185	-24
23	-74	-27	-1
24	876	-830	12
25	421	268	19

9 5 1

0	289	266	3
1	926	-795	39
2	1324	-1321	1
3	519	501	3
4	1264	1297	-11
5	393	63	34
6	1467	-1475	-2
7	489	-399	17
8	1765	1755	3
9	524	369	29
10	588	-604	-3
11	458	-491	-6
12	311	-414	-16
13	314	426	-18
14	98	340	-24
15	586	-442	24
16	1260	-1246	4
17	182	116	4
18	765	869	-28
19	269	187	7
20	885	-895	-2

10 5 1

0	1336	-1283	17
1	343	-137	22

2	1641	1583	19
3	359	9	28
4	1614	-1604	3
5	342	231	14
6	1398	1361	12
7	502	-242	39
8	1116	-999	36
9	131	307	-17
10	313	337	-3
11	65	-285	-16
12	302	336	-4
13	139	227	-6

-10 6 1

1	353	396	-7
2	969	-947	6
3	-272	-100	-20
4	250	323	-9
5	-22	-319	-24
6	768	-690	20
7	105	276	-15
8	187	328	-16
9	961	-976	-4
10	-273	24	-18
11	679	809	-36
12	253	192	5
13	1376	-1379	0
14	375	190	21
15	773	818	-12
16	421	-394	4
17	485	-572	-18
18	782	768	3

-9 6 1

1	413	518	-22
2	336	356	-3
3	262	169	9
4	192	-287	-11
5	780	-723	16
6	279	-12	18
7	1330	1275	19
8	476	317	27
9	1522	-1531	-3
10	615	-412	42
11	1360	1354	2
12	601	471	28
13	1193	-1084	36
14	423	-328	15
15	518	494	5
16	368	349	3
17	271	190	8
18	-93	-175	-9
19	852	-862	-2
20	302	-27	19
21	1403	1383	6
22	529	316	35
23	1745	-1771	-8
24	670	-262	67
25	1523	1538	-4

-8 6 1

1	-184	71	-10
2	1295	1283	4
3	941	-993	-18
4	918	-870	15
5	1328	1418	-34
6	919	926	-2
7	1157	-1156	0
8	112	7	3
9	1393	1436	-16
10	328	-263	9
11	1151	-1157	-2
12	295	-297	0
13	1108	1094	4
14	565	-519	10
15	918	-864	17
16	-27	-125	-4
17	360	345	2
18	1274	-1221	18
19	353	477	-23
20	524	491	7
21	1413	-1413	0
22	520	-409	21
23	1725	1711	4
24	603	434	33
25	1658	-1644	4
26	439	-241	27
27	1152	1234	-26
28	597	-499	19
29	519	-539	-3
30	643	628	3

-7 6 1

1	582	626	-12
2	545	-497	12
3	1280	-1279	0
4	343	71	30
5	1950	1992	-16
6	556	310	51
7	2083	-2058	9
8	555	-501	13
9	1604	1580	9
10	752	624	37
11	1200	-1184	5
12	955	-1024	-25
13	353	319	5
14	649	646	1
15	466	568	-25
16	334	-362	-4
17	992	-998	-2
18	521	299	40
19	1657	1681	-8
20	628	272	66
21	1608	-1576	11
22	725	-520	48
23	1632	1588	15
24	914	726	51
25	1446	-1369	25
26	790	-639	37
27	683	574	25
28	790	702	22
29	280	238	4
30	433	-390	6
31	1056	-991	18
32	434	39	35
33	1503	1469	10

-6 6 1

1	966	-986	-7
2	1793	-1721	28
3	2575	2603	-9
4	2004	1974	11
5	2662	-2609	17
6	1338	-1271	27
7	2561	2561	0
8	801	698	34
9	1721	-1734	-5
10	297	166	17
11	1141	1165	-9
12	605	-572	9
13	459	-549	-23
14	342	327	2
15	565	-668	-30
16	887	-794	30
17	1130	1117	4
18	1259	1294	-13
19	1611	-1611	0
20	394	-207	26
21	2215	2140	25
22	855	765	26
23	1868	-1836	11
24	441	248	29
25	2226	2227	0
26	238	1	12
27	374	-489	-20
28	270	-263	0
29	331	341	-1
30	939	-924	4
31	891	926	-9
32	996	913	23
33	1688	-1677	3
34	773	-585	40
35	1772	1679	28
36	644	309	51

-5 6 1

1	1456	-1518	-27
2	430	175	50
3	2106	2210	-42
4	749	613	48
5	1965	-2007	-17
6	766	-662	38
7	1793	1805	-4
8	485	357	33
9	1311	-1279	13
10	598	-605	-2
11	19	-25	0
12	666	670	-1
13	685	634	16
14	715	-752	-13
15	1030	-971	22
16	563	523	10
17	1417	1430	-5
18	292	-142	17
19	1321	-1319	0
20	294	-227	9
21	1055	1052	1
22	441	353	16
23	885	-948	-21
24	757	-678	21
25	506	527	-4
26	775	691	22
27	262	-146	10
28	635	-643	-1
29	512	-602	-19
30	505	332	27
31	1100	1103	-1
32	492	6	45
33	1177	-1188	-3
34	668	-337	55
35	1214	1182	9
36	686	549	26
37	900	-883	4

-4 6 1

1	2146	2148	0
2	1737	1703	14
3	3688	-3693	-1
4	411	-140	54
5	3711	3801	-25
6	1153	1126	12
7	2711	-2678	11
8	514	563	-17
9	1805	1841	-15
10	218	-208	1
11	464	-431	9
12	1087	1035	21
13	1024	-1124	-45
14	1299	-1305	-2
15	1552	1574	-9
16	555	556	0
17	2433	-2546	-40
18	990	-938	19
19	2430	2413	5
20	524	464	14
21	2230	-2225	1
22	172	134	3
23	1888	1870	6
24	842	-741	29
25	1307	-1297	3
26	444	391	9
27	380	-427	-8
28	-91	58	-2
29	734	888	-43
30	1415	1322	29
31	1942	-1980	-12
32	639	-510	25
33	1833	1800	10
34	1035	952	22
35	1746	-1712	10
36	409	-176	23
37	1694	1640	16
38	159	-79	3
39	653	-664	-1

-3 6 1

1	986	1009	-11
2	584	636	-22
3	1014	-975	19
4	946	-989	-21
5	773	705	29
6	1486	1572	-41
7	990	-915	35
8	1614	-1701	-40
9	402	315	22
10	1342	1385	-20
11	454	325	34
12	1440	-1445	-2
13	1026	-926	44
14	1217	1158	25
15	1046	1028	7
16	504	-414	23
17	1050	-1063	-5
18	540	-471	18
19	979	941	14
20	881	838	14
21	701	-612	25
22	1000	-964	13
23	424	363	11
24	1129	1176	-17
25	277	-51	17
26	1158	-1151	2
27	372	-199	20
28	710	718	-1
29	418	597	-35
30	-195	-161	-13
31	891	-922	-8
32	269	-131	10
33	750	737	2
34	505	362	21
35	676	-722	-10
36	788	-794	-1
37	304	284	2
38	599	697	-19
39	-322	25	-18
40	514	-690	-32

-2 6 1

1	3892	-3900	-2
2	1659	-1684	-11
3	3992	3937	14
4	1511	1583	-35
5	2929	-2857	24
6	1377	-1380	-1
7	2054	2078	-10
8	721	-646	30
9	1103	-1061	19
10	253	178	12
11	1272	-1158	50
12	1683	-1621	26
13	2151	2142	3
14	1941	1842	39
15	3715	-3683	8

16	881	-860	8
17	3476	3443	9
18	592	426	42
19	2958	-2793	50
20	989	-886	35
21	1309	1319	-3
22	328	-387	-10
23	276	-363	-13
24	445	569	-26
25	379	-477	-17
26	450	-388	10
27	1603	1577	8
28	542	431	20
29	1783	-1759	7
30	549	-437	19
31	1971	1971	0
32	469	160	33
33	2003	-1987	4
34	1087	-951	35
35	1486	1502	-4
36	245	83	9
37	1072	-1170	-27
38	-269	-215	-21
39	-288	-91	-16
40	559	-634	-13

-1	6	1	
1	374	-340	10
2	888	-906	-8
3	223	76	18
4	1034	999	16
5	343	332	2
6	993	-952	19
7	293	-295	0
8	1083	1011	32
9	584	506	26
10	789	-773	6
11	514	-485	8
12	662	597	22
13	693	697	-1
14	-159	-22	-8
15	496	-448	12
16	233	-224	1
17	256	125	14
18	880	853	9
19	191	-138	4
20	1048	-1100	-18
21	374	-228	20
22	913	920	-2
23	501	410	17
24	737	-872	-39
25	611	-597	3
26	854	861	-1
27	785	816	-8
28	502	-532	-5
29	403	-423	-3
30	-288	51	-17
31	-408	282	-50
32	-265	394	-43
33	-136	-221	-12
34	726	-722	0
35	179	85	4
36	888	1008	-31
37	-376	29	-27
38	563	-706	-28
39	-379	-16	-26
40	561	568	-1

0	6	1	
0	1596	1520	35
1	3718	3650	21
2	826	855	-19
3	2320	-2239	37
4	750	-798	-30
5	2148	2097	24
6	465	461	1
7	-53	-311	-51
8	339	-335	1
9	255	-300	-11
10	282	-341	-16
11	3029	2963	24
12	1362	1233	66
13	4668	-4664	1
14	957	-788	77
15	4092	4006	24
16	1498	1342	74
17	2764	-2748	6
18	1105	-927	80
19	2714	2734	-7
20	459	-411	13
21	-134	240	-26
22	-180	-201	-24
23	1005	-1042	-16
24	1070	-1023	20
25	1766	1724	18
26	1193	973	89
27	3133	-3177	-14
28	1116	-784	117
29	2708	2698	3
30	591	384	48
31	2005	-2000	1
32	398	66	38
33	1781	1718	25
34	343	282	9
35	400	-582	-43
36	-375	54	-39
37	-326	40	-28
38	-383	-104	-42
39	873	964	-31
40	652	563	22

1	6	1	
0	377	424	-15
1	425	-425	0
2	300	253	11
3	408	368	12
4	853	-815	18
5	722	-725	-1
6	1053	1003	22
7	446	404	12
8	1497	-1432	28
9	282	-37	26
10	1386	1390	-1
11	377	-273	20
12	848	-863	-5
13	577	503	20
14	169	-94	5
15	108	-135	-1
16	362	286	13
17	269	44	18
18	672	-642	8
19	416	-334	14
20	1103	1102	0
21	344	144	21
22	1091	-1130	-13
23	208	-128	5
24	1156	1281	-42
25	298	356	-7
26	737	-743	-1
27	-196	-105	-10
28	-85	151	-6
29	-337	-14	-23
30	-326	130	-24
31	-324	257	-34
32	120	-374	-23
33	76	-324	-18
34	578	697	-24
35	454	325	16
36	829	-851	-5
37	-159	-223	-13
38	440	595	-26
39	-215	67	-9

2	6	1	
0	426	329	30
1	3179	-3185	-1
2	360	229	33
3	1151	1138	6
4	266	-106	26
5	934	906	13
6	1403	-1372	14
7	1969	-2001	-13
8	529	-407	38
9	1993	2026	-13
10	1064	1043	9
11	3681	-3691	-2
12	837	-701	49
13	3362	3459	-29
14	1153	1079	29
15	3076	-3025	15
16	315	-252	10
17	2421	2338	28
18	916	1012	-37
19	967	-953	4
20	-242	32	-15
21	645	-741	-26
22	-274	-240	-31
23	1676	1695	-6
24	860	767	25
25	2978	-2913	18
26	1060	-944	33
27	3165	3136	8
28	1033	911	32
29	2257	-2235	6
30	404	55	28
31	1527	1603	-24
32	260	249	0
33	185	-299	-9
34	-403	-259	-44
35	-401	-166	-36
36	-159	-298	-20
37	617	714	-19
38	-243	56	-11

3	6	1	
0	314	202	24
1	782	810	-13
2	921	-914	3
3	465	-405	19
4	1382	1399	-8
5	229	75	19
6	1200	-1200	0
7	213	-27	17
8	1103	1095	3
9	421	-298	30
10	674	-659	5
11	1161	1060	42
12	46	43	0
13	1074	-1080	-2
14	340	353	-2
15	832	888	-22
16	852	-834	6
17	592	-598	-1
18	1018	1015	1
19	-222	-41	-13
20	1119	-1158	-13
21	171	176	0
22	954	975	-6
23	462	-472	-1
24	636	-683	-11
25	430	459	-5
26	232	201	2
27	546	-686	-31
28	421	471	-8
29	416	539	-21
30	764	-872	-27
31	341	-361	-2
32	639	697	-12
33	-199	436	-42
34	702	-767	-14
35	257	-230	2
36	675	722	-9
37	-321	29	-18

4	6	1	
0	379	-241	31
1	1253	1239	6
2	1070	-1049	9
3	523	595	-26
4	226	15	19
5	1123	-1130	-2
6	807	818	-4
7	2574	2594	-7
8	295	-228	12
9	2253	-2235	6
10	1142	-1052	37
11	2592	2620	-9
12	882	924	-16
13	2308	-2266	15
14	1255	-1213	16
15	1394	1367	10
16	629	723	-29
17	320	-445	-24
18	573	-528	11
19	155	-337	-22
20	-169	-68	-8
21	1554	1620	-24
22	253	-166	8
23	2812	-2809	0
24	854	-884	-8
25	2407	2256	46
26	1866	1773	30
27	2402	-2467	-20
28	960	-902	15
29	1540	1569	-9
30	-310	-77	-20
31	-277	-242	-26
32	351	-465	-16
33	537	-552	-2
34	-407	65	-32
35	1130	1173	-11

5	6	1	
0	667	-687	-7
1	1101	-1201	-45
2	658	658	0
3	445	411	9
4	896	-941	-19
5	586	570	5
6	1116	1106	3
7	1094	-1063	12
8	898	-904	-2
9	1382	1400	-7
10	487	433	13
11	1375	-1358	6
12	336	166	23
13	1269	1273	-1
14	579	-594	-4
15	753	-785	-10
16	706	647	16
17	-183	205	-20
18	899	-866	10
19	454	470	-3
20	1010	996	4
21	980	-992	-3
22	759	-737	5
23	1127	1100	8
24	426	271	21
25	796	-822	-7
26	424	344	12
27	691	641	11
28	404	-421	-2
29	471	-508	-6
30	561	672	-23
31	-384	65	-31

32	671	-706	-7
33	167	347	-16

6 6 1

0	1212	1139	29
1	-214	3	-15
2	231	-280	-7
3	1915	-1886	11
4	-118	-77	-6
5	2204	2197	2
6	445	140	47
7	2946	-2908	11
8	376	-192	28
9	2529	2419	36
10	1219	1270	-19
11	1167	-1203	-13
12	537	-453	19
13	769	799	-9
14	398	417	-3
15	161	442	-43
16	769	-831	-19
17	887	-786	30
18	169	-84	5
19	487	558	-15
20	609	668	-15
21	1721	-1729	-2
22	563	429	25
23	2118	2079	12
24	832	710	31
25	1685	-1596	28
26	1250	-1249	0
27	1499	1463	11
28	524	595	-14
29	-182	-230	-17
30	-281	-372	-43

7 6 1

0	843	854	-3
1	58	-193	-9
2	935	-982	-17
3	1012	998	4
4	1018	970	18
5	1492	-1457	13
6	632	-517	29
7	1685	1613	26
8	471	366	21
9	1707	-1669	13
10	319	-32	24
11	1215	1213	0
12	664	-655	2
13	501	-528	-6
14	959	962	-1
15	221	70	10
16	978	-963	4
17	292	285	0
18	746	739	1
19	947	-928	5
20	736	-715	5
21	1263	1281	-5
22	450	272	25
23	995	-1084	-27
24	88	104	0
25	615	621	-1
26	487	-488	0
27	112	-226	-7

8 6 1

0	961	-905	18
1	914	-923	-2
2	-152	-241	-21
3	1176	1182	-2
4	290	-43	20
5	1877	-1891	-4
6	372	-109	29
7	2196	2121	25
8	1072	917	50
9	1025	-1142	-41
10	1342	-1329	4
11	754	825	-21
12	-148	-14	-5
13	102	85	0
14	637	-638	0
15	1175	-1102	23
16	317	272	5
17	1106	1053	17
18	-84	146	-6
19	1364	-1379	-5
20	128	-119	0
21	990	1037	-14
22	400	363	5
23	1082	-1092	-2

9 6 1

0	345	-369	-3
1	1145	1216	-25
2	607	420	39
3	1579	-1577	0
4	615	-473	31
5	1654	1588	22
6	683	570	27
7	1348	-1426	-28
8	267	-128	12
9	935	904	9
10	127	-225	-8
11	143	-271	-12
12	140	224	-6
13	37	-117	-2
14	-249	-235	-27
15	733	717	4
16	477	481	0
17	1027	-1008	5
18	521	-267	37

10 6 1

0	564	588	-5
1	291	386	-14
2	-141	230	-17
3	725	-758	-8
4	353	-387	-5
5	941	965	-7
6	464	470	-1
7	1163	-1151	3
8	831	-739	23
9	821	813	2
10	931	900	8

-10 7 1

1	669	650	4
2	201	-203	0
3	398	-428	-5
4	407	-329	12
5	124	180	-3
6	940	928	3
7	297	139	14
8	1136	-1111	8
9	677	-535	31
10	1252	1236	5
11	698	611	20
12	1058	-997	18
13	753	-644	26

-9 7 1

1	114	286	-16
2	281	197	9
3	1250	-1246	1
4	325	328	0
5	1102	1117	-4
6	460	-416	8
7	632	-588	10
8	486	563	-17
9	1094	1167	-26
10	533	-572	-8
11	-174	-72	-8
12	1041	1039	0
13	430	321	17
14	1503	-1515	-4
15	610	453	32
16	1097	1037	18
17	374	-405	-5
18	-185	-236	-20
19	945	866	22
20	268	-305	-4
21	909	-947	-10
22	1085	1063	6

-8 7 1

1	514	-626	-28
2	456	-453	0
3	189	228	-4
4	1086	1143	-21
5	372	273	15
6	1340	-1381	-15
7	668	-603	17
8	1372	1426	-19
9	799	768	9
10	1176	-1192	-5
11	1175	-1175	0
12	633	512	28
13	1062	1068	-2
14	308	-262	6
15	817	-797	5
16	232	-139	8
17	-64	173	-8
18	794	812	-5
19	415	398	2
20	1277	-1315	-12
21	891	-738	41
22	1457	1459	0
23	1003	842	45
24	1463	-1433	9
25	984	-837	40
26	1107	1071	10
27	809	808	0
28	465	-385	12

-7 7 1

1	1496	-1533	-14
2	445	483	-8
3	1598	1662	-24
4	954	-945	3
5	1889	-1873	5
6	1406	1463	-22
7	1434	1529	-37
8	1255	-1236	6
9	289	-280	1
10	1059	1103	-16
11	319	476	-31
12	969	-1056	-31
13	381	-338	7
14	505	463	9
15	1348	-1389	-15
16	655	-690	-9
17	804	868	-19
18	81	-349	-28
19	502	-518	-3
20	882	940	-18
21	1754	1752	0
22	1393	-1420	-9
23	605	-370	45
24	1647	1671	-8
25	604	474	26
26	1416	-1532	-40
27	64	-75	0
28	980	1014	-10
29	-138	-296	-22
30	190	-108	4
31	1343	1218	37

-6 7 1

1	280	-2	22
2	1726	1742	-6
3	588	495	25
4	1680	-1705	-10
5	722	-596	37
6	1480	1549	-28
7	967	929	13
8	1132	-1172	-15
9	1127	-1072	21
10	520	544	-6
11	843	852	-3
12	97	212	-9
13	864	-868	-1
14	700	-710	-3
15	520	555	-8
16	1128	1147	-7
17	284	-24	20
18	1217	-1271	-21
19	653	-571	21
20	1401	1340	21
21	965	918	15
22	1447	-1395	18
23	979	-866	33
24	748	655	24
25	969	958	3
26	575	-452	24
27	913	-913	0
28	438	-331	16
29	511	363	24
30	898	908	-2
31	458	115	37
32	1242	-1218	7
33	778	-490	56
34	1298	1271	7

-5 7 1

1	618	454	46
2	1870	-1857	5
3	2790	-2739	16
4	2866	2837	9
5	1975	1992	-6
6	2866	-2735	41
7	717	-508	63
8	2190	2232	-16
9	326	111	27
10	1239	-1218	8
11	-113	-86	-6
12	144	221	-8
13	1070	-1036	12
14	269	299	-4
15	1373	1316	21
16	1244	-1181	23
17	1288	-1215	27
18	1674	1822	-58
19	1600	1543	21
20	1769	-1770	0
21	1108	-1044	21
22	1910	1874	12
23	377	-1	31
24	1844	-1912	-24
25	1122	-1014	33
26	794	804	-2
27	707	-706	0
28	192	-252	-5
29	282	279	0
30	412	-370	6
31	1232	-1243	-3
32	1586	1563	7
33	1145	1057	26
34	1918	-1802	34
35	1244	-1079	44
36	1523	1495	8

-4 7 1

1	276	50	26
2	1260	-1317	-26
3	687	-680	2
4	1232	1283	-23
5	1312	1326	-6
6	633	-572	20
7	1471	-1493	-9
8	400	233	33
9	1771	1795	-9
10	361	122	36
11	1703	-1711	-3
12	738	-663	25
13	983	1001	-7
14	1044	1053	-3
15	358	-323	6
16	991	-1109	-48
17	439	-408	6
18	1089	1102	-4
19	1045	1002	15
20	857	-785	22
21	1280	-1233	17
22	418	457	-7
23	1045	1077	-10
24	-144	-131	-9
25	867	-913	-14
26	269	-268	0
27	909	920	-3
28	766	765	0
29	361	-383	-3
30	684	-718	-8
31	427	-107	31
32	933	975	-11
33	728	699	6
34	853	-882	-7
35	916	-800	27
36	617	520	17
37	907	923	-3

-3 7 1

1	750	-787	-15
2	3023	3052	-9
3	1788	1794	-2
4	3640	-3624	4
5	2576	-2569	2
6	3440	3401	11
7	966	951	6
8	2199	-2145	20
9	139	-159	-2
10	1191	1153	16
11	899	-904	-2
12	970	998	-11
13	1093	1025	27
14	2097	-2067	11
15	1555	-1600	-18
16	2302	2396	-34
17	1955	1981	-10
18	1920	-1933	-4
19	1225	-1196	11
20	1399	1423	-9
21	279	254	3
22	1342	-1360	-6
23	-239	226	-26
24	942	913	9
25	422	-437	-2
26	-301	-188	-28
27	944	922	6
28	271	-343	-8
29	918	-867	13
30	1413	1396	5
31	1330	1305	8
32	1675	-1695	-6
33	766	-768	0
34	1796	1876	-25
35	895	842	12
36	1551	-1580	-8
37	669	-564	19
38	1016	962	12

-2 7 1

1	186	-4	14
2	467	320	42
3	564	548	6
4	504	-506	0
5	1018	-988	13
6	331	-75	38
7	1165	1144	9
8	767	674	35
9	1224	-1156	29
10	863	-738	48
11	1139	1065	30
12	1235	1161	30
13	563	-500	18
14	1249	-1227	9
15	341	-108	30
16	1245	1261	-6
17	688	624	19
18	584	-593	-2
19	912	-912	0
20	257	-35	15
21	1029	1056	-9
22	380	398	-3
23	896	-993	-30
24	605	-562	9
25	700	775	-19
26	821	822	0
27	578	-593	-3
28	882	-950	-18
29	-338	132	-27
30	574	647	-15
31	224	251	-2
32	465	-535	-12
33	424	-523	-16
34	369	273	10
35	616	744	-27
36	-209	114	-10
37	522	-660	-25
38	111	-321	-15
39	143	382	-20

-1 7 1

1	1201	1165	17
2	3061	-3068	-2
3	1636	-1598	16
4	2885	2770	37
5	920	1004	-38
6	2100	-2022	30
7	1109	-951	64
8	520	403	32
9	231	57	16
10	693	694	0
11	2569	2428	47
12	2522	-2389	44
13	1326	-1290	14
14	3342	3369	-7
15	2359	2195	54
16	3147	-3114	9
17	1205	-1191	5
18	2473	2458	5
19	1686	1685	0
20	1244	-1344	-38
21	88	-262	-13
22	-263	177	-22
23	1065	-1108	-14
24	332	517	-31
25	591	600	-1
26	1390	-1441	-16
27	1004	-836	43
28	2005	2028	-7
29	1673	1565	33
30	1645	-1732	-27
31	890	-754	31
32	1467	1579	-35
33	734	695	8
34	1274	-1311	-10
35	682	-791	-24
36	433	656	-40
37	-412	74	-33
38	341	-340	0
39	1035	1098	-16

0 7 1

1	308	322	-4
2	226	-23	28
3	1063	-1093	-18
4	448	-358	35
5	1656	1673	-9
6	485	280	68
7	1704	-1654	25
8	949	-806	72
9	1443	1388	28
10	1098	971	63
11	1320	-1270	25
12	586	-493	33
13	658	628	11
14	26	-90	-2
15	114	0	4
16	-211	-111	-20
17	353	-414	-15
18	617	-585	10
19	728	746	-6
20	874	878	-1
21	808	-850	-16
22	901	-890	4
23	772	819	-17
24	712	725	-4
25	763	-831	-24
26	428	-470	-9
27	400	440	-8
28	-187	349	-43
29	-221	-85	-15
30	-276	-133	-25
31	-306	-204	-36
32	-208	-16	-11
33	425	519	-21
34	-198	205	-21
35	588	-699	-31
36	210	-402	-29
37	611	727	-33
38	-206	241	-24
39	517	-645	-15

1 7 1

0	2010	-1982	11
1	949	-946	1
2	1421	1385	17
3	1792	1808	-7
4	644	-649	-1
5	839	-838	0
6	-126	-97	-9
7	107	222	-13
8	406	334	15
9	138	55	5
10	1246	-1195	20
11	3378	-3294	23
12	2881	2870	3
13	2543	2507	11
14	3318	-3327	-2
15	1591	-1635	-16
16	2616	2595	6
17	1265	1138	45
18	2272	-2287	-4
19	1426	-1406	6
20	347	361	-2
21	443	-501	-10
22	783	945	-47
23	868	888	-5
24	1761	-1728	10
25	1394	-1282	34
26	2661	2633	8
27	2089	2026	19
28	2311	-2252	17
29	1453	-1419	10
30	1506	1494	3
31	715	680	7
32	1321	-1351	-8
33	417	-466	-7
34	541	564	-4
35	310	489	-24
36	-422	98	-36
37	-190	146	-10
38	326	-355	-3

2 7 1

0	693	505	70
1	490	-539	-18
2	720	-662	23
3	871	944	-34
4	593	545	17
5	1190	-1166	11
6	338	-159	32
7	1330	1265	28
8	273	207	11
9	1287	-1288	0
10	142	37	6
11	582	587	-1
12	-164	-155	-16
13	90	23	2
14	546	569	-6
15	603	-684	-24
16	705	-709	-1
17	1332	1367	-13
18	538	448	19
19	1336	-1351	-5
20	487	-436	9
21	1313	1291	7
22	481	355	20
23	1002	-931	20
24	-131	-246	-16
25	395	512	-20
26	-337	243	-35
27	-225	-77	-11
28	-292	215	-25
29	124	-203	-4
30	582	-608	-5
31	269	391	-14
32	643	553	16
33	660	-714	-11
34	479	-571	-15
35	508	592	-14
36	483	588	-17
37	288	-478	-24

3 7 1

0	1775	1801	-11
1	2160	2098	24
2	837	-799	17
3	275	76	26
4	149	-155	0
5	85	-93	0
6	938	1035	-44
7	336	267	14
8	1700	-1723	-9
9	1213	-1139	31
10	2065	2090	-9
11	2302	2349	-17
12	2288	-2343	-20
13	1497	-1412	33
14	2150	2178	-10
15	1521	1515	2
16	1353	-1410	-22
17	1043	-1093	-18
18	411	499	-18

19	-180	66	-9
20	321	321	0
21	-131	309	-26
22	1378	-1518	-50
23	1093	-1117	-7
24	2398	2426	-8
25	1318	1255	19
26	2426	-2311	34
27	1647	-1634	4
28	2009	1931	24
29	1110	1116	-1
30	552	-796	-55
31	79	-396	-27
32	-420	8	-34
33	-274	-233	-23
34	249	609	-52
35	258	-160	6
36	1033	-990	10

4 7 1

0	1062	-1067	-2
1	880	869	4
2	939	897	17
3	1156	-1199	-19
4	670	-758	-34
5	1212	1261	-21
6	307	198	17
7	1003	-1066	-27
8	269	266	0
9	580	611	-9
10	753	-774	-7
11	423	-386	8
12	961	1090	-53
13	348	-302	8
14	1012	-1041	-10
15	652	675	-6
16	751	793	-13
17	728	-803	-23
18	752	-796	-13
19	814	851	-11
20	119	144	-1
21	954	-926	2
22	464	548	-17
23	736	786	-13
24	527	-605	-16
25	410	-299	15
26	570	601	-6
27	79	100	0
28	616	-667	-11
29	470	368	15
30	705	806	-23
31	416	-572	-26
32	424	-553	-21
33	638	682	-8
34	230	383	-16

5 7 1

0	503	-574	-21
1	1052	-1087	-14
2	1090	-1082	3
3	229	-273	-6
4	1886	1867	7
5	434	220	39
6	1875	-1885	-3
7	874	-848	9
8	2383	2407	-3
9	1321	1305	6
10	1671	-1630	15
11	1259	-1256	1
12	1257	1365	-43
13	1142	1199	-21
14	744	-819	-24
15	583	-652	-19
16	-198	-31	-10
17	-129	-116	-7
18	-188	-11	-8
19	-163	-290	-26
20	1046	-1123	-25
21	801	-759	11
22	1758	1733	8
23	1809	1758	16
24	1825	-1808	5
25	981	-969	3
26	1732	1717	4
27	1341	1333	2
28	1020	-969	14
29	650	-814	-39
30	-405	-4	-33
31	-190	355	-30

6 7 1

0	1321	1387	-26
1	550	-513	9
2	280	-331	-8
3	1001	998	1
4	356	-273	14
5	1029	-1008	8
6	1063	1075	-4
7	945	1005	-22
8	1432	-1332	37
9	634	-677	-12
10	1525	1518	2
11	333	117	24
12	1487	-1537	-18
13	409	346	11
14	1094	1097	-1
15	617	-674	-15
16	485	-472	2
17	911	894	5
18	221	-95	9
19	877	-882	-1
20	614	528	18
21	486	404	14
22	811	-840	-8
23	208	-175	2
24	873	889	-4
25	221	152	5
26	849	-835	3
27	182	381	-21
28	368	370	0
29	379	-517	-22

7 7 1

0	744	-705	11
1	303	305	0
2	1344	1341	1
3	755	769	-4
4	1651	-1622	10
5	484	-473	2
6	2289	2355	-22
7	1242	1266	-9
8	1801	-1770	11
9	640	-569	18
10	1126	1168	-14
11	1244	1241	1
12	257	-185	7
13	1174	-1094	26
14	719	-695	6
15	186	-153	2
16	1338	1308	10
17	362	-226	17
18	1194	-1132	20
19	642	-549	20
20	979	1041	-19
21	308	526	-37
22	1161	-1148	4
23	734	-709	6
24	936	896	10
25	1179	1094	25

8 7 1

0	196	123	5
1	871	906	-11
2	643	-541	24
3	840	-874	-10
4	1145	1092	17
5	904	853	15
6	1458	-1459	0
7	856	-819	11
8	1232	1240	-2
9	623	470	33
10	878	-820	17
11	113	-71	1
12	403	388	2
13	-303	-327	-48
14	-156	-57	-6
15	365	473	-19
16	125	-247	-10
17	730	-717	3
18	913	859	15
19	865	782	21
20	1319	-1170	44
21	796	-639	36

9 7 1

0	342	332	1
1	-229	-124	-16
2	929	-918	3
3	229	-45	11
4	1086	1120	-11
5	933	951	-5
6	1212	-1134	25
7	1100	-1087	4
8	1029	1127	-32
9	954	785	46
10	301	-348	-6
11	386	-495	-19
12	274	-378	-14
13	881	846	9
14	822	829	-1
15	323	-240	9

10 7 1

0	774	-736	10
1	1060	-935	36
2	1179	1167	3
3	1143	936	59
4	1138	-1155	-5
5	717	-574	32

-9 8 1

1	-122	-216	-14
2	426	501	-14
3	492	482	2
4	-199	78	-10
5	781	-781	0
6	586	-429	31
7	1281	1238	14
8	1008	954	16
9	1181	-1199	-6
10	1275	-1256	6
11	1046	982	19
12	966	990	-7
13	740	-730	2
14	733	-776	-11
15	-176	35	-7
16	89	166	-4
17	293	281	1
18	453	377	12

-8 8 1

1	528	-505	5
2	584	617	-8
3	113	233	-10
4	1413	-1339	25
5	508	476	6
6	1189	1313	-44
7	384	-342	6
8	955	-989	-11
9	438	458	-3
10	1042	1044	0
11	624	-627	0
12	755	-774	-5
13	928	908	6
14	423	-318	16
15	1325	-1326	0
16	600	442	32
17	527	598	-16
18	1328	-1354	-8
19	447	-336	17
20	941	910	8
21	719	-644	18
22	1248	-1198	15
23	1286	1255	9
24	581	523	11
25	1338	-1336	0

-7 8 1

1	601	605	0
2	209	-87	9
3	1013	-1016	0
4	222	-176	4
5	1289	1304	-5
6	720	750	-8
7	1029	-998	10
8	1027	-989	12
9	820	741	23
10	1234	1248	-4
11	513	-359	29
12	1377	-1435	-21
13	349	-269	11
14	761	716	12
15	927	907	6
16	306	-92	19
17	1042	-1036	1
18	443	-378	11
19	1128	1147	-6
20	935	906	8
21	1134	-1031	32
22	1152	-1038	35
23	868	873	-1
24	1197	1106	28
25	583	-543	8
26	833	-859	-7
27	230	61	10
28	524	566	-8
29	562	540	4

-6 8 1

1	317	-282	5
2	1900	-1956	-21
3	744	737	1
4	1220	1277	-22
5	1100	-1064	13
6	1656	-1653	1
7	1511	1536	-9
8	1525	1482	16
9	694	-682	3
10	437	-371	13
11	543	650	-29
12	100	-116	-6
13	307	-231	10
14	480	528	-11
15	488	426	12
16	919	-1015	-33
17	239	-13	13
18	2015	1956	20
19	668	-700	-8
20	846	-935	-28
21	587	504	18
22	1306	1254	18

23	1578	-1593	-5
24	829	-817	3
25	1316	1365	-16
26	415	167	29
27	753	-875	-33
28	-23	11	0
29	628	630	0
30	1111	-1121	-3
31	503	247	34
32	1387	1354	9

-5 8 1

1	1611	-1597	5
2	555	-501	14
3	1488	1519	-12
4	1227	1283	-22
5	1000	-1029	-10
6	1419	-1430	-4
7	675	638	11
8	1556	1561	-1
9	419	301	22
10	1454	-1471	-6
11	883	-817	22
12	937	980	-15
13	1230	1198	12
14	401	-432	-6
15	1268	-1249	6
16	440	-321	21
17	1200	1175	9
18	700	693	2
19	988	-898	28
20	1061	-1107	-15
21	388	197	24
22	1052	1059	-2
23	364	-196	20
24	988	-964	7
25	423	-199	28
26	1146	1101	14
27	827	755	18
28	575	-464	21
29	719	-722	0
30	334	-2	21
31	902	811	23
32	575	484	16
33	733	-616	24
34	928	-862	16

-4 8 1

1	1248	1264	-6
2	2816	2894	-26
3	1992	-2048	-22
4	2652	-2694	-14
5	2780	2767	4
6	2616	2512	35
7	2187	-2196	-3
8	961	-936	9
9	1569	1594	-10
10	491	546	-15
11	283	-50	22
12	519	516	0
13	217	-293	-10
14	1656	-1568	32
15	869	807	20
16	2286	2304	-6
17	1336	-1299	13
18	1204	-1262	-21
19	876	818	18
20	1875	1874	0
21	1546	-1421	42
22	1381	-1358	8
23	1414	1411	1
24	382	-292	12
25	952	-908	13
26	195	-226	-2
27	606	639	-7
28	101	-219	-7
29	424	300	16
30	1706	1816	-36
31	1075	-945	35
32	1130	-1132	0
33	1571	1494	22
34	1669	1603	19
35	1425	-1338	25

-3 8 1

1	1073	1022	21
2	84	100	-1
3	476	-450	7
4	684	-607	26
5	461	-463	0
6	1294	1244	21
7	812	776	13
8	1384	-1400	-6
9	1222	-1152	28
10	1372	1357	6
11	1305	1280	10
12	1027	-955	28
13	1130	-1137	-2
14	440	308	25
15	860	886	-9
16	389	263	20
17	625	-597	7
18	999	-1020	-7
19	356	97	27
20	1135	1143	-2
21	527	359	31
22	1138	-1174	-12
23	725	-637	21
24	1061	1060	0
25	805	676	31
26	616	-550	13
27	817	-886	-18
28	202	183	1
29	883	878	1
30	252	191	5
31	790	-770	4
32	532	-476	9
33	326	372	-5
34	578	510	11
35	134	-182	-2
36	657	-730	-14

-2 8 1

1	1498	-1508	-4
2	3315	-3207	32
3	2232	2209	8
4	2006	2097	-37
5	2463	-2411	18
6	1555	-1650	-41
7	1903	1851	20
8	323	-153	25
9	994	-916	30
10	413	427	-3
11	159	-137	2
12	2228	-2235	-2
13	1801	1768	12
14	2151	2287	-50
15	1927	-1944	-6
16	1962	-1975	-4
17	1995	1926	24
18	2013	1941	25
19	1402	-1425	-8
20	1113	-1141	-9
21	828	835	-2
22	-227	313	-33
23	479	-493	-2
24	370	409	-5
25	83	-83	0
26	1195	-1200	-1
27	93	136	-1
28	1335	1343	-2
29	519	-510	1
30	1632	-1659	-8
31	972	1038	-17
32	1038	1082	-11
33	1457	-1374	24
34	1414	-1296	33
35	1540	1542	0
36	341	336	0
37	904	-933	-6

-1 8 1

1	791	-792	0
2	758	-780	-9
3	267	-147	16
4	992	1012	-8
5	1168	1194	-11
6	961	-924	15
7	1383	-1377	2
8	764	657	35
9	1648	1650	0
10	682	-552	38
11	1594	-1632	-15
12	479	371	22
13	1256	1204	19
14	303	1	23
15	656	-607	12
16	347	-371	-4
17	288	82	17
18	509	569	-13
19	-193	288	-27
20	765	-808	-11
21	848	-851	0
22	740	685	13
23	1123	1144	-6
24	624	-639	-3
25	1089	-1077	3
26	513	504	1
27	740	767	-6
28	-256	-107	-14
29	-145	-386	-31
30	-266	-189	-19
31	-224	72	-10
32	481	520	-6
33	259	32	11
34	587	-726	-28
35	-250	-69	-12
36	822	813	2
37	525	490	5

0 8 1

0	2115	-2100	5
1	1095	1100	-3
2	2151	2168	-8
3	1956	-1986	-14
4	1292	-1269	13
5	1787	1749	19
6	514	349	55
7	1049	-1027	11
8	864	736	58
9	277	204	13
10	1563	-1554	4
11	1192	1220	-14
12	2055	2093	-17
13	2865	-2888	-8
14	2359	-2308	20
15	2873	2837	13
16	2473	2395	30
17	2328	-2329	0
18	1773	-1722	21
19	1101	1103	-1
20	308	446	-28
21	-367	-36	-40
22	-324	11	-30
23	531	-600	-19
24	1549	-1534	6
25	1224	1220	1
26	1652	1647	2
27	1451	-1503	-21
28	1970	-1995	-9
29	1167	1142	9
30	1609	1649	-16
31	910	-949	-13
32	1146	-1110	13
33	934	974	-14
34	1035	977	20
35	145	-452	-45
36	-376	-23	-36
37	-331	196	-37

1 8 1

0	760	813	-21
1	1265	-1286	-9
2	381	-223	33
3	1504	1574	-31
4	597	-570	9
5	1396	-1421	-10
6	901	961	-23
7	1060	1006	21
8	1290	-1276	5
9	569	-487	20
10	1113	1112	0
11	211	55	10
12	703	-686	4
13	297	93	19
14	-282	190	-28
15	537	-477	12
16	453	411	7
17	878	847	8
18	698	-649	11
19	1018	-1061	-13
20	917	875	11
21	1202	1225	-7
22	713	-664	11
23	862	-819	11
24	608	565	8
25	600	707	-23
26	344	-447	-14
27	-368	-249	-38
28	-466	150	-48
29	-100	-235	-11
30	-440	89	-39
31	370	490	-17
32	185	-270	-6
33	393	-564	-27
34	385	594	-34
35	307	494	-24
36	600	-662	-11

2 8 1

0	1994	1891	40
1	607	-554	18
2	1380	-1306	32
3	587	521	21
4	1093	1050	18
5	390	488	-28
6	448	-454	-1
7	633	-704	-25
8	992	-981	4
9	1119	1082	15
10	2395	2404	-3
11	1302	-1348	-18
12	2356	-2333	8
13	1168	1206	-14
14	2718	2766	-15
15	1723	-1715	2
16	2196	-2157	13
17	1006	1091	-30
18	943	937	1
19	104	-344	-23
20	-191	161	-13
21	393	-597	-39
22	779	-739	10
23	1632	1641	-2

24	2010	2029	-6
25	1945	-1847	30
26	1754	-1742	3
27	1694	1695	0
28	1729	1723	1
29	1071	-1074	0
30	960	-978	-4
31	520	549	-5
32	755	866	-26
33	-275	-156	-18
34	-327	-270	-32
35	248	-482	-28

3 8 1

0	407	369	9
1	1359	1419	-26
2	764	-758	2
3	952	-927	10
4	989	1032	-18
5	617	554	20
6	1152	-1150	1
7	427	-417	2
8	1026	1030	-1
9	52	233	-15
10	1035	-980	20
11	532	532	0
12	485	413	16
13	951	-1021	-25
14	199	48	9
15	950	941	2
16	577	-527	11
17	1090	-1059	10
18	968	1002	-11
19	832	852	-5
20	945	-988	-13
21	670	-749	-20
22	886	934	-13
23	419	440	-3
24	685	-666	4
25	-342	78	-25
26	500	329	24
27	595	-538	11
28	-149	-100	-6
29	734	699	7
30	-53	-270	-13
31	688	-784	-21
32	425	485	-8
33	902	910	-1
34	615	-635	-3

4 8 1

0	1980	-1808	64
1	282	246	5
2	768	724	15
3	917	867	19
4	273	429	-33
5	962	-936	9
6	712	-631	25
7	1636	1613	8
8	1141	980	58
9	1513	-1465	18
10	1927	-2015	-33
11	1178	1123	20
12	2298	2331	-11
13	1314	-1346	-12
14	1157	-1056	35
15	540	618	-20
16	815	892	-24
17	181	-445	-39
18	474	-513	-8
19	-291	-36	-20
20	1339	-1290	16
21	961	1027	-20
22	749	661	21
23	1247	-1288	-13
24	1369	-1354	4
25	1781	1727	17
26	2117	2144	-8
27	1060	-1087	-7
28	1171	-1230	-17
29	115	478	-40
30	173	440	-29
31	-523	147	-59
32	-328	-281	-34

5 8 1

0	400	-149	37
1	1343	-1413	-28
2	877	816	21
3	840	831	2
4	1157	-1106	19
5	186	33	9
6	1317	1225	34
7	563	-428	32
8	1249	-1169	30
9	924	840	28
10	753	683	20
11	1133	-1160	-9
12	438	-352	16
13	1290	1248	14
14	447	-428	3
15	1185	-1126	20
16	692	702	-2
17	745	749	-1
18	643	-687	-11
19	-151	-68	-6
20	848	835	3
21	397	-336	9
22	620	-645	-5
23	224	248	-2
24	512	565	-10
25	458	-517	-10
26	353	-302	6
27	854	870	-4
28	-193	27	-7
29	704	-782	-17

6 8 1

0	831	951	-43
1	1098	1067	11
2	440	317	22
3	1128	-1213	-32
4	620	-633	-3
5	2081	2130	-17
6	1089	995	32
7	2048	-1987	21
8	1479	-1448	11
9	1139	1075	22
10	2387	2388	0
11	514	-397	23
12	755	-789	-10
13	312	-416	-17
14	1061	1134	-25
15	491	397	17
16	865	-890	-7
17	612	-547	14
18	1082	-1080	0
19	362	445	-13
20	874	928	-15
21	834	-902	-19
22	657	-578	17
23	825	804	5
24	1253	1346	-30
25	969	-850	30
26	1156	-1178	-6

7 8 1

0	596	547	12
1	287	247	5
2	901	-898	1
3	399	279	19
4	1043	1039	1
5	609	-600	2
6	959	-943	5
7	693	694	0
8	722	739	-4
9	1031	-1124	-32
10	777	-675	27
11	1094	1035	19
12	330	55	23
13	683	-637	11
14	402	426	-4
15	360	253	14
16	762	-777	-4
17	-139	20	-4
18	952	992	-11
19	560	-448	21
20	849	-778	18
21	824	849	-6
22	646	521	25
23	774	-838	-16

8 8 1

0	402	-412	-1
1	906	-891	4
2	559	-500	13
3	1456	1452	1
4	1061	1043	6
5	1187	-1138	16
6	1210	-1217	-2
7	1034	1026	2
8	1154	1174	-6
9	695	-649	11
10	1400	-1361	13
11	85	-44	1
12	505	397	19
13	960	922	11
14	319	-150	16
15	978	-1040	-19
16	-141	-97	-6
17	986	947	11
18	523	484	7

9 8 1

0	825	-860	-10
1	382	303	11
2	1080	1100	-6
3	736	-739	0
4	1079	-1047	9
5	911	902	2
6	1054	993	18
7	894	-804	24
8	682	-640	10
9	795	804	-2
10	347	48	24
11	596	-569	5

-9 9 1

1	343	23	24
2	695	649	11
3	372	-488	-20
4	612	-666	-12
5	903	824	21
6	860	749	29
7	1051	-1012	11
8	421	83	34
9	1328	1393	-21
10	270	-99	13
11	894	-940	-13
12	780	784	-1

-8 9 1

1	273	-399	-19
2	581	-596	-3
3	-203	-92	-12
4	710	679	8
5	645	669	-6
6	677	-623	13
7	991	-999	-2
8	739	668	18
9	1189	1197	-2
10	628	-452	37
11	1267	-1276	-3
12	199	105	6
13	821	895	-22
14	194	-31	8
15	343	-425	-13
16	252	-417	-24
17	-35	-246	-13
18	689	695	-1
19	904	880	6
20	804	-763	10
21	1111	-1034	22

-7 9 1

1	435	-439	0
2	416	-403	2
3	1193	1270	-27
4	187	-12	8
5	1346	-1397	-18
6	448	336	19
7	1130	1203	-26
8	534	-356	34
9	791	-770	6
10	485	579	-21
11	760	885	-38
12	421	-415	1
13	327	-275	7
14	750	660	23
15	849	-850	0
16	857	-809	13
17	1227	1312	-30
18	669	700	-7
19	1227	-1319	-31
20	232	-204	2
21	1534	1580	-15
22	553	-466	17
23	1133	-1040	27
24	1368	1363	1
25	778	723	13
26	1096	-1214	-25

-6 9 1

1	-217	-63	-13
2	1020	1103	-31
3	638	567	18
4	749	-773	-7
5	854	-955	-34
6	483	410	15
7	1194	1282	-33
8	385	-198	26
9	1201	-1116	29
10	272	-56	17
11	989	993	-1
12	574	543	7
13	761	-723	10
14	918	-1021	-34
15	285	-27	18
16	1004	1046	-13
17	527	449	15
18	1031	-922	33
19	979	-988	-2
20	700	524	40
21	1344	1289	18
22	561	-318	41
23	1165	-1124	12
24	242	-65	11
25	931	1001	-20
26	380	315	8
27	687	-665	5
28	760	-708	12

29	-158	128	-8

-5 9 1

1	1356	1337	7
2	480	-295	35
3	2293	-2390	-34
4	1192	1265	-29
5	2090	2119	-10
6	1188	-1153	13
7	1514	-1549	-13
8	1101	1156	-20
9	1018	962	19
10	490	-492	0
11	655	-633	6
12	602	539	15
13	291	-276	2
14	291	-24	20
15	1455	1496	-15
16	351	137	24
17	1589	-1643	-19
18	567	-411	31
19	1754	1739	5
20	675	-506	38
21	1823	-1845	-7
22	507	478	5
23	646	666	-4
24	970	-1048	-24
25	810	-793	4
26	1014	1071	-17
27	196	-140	3
28	785	-615	38
29	1175	1186	-3
30	583	431	26
31	1661	-1559	30

-4 9 1

1	271	310	-6
2	613	-610	0
3	709	-736	-9
4	258	19	18
5	1136	1105	11
6	565	559	6
7	1319	-1314	1
8	838	-829	3
9	1183	1198	-6
10	1032	1040	-3
11	952	-998	-16
12	1303	-1306	0
13	457	307	27
14	1455	1453	0
15	375	171	26
16	1095	-1078	5
17	906	-951	-14
18	481	518	-8
19	1057	1115	-20
20	304	-84	18
21	963	-899	19
22	477	-442	6
23	1044	1064	-6
24	779	696	20
25	539	-564	-5
26	692	-814	-31
27	342	216	13
28	917	997	-22
29	53	127	-2
30	721	-766	-10
31	581	-530	9
32	602	588	2
33	536	615	-14

-3 9 1

1	2867	-2932	-21
2	945	831	41
3	3248	3188	17
4	1461	-1377	32
5	2555	-2648	-32
6	1477	1495	-7
7	1790	1721	26
8	1327	-1362	-14
9	591	-637	-13
10	362	402	-8
11	509	-433	17
12	579	425	35
13	1335	1308	9
14	793	-918	-42
15	2365	-2350	5
16	1086	964	41
17	2302	2246	18
18	937	-839	29
19	2138	-2206	-23
20	411	273	20
21	1337	1293	14
22	806	-881	-21
23	373	-315	8
24	927	941	-4
25	-223	-88	-12
26	616	-617	0
27	799	863	-16
28	487	415	11
29	1380	-1475	-30
30	269	194	6
31	1621	1602	5
32	980	-876	25
33	1465	-1351	32
34	1235	1125	28

-2 9 1

1	187	-158	3
2	215	-146	7
3	579	601	-6
4	752	655	32
5	757	-746	3
6	1055	-1022	13
7	704	602	30
8	1246	1197	19
9	383	-303	14
10	1346	-1357	-4
11	407	213	30
12	1511	1554	-16
13	368	-61	31
14	1055	-1071	-5
15	485	-484	0
16	603	555	11
17	631	680	-12
18	328	320	1
19	765	-810	-12
20	980	-912	19
21	813	763	12
22	1099	1137	-11
23	506	-386	19
24	1262	-1196	19
25	477	254	28
26	1219	1259	-12
27	95	99	0
28	989	-936	13
29	531	-509	3
30	515	433	12
31	587	743	-32
32	-145	-233	-13
33	491	-613	-21
34	-371	-42	-24
35	460	482	-3

-1 9 1

1	2349	2290	20
2	1167	-1129	14
3	2727	-2708	6
4	2497	2482	4
5	1983	2017	-12
6	844	-781	21
7	304	-280	3
8	958	1024	-25
9	154	-69	5
10	226	-272	-5
11	1529	1551	-8
12	1096	-1070	8
13	2634	-2555	24
14	1582	1557	8
15	2845	2734	33
16	1644	-1596	16
17	2021	-2052	-10
18	1022	982	12
19	1772	1797	-8
20	386	-434	-7
21	383	-567	-33
22	145	-329	-16
23	-318	-277	-35
24	-225	240	-20
25	925	1029	-28
26	153	-248	-6
27	1272	-1314	-12
28	468	297	21
29	1818	1761	16
30	623	-356	40
31	1773	-1725	14
32	710	655	10
33	1155	1154	0
34	405	-523	-17
35	837	-914	-17

0 9 1

1	392	347	13
2	611	583	11
3	629	-576	22
4	955	-951	2
5	897	898	0
6	1379	1292	43
7	912	-826	39
8	1673	-1561	52
9	595	503	30
10	1429	1389	18
11	503	-325	43
12	1015	-1013	0
13	-186	-61	-12
14	240	329	-14
15	-239	143	-23
16	-250	103	-21
17	225	-339	-17
18	687	-645	13
19	515	543	-7
20	1105	1080	9
21	611	-600	3
22	1263	-1226	14
23	628	586	11
24	1175	1162	5
25	489	-442	10
26	864	-860	1
27	263	245	2
28	216	372	-22
29	-216	66	-13
30	-187	176	-16
31	-365	-166	-42
32	392	-511	-24
33	504	514	-2
34	705	744	-11
35	662	-735	-20

1 9 1

0	540	-328	48
1	3021	-2958	19
2	1271	1192	31
3	2182	2223	-15
4	394	325	14
5	277	-138	16
6	-152	190	-16
7	112	-26	3
8	517	-555	-9
9	1370	1470	-37
10	446	-150	38
11	2905	-3036	-40
12	748	881	-39
13	2923	2968	-13
14	1410	-1445	-11
15	2441	-2330	34
16	1499	1498	0
17	1464	1447	5
18	955	-928	7
19	906	-943	-10
20	-384	164	-36
21	-238	-240	-22
22	775	848	-18
23	1017	1073	-15
24	899	-912	-3
25	1594	-1630	-10
26	916	855	14
27	2165	2149	4
28	661	-392	43
29	2154	-2178	-7
30	514	408	15
31	1431	1346	23
32	-175	-62	-6
33	611	-712	-19
34	-408	62	-30

2 9 1

0	516	533	-5
1	186	12	11
2	1179	-1186	-3
3	606	530	22
4	1501	1437	25
5	803	-657	48
6	1339	-1315	9
7	748	674	23
8	1116	1142	-10
9	1074	-1096	-8
10	708	-821	-36
11	775	832	-18
12	-169	-32	-7
13	194	-385	-26
14	586	643	-14
15	-322	-31	-25
16	1001	-978	6
17	262	352	-11
18	1213	1161	16
19	542	-346	32
20	1353	-1348	1
21	442	368	11
22	1246	1336	-28
23	582	-550	6
24	1064	-1148	-26
25	374	357	2
26	378	525	-22
27	-166	-174	-10
28	330	380	-6
29	-306	28	-17
30	890	-928	-9
31	-273	85	-14
32	768	875	-24
33	478	-213	28

3 9 1

0	322	194	19
1	1686	1698	-4
2	158	180	-2
3	460	-414	10
4	483	-591	-30
5	603	-701	-31
6	1203	1251	-19
7	1142	1108	13
8	647	-704	-17
9	1873	-1976	-39
10	599	478	29
11	2445	2514	-23

12	672	-674	0
13	2002	-2081	-28
14	607	649	-10
15	1620	1644	-8
16	716	-666	13
17	663	-654	2
18	-155	-110	-8
19	298	-334	-4
20	265	312	-5
21	806	807	0
22	1039	-1039	0
23	1637	-1619	5
24	1280	1171	32
25	1890	1883	2
26	662	-651	2
27	1671	-1792	-38
28	693	615	15
29	1320	1345	-7
30	-318	-230	-28
31	630	-722	-18

4 9 1

0	1147	-1141	2
1	475	320	31
2	1361	1366	-1
3	651	-654	0
4	1377	-1402	-9
5	914	959	-17
6	982	936	16
7	1042	-1013	10
8	331	-288	6
9	883	858	8
10	299	-104	19
11	906	-918	-4
12	907	810	29
13	482	466	3
14	1043	-1095	-17
15	48	65	0
16	1004	1003	0
17	331	-297	4
18	1115	-1184	-24
19	666	711	-11
20	855	934	-23
21	882	-846	9
22	551	-541	1
23	827	773	13
24	-62	91	-2
25	687	-759	-17
26	339	408	-9
27	425	471	-7
28	833	-894	-15
29	300	22	15

5 9 1

0	538	499	9
1	779	-883	-35
2	696	-728	-9
3	370	-387	-3
4	1341	1378	-13
5	949	988	-13
6	1199	-1269	-27
7	1618	-1516	36
8	1153	1032	43
9	1781	1810	-10
10	401	115	34
11	1934	-2098	-60
12	383	121	27
13	1806	1655	51
14	127	-200	-5
15	672	-718	-12
16	462	-452	2
17	-106	135	-6
18	293	-318	-3
19	181	286	-10
20	329	-404	-11
21	900	-921	-5
22	1013	1047	-10
23	1101	1148	-14
24	719	-634	19
25	1514	-1420	28
26	527	467	10
27	1057	1157	-28

6 9 1

0	1190	1230	-16
1	305	-300	0
2	942	-963	-7
3	837	759	23
4	493	409	17
5	1010	-957	17
6	112	129	-1
7	913	918	-1
8	433	-259	27
9	1053	-1058	-1
10	877	854	7
11	528	452	15
12	1094	-1120	-8
13	298	60	19
14	894	881	3
15	309	-223	10
16	626	-613	3
17	537	584	-10
18	458	491	-6
19	672	-762	-23
20	-164	-118	-8
21	610	736	-30
22	-124	-170	-9
23	449	-457	-1
24	449	483	-5

7 9 1

0	708	-652	14
1	238	8	13
2	1010	1054	-14
3	960	998	-12
4	1406	-1374	10
5	1352	-1278	25
6	1364	1309	19
7	1206	1193	4
8	785	-700	22
9	1345	-1430	-30
10	311	-176	14
11	1283	1287	-1
12	526	474	10
13	732	-605	30
14	1138	-1155	-5
15	452	370	13
16	1102	1060	12
17	725	675	12
18	883	-672	51
19	1101	-1080	6
20	328	428	-14

8 9 1

0	170	-434	-37
1	887	874	3
2	360	7	28
3	1090	-1085	1
4	402	272	18
5	1127	1049	24
6	584	-543	9
7	1011	-969	13
8	708	708	0
9	791	791	0
10	709	-685	5
11	365	-324	5
12	698	625	16
13	175	-211	-2
14	627	-547	16

9 9 1

0	872	840	8
1	577	556	4
2	449	-456	-1
3	748	-783	-9
4	598	611	-2

-8 10 1

1	409	-411	0
2	261	155	9
3	679	679	0
4	563	-588	-5
5	449	-516	-13
6	981	1000	-5
7	320	187	14
8	997	-1073	-24
9	386	-116	28
10	942	1145	-66
11	331	-188	15
12	973	-970	0
13	885	859	7
14	467	456	2
15	1419	-1242	53

-7 10 1

1	769	826	-16
2	269	214	6
3	733	-753	-5
4	758	-698	16
5	627	650	-6
6	955	949	1
7	265	-263	0
8	945	-1005	-19
9	221	-5	11
10	818	932	-35
11	411	294	17
12	646	-735	-23
13	666	-589	18
14	315	320	0
15	616	687	-17
16	340	209	15
17	578	-659	-19
18	656	-633	5
19	451	456	0
20	1005	1040	-10
21	445	-234	27

-6 10 1

1	665	508	37
2	1061	-1050	3
3	406	-277	20
4	1576	1584	-2
5	296	-208	10
6	1452	-1503	-18
7	528	377	29
8	1050	1080	-10
9	525	-590	-15
10	809	-802	2
11	339	435	-17
12	681	669	3
13	561	-593	-7
14	356	158	22
15	674	709	-9
16	1077	-1154	-25
17	890	-787	28
18	1347	1349	0
19	922	808	31
20	1662	-1662	0
21	428	-160	31
22	1400	1435	-11
23	581	-623	-9
24	740	-770	-7
25	995	956	10

-5 10 1

1	1005	-989	5
2	825	-798	8
3	699	622	20
4	1180	1254	-28
5	370	-85	31
6	1186	-1199	-4
7	425	-439	-2
8	1005	935	23
9	879	967	-29
10	724	-702	6
11	1202	-1248	-17
12	369	290	11
13	1400	1497	-35
14	320	26	23
15	1156	-1149	2
16	765	-651	29
17	730	670	15
18	1194	1216	-7
19	475	-254	32
20	1026	-1040	-4
21	495	-337	25
22	874	897	-6
23	712	647	15
24	627	-605	4
25	751	-767	-4
26	441	362	11
27	946	981	-9
28	298	-48	16

-4 10 1

1	497	-387	23
2	2141	2222	-29
3	427	270	26
4	2244	-2353	-39
5	663	478	45
6	2140	2200	-21
7	849	-839	2
8	1390	-1320	25
9	597	623	-7
10	804	782	6
11	381	-196	25
12	48	-267	-17
13	331	285	6
14	920	-915	1
15	392	-190	26
16	1908	1926	-6
17	349	-322	4
18	1921	-1957	-12
19	872	-691	47
20	2192	2238	-15
21	457	72	40
22	1664	-1463	62
23	1038	1011	7
24	598	572	5
25	649	-683	-7
26	-212	-85	-10
27	856	948	-25
28	763	-670	20
29	826	-739	20
30	1394	1346	13

-3 10 1

1	732	724	2
2	540	492	12
3	257	-87	15
4	541	-522	4
5	681	-709	-8
6	585	548	9
7	1210	1164	17
8	552	-497	13
9	1448	-1394	19
10	272	28	18
11	1517	1451	23
12	286	72	18
13	1335	-1368	-12

14	386	-411	-4
15	962	986	-7
16	718	692	6
17	433	-309	19
18	851	-752	26
19	393	-312	11
20	998	1011	-3
21	826	797	7
22	473	-370	16
23	942	-1031	-26
24	216	-1	9
25	1051	1063	-3
26	387	180	21
27	922	-1030	-29
28	692	-520	32
29	666	674	-1
30	630	573	10
31	326	-325	0

-2 10 1

1	463	-7	54
2	2684	-2676	2
3	894	754	45
4	2699	2817	-39
5	763	-632	38
6	1792	-1775	6
7	1002	1094	-34
8	484	348	26
9	494	-467	6
10	325	228	12
11	356	167	22
12	1338	-1443	-38
13	261	224	4
14	2164	2170	-2
15	960	-825	38
16	2199	-2181	5
17	586	306	47
18	1947	2024	-26
19	504	276	33
20	1839	-1872	-10
21	189	122	4
22	1110	1095	4
23	42	135	-3
24	-336	28	-22
25	506	477	4
26	659	-741	-18
27	781	-688	20
28	1639	1680	-12
29	670	342	50
30	1978	-1973	1
31	543	-81	44
32	1674	1657	4

-1 10 1

1	205	-54	9
2	315	-305	1
3	850	-778	22
4	518	453	14
5	1352	1369	-6
6	474	-204	41
7	1788	-1821	-12
8	426	-157	35
9	1588	1550	13
10	294	-22	19
11	1369	-1346	8
12	437	-342	15
13	834	881	-13
14	443	532	-17
15	302	-215	9
16	591	-682	-21
17	306	-278	3
18	631	485	28
19	973	962	3
20	572	-309	39
21	1500	-1483	5
22	584	241	46
23	1630	1578	15
24	501	-68	41
25	1427	-1382	13
26	438	-164	27
27	740	730	2
28	342	343	0
29	-215	-239	-18
30	322	-448	-16
31	252	-329	-7
32	343	497	-20

0 10 1

0	2771	-2783	-4
1	492	252	60
2	2265	2241	10
3	459	328	35
4	1530	-1573	-21
5	749	673	31
6	674	607	25
7	484	-516	-10
8	396	458	-16
9	718	874	-65
10	1486	-1506	-9
11	262	-167	12
12	1838	1754	35
13	581	-575	1
14	2104	-2167	-26
15	888	821	24
16	1933	1949	-6
17	851	-943	-34
18	1674	-1660	5
19	-97	-157	-8
20	979	1053	-28
21	-176	137	-12
22	-325	-231	-41
23	-281	-137	-24
24	715	-875	-52
25	-178	28	-8
26	1590	1666	-30
27	264	76	15
28	1954	-1932	8
29	442	-134	40
30	1682	1704	-8
31	190	185	0
32	1273	-1367	-37

1 10 1

0	401	542	-31
1	697	-747	-15
2	383	136	31
3	1464	1496	-12
4	601	-529	19
5	1654	-1700	-17
6	447	230	32
7	1575	1524	17
8	602	-375	42
9	1377	-1345	10
10	392	342	7
11	867	830	10
12	289	-381	-12
13	380	-304	9
14	-221	209	-18
15	398	-359	5
16	103	-20	1
17	908	955	-12
18	237	-93	8
19	1363	-1359	1
20	402	-1	28
21	1675	1665	3
22	464	-58	35
23	1475	-1440	10
24	439	149	28
25	957	970	-3
26	228	-36	8
27	214	-333	-11
28	-168	24	-5
29	-183	-312	-22
30	-143	171	-8
31	793	734	12

2 10 1

0	2395	2486	-32
1	462	213	43
2	1454	-1529	-30
3	306	-338	-5
4	921	970	-17
5	638	705	-20
6	244	206	4
7	445	-509	-14
8	1131	-1150	-7
9	536	-490	10
10	1862	1943	-29
11	326	64	23
12	2696	-2764	-21
13	454	117	39
14	2001	2020	-6
15	427	-403	3
16	1119	-1249	-45
17	401	403	0
18	497	622	-25
19	-328	-73	-23
20	-272	31	-14
21	430	-558	-22
22	577	-824	-56
23	302	166	11
24	1398	1547	-46
25	460	-281	21
26	1921	-1920	0
27	446	74	31
28	1887	1996	-33
29	347	297	5
30	1126	-1201	-20

3 10 1

0	281	-175	13
1	1226	1224	0
2	235	56	14
3	1565	-1507	21
4	550	267	54
5	1671	1597	27
6	583	-475	25
7	1393	-1359	12
8	583	634	-13
9	1010	1017	-2
10	687	-594	24
11	-104	-208	-13
12	807	777	8
13	550	-521	6
14	453	-479	-5
15	952	954	0
16	449	285	24
17	1188	-1214	-8
18	379	1	28
19	1306	1346	-13
20	543	-446	17
21	1017	-1060	-12
22	666	579	17
23	714	762	-11
24	541	-546	0
25	-248	-247	-23
26	429	460	-4
27	131	-347	-18
28	213	-332	-11
29	576	707	-25

4 10 1

0	1410	-1424	-5
1	1067	-1125	-22
2	564	579	-4
3	1227	1242	-5
4	517	580	-15
5	804	-834	-9
6	1144	-1070	25
7	528	491	8
8	1663	1702	-14
9	596	413	39
10	2359	-2337	7
11	365	-135	26
12	2054	2189	-47
13	726	635	23
14	1125	-1072	17
15	-79	87	-3
16	941	996	-16
17	-13	-48	0
18	-124	229	-14
19	667	-564	22
20	662	-691	-6
21	-331	162	-29
22	740	745	-1
23	526	-522	0
24	1441	-1574	-42
25	504	430	11
26	1579	1652	-22
27	132	58	2

5 10 1

0	454	370	16
1	1234	-1283	-18
2	393	219	25
3	1127	1145	-6
4	628	-587	10
5	803	-748	16
6	786	730	16
7	530	451	16
8	949	-981	-10
9	385	-11	33
10	954	976	-7
11	643	-659	-4
12	741	-744	0
13	875	911	-11
14	394	270	17
15	1102	-1173	-23
16	320	20	21
17	1075	1072	0
18	358	-278	10
19	737	-799	-16
20	497	580	-16
21	350	387	-5
22	682	-816	-33
23	-117	-125	-5
24	678	707	-6

6 10 1

0	295	390	-15
1	815	800	4
2	309	232	9
3	952	-974	-7
4	1082	-1192	-40
5	1218	1264	-16
6	1184	1098	28
7	544	-465	16
8	1611	-1606	1
9	520	-333	33
10	1947	2032	-29
11	784	632	38
12	1475	-1440	11
13	1061	-999	18
14	708	648	14
15	892	872	5
16	236	-5	11
17	308	-360	-7
18	808	-879	-19
19	237	256	-1
20	1219	1180	11

7 10 1

0	338	140	21
1	745	776	-8
2	634	-723	-23
3	628	-601	6
4	890	958	-21
5	312	224	10
6	918	-929	-3
7	313	126	18
8	912	929	-5
9	412	-431	-3
10	812	-769	11
11	827	845	-5
12	555	432	23
13	777	-821	-11
14	296	1	18
15	724	731	-1

8 10 1

0	187	196	0
1	702	-645	13
2	1029	-1059	-9
3	646	610	8
4	1158	1132	8
5	477	-563	-17
6	1096	-1178	-27
7	134	113	1
8	1179	1204	-7

-7 11 1

1	-144	-132	-8
2	359	-418	-9
3	513	480	6
4	438	254	26
5	1120	-1079	13
6	615	-500	24
7	1182	1150	10
8	329	-45	22
9	950	-864	24
10	395	161	26
11	989	1028	-11
12	599	-438	31
13	680	-637	10
14	1006	914	26
15	384	155	24
16	1468	-1431	8

-6 11 1

1	589	-606	-4
2	734	728	1
3	855	851	1
4	418	-295	19
5	1111	-1144	-11
6	412	-280	20
7	993	1077	-27
8	809	801	2
9	738	-726	3
10	955	-951	1
11	589	402	36
12	1086	1067	6
13	458	172	37
14	1037	-1082	-14
15	587	-392	36
16	705	659	11
17	738	708	7
18	445	-227	28
19	702	-776	-19
20	96	-192	-5
21	731	834	-26

-5 11 1

1	718	708	2
2	684	675	2
3	1135	-1103	11
4	615	-514	23
5	1599	1655	-20
6	335	285	7
7	1430	-1378	18
8	398	443	-8
9	942	884	18
10	383	37	32
11	971	-1000	-9
12	577	482	20
13	431	356	12
14	1011	-910	31
15	741	734	1
16	881	850	8
17	1071	-1040	9
18	942	-928	3
19	1555	1581	-8
20	778	695	20
21	1761	-1771	-3
22	590	316	44
23	1222	1202	6
24	569	-375	31

-4 11 1

1	911	831	24
2	493	-468	5
3	928	-873	17
4	258	-23	16
5	771	632	37
6	604	606	0
7	516	-339	32
8	987	-983	1
9	255	2	15
10	1130	1106	8
11	394	163	28
12	1154	-1129	8
13	921	-777	40
14	1152	1118	10
15	1130	1009	37
16	885	-785	27
17	966	-883	24
18	493	201	39
19	947	804	38
20	547	412	24
21	653	-604	10
22	1001	-1021	-6
23	414	401	1
24	1097	1026	19
25	488	-28	41
26	1139	-1128	3
27	658	-464	34

-3 11 1

1	1637	-1740	-39
2	696	-619	21
3	2086	2136	-17
4	472	166	44
5	2034	-2106	-25
6	440	324	20
7	1038	1039	0
8	462	-399	12
9	480	-354	23
10	808	749	16
11	-191	-6	-8
12	467	-550	-17
13	400	479	-14
14	301	-392	-13
15	1264	-1271	-2
16	979	-810	46
17	1897	1920	-7
18	828	629	47
19	2111	-2092	6
20	554	-26	55
21	1901	1809	28
22	548	472	13
23	876	-862	3
24	321	419	-13
25	191	-153	2
26	886	-896	-2
27	715	737	-4
28	873	746	28

-2 11 1

1	506	-444	13
2	93	44	1
3	284	300	-2
4	751	713	10
5	235	-95	11
6	1229	-1205	8
7	526	-420	21
8	1298	1349	-18
9	676	655	5
10	1274	-1360	-30
11	670	-618	12
12	1239	1205	11
13	354	336	2
14	682	-623	13
15	548	-518	6
16	338	291	5
17	606	605	0
18	-90	299	-19
19	219	-88	7
20	1067	-1063	1
21	423	18	32
22	1213	1284	-22
23	344	134	17
24	1261	-1289	-8
25	678	-499	32
26	1001	925	19
27	539	493	7
28	453	-469	-2
29	608	-635	-4

-1 11 1

1	2473	2512	-12
2	467	140	41
3	2004	-2048	-15
4	421	19	37
5	1847	1877	-10
6	286	144	13
7	804	-809	-1
8	548	489	12
9	260	-334	-9
10	689	-819	-35
11	719	765	-12
12	195	21	7
13	1519	-1584	-21
14	387	-144	24
15	1603	1688	-28
16	407	94	28
17	1662	-1608	16
18	426	-183	26
19	1899	1888	3
20	609	483	22
21	1152	-1169	-4
22	-106	-73	-3
23	172	81	4
24	404	-424	-2
25	670	693	-4
26	400	356	5
27	1247	-1298	-14
28	958	-990	-7
29	1597	1636	-11

0 11 1

1	289	-182	16
2	465	542	-24
3	667	664	1
4	1030	-1009	9
5	376	-211	31
6	1444	1414	14
7	551	392	43
8	1547	-1532	6
9	612	-482	37
10	1336	1343	-3
11	421	247	31
12	814	-866	-19
13	131	-50	4
14	-102	317	-30
15	-266	-211	-31
16	384	415	-6
17	91	262	-15
18	985	-938	16
19	417	-90	38
20	1397	1381	6
21	566	185	62
22	1664	-1615	19
23	652	-378	58
24	1413	1368	17
25	319	419	-16
26	894	-906	-3
27	193	-248	-5
28	-254	247	-29
29	-192	235	-21

1 11 1

0	1626	1648	-7
1	2266	-2248	5
2	521	-143	51
3	1793	1845	-18
4	656	523	33
5	745	-834	-25
6	305	100	17
7	537	-544	-1
8	556	-554	0
9	1674	1737	-20
10	813	644	38
11	2162	-2222	-19
12	615	-565	10
13	2143	2296	-49
14	428	224	23
15	1726	-1713	3
16	193	212	-1
17	1111	1154	-12
18	-231	174	-15
19	964	-944	4
20	185	-112	3
21	-160	274	-17
22	210	-203	0
23	407	600	-31
24	160	-111	2
25	1346	-1363	-4
26	450	-329	14
27	1758	1867	-32
28	663	732	-13

2 11 1

0	761	672	25
1	601	411	42
2	1359	-1343	5
3	745	-634	31
4	1710	1772	-23
5	592	265	61
6	1838	-1901	-23
7	482	-45	51
8	1490	1498	-2
9	388	-151	27
10	1016	-1026	-3
11	494	464	5
12	-137	274	-20
13	272	-377	-13
14	190	331	-14
15	501	484	3
16	757	-683	17
17	612	-409	35
18	963	959	1
19	445	231	25
20	1096	-1211	-34
21	257	-62	11

22	1168	1258	-26
23	315	-131	13
24	740	-949	-50
25	-116	106	-4
26	292	504	-27
27	-383	-34	-26

3 11 1

0	1189	-1112	27
1	1167	1212	-17
2	924	975	-17
3	552	-538	3
4	1008	-1052	-16
5	398	-511	-24
6	477	530	-11
7	1247	1157	31
8	440	-81	41
9	1798	-1802	-1
10	762	-705	15
11	2198	2248	-16
12	1117	1085	10
13	1696	-1679	5
14	-75	-52	-1
15	863	801	16
16	936	915	5
17	339	-394	-7
18	-169	-8	-5
19	379	-249	15
20	-174	-190	-13
21	531	686	-32
22	352	-281	8
23	1120	-1152	-9
24	173	-123	2
25	1541	1489	14

4 11 1

0	884	-848	11
1	615	-534	19
2	1261	1279	-6
3	296	5	21
4	1305	-1303	0
5	401	284	18
6	1261	1222	13
7	521	-270	42
8	941	-904	11
9	550	493	12
10	457	372	15
11	708	-744	-9
12	532	357	31
13	775	655	30
14	1059	-1006	16
15	652	-606	10
16	1128	1045	24
17	236	80	10
18	1234	-1240	-2
19	275	12	14
20	945	1038	-26
21	558	-408	24
22	608	-714	-23
23	542	499	7

5 11 1

0	1169	1131	14
1	146	-326	-20
2	1052	-967	28
3	637	-587	12
4	938	832	31
5	1046	1018	9
6	683	-702	-5
7	1262	-1181	28
8	596	-566	7
9	1879	1885	-2
10	936	893	12
11	1656	-1712	-19
12	1359	-1344	4
13	879	826	14
14	1093	1031	19
15	195	-270	-7
16	596	-641	-10
17	514	-559	-8
18	51	44	0
19	878	848	7
20	378	-306	9

6 11 1

0	1002	1022	-6
1	354	226	16
2	1116	-1129	-4
3	446	366	13
4	952	879	21
5	648	-705	-14
6	538	-450	17
7	683	750	-18
8	322	288	4
9	741	-812	-19
10	452	350	16
11	811	792	5
12	744	-746	0
13	493	-444	8
14	821	829	-2
15	445	368	12
16	926	-925	0

7 11 1

0	779	-759	5
1	536	-462	14
2	468	346	20
3	1052	1020	9
4	514	-493	4
5	1099	-1112	-3
6	272	241	3
7	1194	1156	12
8	273	272	0
9	1087	-1073	4
10	832	-715	29

-6 12 1

1	566	638	-16
2	65	-306	-20
3	801	-882	-23
4	808	877	-20
5	585	448	27
6	1180	-1215	-11
7	612	-586	6
8	1181	1167	4
9	448	325	19
10	1033	-1064	-9
11	342	24	24
12	1026	1107	-25
13	820	-765	14
14	421	-417	0

-5 12 1

1	691	-614	19
2	700	-729	-7
3	507	417	17
4	698	752	-14
5	350	243	13
6	508	-461	9
7	768	-739	7
8	305	164	14
9	1017	972	13
10	461	188	36
11	1223	-1274	-17
12	637	-436	40
13	1244	1257	-4
14	716	613	24
15	899	-803	25
16	861	-891	-8
17	400	221	21
18	779	885	-28
19	250	190	5

-4 12 1

1	1211	-1282	-26
2	751	711	10
3	881	838	12
4	1130	-1148	-6
5	667	-532	31
6	1259	1269	-3
7	310	69	20
8	810	-699	29
9	176	0	7
10	727	825	-28
11	103	-116	0
12	411	-525	-22
13	771	804	-9
14	357	-331	3
15	1375	-1297	25
16	683	592	20
17	1133	998	39
18	1144	-1175	-9
19	1197	-1187	3
20	1717	1781	-20
21	624	417	36
22	1170	-1265	-28

-3 12 1

1	634	534	23
2	560	547	3
3	334	242	12
4	348	-141	22
5	727	-804	-22
6	409	233	24
7	1106	1054	16
8	387	11	32
9	1119	-1032	27
10	871	-804	19
11	1176	1198	-7
12	997	888	31
13	867	-873	-1
14	831	-764	17
15	486	291	29
16	820	785	9
17	294	166	11
18	432	-392	6
19	666	-698	-7
20	410	400	1
21	858	806	12
22	-223	51	-10
23	1035	-1108	-20
24	595	-430	26

-2 12 1

1	1302	1317	-5
2	1888	-1955	-23
3	1446	-1424	7
4	1800	1925	-44
5	455	328	20
6	916	-937	-6
7	514	401	20
8	327	213	13
9	-87	127	-5
10	258	-33	13
11	418	305	16
12	709	-649	14
13	1187	-1022	47
14	1383	1440	-18
15	632	644	-2
16	1018	-1028	-2
17	635	-540	18
18	1540	1546	-1
19	1005	957	12
20	1686	-1726	-12
21	234	-27	9
22	782	821	-9
23	-249	-116	-13
24	289	-386	-11
25	472	495	-3

-1 12 1

1	220	-258	-3
2	308	-43	18
3	370	-430	-9
4	500	-406	16
5	1187	1284	-31
6	948	827	32
7	1432	-1459	-8
8	954	-831	33
9	1392	1291	31
10	950	800	39
11	1072	-900	47
12	1000	-904	26
13	723	675	11
14	520	513	1
15	206	19	8
16	225	248	-2
17	657	-737	-17
18	584	-490	16
19	751	733	3
20	606	467	23
21	1186	-1207	-5
22	884	-628	52
23	1139	1124	3
24	570	512	9
25	741	-770	-5

0 12 1

0	1543	-1579	-12
1	1468	-1400	30
2	1775	1780	-1
3	1244	1199	20
4	1343	-1338	2
5	278	-156	16
6	323	248	13
7	197	5	11
8	719	721	0
9	953	1084	-55
10	774	-761	4
11	1000	-928	27
12	1125	1173	-19
13	965	903	22
14	1229	-1194	13
15	852	-789	20
16	1234	1236	0
17	719	604	31
18	1178	-1121	20
19	160	-21	5
20	730	856	-39
21	-320	133	-29
22	210	-415	-29
23	-338	-115	-30
24	615	-712	-25
25	691	-678	3

1 12 1

0	569	533	7
1	928	-869	16
2	746	-668	18
3	1229	1139	28
4	932	653	70
5	1460	-1410	16
6	1265	-1156	32
7	1451	1417	10
8	986	880	27
9	1199	-1087	31
10	739	-722	3
11	949	884	16
12	97	72	0

13	361	-260	10
14	260	257	0
15	255	-234	1
16	691	-595	18
17	468	448	2
18	746	652	18
19	966	-979	-3
20	826	-711	23
21	1147	1150	0
22	544	529	2
23	1061	-1126	-16
24	424	-403	2
25	838	828	1

2 12 1

0	1303	1302	0
1	1114	937	55
2	1426	-1456	-10
3	1438	-1447	-3
4	523	434	18
5	378	86	30
6	367	44	29
7	243	6	13
8	920	-1031	-35
9	1196	-1219	-7
10	1858	1873	-4
11	754	643	26
12	1571	-1687	-39
13	1411	-1376	11
14	1769	1822	-16
15	847	648	44
16	833	-779	12
17	-253	79	-13
18	71	300	-15
19	-182	256	-18
20	-232	-197	-16
21	-338	-149	-24
22	746	-710	7
23	404	-452	-6

3 12 1

0	980	-878	31
1	1140	1092	17
2	926	964	-12
3	1380	-1403	-8
4	745	-603	36
5	1563	1613	-18
6	773	579	48
7	1263	-1249	4
8	398	-77	32
9	944	1057	-36
10	318	101	19
11	309	-329	-2
12	631	543	18
13	589	-497	18
14	629	-697	-16
15	894	889	1
16	782	748	8
17	1138	-1107	8
18	748	-613	28
19	1044	1025	5
20	458	268	23
21	1000	-988	2

4 12 1

0	672	-655	4
1	1066	-1063	0
2	245	0	14
3	876	810	19
4	498	505	-1
5	411	-297	17
6	831	-839	-2
7	372	77	28
8	1411	1410	0
9	1039	1094	-17
10	1267	-1345	-26
11	1039	-991	14
12	1170	1221	-16
13	1341	1382	-13
14	730	-721	2
15	602	-627	-5
16	101	-192	-5
17	382	298	10
18	301	380	-10
19	-175	54	-6

5 12 1

0	651	694	-11
1	1023	-1013	3
2	602	-572	6
3	1131	1130	0
4	256	70	13
5	862	-829	9
6	-93	80	-3
7	861	782	21
8	510	-453	11
9	384	-471	-15
10	561	659	-23
11	251	-118	10
12	679	-627	12
13	495	474	3
14	645	617	6
15	918	-875	11

6 12 1

0	212	-200	1
1	313	280	4
2	562	502	12
3	345	-316	3
4	857	-915	-17
5	250	163	7
6	903	868	9
7	222	316	-10
8	1110	-1090	6
9	821	-753	17

-5 13 1

1	224	-119	7
2	842	889	-13
3	357	-130	23
4	989	-1008	-5
5	1041	1084	-13
6	832	842	-2
7	643	-691	-11
8	362	-327	4
9	1090	937	43
10	522	374	24
11	1150	-1260	-24

-4 13 1

1	919	996	-24
2	372	-111	27
3	618	-718	-25
4	304	-212	10
5	271	249	2
6	783	874	-26
7	347	254	11
8	891	-856	10
9	571	-551	4
10	816	699	29
11	700	592	24
12	1014	-896	32
13	981	-993	-3
14	705	652	12
15	849	887	-10
16	426	-160	29

-3 13 1

1	765	-630	33
2	1207	-1205	0
3	705	827	-34
4	845	850	-1
5	1066	-1113	-15
6	255	-311	-6
7	808	769	10
8	369	300	9
9	-154	-254	-19
10	311	330	-2
11	411	384	4
12	724	-714	2
13	122	-87	1
14	684	586	20
15	530	-362	26
16	1392	-1405	-4
17	1124	1177	-15
18	1150	1219	-20

-2 13 1

1	692	-664	6
2	283	-65	16
3	225	185	3
4	612	579	7
5	418	312	15
6	930	-843	23
7	1035	-1002	9
8	1214	1214	0
9	1161	1125	11
10	952	-936	4
11	1038	-1044	-1
12	674	593	17
13	719	710	2
14	347	-274	8
15	517	-549	-6
16	290	-259	3
17	224	246	-1
18	314	457	-19
19	273	304	-3
20	942	-931	2

-1 13 1

1	1350	1321	9
2	1185	1112	21
3	868	-755	27
4	894	-921	-7
5	927	932	-1
6	348	290	7
7	460	-499	-7
8	417	323	12
9	411	-236	21
10	607	-746	-32
11	554	619	-13
12	591	608	-3
13	430	-421	1
14	1097	-1056	11
15	1384	1273	33
16	977	914	15
17	1014	-969	11
18	582	-677	-18
19	847	849	0
20	631	594	6

0 13 1

1	428	-243	35
2	501	494	2
3	1025	1010	6
4	839	-719	43
5	892	-822	26
6	894	788	39
7	1129	1136	-2
8	1150	-992	61
9	1313	-1272	17
10	1176	1119	22
11	836	800	12
12	713	-666	14
13	234	-413	-29
14	-236	21	-14
15	-285	-125	-24
16	169	314	-16
17	584	653	-17
18	773	-764	2
19	1030	-906	39
20	766	675	24

1 13 1

0	1837	1931	-30
1	1580	-1585	-1
2	1075	-1075	0
3	632	500	24
4	888	925	-9
5	541	-518	4
6	-70	149	-5
7	644	-730	-18
8	183	-219	-2
9	794	746	10
10	975	1041	-17
11	1220	-1277	-16
12	1485	-1375	31
13	1198	1329	-37
14	752	853	-23
15	352	-497	-20
16	615	-811	-40
17	433	403	3
18	514	624	-18
19	-127	-347	-22
20	-329	-193	-24

2 13 1

0	589	300	50
1	1036	965	21
2	1026	-865	46
3	1420	-1283	44
4	1312	1386	-27
5	1206	1168	12
6	1142	-1059	25
7	1004	-928	22
8	1089	1069	6
9	689	635	12
10	599	-501	19
11	485	-340	21
12	265	321	-6
13	104	-52	1
14	228	267	-3
15	659	594	12
16	733	-660	15
17	810	-897	-20
18	725	702	4

3 13 1

0	1550	-1490	20
1	551	436	23
2	907	1007	-31
3	112	198	-6
4	674	-735	-16
5	532	-464	13
6	326	157	17
7	1012	977	10
8	652	662	-2
9	835	-737	25
10	1079	-1071	2
11	1337	1439	-33
12	1380	1498	-38
13	568	-530	7
14	995	-953	11
15	512	496	2
16	606	767	-36

4 13 1

0	583	-495	18
1	973	-998	-7
2	931	902	8
3	977	911	19
4	1009	-975	10
5	802	-661	35
6	899	915	-4
7	591	467	24
8	898	-957	-17
9	356	-175	19
10	424	468	-7
11	472	-468	0
12	-103	36	-2

5 13 1

0	655	720	-16
1	157	-118	2
2	474	-526	-10
3	797	-919	-35
4	192	58	7
5	806	785	5
6	441	274	23

-3 14 1

1	356	-126	22
2	569	564	0
3	468	475	-1
4	340	43	22
5	710	-723	-3
6	522	-405	20
7	742	612	28
8	758	792	-8
9	731	-566	35

-2 14 1

1	1278	1397	-41
2	663	-758	-23
3	1154	-1210	-17
4	716	693	5
5	800	777	5
6	517	-378	22
7	290	-139	12
8	391	214	19
9	305	-160	12
10	502	-460	7
11	647	634	2
12	-114	82	-3

-1 14 1

1	231	-87	8
2	258	-61	11
3	379	-210	17
4	627	-504	22
5	864	820	10
6	1052	1026	6
7	733	-656	16
8	1218	-1285	-20
9	616	563	9
10	1191	1238	-13
11	647	-459	32
12	1110	-1118	-2
13	426	367	7

0 14 1

0	307	-164	13
1	1410	-1473	-28
2	1112	1059	21
3	1104	1287	-81
4	433	-430	0
5	406	-495	-21
6	-35	-70	-1
7	157	39	6
8	354	488	-29
9	700	763	-20
10	428	-272	26
11	884	-1035	-56
12	406	428	-4
13	1085	1163	-29

1 14 1

0	552	609	-11
1	356	-334	2
2	875	-943	-17
3	361	95	21
4	1241	1269	-8
5	851	-623	53
6	1581	-1528	16
7	763	652	23
8	1209	1250	-11
9	382	-341	4
10	933	-1073	-35
11	405	431	-3
12	196	335	-11

2 14 1

0	451	-29	38
1	1204	1151	16
2	552	-409	25
3	998	-1028	-8
4	337	-245	11
5	363	255	13
6	387	326	8
7	440	430	1
8	769	-712	13
9	908	-998	-25
10	827	818	2

3 14 1

0	1064	-1049	4
1	499	241	37
2	1340	1341	0
3	721	-541	39
4	1235	-1219	4
5	859	757	26
6	1240	1192	14